



UNIVERSITÀ
DEGLI STUDI
DI PADOVA

Head Office: Università degli Studi di Padova
Department of Management and Engineering

Ph.D. COURSE IN: Mechatronics and Product Innovation Engineering
CURRICULUM: Mechanics of Materials
SERIES XXXVI

GEOMETRIC SPECIFICATION MANAGEMENT IN INDUSTRIAL PRODUCT LIFE CYCLE

Coordinator: Ch.ma Prof.sa Daria Battini

Supervisor: Ch.mo Prof. Gianmaria Concheri

Co-Supervisor: Prof. Roberto Meneghello

Ph.D. student : Mattia Maltauro

A chi non ha mai creduto in me
...e a chi ha sempre creduto in me

To who never believed in me
...and, to who always believed in me

Abstract

This thesis delves into multifaceted dimensions of industrial geometric specification management, proffering insights into an innovative framework designed to mitigate complexities encountered during ISO GPS system implementation. Drawing upon a four-year industrial partnership with Electrolux, this work encompasses a spectrum of themes, around the intricate interplay between functional, manufacturing, and verification geometric specifications. Prominence is attributed to the top-down methodology, tolerance stack-ups, alignment intricacies, and the integration nuances pertaining to deformable components. At the end, this work underscores the pertinence of these discoveries in catalyzing future research activities in geometric specification management within industrial paradigms.

Acknowledgements

A successful PhD program cannot be completed in isolation. It is now time to express my gratitude to all the people who have been with me on this journey.

First and foremost, I would like to extend my heartfelt thanks to both my supervisor, prof. Gianmaria Concheri, and my co-supervisor, prof. Roberto Meneghello. This achievement would not have been possible without their guidance and the time they devoted to helping me achieve my research objectives. They were challenging supervisors, pushing me in unexpected ways, which ultimately allowed me to develop independence in my daily activities and research path.

I must also express my gratitude to Prof. Edward Morse, my supervisor at UNC Charlotte (USA), who reminded me, once again, that we work and persevere for the things we love during some particularly stressful times. His support and appreciation for my work were instrumental in keeping me focused and motivated.

I'd also like to thank all my colleagues who have shared this journey with me. I want to express my appreciation to Luca, Pierandrea, and Stefano from the research group. A special mention goes to Andrea, who shared the office with me for most of my journey. Daily life would have been much more challenging without his companionship during both the good and bad times.

Furthermore, I want to acknowledge the other professors in the research group, Prof. Francesca Ucheddu and Prof. Gianpaolo Savio.

Among my colleagues who shared the same spaces, I want to extend my sincere thanks to Prof. Andrea Giordano for creating a relaxed and friendly environment—a true source of light during dark times.

I would also like to remember all the undergraduate and graduate students I had the pleasure of guiding in their final dissertations: Matteo Longo, Daniele Pellegrini, Federico De Checchi, Alberto Andretta, Cristin Campagnaro, Luca Casa, Caterina Fasolo, Gianluca Passarotto, Marco Carraro, Michele Zanin, Arjola Barjami, and Davide Fontana. Not forgetting the students from other universities with whom I had the opportunity to work during their thesis projects: Valerio Cimini, Lorenzo Menarini, Elena Pierantozzi, Livia Palma, Volodymir Kravets, and Federico Tozzi: all working alongside Prof. Leonardo Ciocca from the University of Bologna.

During my time abroad in the USA, I would also like to express my appreciation for the support of the colleagues I met there: Rehab Abdelazim, Sevda Mamaghani, Jacob Brooks, Jessy Redford, Raj Shanmugan, and Dhanooj Bobba.

I also need to thank some of my long-standing friends who have helped me maintain balance in my life. Special thanks go to both Stefano and Davide. Their selfless support has been a lifeline during difficult times.

Lastly, I want to express my deepest gratitude to my family. Beginning with my parents, Arianna and Leonardo, and extending to my grandparents, Adelino, Alessandra, Celestina, and Giuliano. A special acknowledgment goes to my fiancée, Francesca, who has been a stabilizing force and kept me on track when things were challenging.

Index

Introduction	1
1 The ISO GPS System in the Italian Industrial Context	5
1.1 Design of the maturity model	6
1.1.1 Maturity model preparation	7
1.1.2 Model development.....	7
1.1.3 Assessment tool development and testing	9
1.1.4 Evaluation model.....	11
1.2 Model validation	12
1.3 Descriptives results on the Italian market.....	15
1.3.1 Participants description.....	15
1.3.2 Overall results	17
1.3.3 KPIs results	20
1.4 Comparative results on the Italian market	25
1.4.1 Differences between categories overall	25
1.4.2 Differences between KPIs.....	30
1.4.3 Differences between categories per each KPI.....	32
1.5 Conclusions	40
2 A model for tolerance specification management	41
2.1 State of the art	42
2.1.1 Functional tolerancing	42
2.1.2 Manufacturing tolerancing.....	43
2.1.3 Verification tolerancing.....	44
2.1.4 Relations in tolerancing.....	45
2.2 Responsibilities in tolerancing management	45
2.2.1 Design department.....	45
2.2.2 Manufacturing department.....	46
2.2.3 The quality control department	47
2.3 Hierarchy in tolerancing	48

2.3.1	The supply chain	50
2.4	Consequences of the new model.....	51
2.4.1	Tolerance hierarchy	52
2.4.2	The relevance of functional specification	53
2.4.3	The V model as a key to understanding.....	53
2.4.4	Clarifying Examples.....	54
2.4.5	Final remarks.....	59
2.5	Research gaps	59
3 	Classification of functional features.....	63
3.1	Phase 0: definition of functional requirements	63
3.2	A formal methodology for phase 0	64
3.3	Approach validation.....	67
3.3.1	Identification of critical zones.....	69
3.3.2	Disassembly	71
3.3.3	DfA Methodology	73
3.3.4	Functional feature refinement.....	81
3.3.5	Functional surfaces classification	85
3.3.6	Geometric specification	91
3.4	Conclusion.....	97
4 	Creation of functional specifications.....	99
4.1	Phase 1: functional dimensioning scheme.....	101
4.1.1	Phase 1.1: Size dimensions	102
4.1.2	Phase 1.2: Distance dimension.....	104
4.1.3	Phase 1.3: restricted features dimensions	106
4.1.4	Phase 1.4: Non-functional dimension.....	107
4.1.5	Phase 1.5: Dimensioning scheme layout	108
4.2	Phase 2	109
4.2.1	Phase 2.A: Size tolerances	110
4.2.2	Phase 2.B: Geometric tolerances.....	115
4.2.3	Final geometric specifications	127
4.3	Results	127
4.3.1	Assembly drawing	128
4.3.2	Sub-assembly drawings	128
4.3.3	Part drawings.....	130
5 	A top down approach for tolerance synthesis using tolerance stack-up.....	135
5.1	What's the meaning of tolerance stack-up.....	136
5.1.1	Responsibility in Tolerance stack-up.....	139

5.2	Updated mono-dimensional Excel model for tolerance stack-up	140
5.2.1	Tool general hypothesis	144
5.2.2	Compiling examples.....	144
5.3	Traditional approach	146
5.4	Top-Down approach	154
5.5	Discussion	161
6 	Functional definition of Pattern of fits	163
6.1	Methodology development	166
6.1.1	General Hypothesis	166
6.2	External vs Intrinsic datum system	166
6.2.1	Datum system transformation	168
6.3	2x Patterns stack-up	169
6.3.1	Stack-up by cases.....	169
6.3.2	Symmetric stack-up	171
6.3.3	Symmetric adjusted stack up	172
6.3.4	Symmetric optimized stack up	172
6.3.5	Monte Carlo Verification.....	173
6.4	Path towards generalization	173
6.5	The case study	174
6.6	Conclusions	176
7 	Tolerance stack-up: yet another proof for alignment design rules and design for maintenance.....	179
7.1	Functional requirements	180
7.2	Explicit alignment feature.....	181
7.2.1	Total length stack-up with external alignment feature	182
7.2.2	Hole alignment stack-up without material condition.....	184
7.2.3	Hole alignment stack-up with material condition.....	186
7.2.4	Maximum Material Condition vs Regardless of Feature size	187
7.3	Alignment through the fastener	188
7.3.1	Total length stack-up without external alignment feature and non-functional specification without material condition.....	188
7.3.2	Total length stack-up without external alignment feature and non-functional specification with material condition.....	191
7.3.3	Total length stack-up without external alignment feature and functional specification without material condition.....	193
7.3.4	Total length stack-up without external alignment feature and functional specification with material condition.....	195
7.3.5	Comparison.....	198

7.4	Conclusions	200
8 	Correlation of functional and manufacturing specifications for deformable assembly	203
8.1	Methodology description	205
8.1.1	Matrix computation	207
8.1.2	Assembly feature deviation	208
8.1.3	Deviation of other functional elements	209
8.1.4	Specification Correlation.....	211
8.1.5	Model validation.....	211
8.2	Results	218
8.2.1	Results case study 1	218
8.2.2	Results case study 2	221
8.2.3	Results case study 3	221
8.2.4	Results case study 4	223
8.3	Considerations on the model	224
8.3.1	Limits of application	224
8.3.2	Assembly with more than two parts.....	225
8.3.3	The advantages of a hybrid approach.....	226
8.3.4	Experimental validation	227
8.4	A possible application	227
9 	Definition of Verification specification within the ISO GPS system	231
9.1.1	Geometric verification specification	231
9.2	Verification purpose	232
9.2.1	Supplier qualification	233
9.2.2	Inbound batch approval	233
9.2.3	Selective assembly.....	233
9.2.4	Manufacturing/assembly process tuning	234
9.2.5	Statistical process control.....	234
9.2.6	In-line checks.....	234
9.3	Contents of the verification specification.....	235
9.4	Case study	236
9.5	Conclusions.....	240
10 	Use of real statistics for statistical assembly simulation	243
10.1	Method of System Moments	244
10.1.1	Linear Model limits.....	244
10.1.2	Second-order model contributions	246
10.2	Case Study.....	247

10.2.1	The assembly	248
10.3	Results	250
10.3.1	Critical dimension “Y-POS”	250
10.3.2	Critical dimension “X-POS”	252
10.4	Discussion	253
10.4.1	The mean shift	253
10.4.2	Critical dimension “Y-POS”	253
10.5	Conclusions	254
11 	An industrial application, the ELECTROLUX case study	255
11.1	Technical committee	257
11.2	Training	259
11.2.1	Training modules.....	259
11.2.2	Ambassador phase	260
11.2.3	Initial dissemination phase	261
11.3	Technical documentation.....	262
11.3.1	Guideline ISO GPS	262
11.3.2	Drawing standard	262
11.3.3	Working Instructions	263
11.3.4	Drawings management	263
11.4	Deployment in Electrolux	265
12 	Conclusions.....	267
13 	Future research agenda	271
	Appendices	275
A 	Geometric Specification 2D drawings for the case study of chapter 4	279
A.1	Assembly Drawing	277
A.2	Sub-assembly Drawings	281
A.3	Part Drawings	287
B 	Derivation of equation for statistical tolerance analysis	299
C 	Training agenda.....	301
D 	Scientific production and tutored dissertations	305
D.1	Journal publications	305
D.2	Full paper peer review conference proceedings	306

D.3	Full paper non peer review conference proceedings	306
D.4	Abstract conference proceedings.....	306
D.5	Pre-prints.....	307
D.6	Co-tutored students' dissertations.....	307
Bibliography		309

List of figures

Fig. 1.1: Example of knowledge or usage distribution curves.	8
Fig. 1.2: general questionnaire scheme.	9
Fig. 1.3: Example of self-assessment questions from the beginner's subsection of KPI 1 (Geometric tolerances).	10
Fig. 1.4: Example of check question from the advanced subsection of KPI 2 (Datum systems) on the right.	11
Fig. 1.5: Example of descriptive statistics for a self-assessment question (KPI 1: Geometric tolerances, beginner level).	13
Fig. 1.6: Example of descriptive statistics for check question (KPI 2: Datum systems, beginner level).	14
Fig. 1.7: Example of Knowledge and usage distribution across the population.	14
Fig. 1.8: Industrial sectors covered by the survey.	17
Fig. 1.9: Beginner/Experienced distribution for all KPIs.	18
Fig. 1.10: Overall knowledge and usage distribution found averaging KPIs from 1 to 4.	19
Fig. 1.11: Differences in Knowledge, usage, applied knowledge, and applied usage overall.	19
Fig. 1.12: Results for KPI 0.	21
Fig. 1.13: Knowledge and usage distribution for KPI 1.	21
Fig. 1.14: Knowledge and usage distribution for KPI 2.	22
Fig. 1.15: Knowledge and usage distribution for KPI 3.	23
Fig. 1.16: Knowledge and usage distribution for KPI 4.	23
Fig. 1.17: Overview of approaches used for tolerance stack-up.	24
Fig. 1.18: Result for the check question of KPI 5 (Tolerance stack-up).	24
Fig. 1.19: Grade overview per each KPI.	25
Fig. 1.20: Beginner/Experienced comparison overall.	26
Fig. 1.21: Industry/academia comparison overall.	26
Fig. 1.22: With training/without training comparison overall.	27
Fig. 1.23: Write/read geometric specification comparison overall.	28
Fig. 1.24: Overall grades comparison between categories.	28
Fig. 1.25: Knowledge and usage distribution comparison among KPIs.	31
Fig. 1.26: Grade comparison among KPIs.	32

Fig. 1.27: Knowledge and usage distribution comparison between categories for KPI 1.....	34
Fig. 1.28: Knowledge and usage distribution comparison between categories for KPI 2.....	35
Fig. 1.29: Knowledge and usage distribution comparison between categories for KPI 3.....	36
Fig. 1.30: Knowledge and usage distribution comparison between categories for KPI 4.....	37
Fig. 2.1: Input/Output diagram that describes the functional tolerancing activity that takes place inside the design department. Other tasks performed by the design department are omitted.....	46
Fig. 2.2: Input/Output diagram that describes the manufacturing tolerancing activity taking place inside the manufacturing department. Other tasks performed by the manufacturing department are omitted.....	47
Fig. 2.3: Input/Output diagram that describes the verification tolerancing activity taking place inside the quality control department. Other tasks performed by the quality control department are omitted.....	48
Fig. 2.4: Hierarchical relations (as described by the ISO/TS 21619) among different specifications: Functional, Manufacturing and Verification, inspired by [37].	48
Fig. 2.5: The scheme represents the relations among the different departments involved in product development for what concern the tolerancing activities. Each department block is the zoom out from the diagrams represented in Fig. 2.1, Fig. 2.2 and Fig. 2.3, the solid arrows represent an information flow, while the dashed arrow the transfer of a physical entity. FUN-SPEC stands for Functional Specification, MAN-SPEC stands for Manufacturing Specification, VERI-SPEC stands for Verification Specification and ECR stands for Engineering Change Request.....	49
Fig. 2.6: The scheme represents the relations among different departments and different business units (or different companies) along the supply chain that are involved in the product development for what concern the tolerancing activities, each horizontal layer follows the scheme represented in Fig. 2.5.	51
Fig. 2.7: The scheme represents the functional hierarchy among product, system, sub-system and component levels depicting a case in which one component inherit functionality from two distinct subsystems. It could represent a case of a standardized component used in different sub-systems or a complex component that is required for different functions (e.g., Structural and aerodynamic).	52
Fig. 2.8: A simplified V-Model framework used to describe the product development (Adapted from: [72]).	54
Fig. 2.9: Submersible pump assembly functional specification.	55
Fig. 2.10: Impeller functional specification.	56
Fig. 2.11: Pump case base functional specification.....	56
Fig. 2.12: Pump case functional specification.....	56
Fig. 2.13: Functional specification for a spacer plate.....	57
Fig. 2.14: Manufacturing specification for a spacer plate.	58
Fig. 2.15: graphical representation of the research gaps that were identified.	60
Fig. 3.1: Proposed workflow.....	65

Fig. 3.2: The actual model used consists of the following components: the red Pulley component, the blue Base component, the two green Uprights, the white Bearings, the light gray Shaft, and the purple M10 Screws.....	68
Fig. 3.3: Identification of critical zones.	69
Fig. 3.4: The critical zones identified in the caster are as follows: Zone 1: Gap between the Bushings and Wheel. Zone 2: Gap between the Wheel and Base.	70
Fig. 3.5: Disassembly phase.	71
Fig. 3.6: Sub-assembly “wheel_asm” (3), “riser_asm” (2), and Base component (1).	72
Fig. 3.7: DfA methodology phase.	73
Fig. 3.8: Base posing on the fixturing base.	76
Fig. 3.9: assembly procedure to obtain the “riser_asm” and the “wheel_asm” sub-assemblies.	77
Fig. 3.10: “riser_asm” sub-assembly posing on the base component.....	77
Fig. 3.11: Pre-mounting of M10 screws.....	78
Fig. 3.12: “wheel_asm” insection.....	78
Fig. 3.13: assembly of the second “riser_asm” sub-assembly.	79
Fig. 3.14: tightening of all M10 screws.	80
Fig. 3.15: Refinement of assembly surfaces phase.	81
Fig. 3.16: Exploded view with all components where functional features are highlighted.	83
Fig. 3.17: Comparison between the solid model and the one with just the functional features.	84
Fig. 3.18: Classification of functional features phase.....	85
Fig. 3.19: Base component functional feature classification. A) Assembly features at the next level, B) Assembly features at the next level, C) Other functional features, D) Chain features, E) Other functional features.	86
Fig. 3.20: “riser_asm” sub-assembly functional feature classification. H) Assembly features at the previous level, I) Assembly features at the previous level, J) Assembly features at the previous level, K) Other functional features, L) Chain features / Assembly features at the next level, M) Assembly features at the next level.....	87
Fig. 3.21: Riser component functional feature classification. F) Assembly features at the next level, G) Assembly features at the next level, H) Assembly features at the previous level, I) Assembly features at the previous level, J) Assembly features at the previous level, K) Other functional features.....	88
Fig. 3.22: Bushing component functional feature classification. L) Chain features / Assembly features at the next level, M) Assembly features at the next level, N) Assembly features at the previous level, O) Assembly features at the previous level.....	88
Fig. 3.23: – “wheel_asm” sub-assembly functional feature classification. P) Assembly features at the previous level, Q) Chain features / Assembly features at the previous level, S) Chain features / Assembly features at the previous level, U) Chain features.	89

Fig. 3.24: Shaft component functional feature classification. P) Assembly features at the previous level, Q) Chain features / Assembly features at the previous level, R) Assembly features at the next level.	89
Fig. 3.25: Wheel component functional feature classification. S) Chain feature / Assembly features at the previous level, T) Assembly features at the previous level, U) Chain feature.	90
Fig. 3.26: Exploded view with all functional features highlighted.	91
Fig. 3.27: Geometric specification phase.	91
Fig. 3.28: Base component Datum System description.	93
Fig. 3.29: "Riser_asm" Datum System description.	94
Fig. 3.30: Riser Datum System description.	94
Fig. 3.31: Bushing Datum System description.	95
Fig. 3.32: "Wheel_asm" Datum System description.	95
Fig. 3.33: Shaft Datum System description.	96
Fig. 3.34: Wheel Datum System description.	96
Fig. 4.1: Schematic view of the methodology to create functional specification.	99
Fig. 4.2: orthogonal views of the risers.	102
Fig. 4.3: orthogonal views of the risers with mating features (feature of size) highlighted.	103
Fig. 4.4: orthogonal views of the risers with size dimension.	104
Fig. 4.5: orthogonal views of the risers with reference and referenced mating features highlighted.	105
Fig. 4.6: orthogonal views of the risers with distance dimension.	106
Fig. 4.7: orthogonal views of the risers with dimension to specified restricted features extension.	107
Fig. 4.8: orthogonal views of the risers with non-functional dimensions.	108
Fig. 4.9: Functional dimensioning scheme at the end of phase 1.	109
Fig. 4.10: orthogonal views of the risers with size dimension and their variability.	112
Fig. 4.11: orthogonal views of the risers with size dimension and their variability and modifiers.	115
Fig. 4.12: H-Matrix, Geometrical tolerance hierarchical matrix.	116
Fig. 4.13: orthogonal views of the risers with datum features tolerance zone and datum features naming.	118
Fig. 4.14: orthogonal views of the risers with datum features geometric specification.	119
Fig. 4.15: orthogonal views of the risers with datum features geometric specification with modifiers.	121
Fig. 4.16: orthogonal views of the risers with referenced features tolerance zone.	122
Fig. 4.17: orthogonal views of the risers with referenced features tolerance zone and TEDs. ...	123
Fig. 4.18: orthogonal views of the risers with referenced features specification.	124
Fig. 4.19: orthogonal views of the risers with referenced feature full geometric specification.	125
Fig. 4.20: orthogonal views of the risers with full geometric specification.	127
Fig. 4.21: Extract from the full assembly 2D drawing.	128
Fig. 4.22: Extract from the "riser_asm" 2D drawing.	129

Fig. 4.23: Extract from the “wheel_asm” 2D drawing.	130
Fig. 4.24: Extract from the base component 2D drawing.	131
Fig. 4.25: Extract form the riser component 2D drawing.	132
Fig. 4.26: Extract form the bushing 2D drawing.	133
Fig. 4.27: Extract form the shaft component 2D drawing.	133
Fig. 4.28: Extract from the wheel component 2D drawing.	134
Fig. 5.1: Input-output relation for tolerance stack-up simulation.	137
Fig. 5.2: Input tab for the Excel tool.	142
Fig. 5.3: Output tab for the excel tool.	143
Fig. 5.4: Template for input quantities based on the type of tolerance.	145
Fig. 5.5: Case study assembly 2D drawing.	146
Fig. 5.6: Slot geometric specification.	147
Fig. 5.7: Component A1 geometric specification.	147
Fig. 5.8: Component B1 geometric specification.	148
Fig. 5.9: Component C1 geometric specification.	148
Fig. 5.10: Component A2 geometric specification.	149
Fig. 5.11: Component B2 geometric specification.	149
Fig. 5.12: Component C2 geometric specification.	150
Fig. 5.13: Stack-up scheme, still not displaying UZ contribution.	151
Fig. 5.14: Stack-up scheme, displaying UZ contribution.	151
Fig. 5.15: Extract from the input tab of the Excel tool.	152
Fig. 5.16: Tolerance stack-up result after tolerance synthesis.	153
Fig. 5.17: Sub-assembly 1+2 geometric specification.	154
Fig. 5.18: Sub-assembly 1 geometric specification.	154
Fig. 5.19: Sub-assembly 2 geometric specification.	155
Fig. 5.20: Extract from the input tab of the Excel tool for the highest level (product).	155
Fig. 5.21: Tolerance stack-up scheme for the second level (system).	156
Fig. 5.22: Extract from the input tab of the Excel tool for the second level (system).	156
Fig. 5.23: Tolerance stack-up scheme for the third level (sub-system 1).	157
Fig. 5.24: Extract from the input tab of the Excel tool for the third level (sub-system 1).	157
Fig. 5.25: Tolerance stack-up scheme for the third level (sub-system 2).	158
Fig. 5.26: Extract from the input tab of the Excel tool for the third level (sub-system 2).	158
Fig. 5.27: Result for the highest level stack-up (product).	159
Fig. 5.28: Result for the second level stack-up (system).	160
Fig. 5.29: Result for the second third stack-up (sub-system 1).	160
Fig. 5.30: Result for the second third stack-up (sub-system 2).	160
Fig. 6.1: External Datum System for a spacer.	164
Fig. 6.2: Intrinsic Datum System for a spacer.	165
Fig. 6.3: Geometric specification for a two shafts cap.	169

Fig. 6.4: Stack-up scheme.	170
Fig. 6.5: External and Internal gap distribution and rejection rate, stack-up by cases.	170
Fig. 6.6: Generalized Gap distribution and Rejection Rate, stack-up by cases.....	170
Fig. 6.7: Stack-up scheme for all symmetric cases: a) Internal and external gaps for the symmetric stack-up; b) Elements use in the symmetric adjusted stack-up.....	171
Fig. 6.8: Generalized Gap distribution and Rejection Rate, symmetric stack-up.	171
Fig. 6.9: Generalized Gap distribution and Rejection Rate, symmetric adjusted stack-up.....	172
Fig. 6.10: Case study geometric specification for the spacer.	175
Fig. 6.11: Case study geometric specification for the two shafts cap.....	176
Fig. 7.1: Case study functional requirements.....	180
Fig. 7.2: Functional specification for both parts considering the alignment feature without material conditions.	181
Fig. 7.3: Functional specification for both parts considering the alignment feature with material conditions.	182
Fig. 7.4: Total length stack up scheme using an explicit alignment feature.	183
Fig. 7.5: Extract from the input and output for the total length tolerance stack-up.	183
Fig. 7.6: Hole alignment without material condition stack-up scheme using an explicit alignment feature.	185
Fig. 7.7: Extract from the input and output for the Hole alignment without material condition tolerances stack-up.	185
Fig. 7.8: Extract from the input and output for the Hole alignment with material condition tolerances stack-up.....	186
Fig. 7.9: Tolerance stack-up output statistical distribution comparison between the case without and with material condition.....	187
Fig. 7.10: Case study functional requirements.....	188
Fig. 7.11: Total length stack-up scheme using the bolt as alignment with non-functional specification.	189
Fig. 7.12: Extract from the input for the total length stack-up using the bolt as alignment without material condition and non-functional specification.	190
Fig. 7.13: Extract from the output for the total length stack-up using the bolt as alignment without material condition and non-functional specification.	191
Fig. 7.14: Extract from the input for the total length stack-up using the bolt as alignment with material condition and non-functional specification.	192
Fig. 7.15: Extract from the output for the total length stack-up using the bolt as alignment with material condition and non-functional specification.	193
Fig. 7.16: Functional specification for both parts considering the alignment through the bolt without material condition.....	193
Fig. 7.17: Total length stack-up scheme using the bolt as alignment with functional specification.	194

Fig. 7.18: Extract from the input for the total length stack-up using the bolt as alignment without material condition and functional specification.	194
Fig. 7.19: Extract from the outputs for the total length stack-up using the bolt as alignment without material condition and functional specification.	195
Fig. 7.20: Functional specification for both parts considering the alignment through the bolt with material condition.....	196
Fig. 7.21: Extract from the input for the total length stack-up using the bolt as alignment with material condition and functional specification.	197
Fig. 7.22: Extract from the outputs for the total length stack-up using the bolt as alignment with material condition and functional specification.	197
Fig. 7.23: Comparison between the result obtained with the same geometric specification changing the assembly condition.	198
Fig. 7.24: Comparison between the result obtained with different geometric specifications with the same assembly condition.	199
Fig. 8.1: General workflow to correlate functional (design) and manufacturing specifications. ...	206
Fig. 8.2 : Types of possible input-output degrees of freedom.	207
Fig. 8.3 : The input degrees of freedom are mapped on the second part mating feature creating an assembly link per each of them.	208
Fig. 8.4 : The general workflow to generate the proposed linearized model. DoF stands for Degree of Freedom.	210
Fig. 8.5 : The monodimensional case study.	212
Fig. 8.6: The case study used to prove the sensitivity matrix's effectiveness, a) CAD model, b) FEM model.	214
Fig. 8.7: The case study used to test the elastic spring back.....	215
Fig. 8.8: The geometry used to test the instability of the problem.....	216
Fig. 8.9: Effect of the truncation of the stiffness matrices on the elastic spring back simulation.	216
Fig. 8.10: Actual geometries used for case study 4.	218
Fig. 8.11: Result for test case 7.	221
Fig. 8.12: Result for case study 3.	223
Fig. 8.13: Comparison between the result obtained with the proposed framework and the actual values measure in the assembly.	224
Fig. 8.14: Functional specification for the tank assembly.	228
Fig. 8.15: Functional and manufacturing specifications for the tank top.	229
Fig. 9.1: Geometric functional specification for the case study.	237
Fig. 9.2: Geometric verification specification dedicated to in-line functional check.	238
Fig. 9.3: Geometric manufacturing specification for the case study.....	238
Fig. 9.4: Geometric verification specification dedicated to process tuning	239
Fig. 9.5: Example of posing described by the verification geometric specification in Fig. 9.4	240

Fig. 10.1: Input and output probability distribution for a single-input/single-output system, comparison among actual non-linear assembly function, linear approximation, and a quadratic approximation.....	246
Fig. 10.2: SMLambda distribution with a mean value of 0, standard deviation, skewness and excess kurtosis of 1; compared with a normal distribution (dashed line) and a uniform distribution (dash dotted line).....	248
Fig. 10.3: Simulated real geometries, surface comparison in GOM Inspect.	249
Fig. 10.4: Distribution for rotation about y-axes for the cylinder marked as Cylinder 2.	250
Fig. 10.5: Output statistical distribution for the analysis centred with the input tolerance midpoint.	251
Fig. 10.6: Output statistical distribution for the analysis centred with the input distributions means.	251
Fig. 10.7: Comparison among the output statistical distribution obtained for the critical dimension “Y-POS”.....	252
Fig. 10.8: Comparison among the output statistical distribution obtained for the critical dimension “X-POS”.....	252
Fig. 11.1: Pillars for the ISO GPS implementation in Industry.	256
Fig. 11.2: Competence and Training matrix (example).....	261
Fig. 11.3: Drawings management.	264
Fig. 13.1: graphical representation of the research gaps and the contributions in this thesis.	272

List of tables

Tab. 1.1: Summary of the participants to the survey.....	16
Tab. 1.2: Quantitative differences in overall Knowledge and usage between categories.....	29
Tab. 1.3: Quantitative differences in overall applied Knowledge and usage and overall grade between categories.	30
Tab. 1.4: Quantitative differences in grade between categories.	32
Tab. 1.5: Case study 2, reduced model results compared to full FEM model results.....	39
Tab. 3.1: Assembly procedure with sub-assembly.....	74
Tab. 4.1: Fits requirements based on application, from [84].	110
Tab. 4.2: Usual Fit tolerances table, from [85].	111
Tab. 4.3: Size modifiers according to ISO 14405-1:2016.	113
Tab. 5.1: Responsibilities in tolerance stack-up.....	140
Tab. 5.2: Tolerance values after traditional tolerance synthesis.	153
Tab. 5.3: Tolerance values after traditional tolerance synthesis.	159
Tab. 6.1: Monte Carlo simulation results for 2x pattern.....	168
Tab. 6.2: Monte Carlo simulation results for 3x pattern.....	168
Tab. 8.1: Configurations tested to verify the framework.....	212
Tab. 8.2: Expected simulation results.....	213
Tab. 8.3: Configuration tested for case study 2.....	214
Tab. 8.4: Configuration tested for case study 3.....	217
Tab. 8.5: Simulation results.	220
Tab. 8.6: Case study 2, reduced model results compared to full FEM model results.....	222
Tab. 8.7: Configuration tested for case study 3.....	223

Prologue

Much of the content in this volume can be traced back to 1995.

In that year, significant technological advancements were made. One notable introduction was the DVD (Digital Versatile Disc) format, which revolutionized digital storage by providing a new medium for data. Even though almost 30 years have passed since then and more advanced storage technologies have been introduced, DVDs are still widely used and familiar to younger generations. Around the same time, the Java programming language was released, having a profound impact on software development and internet applications.

1995 also marked a milestone in space exploration as the Galileo spacecraft successfully entered orbit around Jupiter, becoming the first spacecraft to do so. This achievement expanded our understanding of the solar system and provided valuable insights into Jupiter's composition and environment.

In the field of biology, 1995 saw a groundbreaking development with the announcement of the successful cloning of a mammal. Scientists in Scotland revealed the cloning of a sheep named Dolly, the first mammal to be cloned from an adult somatic cell.

This is just a glimpse of what happened in 1995. However, none of these achievements are directly relevant to this work.

The first milestone relevant to this work that I want to highlight occurred in November 1995 when ISO (International Organization for Standardization) published a technical report named ISO/TR 14638:1995, also known as the Masterplan for Geometric Product Specification (GPS).

This led in 1996 to the initial establishment of the ISO/TC 213.

In the same year, another event took place, which may be irrelevant to most but extremely relevant to this work. On May 28th, I was born, coinciding with the birth of the ISO GPS system. Whether we are considered old or young is not for me to judge.

Now, after nearly 28 years, I find myself sitting in front of my personal computer, building upon the foundation laid by those who came before me, to explore the current state of the ISO GPS system and facilitate its industrial application. This volume presents a management model for the information conveyed through geometric specification throughout the lifecycle of an industrial product. The task is not simple, the outcome is not trivial, and success is not guaranteed. However, goals and ambitions should not be chosen based on ease; they should be chosen based on the

passion they evoke. As John F. Kennedy once said, “We choose to go to the Moon in this decade and do the other things, not because they are easy, but because they are hard.”

Although I did not decide to go to the Moon, the following pages can be seen as my journey to the Moon and back. This journey spanned three years during my Ph.D. studies and took off nearly one year before when I began working on my M.Sc. dissertation.

I genuinely hope that every reader of this document can sense the passion and dedication I have poured into my research and the writing of this thesis.

See you at the end.

Mattia Maltauro

Introduction

A product geometric specification [1,2] is the result of the so-called tolerancing activity [3]. A product specification represents the information contained in the technical product documentation (TPD) stating the product requirements [4]. The TPD can therefore be defined as the comprehensive set of documents needed to describe all the significant characteristics of a product from a technical point of view (i.e., geometrical and functional, but also manufacturing, maintenance, etc.). The geometric specification is created during the product development phase and allows the transposition of definite functional requirements into geometrical requirements assigned to actual product features [5–7].

The information contained herein is transmitted throughout the product lifecycle and used by all the different actors that collaborate to bring the final product to the market and provide subsequent services during usage. The key to the success of a project, which involves the design, manufacturing, inspection, service, and disposal of a mechanical/mechatronic product, can be individuated as the proper communication among the involved actors.

In this framework, during the last century, the technical language to translate functional requirements into geometrical requirements applied to product features was developed. The base assumption is that the difference (deviation) between ideal (nominal) and actual geometry (Skin Model) is inevitable and depends on the technological process. The difference between the ideal, therefore nominal, machine and the real machine, as produced by an actual manufacturing process, should not compromise its functionality. It is the task of the designer to define the permissible differences (“deviations” or “tolerances”) between ideal dimensions/geometry and actual dimensions/geometry that ensure proper functionality.

Historically, in the 1920s, initial proposals were formulated by National Standardization Bodies regarding standards unification for couplings. In April 1926, the International Federation of the National Standardizing Associations (ISA) was founded in New York. One of the main topics discussed was the unification of the various national systems covering mechanical couplings (limits and fits). The Secretariat of ISA Committee 3, covering Limits and Fits, was entrusted to the German Standardizing Association the same year. The ISA System of Limits and Fits was finally published in ISA Bulletin 25 (1940) [8].

During the same time period, in the United States, the American Standards Association (ASA) published the first standards on drafting: “American Standard Drawing and Drafting Room

Practices," first published in 1935 [9] and later revised 1946 [10]. At this stage, the focus was only on dimensional tolerance. The evolution of these concepts is still used today and can be found in ISO 286-1:2010 [11].

Starting from the 1940s, the concept of geometrical tolerances emerged. In 1940, Stanley Parker introduced the concept of tolerance zone, the circular tolerance zone for hole/shaft location, and the concept of "true location" [12]. Around the same time, Chevrolet published the "Chevrolet draftsman's handbook," which was among the first publications to mention location tolerances and introduced the concept of Maximum Material Condition [13]. In 1943, the British Standard's BS 308:1943 figure 29 at page 27 [14] first used the Datum concept as a reference element to clarify the meaning and orientation of linear dimensions. The integration of Stanley Parker's studies into this standard led to the 1953 edition (BS 308:1953), which formally introduced the concept of geometrical tolerances in a standard, yet without standardized symbology. Tolerances and datums were assigned by means of words [15]. In the United States of America, the military standard MIL-STD-8 covering dimensioning and tolerancing was first published in 1949. It was updated in 1953 (MIL-STD-8A), 1959 (MIL-STD-8B), and 1963 (MIL-STD-8C) before being suspended and superseded by ANSI-Y14.5:1966. It is thanks to this military standard that graphical symbols for tolerances were first introduced.

While the ANSI standard is still independent today with its latest edition ANSI-Y14.5:2018 [5], at the international level, the good practice initiated by the British Standard and ANSI was collected into a first ISO publication in 1969, the ISO/R 1101-1:1969 under the control of the Technical Committee ISO/TC 10 [Drawing (General principles)], which introduced the geometric tolerances in the ISO system [16]. For the first 25 years, concepts related to geometrical tolerances and geometric specification, in general, kept evolving in a non-structured way within the ISO System. This led to multiple standards being overlapped and not always coherent. For this reason, in 1995, a project was laid out aiming to restructure the system. It was synthesized in the ISO/TR 14638:1995 [2], also known as the Masterplan for Geometric Product Specification (GPS). The year after, the ISO/TC 213 was founded under the secretariat of the Danish Standard, formally establishing the ISO GPS System.

According to one of the fathers of the system, Henrik S. Nielsen, former chairman of the ISO/TC 213, the Geometric Product Specification, or GPS, is a language defined by symbols endorsed internationally to state tolerances on engineering drawings [17]. Indeed, one of the fathers of geometrical tolerancing, Stanley Parker, in a publication dating back to 1956, said: "Experiences of co-related problems of designers, manufacturers, and inspectors, together with an intimate knowledge of the troubles and misunderstandings which frequently occur between these three broad groups of specialists, convinced me, nearly twenty years ago, of the necessity for the establishment of a standard and logical language for the expression of dimensions and tolerances on engineering drawings" [18]. Therefore, reiterating the concept that the ISO GPS system is a language. In other words, the ISO GPS language aims to give designers a common language to translate functional requirements into admissible geometrical and dimensional deviations (i.e., tolerances). These deviations are defined as the difference between the actual artifact, as produced

by the manufacturing process (non-ideal surface model or skin model), and the intended perfect geometry defined by the designer (CAD model).

Being a language, it is the means of communication between the actors involved in the product development cycle, conveying the information relevant to the design, manufacturing, and inspection of a product. The information needs to be (correctly) interpreted by a reader, but at the same time, it needs to be correctly written by the writer. The users of the GPS System can be clustered into two groups: writers and readers. Communication issues may arise at both ends: a requirement may be poorly/inadequately described in the TPD, or the reader might misinterpret a specification, leading to possible unexpected problems. If the functional requirements are not transmitted clearly and coherently, different unwanted scenarios may arise. On one side, it is possible to experience a loss in performance in the final product. On the other side, an increase in scraps during manufacturing can occur, increasing the overall manufacturing cost.

The first question that arises regarding the implementation of the system in industry is: how much is the system known and used? Since its introduction in the mid-'90s, the ISO GPS language has proved itself as a great tool to decrease ambiguity compared to the previous linear dimensioning scheme [19,20]. It has also proved to be a great tool to improve the functional description of assemblies and parts. An emblematic example is given by the location tolerance assigned to a hole: using geometric tolerances, it is possible to increase the tolerance zone by 57% while maintaining functionality. Similarly, the use of material conditions/requirements for mating features of size can exactly describe the mating requirements [7]. However, so far, there is no quantification of the actual knowledge and usage of the system. The first chapter of this manuscript will give an answer to this question, limited to the Italian market. The findings clearly state that the implementation is not sufficient, as also confirmed by evidence collected through experiences with consultants from all over the world.

A new management model for tolerance specification is also presented, aiming to propose a structured way to implement the GPS system that shares and gives the responsibility to the appropriate actors involved in product development. The analysis of the proposed model allows defining multiple research gaps and research questions that this manuscript aspires to identify and provide possible preliminary answers to as many of them as possible.

It should be noted that this work cannot aspire to cover all the gaps or propose definitive answers to each and every question. The main purpose of this document is to establish a new vision for the system and be the starting point for future research lines and activities, which will be summarized at the end of the manuscript.

1 || The ISO GPS System in the Italian Industrial Context¹

"The greatest enemy of knowledge is not ignorance, it is the illusion of knowledge."

Stephen Hawking

As stated in the introduction, this first chapter will provide an overview of the implementation of the ISO GPS system in industry and academia. The experience gained by the author in his work within the Design Tools and Methods in Industrial Engineering Laboratory at the University of Padova, collaborating with Italian firms, including small and medium enterprises (SMEs) and multinational enterprises, has shown that the overall implementation of the ISO GPS system is lacking. Similar findings were collected in Germany, with a particular focus on SMEs, revealing that they struggle with the task of ISO GPS implementation, and only 30% of them are familiar with the system [21,22]. At the same time, it is recognized that a comprehensive application of the ISO GPS system is necessary to obtain the advantages postulated by the system itself, as mentioned previously [23].

For these reasons, it becomes important to assess the current knowledge and usage of the ISO GPS language in industry, mapping critical areas in the standard system and guiding the transition towards a better implementation of the ISO GPS system. The idea is to develop a survey to gather insights from individuals in industry and academia, aiming to create a snapshot of the current implementation of the system.

Examples of surveys regarding the ISO GPS system can be found in the literature [22,24–26]. In 2017, a survey was conducted to compare the usage of the ISO GPS system versus ASME Y14.5, which revealed that the ASME standard is more widely used worldwide. In China, a survey was used to assess the delivery status of ISO GPS, highlighting a significant gap between education and industry [25]. In Germany, a survey was conducted to test the awareness, use, and need for statistical tolerance analysis, revealing that tolerance analysis is not systematically used in most of

¹ Most of the content of this chapter was presented at the ADM2023 International Conference and will be featured in an upcoming publication in Lecture Notes in Mechanical Engineering.

the companies interviewed, although there is a high awareness of the importance of managing geometric deviations [26]. In Germany, after evaluating the implementation of a maturity model for assessing the current integration of the ISO GPS system in companies [21], Schuldt and Gröger developed a tool based on a survey to drive the systematic implementation of the ISO GPS system within companies [22].

In the literature, surveys in the field of ISO GPS have mainly focused on three areas: the education gap, tolerance analysis, and the implementation of the ISO GPS system within companies. However, none of them were designed to assess the current implementation of the system over a geographic area or a specific industrial sector.

Therefore, building upon the experience of the research group in Chemnitz, Germany [21,22], which has come closest to implementing a survey for the scope covered in this document, the aim is to propose a tool to assess the actual knowledge and usage of the ISO GPS language in industry and academia. This tool will be used to provide evidence of knowledge gaps between the industry and the research/education world, with the goal of defining systematic actions in industry, standards, education, and research.

In the following sections, the development of the tool will be presented first, followed by the results collected thus far (08/08/2023), which will be presented and discussed.

1.1 || Design of the maturity model

In the literature, the application of the maturity model for assessing ISO GPS implementation within companies has proven to be a valid approach [21,22]. Maturity models are commonly used to determine the current performance and level of penetration in a specific field of application [27]. In this case, the maturity model is used to assess the knowledge and usage of the ISO GPS language in industry and academia.

The design steps required to develop a maturity model are well-discussed in the literature, and a detailed analysis of the design procedure is presented in [22]. Generally, the design of a maturity model can be divided into three main phases: preparation, model development, and application of the model. Each phase will be further analyzed in the following sections.

Maturity models can be categorized into three different groups based on their structure: the quick test, the topic generator, and the individual transformation [28]. The quick test approach involves a quick and simple questionnaire. The topic generator delves deeper into the topic with general questions. The individual transformations approach focuses on in-depth analysis, targeting even personal and cultural aspects.

It is known that maturity models tend to fail if they become too complex [29]. Therefore, for the purpose of this study, the quick test structure was chosen. This choice is also driven by the intended widespread distribution of the maturity model among a large population.

1.1.1 Maturity model preparation

During the preparation phase, three key aspects need to be considered: the problem definition, the target of the assessment, and the analysis of defined models.

While the analysis of the defined model has been presented in the introduction to this chapter. The problem definition in this case is to assess the current knowledge and usage of the ISO GPS language and identify any gaps that exist between industry, research/education, and standards.

To address this problem, the target population includes technicians, academic researchers, professors, and students who are involved or prospectively involved in the development of industrial products.

Regarding technicians, the focus is on three main departments involved in product development: R&D/design, manufacturing, and quality control. Additionally, the assessment includes professionals in the maintenance sector who may need to consult technical product documentation. It is expected that there will be varying levels of knowledge among these departments, and identifying significant differences will help pinpoint bottlenecks in the implementation of the ISO GPS system. The assessment is intended to cover all industries without being limited to specific application sectors.

The target population also includes students at both the university level (undergraduate and graduate) and high school level. The aim is to evaluate the adequacy of current training on ISO GPS-related content.

Furthermore, it is important to differentiate between individuals who need to read geometrical specifications and those who create geometrical specifications. This distinction aligns with the Geometric Dimensioning and Tolerancing Professional (GDTP) Certification Program offered by the American Society of Mechanical Engineers (ASME), which offers two levels of assessment: technologist level and senior level [30].

1.1.2 Model development

In the model development phase, three main steps are involved: defining the maturity levels, mapping the maturity dimensions and indicators, and determining the degree of maturity.

The first step is to define the levels of maturity. In the referenced work [22], the maturity level was defined based on ISO GPS competence. However, assessing competence through a short questionnaire can be challenging, as competence is typically assessed through a larger number of questions. For example, the GDTP Certification Program uses 150 questions to assess competence [30], which is impractical for the proposed maturity model. In this model, the level of maturity is defined based on both knowledge and usage of the ISO GPS language. Knowledge is considered a contributor to competence [31], and is defined as the recognition of an ISO GPS operator. Therefore, the level of competence can only be less than or equal to the level of usage,

which can only be less than or equal to the level of knowledge. The level of competence is estimated based on questions applied to actual cases.

The ISO GPS language is divided into six distinct sectors, referred to as Key Performance Indicators (KPIs) in the proposed model. These sectors include general concepts, geometric tolerances, datum systems, dimensional tolerance, modifiers and indications, and tolerance stack-up. It is important to note that not all areas of the ISO GPS system are covered in the model (e.g., surface roughness), and the six KPIs were identified based on minimum requirements for the implementation of the ISO GPS system, derived from discussions with members of the Design Tools and Methods in Industrial Engineering Laboratory who have experience in training and consulting. Additionally, the section on tolerance stack-up is specifically intended for those who create specifications. Each section or KPI is associated with a set of indicators that are used to structure the assessment tool.

For each section, the maturity level needs to be determined. The proposed model defines three levels of assessment: single entry rating, population distribution, and population rating. The rating is based on a scale from zero to ten, representing the percentage of knowledge and usage. Every single entry in the questionnaire receives a rating, but the assessment target is the population as a whole, rather than individual entries. To map the knowledge and usage across a population, the distribution of knowledge and usage is analyzed, indicating the percentage of the population that knows and/or uses a specific percentage of the ISO GPS language.

The results are presented as distribution curves on a Cartesian plane, as shown in Fig. 1.1. The population rating is determined based on the integral of the distribution curves, which represents the marked area in Fig. 1.1. In an ideal implementation, where 100% of the population knows and uses 100% of the ISO GPS language, the marked area would cover the entire graph, and the integral of the distribution would be equal to 1. The population rating is calculated by multiplying the integral by ten, as shown in Equation (1-1).

$$r = 10 \cdot \int_0^1 f(x) \partial x \tag{1-1}$$

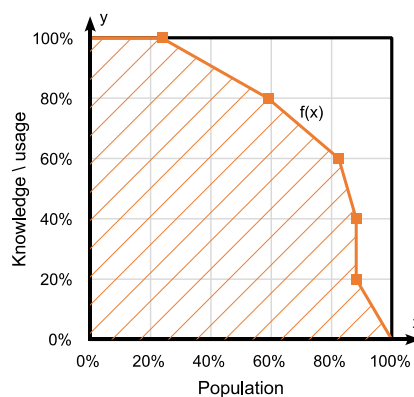


Fig. 1.1: Example of knowledge or usage distribution curves.

1.1.3 Assessment tool development and testing

As the assessment tool, a questionnaire is created and implemented through a Google Form. The structure of the questionnaire can be seen in Fig. 1.2. To comply with GDPR [32] the questionnaire is designed to be completely anonymous: no open-ended questions are provided, and no personal data is collected.

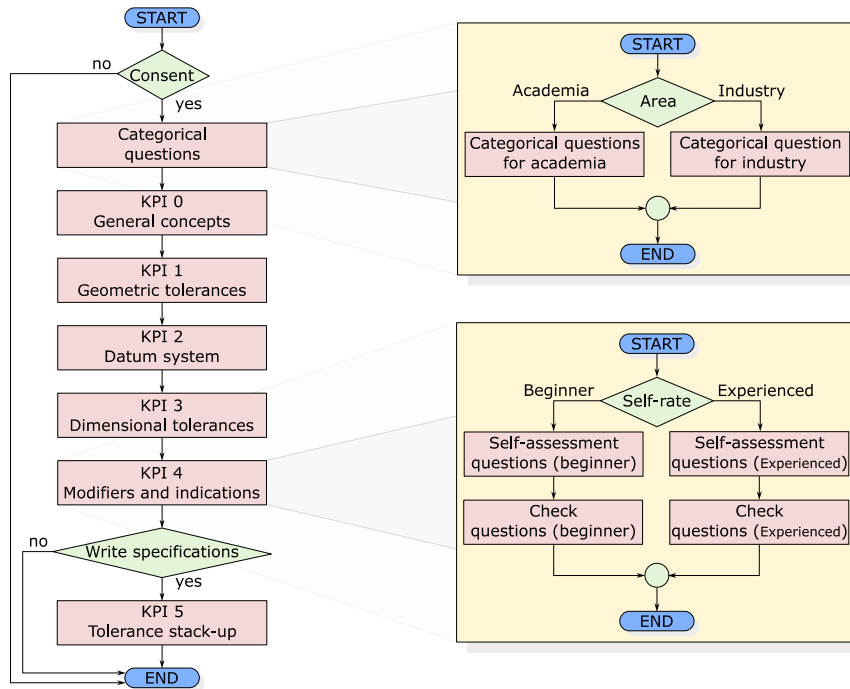


Fig. 1.2: general questionnaire scheme.

The questionnaire is composed of eight sections. In the first section, information about the questionnaire is presented, and consent is requested. The second section contains all the categorical questions necessary for statistical analysis. This section is subdivided into two subsections: one for industry and one for academia.

In the industry subsection, participants are asked to indicate their industrial sector (e.g., automotive, aerospace and defense, etc.), their area of work (design, manufacturing, quality control, and maintenance), and years of experience. The industrial sector list was derived from the Global Industry Classification Standard (GICS®) [33], resulting in a list of fifteen possibilities. In the education subsection, participants are asked to indicate whether they are a student or a teacher/researcher/technician, and their level of education (high school, university). For both subsections, participants are also asked to indicate whether they use geometric specifications (read or create) and whether they have received specific ISO GPS training in the past.

The subsequent section contains questions for each Key Performance Indicator (KPI), with three levels of assessment provided. The first level asks for a self-rating between beginner and experienced. Based on this initial question, participants are divided into two adaptive subsections. The use of adaptive subsections allows for a reduced number of questions while still assessing overall knowledge and usage at an appropriate level of difficulty for the participants. In each of these subsections, a second self-assessment is provided where participants are asked about specific ISO GPS symbology and whether the symbol is “Known but not used/seen in actual specifications,” “Known and used/seen in actual specifications,” or “Not Known.” An example of a self-assessment question for the beginner’s subsection of KPI 1 (Geometric tolerances) can be seen in Fig. 1.3.

Per each symbol select whether you know and use/see the symbol:






Symbol 01:	Symbol 02:	Symbol 03:	Symbol 04:	Symbol 05:
				
	Known but not used/seen in actual specifications	Known and used/seen in actual specifications	Not Known	
Symbol 01	<input type="radio"/>	<input type="radio"/>	<input type="radio"/>	
Symbol 02	<input type="radio"/>	<input type="radio"/>	<input type="radio"/>	
Symbol 03	<input type="radio"/>	<input type="radio"/>	<input type="radio"/>	
Symbol 04	<input type="radio"/>	<input type="radio"/>	<input type="radio"/>	
Symbol 05	<input type="radio"/>	<input type="radio"/>	<input type="radio"/>	

Fig. 1.3: Example of self-assessment questions from the beginner’s subsection of KPI 1 (Geometric tolerances).

Self-rating questions are inherently biased as they rely on self-perception rather than objective knowledge assessment. To address this limitation, an adaptive check layer of unbiased application-based questions is included to validate the self-assessment. These application questions primarily focus on ISO GPS symbology that is not covered in the self-assessment, maximizing variability. The option “I don’t know” is always available to provide a more accurate evaluation, as described in the next paragraph. An example of a check question for the advanced subsection of KPI 2 (Datum System) can be seen in Fig. 1.4.

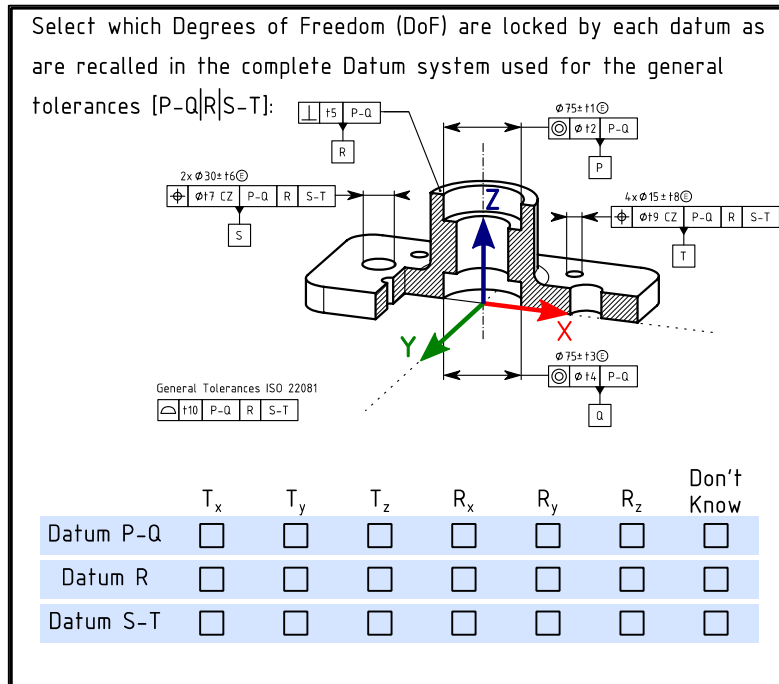


Fig. 1.4: Example of check question from the advanced subsection of KPI 2 (Datum systems) on the right.

Sections related to KPI 0 (General concepts) and KPI 5 (Tolerance stack-up) have slight differences. For KPI 0 (General concepts), there are no distinctions between beginners and advanced levels. The evaluation is based solely on the self-assessment related to the awareness of specific areas of the ISO GPS system. For KPI 5, the self-assessment is based on the utilization of tools to compute tolerance stack-ups.

1.1.4 Evaluation model

The evaluation is conducted using MS Excel. The categorical questions are utilized to group entries together for statistical analysis.

For KPI 0, a rating is assigned based on the proportion of known topics, as indicated in equation (1-2). Additionally, a descriptive analysis of the results is generated.

$$r = 10 \cdot \frac{K}{T} \quad (1-2)$$

Where, r is the rating, K is the number of Known topics, and T is the number of topics that are asked in the section. Therefore, the rating is a value between 0 (minimum) and 10 (maximum).

For KPI 1, 2, 3, and 4 the percentage of “not known”, “Known but not used/seen in actual specifications”, and “Known and used/seen in actual specification” is computed. The knowledge percentage is given by the sum of the last two options; the percentage of usage is considered the last value, see equations (1-3), and (1-4).

$$knowledge_{self-assessment} = \frac{KNU + K\&U}{T} \cdot 100\% \quad (1-3)$$

$$usage_{self-assessment} = \frac{K\&U}{T} \cdot 100\% \quad (1-4)$$

Where, KNU is the number of symbols “Known but not used/seen in actual specifications”, $K\&U$ is the number of symbols “Known and used/seen in actual specification”, and T is the number of symbols asked in the self-assessment question.

The percentages of correct, incorrect, and unanswered check questions are also calculated. For each entry, the knowledge and usage percentages are adjusted based on the incorrect answers to estimate the competence level. Unanswered questions are not taken into account as they indicate an honest acknowledgment of non-knowledge and do not imply an incorrect application of the ISO GPS system.

$$knowledge_{competence} = knowledge_{self-assessment} \cdot \left(1 - \frac{I}{T}\right) \quad (1-5)$$

$$usage_{competence} = usage_{self-assessment} \cdot \left(1 - \frac{I}{T}\right) \quad (1-6)$$

Where, I is the number of incorrect check answers, and T is the total number of check questions.

The evaluation of KPI 5 is based only on a descriptive analysis of the entries.

The aggregate rating for KPI 1, 2, 3, and 4 are found integrating the Knowledge and usage curve as described in section 1.1.2. An overall rating is found by averaging the ratings of these KPIs.

1.2 || Model validation

In this section, an overview of the results obtained during the first testing phase is presented to validate the model. During this phase, twenty entries to the questionnaire were collected.

A descriptive analysis is conducted for each question. One interesting finding is the percentage of people who have received ISO GPS training in the past. A low number of individuals having received such training may indicate a problem in the education and training of professionals.

Fig. 1.5 illustrates the descriptive analysis for the self-assessment of KPI 1 (Geometric tolerances) at the beginner level. Upon initial examination, it is notable that a significant number of participants indicated “not known” for certain symbols. For example, in this example, it is observed that some individuals do not recognize the symbol for location tolerance, yet they are familiar with the symbols for flatness and perpendicularity tolerances. Additionally, the circularity symbol is more widely known than the location symbol. This observation may be attributed to the prevalence of linear positioning schemes over geometric ones, leading to ambiguity [19].

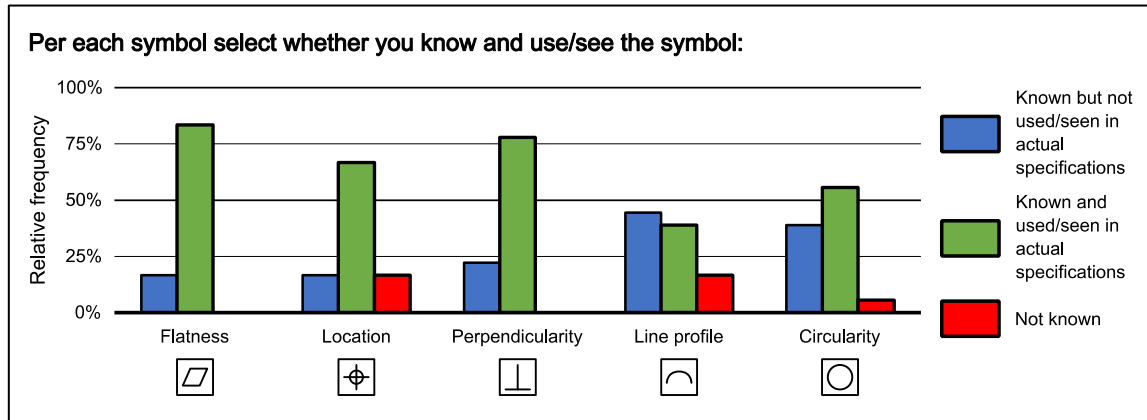


Fig. 1.5: Example of descriptive statistics for a self-assessment question (KPI 1: Geometric tolerances, beginner level).

Fig. 1.6 illustrates the descriptive analysis for the check questions from KPI 2 (Datum systems) at the beginner level, with the correct answers marked with *. The analysis of the “not known” responses and their distribution provides interesting insights. In this case, it is observed that 35% of the interviewees were not familiar with the cylindricity symbol.

Furthermore, the analysis of the distribution of answers compared to the correct one reveals three different patterns. Firstly, in cases where the correct answer is predominant (as seen in symmetry, cylindricity, and perpendicularity), there is a clear understanding among the participants. Secondly, when a specific incorrect answer is predominantly selected (as indicated by no occurrences), it suggests a flaw in education and training where participants are consistently misinformed. Lastly, when there is a balance between the correct and incorrect answers (as seen in surface profile), it indicates a challenge in communication as there are different interpretations, both correct and incorrect.

Identifying these patterns is crucial for understanding the effectiveness of education and training in conveying the intended meanings of ISO GPS symbols.

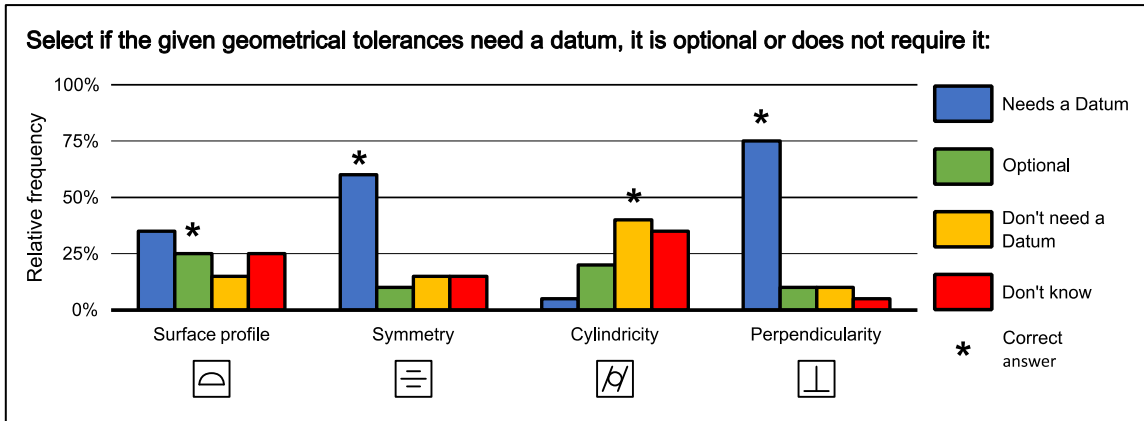


Fig. 1.6: Example of descriptive statistics for check question (KPI 2: Datum systems, beginner level).

Fig. 1.7 illustrates the distribution of knowledge usage across the population for KPI 1 (Geometric tolerances) based on both the self-assessment (a) and the check questions (b). In Fig. 1.7.a), the graph can be interpreted as follows: approximately 80% of the respondents claim to have knowledge of 100% of the ISO GPS system related to the given topic, while 100% of the respondents have a minimum knowledge level of 60%.

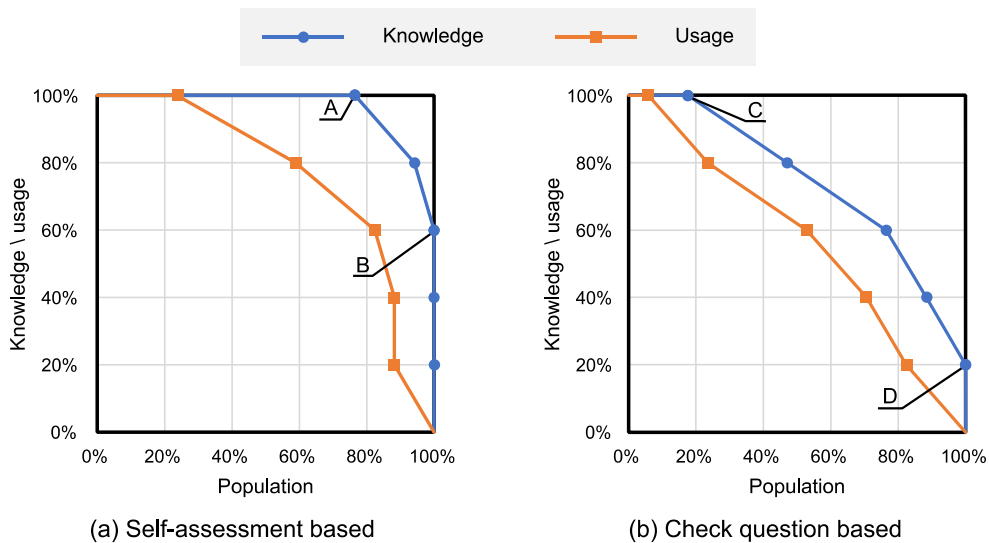


Fig. 1.7: Example of Knowledge and usage distribution across the population.

It is worth noting that the disparity between knowledge and usage becomes more pronounced as knowledge increases. This observation could indicate a constraint within a specific supply chain: even if professionals understand how to use the symbols in the ISO GPS system correctly, they may be unable to use them effectively because downstream stakeholders do not understand them. By comparing the gaps between the two curves (knowledge and usage) across

different industrial sectors, it may be possible to identify sectors that are facing challenges in implementing the system due to supply chain issues.

In Fig. 1.7.b), both curves shift to the left. It is important to highlight that this shift becomes more significant as the self-assessed knowledge increases. This suggests that individuals may have a higher self-perception of their knowledge and usage, but in practice, they struggle with proper application. As a result, the distance between the two curves becomes more uniform.

Based on these graphs, the rating for knowledge is 9.6, and for usage is 7.6. However, when considering the application aspect, the ratings decrease to 7.4 for knowledge and 5.6 for usage.

It is important to keep in mind that these results are based on a small sample size, and therefore cannot provide statistically significant information. Nevertheless, based on this initial insight, it can be concluded that the presented tool is suitable for assessing the current knowledge and usage of the ISO GPS system. Furthermore, it is capable of identifying specific constraints in the system implementation, such as misinterpretation of symbology.

1.3 || Descriptives results on the Italian market

The questionnaire that has been described so far was distributed across the Italian market to gauge the current knowledge and usage of the ISO GPS system. The results should be considered as preliminary, as they are based on data collected up until the beginning of August 2023. However, the data collection is ongoing, and the questionnaire will remain open for an indefinite period of time.

In the following sections, some preliminary results will be presented. First, the participants will be described, and then the actual data will be presented. The subsequent section will also include a comparative analysis.

1.3.1 Participants description

As of August 8th, 2023, a total of 143 responses to the questionnaire were collected in Italy. A possible classification of the participants is presented in Tab. 1.1. In brief, 83 responses were collected from the industry, while 60 were from academia. Less than one-third of the participants had participated in specific ISO GPS training in the past (30.77%), with a higher percentage among the industry respondents (38.55% versus 20.34% in academia). Only 20.28% of the participants indicated that they actually write specifications. Once again, the percentage was slightly higher for the industry compared to academia (26.51% versus 11.86%).

Tab. 1.1: Summary of the participants to the survey.

	Total		Industry		Academia	
Participants:	143		83	58.04%	60	41.96%
With ISO GPS training:	44	30.77%	32	38.55%	12	20.00%
Write geometric specification:	29	20.28%	22	26.51%	7	11.67%
Read geometric specificaiton	114	79.72%	61	73.49%	53	88.33%

The distribution of people who have received specific ISO GPS training is of interest. Only 30.70% of the respondents have participated in such training. Given the intrinsic complexity of the ISO GPS system, this figure might indicate a lack of awareness regarding the importance of receiving proper training to master the topic. It can be observed that this percentage increases in the industry compared to academia. On one hand, this result is positive as it highlights that the industry can, at times, bridge the knowledge gap between itself and academia. On the other hand, this result might be biased due to the nature of the questionnaire and the collaborators and sponsors involved in its distribution. People who have previously received training were more likely to come across the questionnaire, potentially making the actual percentage of those trained even lower. Nevertheless, the doubling of the training percentage in the industry certainly emphasizes that the ISO GPS system is not highly regarded in academia, creating a significant knowledge gap that the industry needs to address whenever possible.

The percentage of individuals actually writing geometric specifications is very low, at 20.28% overall. This means that the responsibility for the content of the specification lies with a few professionals who must take charge of overall geometric specification management, as will be discussed in Chapter 2. Those writing geometric specifications primarily come from the Design/R&D department, while no one from the manufacturing or quality control department is involved in writing geometric specifications. Consequently, whenever specific needs arise from manufacturing or quality control, the request for integrating these needs into the geometric specification is directed to the designer. As a result, each time a modification is requested by the manufacturing or quality control department, it is initiated by someone unfamiliar with writing a geometric specification, potentially leading to misunderstandings.

Looking exclusively at the Industrial sector, the distribution of entries among different industrial sectors is shown in Fig. 1.8. The majority of entries were collected from the automotive sector, totaling 31 entries. The second most represented sector is household consumer durables with 18 entries, followed by Metal and Mining with 13 entries. All other possible industrial sectors have fewer than 10 entries each. Consequently, a comparative analysis among different industrial sectors will not be conducted at this time, as the collected data are not sufficiently distributed to make reliable considerations. This type of analysis will be explored in future research.

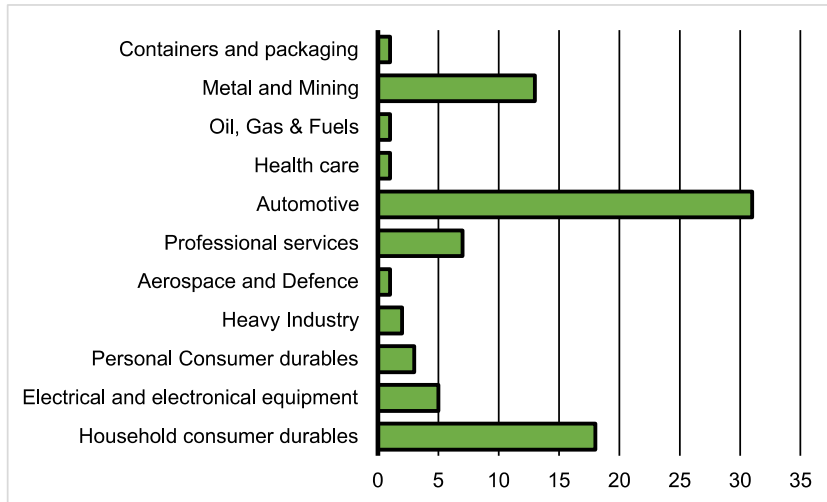


Fig. 1.8: Industrial sectors covered by the survey.

1.3.2 Overall results

In this sub-section, the aggregate results of the descriptive analysis will be presented. Firstly, the self-assessment results between beginners and experienced participants for each KPI will be shown in Fig. 1.9. Secondly, the knowledge and usage curves derived from KPI 1 to 4 are shown in Fig. 1.10. Finally, the differences in knowledge, usage, applied knowledge, and applied usage in percentage are displayed in Fig. 1.11.

Fig. 1.9 displays the self-assessment results between beginners and experienced participants. Among the KPIs, KPI 1 (Geometric Tolerances) has the highest percentage of experienced entries at 31%, followed by KPI 3 (Dimensional Tolerances) with 28% of experienced entries. KPI 4 (Modifiers and Indications) has the fewest experienced entries, with only 13%. KPI 0 (General Concepts) and KPI 2 (Datum Systems) fall in the middle, with 24% and 20% experienced entries, respectively. The results for KPI 5 (Tolerance Stack-ups) are slightly different due to three possibilities (Beginner, Experienced, and Read Only). Looking at absolute values, only 8% of entries classify themselves as experienced. However, when considering relative values, this percentage increases to 24%, aligning with KPI 0 and KPI 2.

Excluding KPI 4, the distribution of beginners and experienced participants is balanced across different KPIs, with an average of experienced entries ranging between 20% and 30%. The lower percentage of experienced entries in KPI 4 was anticipated, as it is a topic that can be mastered primarily through specific training. As previously discussed, the percentage of individuals who have received such training is low. Moreover, the ISO GPS system is renowned for its complex system of modifiers and indications, which may deter users.

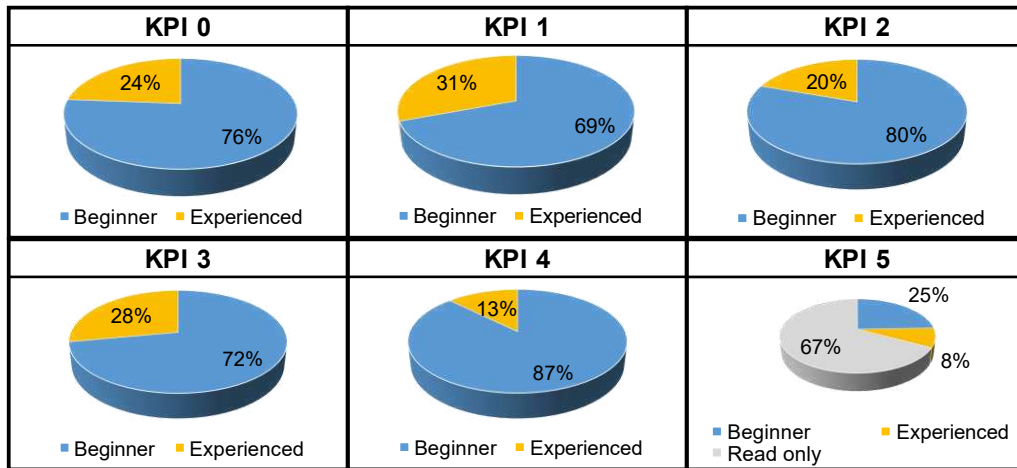


Fig. 1.9: Beginner/Experienced distribution for all KPIs.

In Fig. 1.10 the knowledge and usage curves are presented, considering the responses for KPI 1 to KPI 4 (Geometric Tolerances, Datum Systems, Dimensional Tolerances, and Modifiers and Indications). The overall curves are derived by averaging the curves obtained for each individual KPI.

The knowledge curve is noticeably suboptimal, with an overall knowledge rating of 6.4, while the usage rating remains at 4.7. Comparing the usage curve with the applied knowledge curve, a significant overlap is observed. Specifically, the applied knowledge rating matches the usage rating at 4.7. Interestingly, the applied knowledge, reflecting unbiased knowledge, aligns closely with actual usage: only what is practically used is also genuinely understood. Lastly, the applied usage rating stands at 3.4.

As anticipated, the application-based curve shifts to the left, resulting in lower ratings. This suggests that the ISO GPS system is frequently misapplied by users. A noteworthy observation is that a substantial number of application-based questions received incorrect answers, even when the “don't know” option was available. These incorrect responses indicate instances of misuse or misinterpretation of the system in real-world applications.

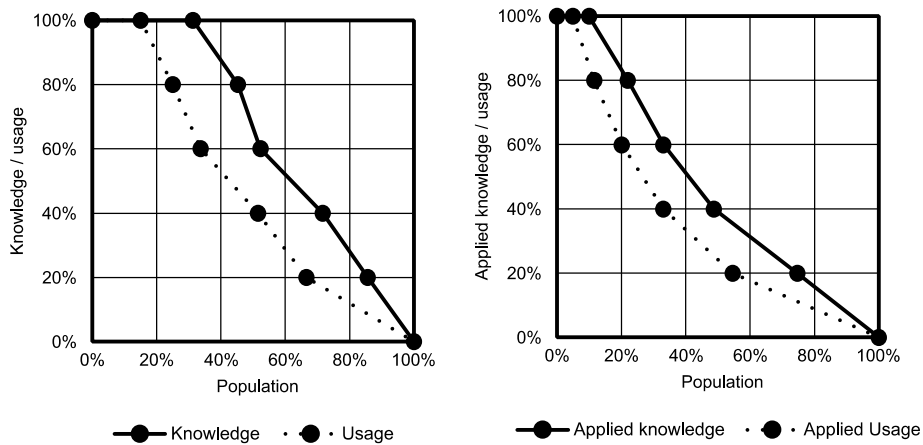


Fig. 1.10: Overall knowledge and usage distribution found averaging KPIs from 1 to 4.

In Fig. 1.11, box plots for knowledge, usage, applied knowledge, and applied usage are displayed. Notably, the knowledge and usage box plots span the entire range of percentages (from 0% to 100%), yet the knowledge distribution skews toward the upper limits (100%) while the usage distribution skews toward the lower limit (0%).

Upon examining the applied knowledge and applied usage distributions, it is apparent that the box plots do not extend to the upper limit, despite the presence of some outliers. In both cases, only one entry achieved a score of 100%. This indicates that among the participants who scored 100% in knowledge and usage, only a single entry answered all application-based questions correctly. This outcome implies that most individuals who attained the maximum self-assessment scores provided incorrect responses to the application-based questions. This finding underscores the bias inherent in the self-assessment and reaffirms that the check question level effectively compensates for this bias.

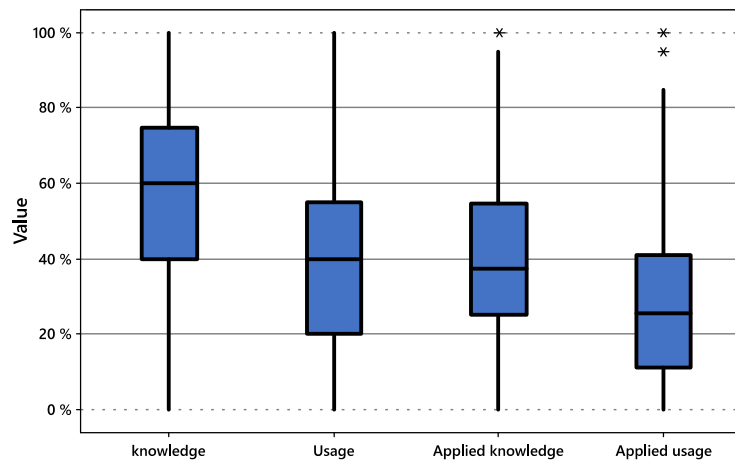


Fig. 1.11: Differences in Knowledge, usage, applied knowledge, and applied usage overall.

Once again, it appears that there are no noticeable differences between usage and applied knowledge.

To investigate potential significant differences among knowledge, usage, applied knowledge, and applied usage, a one-way ANOVA was conducted. The Tukey Method with a 95% confidence level was employed for grouping. The results of this analysis corroborated the observations made from the population curves (Fig. 1.10) and on the boxplots (Fig. 1.11): there were no significant differences between usage and applied knowledge. However, notable differences were observed between knowledge and applied usage, as well as between the usage and applied knowledge clusters.

1.3.3 KPIs results

In this subsection, the descriptive analysis for each KPI will be presented. Fig. 1.12 shows the results for KPI 0 (General concepts). Knowledge and usage curves for KPIs 1 to 4 are displayed in Fig. 1.13 to Fig. 1.16 respectively. Fig. 1.17 and Fig. 1.18 present the results for KPI 5 (Tolerance stack-up). Finally, Fig. 1.19 illustrates the comparison of grades assigned to each entry for each KPI.

The outcomes for KPI 0 (General concepts) are depicted in Fig. 1.12. Notably, the ISO GPS system seems to be more familiar to respondents than the ASME GD&T system. This outcome contrasts with previous surveys conducted in the USA, which is understandable due to the differences in the surveyed populations. A clear result concerns MBD (Model Based Definition), which is generally not well-known among participants. Therefore, it is crucial to invest in raising awareness about MBD and its potential for managing geometric specifications. Other concepts like the Independence principle, Envelope principle, Datum System, and TEDs show balanced results, without evident differences.

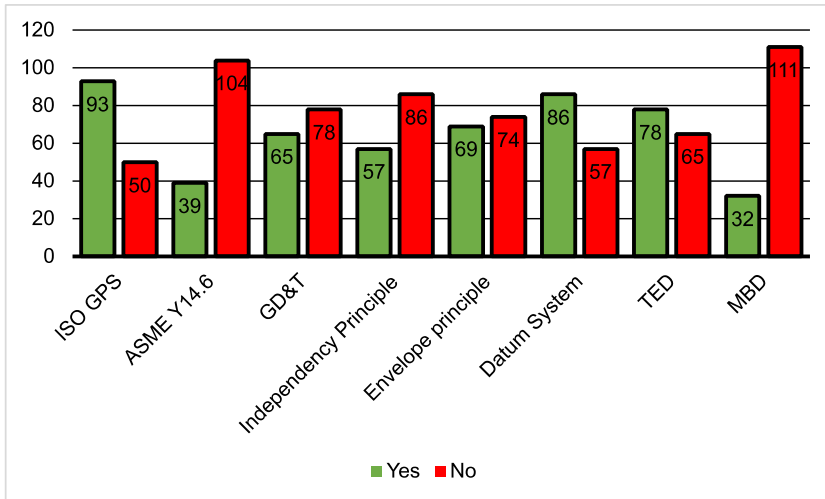


Fig. 1.12: Results for KPI 0.

The knowledge and usage curves for KPI 1 (Geometric tolerances) are depicted in Fig. 1.13. In this instance, the knowledge curve appears favorable, with almost 90% of users familiar with 100% of the system. A comparison between the knowledge and usage curves reveals that the gap between them widens as the levels of knowledge and usage increase. This indicates the presence of a bottleneck that hinders the optimal utilization of the system, particularly concerning geometric tolerances. When comparing the knowledge curve to the applied knowledge curve, it becomes evident that the leftward shift is not uniform but intensifies as the level of knowledge rises. The same trend is observed for usage. This implies that individuals are confident in their understanding of geometric tolerances, but struggle with their practical application. Consequently, many self-proclaimed experts seem to lack proficiency in applying these concepts. The consequence of this shift is that the difference between applied knowledge and applied usage remains relatively constant.

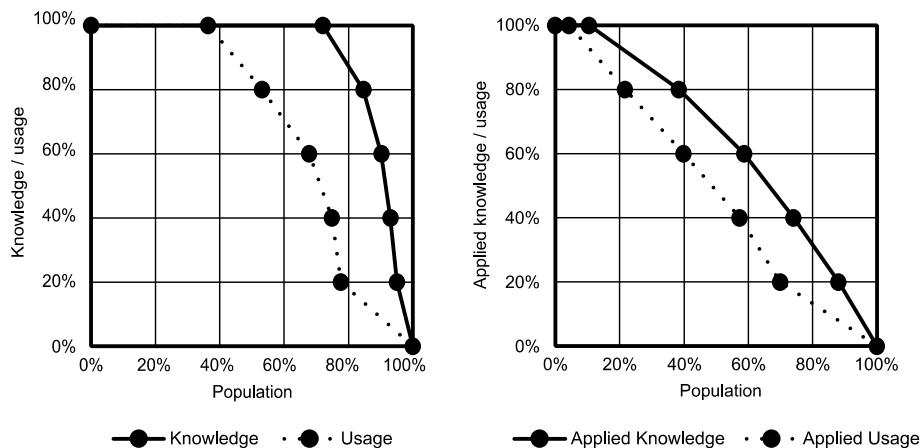


Fig. 1.13: Knowledge and usage distribution for KPI 1.

The curves pertaining to KPI 2 (Datum system) are presented in Fig. 1.14. In this scenario, the knowledge curve is notably lower compared to the previous case. Only 20% of the surveyed population claims to possess a comprehensive understanding of the ISO GPS system with respect to Datum Systems. The discrepancy between knowledge and usage remains relatively constant and minimal in contrast to the previous scenario. This suggests that individuals' perceived knowledge closely aligns with their practical usage. The proximity between the knowledge and usage curves influences the leftward shift of applied knowledge and usage, which, in this instance, is moderate compared to the previous case, even though the applied knowledge curve remains below the usage curve.

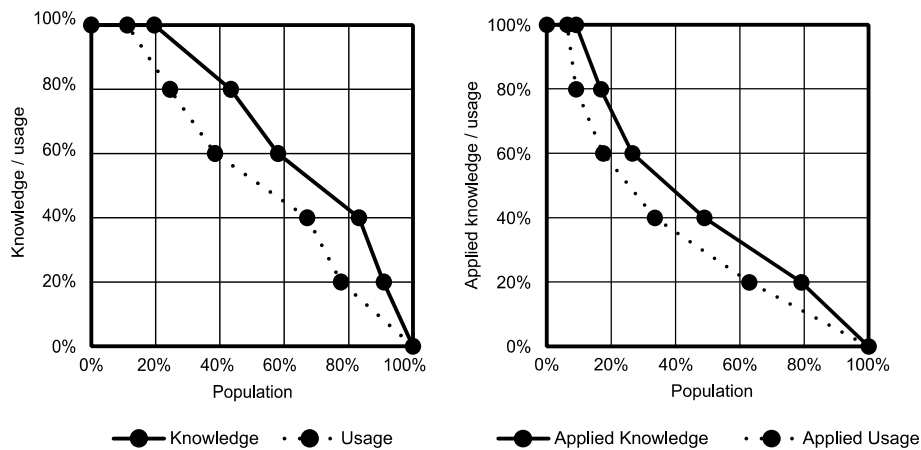


Fig. 1.14: Knowledge and usage distribution for KPI 2.

The curves corresponding to KPI 3 (Dimensional tolerances) are depicted in Fig. 1.15. In this scenario, the knowledge curve is even lower than that of datum systems. Specifically, only slightly over 20% of the participants claim to have familiarity with more than 60% of the system. The gap between the knowledge and usage curve remains constant and moderate. Moreover, the disparity between knowledge and applied knowledge is even smaller compared to the previous case. Consequently, the curves for applied knowledge and applied usage closely resemble those of the previous scenario.

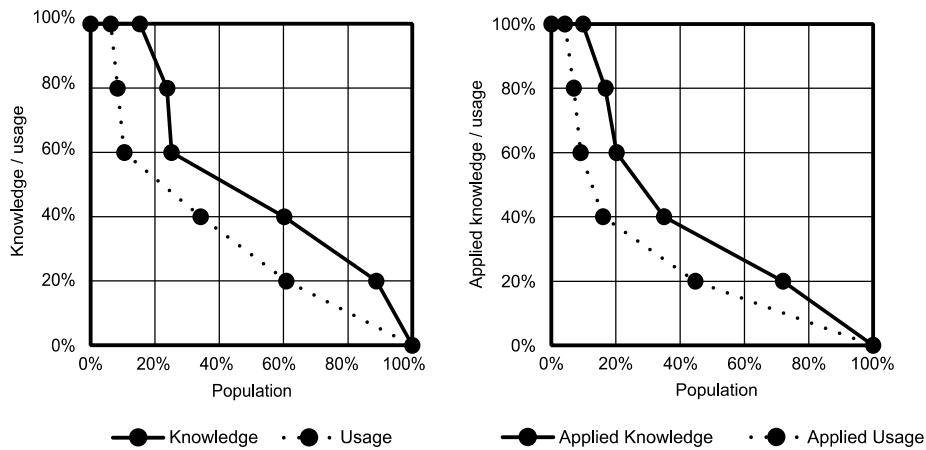


Fig. 1.15: Knowledge and usage distribution for KPI 3.

Finally, the curves pertaining to KPI 4 (Modifiers and indications) are presented in Fig. 1.16. In this instance, the behavior of the curves closely resembles the previous case (KPI 3, dimensional tolerances). The only noticeable distinction is that both the knowledge and usage curves exhibit a smoother transition towards high knowledge/usage values.

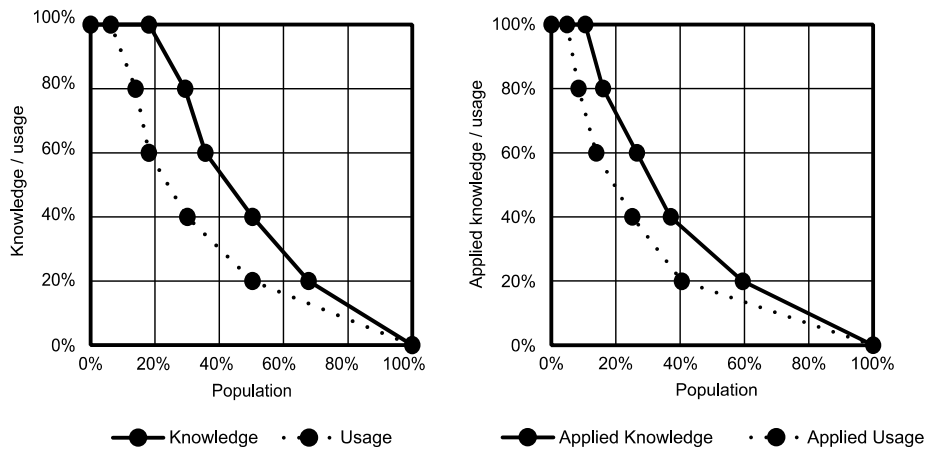


Fig. 1.16: Knowledge and usage distribution for KPI 4.

In Fig. 1.17, an overview of the different tolerance stack-up strategies is presented. It can be observed that the most commonly used approach is the worst-case approach, employed by over 50% of individuals who write geometric specifications. Statistical approaches are used by 21.3% of these individuals. Dedicated software is utilized by only 12.8% of those who write geometric specifications. These results indicate that tolerance stack-up methods are not widely adopted, suggesting ample room for improvement in this area.

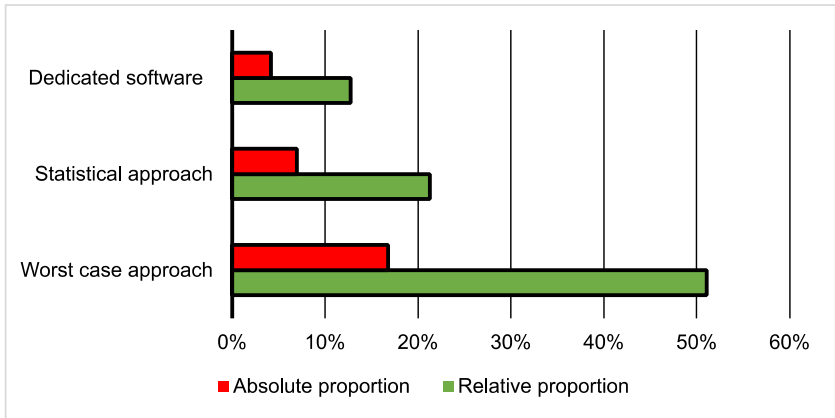


Fig. 1.17: Overview of approaches used for tolerance stack-up.

In Fig. 1.18, an overview of the results for the check questions of KPI 5 is presented. It is evident that a majority of the answers were incorrect, accounting for 36% of the replies. Only 30% of the answers were correct. This reinforces the observation made in the previous figure, indicating that tolerance stack-up methods are not widely utilized and there is substantial room for improvement.

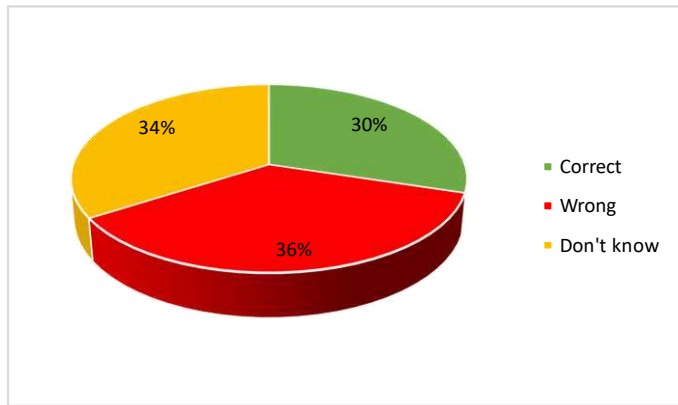


Fig. 1.18: Result for the check question of KPI 5 (Tolerance stack-up).

Finally, in Fig. 1.19, the comparison among the grades given to KPIs from KPI 0 to KPI 4 is shown. The distribution of grades for KPI 0 and KPI 1 appears almost identical. Similar observations can be made for KPI 2 and KPI 3, where a significant number of outliers are noticeable. On the other hand, the distribution of grades for KPI 4 displays a distinct behavior: it is the most skewed and uniformly covers all possible values.

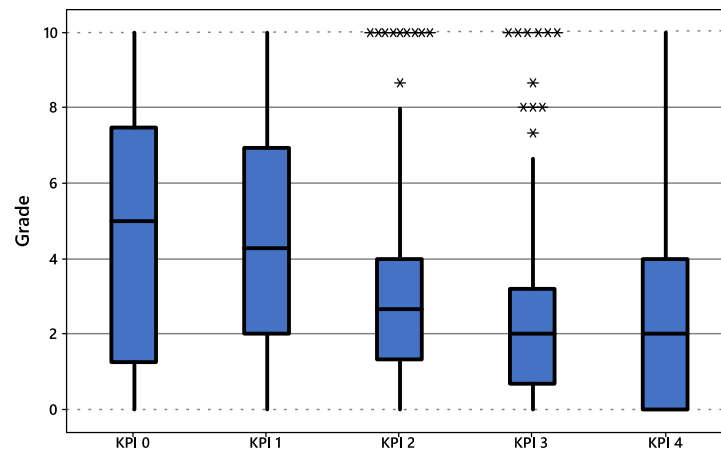


Fig. 1.19: Grade overview per each KPI.

1.4 || Comparative results on the Italian market

In the following section, a comparative analysis of the collected data presented so far will be shown. Three levels of comparison will be conducted. Firstly, differences between categories such as Beginner versus Experienced, Industry versus Academia, with training versus without training, and writing versus reading geometric specifications will be studied. Secondly, differences between Key Performance Indicators (KPIs) will be investigated. Lastly, differences within each category will be presented.

The comparative analysis will be performed using one-way ANOVA, considering the null hypothesis that no differences exist. Differences will be considered significant (and the null hypothesis will be rejected) if the p-value is lower than 0.05.

1.4.1 Differences between categories overall

The first level of comparative analysis involves comparing different categories, including Beginner versus Experienced, Industry versus Academia, with training versus without training, and writing versus reading geometric specifications, considering the overall results.

In Fig. 1.20, a comparison of knowledge and usage curves between beginners (black curves) and experienced (red curves) individuals is shown. It's evident that the two sets of curves do not overlap, indicating significant differences. An interesting observation is that the usage curves for experienced users are very close to the knowledge curves for beginners. This might suggest that experienced users need to adjust their usage to accommodate less experienced professionals.

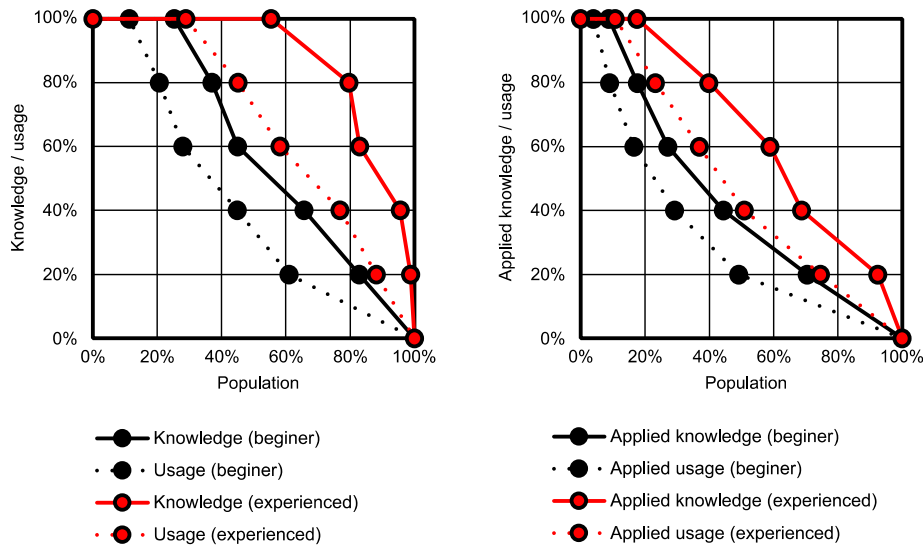


Fig. 1.20: Beginner/Experienced comparison overall.

In Fig. 1.21, a comparison of knowledge and usage curves between Industry (black curves) and academia (red curves) is presented. It's evident that the curves are nearly overlapping, with the industry curves being slightly higher than the academia curves. This suggests that no significant differences exist between these categories. It's important to note that for academia, both students and researchers are considered together; differences between these two sub-categories are not investigated in this analysis.

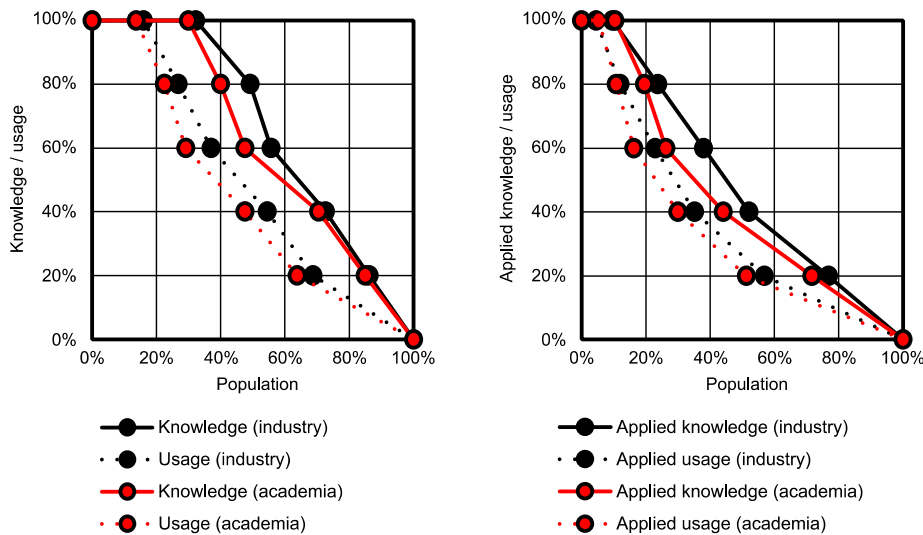


Fig. 1.21: Industry/academia comparison overall.

In Fig. 1.22, a comparison of knowledge and usage curves between people with training (black curves) and people without training (red curves) is presented. Similar to the comparison

between beginners and experienced users, the curves show separation, with the usage curve for trained individuals almost overlapping with the knowledge curve for those without training. Once again, this suggests that individuals with training are confined in their system usage to levels comparable to those without training. This indicates the essential nature of ISO GPS training for comprehensive system application. It can also be assumed that significant differences exist.

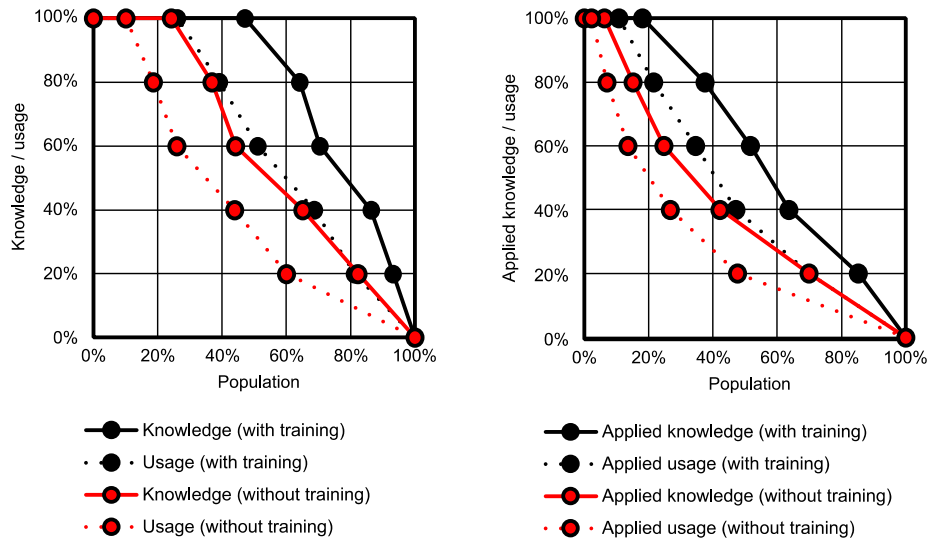


Fig. 1.22: With training/without training comparison overall.

In Fig. 1.23, a comparison of knowledge and usage curves is presented between people who write geometric specifications (black curves) and people who read geometric specifications (red curves). In this case, it can be observed that the usage curves are relatively close to each other, although they do not overlap. If we examine the knowledge curves, the differences between the two categories become more pronounced if compare to usage curves differences, with the knowledge curve for individuals who write geometric specifications being higher than the one for those who read geometric specifications. This suggests that there is likely no significant difference in usage between the two categories, but there are significant differences in knowledge.

The absence of usage differences is to be expected, as readers rely on the content written by the writers. However, the significant difference in favor of people who write geometric specifications in terms of knowledge indicates that not all available knowledge can be fully utilized by the writers. This has two implications. First, it has already been demonstrated that application-based knowledge is more closely aligned with actual usage (as shown in sub-section 1.3.2 on page 17), meaning that not fully utilizing parts of the system hinders a comprehensive understanding. Second, training efforts should be focused more on people who read geometric specifications. As indicated in the participant description, individuals from manufacturing and quality control departments mainly fall into the category of reading geometric specifications in the survey. Therefore, these categories should be targeted for specific training to bridge the knowledge gap.

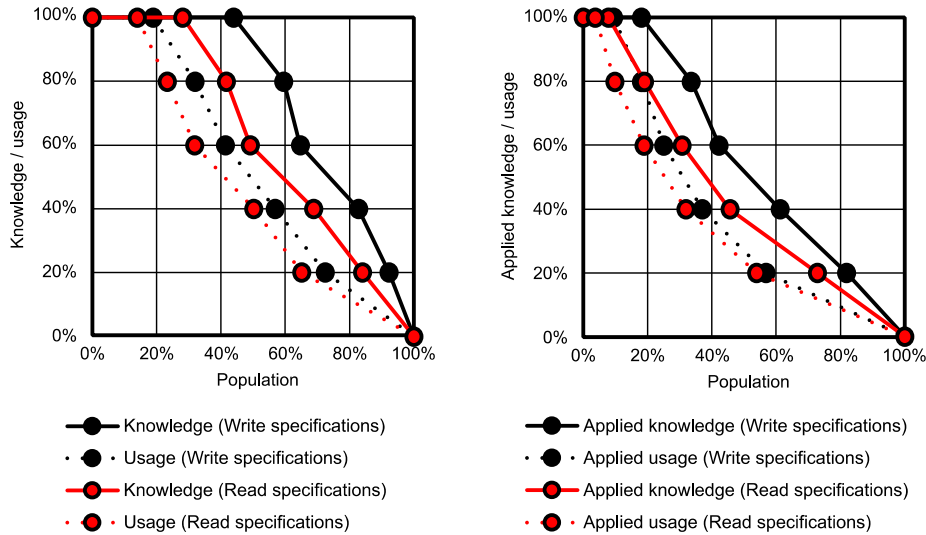


Fig. 1.23: Write/read geometric specification comparison overall.

In Fig. 1.24, a comparison of the overall grades received by different categories is presented. It's apparent that there are no significant differences between the industry and academia, as previously shown in Fig. 1.21, which confirms the initial assumption. Additionally, the dispersion of grades for academia is lower than that for industry, with just one outlier near grade 10. This might suggest that the distinction between students and researchers could be less pronounced than anticipated. Further analysis of the dataset is needed to explore this aspect more thoroughly.

Regarding the grades for individuals with training versus those without training, differences are evident. The distribution of grades for those with training appears to be almost symmetrical, whereas the distribution for those without training is skewed, with a higher concentration of grades towards lower values. As for the distribution of grades for people who write and read geometric specifications, it's noticeable that the grades distribution for those who write geometric specifications is slightly higher. However, determining the significance of these differences solely by examining the boxplots is not straightforward. Further statistical analysis is necessary to make conclusive assessments.

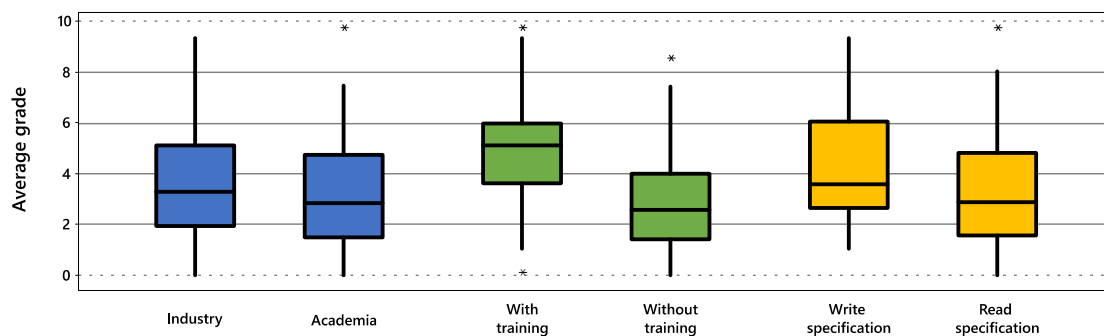


Fig. 1.24: Overall grades comparison between categories.

So far, assumptions of significant differences were based on graphical evidence from curve distributions or box plots. One-way ANOVA was also employed to confirm these assumptions.

Tab. 1.2 presents the results for the one-way ANOVA considering the average knowledge and usage. As anticipated, the differences in both knowledge and usage between the Industry and academia are not significant, with p-values of 0.287 and 0.235 respectively. On the other hand, the differences in both knowledge and usage are significant for people with training versus those without training (p-value < 0.001). With training, both average knowledge and usage increase by about 20%.

Furthermore, when comparing individuals who write geometric specifications to those who read them, the differences in knowledge are confirmed to be significant (p-value 0.006), while the differences in usage are not significant (p-value 0.172).

Tab. 1.2: Quantitative differences in overall Knowledge and usage between categories.

		Average Knowledge			Average usage		
		μ	σ	p-value	μ	σ	p-value
Industry	83	59.16%	25.49%	0.287	40.60%	25.15%	0.235
Academia	60	54.58%	24.96%		35.33%	27.26%	
With training	44	72.27%	21.82%	0.000	53.30%	25.88%	0.000
Without training	99	50.56%	23.89%		31.77%	23.42%	
Write specification	29	68.62%	20.39%	0.006	44.31%	26.62%	0.172
Read specification	114	54.34%	25.66%		36.89%	25.86%	

In Tab. 1.3, the results for the one-way ANOVA considering the average grade, applied knowledge, and applied usage are presented. Concerning the comparison between industry and academia, all differences are confirmed to be not significant (p-values > 0.05). The impact of training is also confirmed to be significant (p-values < 0.001).

The differences in grades between individuals who write and those who read geometric specifications are significant (p-value 0.010). Regarding applied knowledge and usage, the evaluations already made for knowledge and usage (Tab. 1.2) are confirmed: the difference in knowledge is significant (p-value 0.015), while the difference in usage is not significant (p-value 0.187).

Tab. 1.3: Quantitative differences in overall applied Knowledge and usage and overall grade between categories.

		Average grade			Average applied Knowledge			Average applied usage		
		μ	σ	p-value	μ	σ	p-value	μ	σ	p-value
Industry	83	3.632	2.143	0.251	42.70%	22.50%	0.164	29.19%	21.22%	0.286
Academia	60	3.215	2.119		37.49%	21.24%		25.29%	21.80%	
With training	44	4.906	2.105	0.000	53.65%	23.35%	0.000	39.39%	23.34%	0.000
Without training	99	2.813	1.818		34.68%	18.81%		22.29%	18.39%	
Write specification	29	4.365	2.288	0.010	49.37%	24.48%	0.015	32.26%	25.08%	0.187
Read specification	114	3.226	2.042		38.26%	20.92%		26.35%	20.41%	

1.4.2 Differences between KPIs

The second level of analysis aims to determine whether differences exist between different KPIs. Graphical evidence is presented in Fig. 1.25 for KPIs from KPI 1 to KPI 4, including knowledge and usage curves, as well as grades boxplots. Fig. 1.26 focuses on KPIs from KPI 0 to KPI 4, comparing grade 95% confidence intervals.

In Fig. 1.25, a comparison between KPIs from KPI 1 to KPI 4 is presented. Results from KPI 1 are displayed in blue, KPI 2 in green, KPI 3 in yellow, and KPI 4 in red. This matrix enables pairwise comparisons. It's evident that the curves from KPI 1 (geometric tolerances) are visibly higher than the curves from the other three analyzed KPIs (datum systems, dimensional tolerances, and modifiers and indications). Differences in the boxplots can also be observed, suggesting significant differences between KPI 1 and the others. Only the pair of KPI 1 and KPI 2 partially overlap.

The curves for KPI 2 (Datum Systems) are slightly above the curves for KPI 3 and KPI 4. While it might appear that significant differences exist upon first glance, the difference in grades is less evident when examining the boxplots. Consequently, it's challenging to determine whether significant differences exist among these three KPIs.

Lastly, when comparing KPI 3 (dimensional tolerances) and KPI 4 (modifiers and indications), the knowledge and usage curves are completely overlapped. The boxplots are also aligned, suggesting that no significant differences exist between these two KPIs.

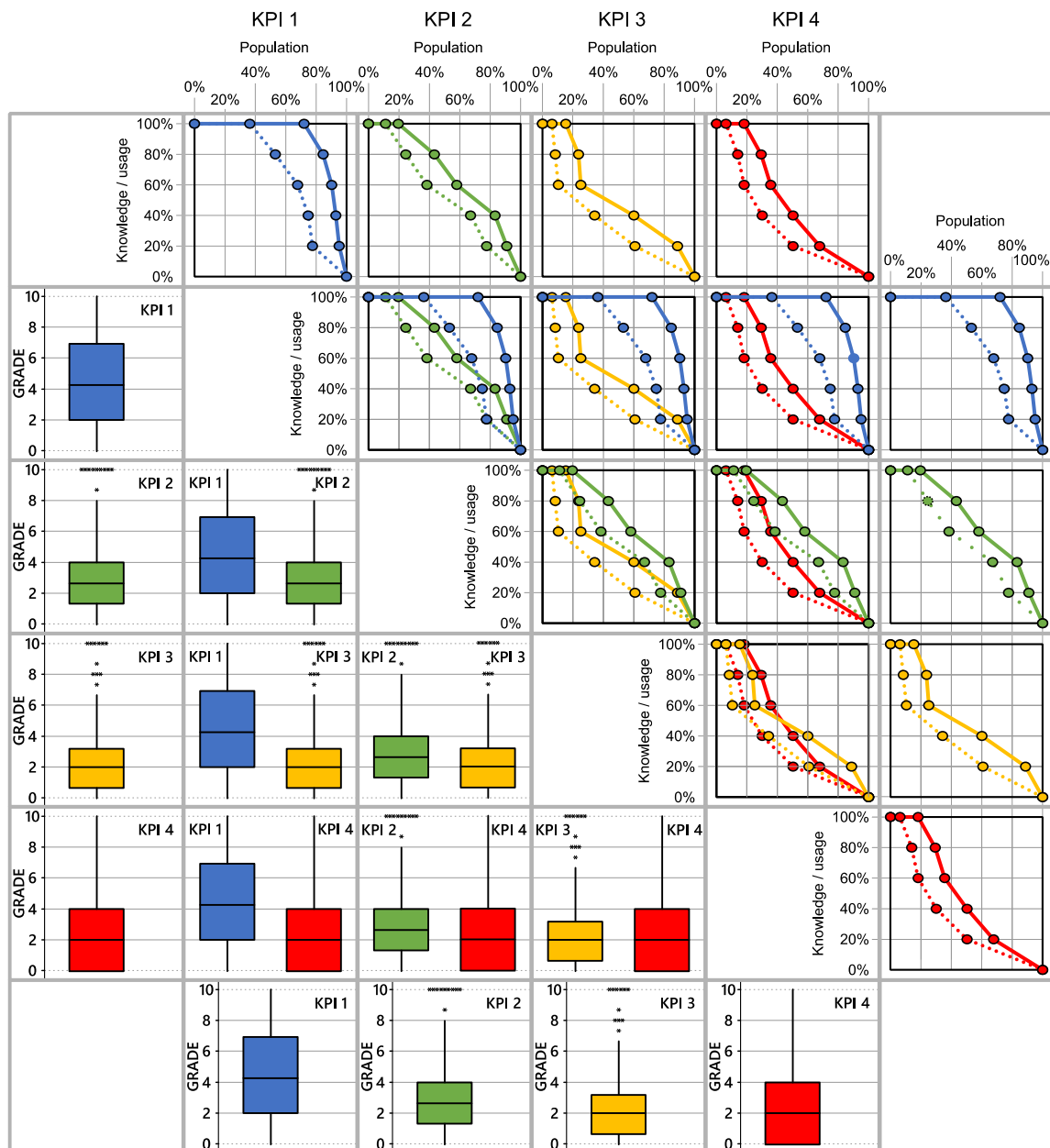


Fig. 1.25: Knowledge and usage distribution comparison among KPIs.

In Fig. 1.26, the confidence intervals for the grades from KPIs 0 to KPI 4 are presented. Again, a notable observation is that the confidence intervals for KPI 3 and KPI 4 are nearly perfectly aligned. Similarly, the confidence intervals for KPI 0 and KPI 1 are also closely aligned. Since knowledge and usage curves were not defined for KPI 0 (general concepts), no prior evidence is available for these.

However, the confidence interval for KPI 2 is distinctly different from those for KPIs 0 and 1, and it is quite close to the intervals for KPIs 3 and 4. Similar to the previous analysis, it remains uncertain whether the grade for KPI 2 is significantly different from those for KPIs 3 and 4.

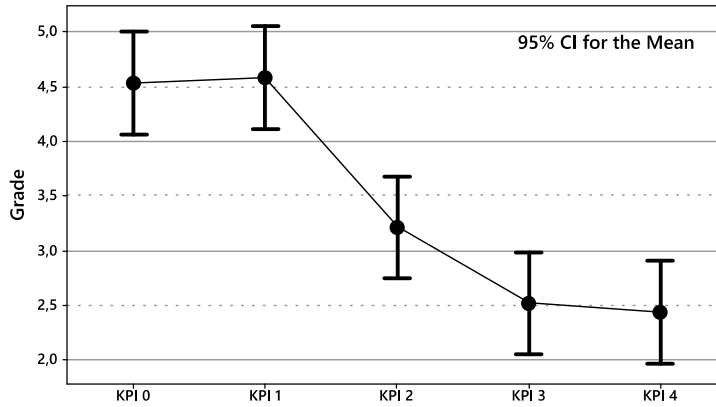


Fig. 1.26: Grade comparison among KPIs.

One-way ANOVA was employed to confirm the differences between KPIs, and the results are presented in Tab. 1.4. It is evident that significant differences exist (p -value < 0.001). In order to determine whether specific KPIs lack significant differences, a grouping analysis was conducted using the Tukey Method with a 95% Confidence level. This analysis revealed the formation of two groups: the first group consists of KPI 0 and KPI 1, while the second group encompasses KPIs 2, 3, and 4. Within these two groups, no significant differences are observed. Hence, the grades for KPIs 0 and KPI 1 are significantly higher than those for the other KPIs.

Tab. 1.4: Quantitative differences in grade between categories.

	μ	σ	p-value	Grouping*
KPI 0	4.537	3.269		A
KPI 1	4.584	2.913		A
KPI 2	3.214	2.734	0.000	B
KPI 3	2.517	2.456		B
KPI 4	2.435	2.844		B

* Using the Tukey Method and 95% Confidence

1.4.3 Differences between categories per each KPI

The third and final level of analysis examines the differences between categories for each KPI. Figures from Fig. 1.27 to Fig. 1.30 provide comparisons of knowledge and usage curves, and Tab. 1.4 presents the results from the one-way ANOVA.

Across all the figures, there seems to be no significant difference between industry and academia, reaffirming the previous overall comparison results (sub-section 1.4.1).

Fig. 1.27 displays the knowledge and usage curves for KPI 1. Although there aren't significant differences among categories, knowledge and usage generally appear to be high. However, observing the applied knowledge and usage curves reveals a notable leftward shift for higher levels of knowledge and usage. This shift leads to a distinction between application-based curves for those with training versus those without training.

In Fig. 1.28, the knowledge and usage curves for KPI 2 are depicted. Here, a clear distinction between the knowledge and usage curves is visible for beginners versus experienced users. This distinction becomes less prominent for the application-based curves, especially at lower levels of knowledge/usage. A similar pattern is seen in the training versus no training comparison. There is a slight separation for the write versus read categories, but it's not substantial enough to suggest a significant difference.

Fig. 1.29 displays the knowledge and usage curves for KPI 3. In this case, a noticeable separation is seen for both beginners versus experienced users and for training versus no training. While the curves for writing versus reading geometric specifications are not entirely overlapped, a distinct separation is not apparent.

Lastly, Fig. 1.30 presents the knowledge and usage curves for KPI 4. Similar to the previous case, a distinction is observable for both beginners versus experienced users and for training versus no training. This distinction is particularly pronounced here. Regarding writing versus reading geometric specifications, no clear separation is evident.

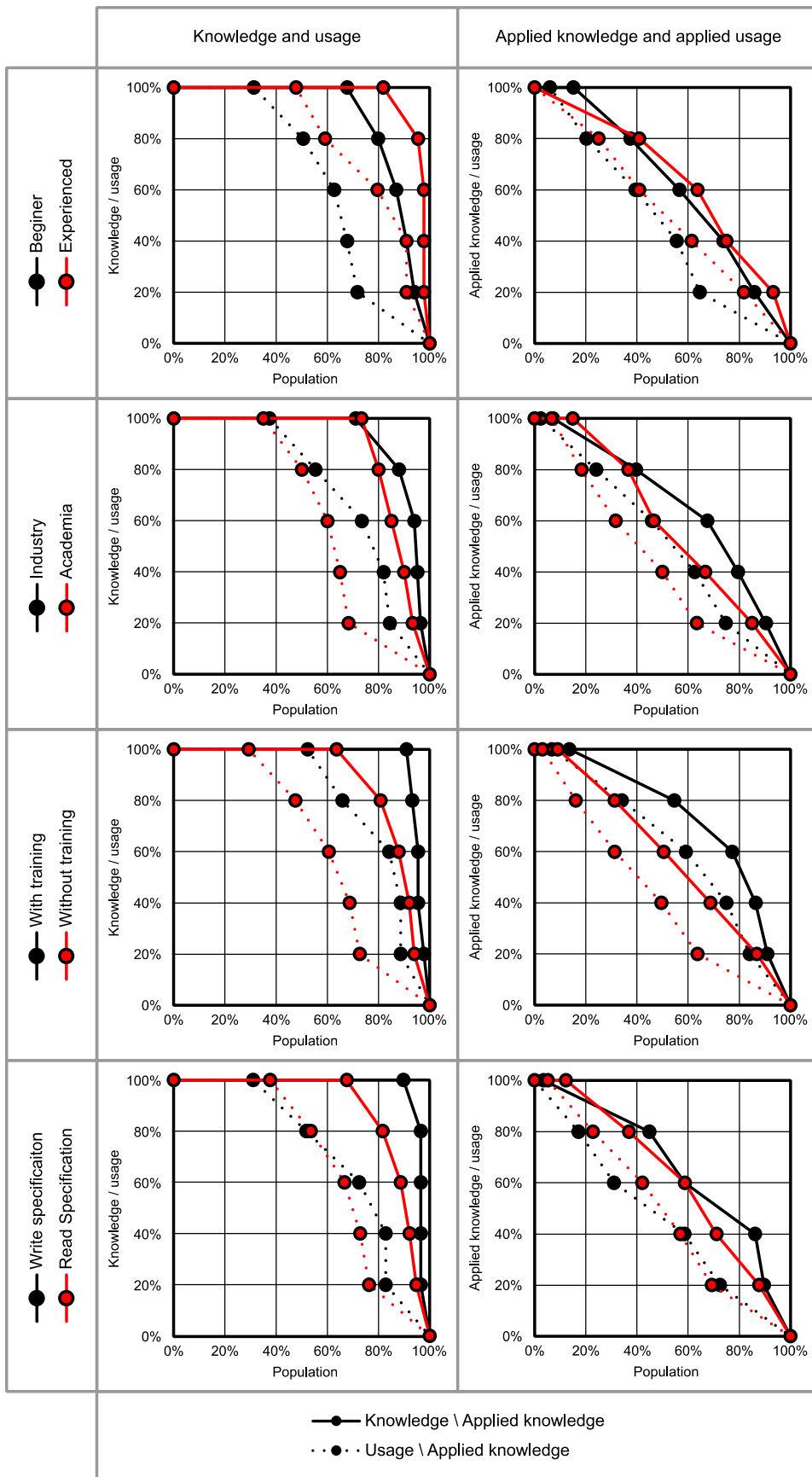


Fig. 1.27: Knowledge and usage distribution comparison between categories for KPI 1.

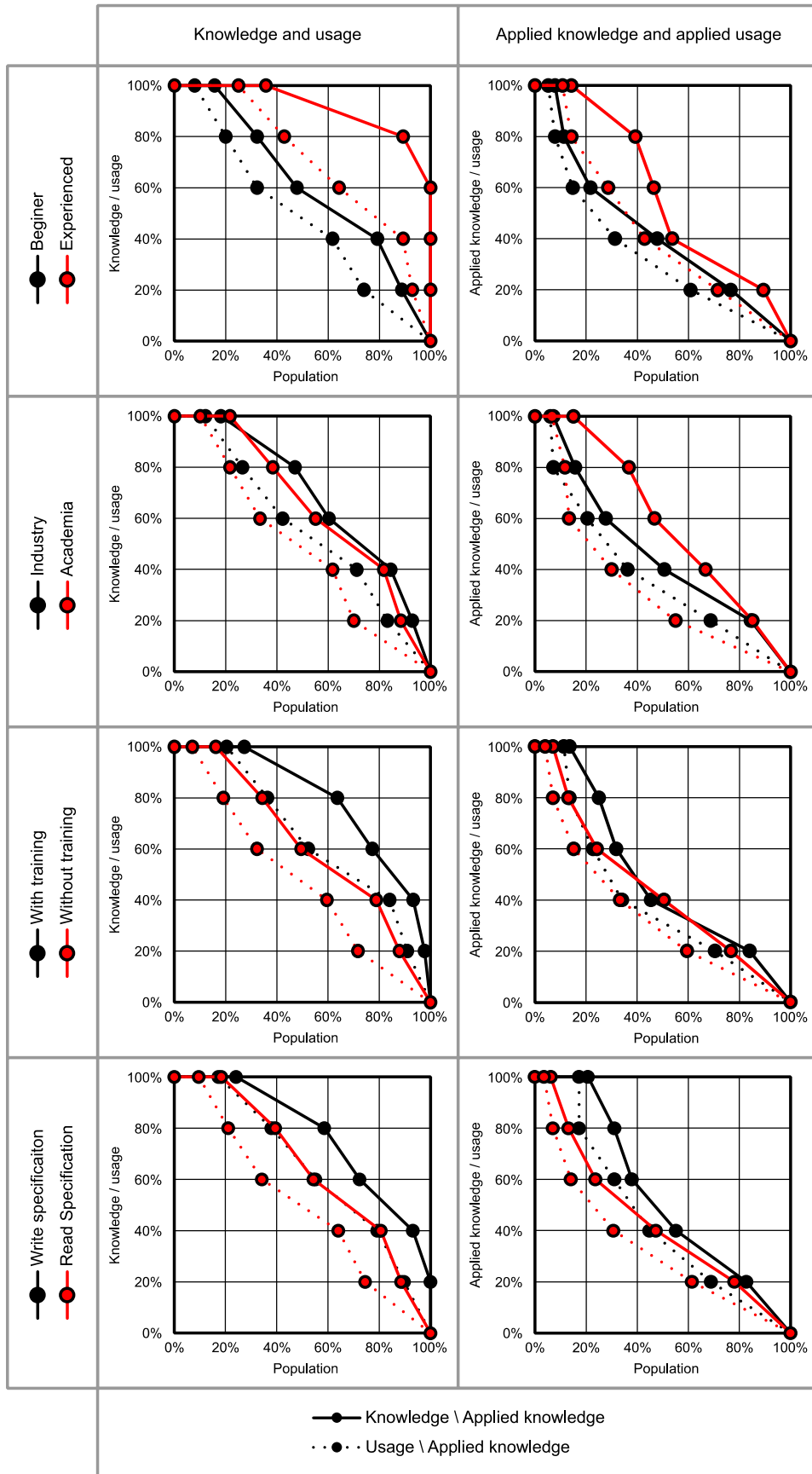


Fig. 1.28: Knowledge and usage distribution comparison between categories for KPI 2.

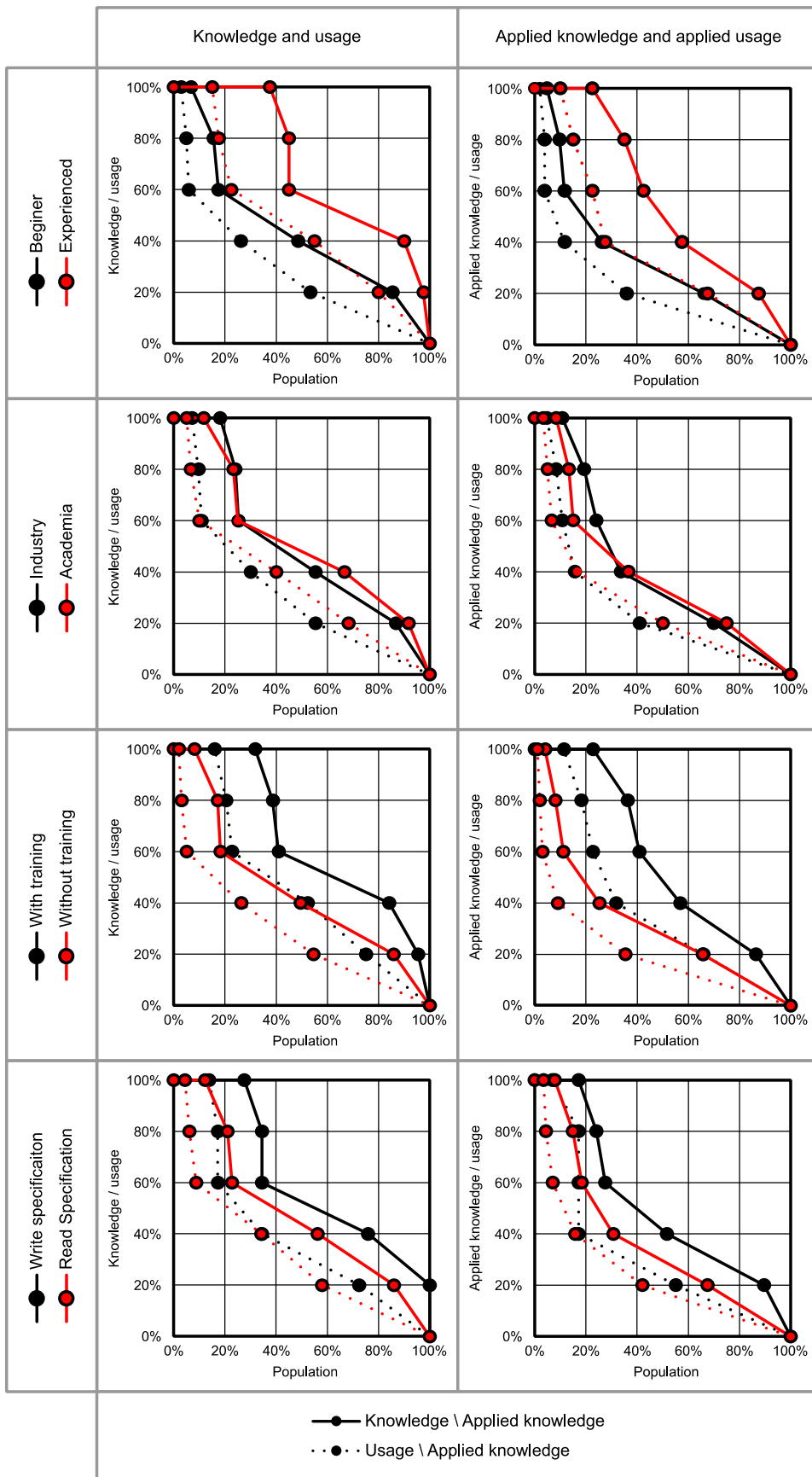


Fig. 1.29: Knowledge and usage distribution comparison between categories for KPI 3.

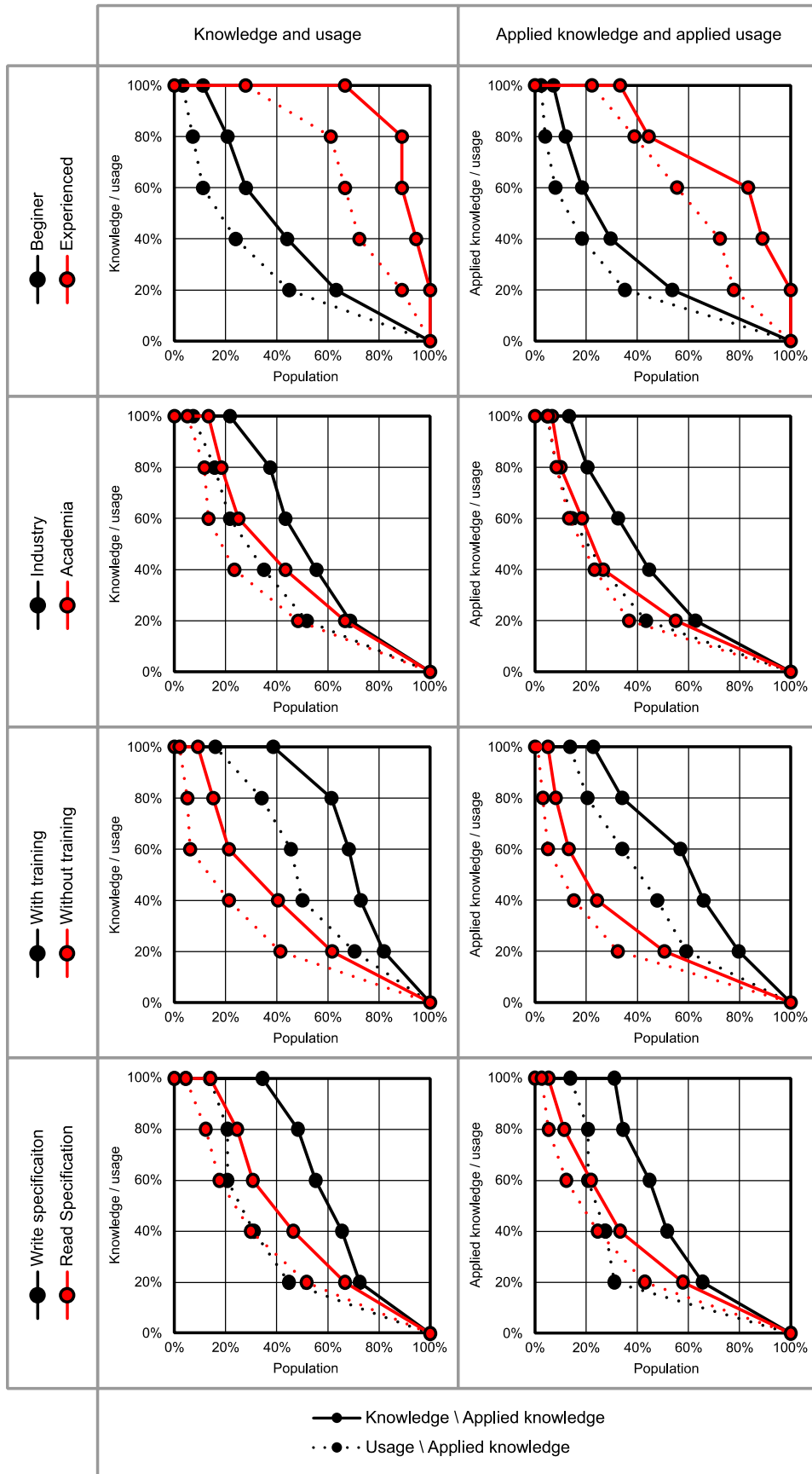


Fig. 1.30: Knowledge and usage distribution comparison between categories for KPI 4.

To confirm or disprove the significance of the separation that is evident in the curves' comparison, one-way ANOVA was conducted. The results are shown in Tab. 1.5. As established in the previous sub-section, no significant differences were detected between the industry and academia. The analysis conducted for each KPI separately reaffirmed that these two categories exhibit no statistical differences. The previous analysis also established the presence of significant differences between individuals with training and those without training. This finding is partly confirmed: significant differences are discerned for KPI 0, 1, 3, and 4, thereby indicating no significant differences for KPI 2 (Datum system). This outcome is unexpected and could potentially be attributed to the lack of proper training in understanding Datum Systems. Observing the curves in Fig. 1.28, it is apparent that the knowledge and usage curves are quite divergent, while the applied knowledge and applied usage curves display more overlap. This suggests that among individuals with training, a higher percentage of incorrect responses were recorded. This phenomenon could signify that participants with training may have initially assessed themselves as experts but subsequently encountered difficulty in responding accurately to advanced questions. Alternatively, individuals without training might have chosen the "don't know" option, therefore selecting less incorrect answers. This subject is indeed intricate, and reaching a consensus is challenging even within ISO/TC 213. This committee is currently working on amending ISO 5459:2011, the standard addressing datum systems, due to its perceived shortcomings. However, the process is progressing gradually due to the complexities involved. At the time of writing, ISO/TC 213, WG 2 (Datums and datum systems) is focused on amending the existing standard to address certain critical aspects before embarking on the task of creating a new edition.

The overall grade difference between those who write and those who read geometric specifications was determined to be significant (Tab. 1.3). Analyzing each KPI individually revealed that significant differences were confined to KPI 0 and KPI 2, while no significant differences were recorded for the other KPIs.

By scrutinizing each KPI separately, it becomes possible to examine the differences between beginner and experienced users. Conducting this analysis overall was not feasible, as each respondent to the questionnaire could independently choose between beginner and experienced status for each KPI. It is noticeable that significant differences are present for all KPIs except KPI 1 (p-value 0.402).

Tab. 1.5: Ratings comparison among different categories and KPIs.

	N	KPI 0			KPI 1			KPI 2			KPI 3			KPI 4		
		μ	σ	p-value	μ	σ	p-value	μ	σ	p-value	μ	σ	p-value	μ	σ	p-value
Beginner		3.54	2.97	0.000	4.45	3.04	0.402	2.97	2.63	0.030	2.00	2.05	0.000	1.89	2.39	0.000
Experienced		7.72	1.86		4.89	2.60		4.21	2.98		3.86	2.90		6.23	2.89	
Industry	83	4.68	3.38	0.529	4.94	2.74	0.089	3.39	2.65	0.361	2.48	2.60	0.829	2.67	2.85	0.249
Academia	60	4.33	3.13		4.10	3.10		2.97	2.86		2.57	2.27		2.11	2.83	
With training	44	6.88	2.62	0.000	5.76	2.78	0.001	3.71	2.97	0.146	3.90	3.10	0.000	4.29	3.35	0.000
Without training	99	3.50	2.99		4.06	2.83		2.99	2.61		1.90	1.82		1.61	2.14	
Write specification	29	6.64	3.14	0.000	4.55	2.60	0.948	4.17	3.29	0.034	3.26	2.85	0.070	3.21	3.63	0.102
Read specification	114	4.00	3.09		4.59	3.00		2.97	2.53		2.33	2.32		2.24	2.59	

1.5 || Conclusions

This first chapter introduced a tool designed to assess the knowledge and usage of the ISO GPS language in both industry and academia. The same tool was utilized in the Italian market to gather data regarding ISO GPS implementation within Italy.

The questionnaire was developed, tested, and proven to be a user-friendly and straightforward tool for evaluating the current dissemination and understanding of the ISO GPS language. Its brevity, requiring only 10 to 15 minutes for completion, makes it suitable for a variety of scenarios, including training, consulting, and invitation-based dissemination.

Indeed, these were the methods employed to gather entries for the Italian market. The Design Tools and Methods in Industrial Engineering Laboratory at the University of Padova distributed the questionnaire during training and consulting sessions. Additionally, the initiative was promoted by various partners, including ADM - Associazione Nazionale Disegno e Metodi dell'Ingegneria Industriale, INRiM - Istituto Nazionale di Ricerca Metrologica, Enginsoft SpA, CMM Club Italia, and DeltaMu, through invitation-based dissemination. The analysis presented in this chapter involved 143 participants, but the questionnaire remains open and continues to accept new responses.

The survey is already available for international use, and its European release is anticipated in the near future (as elaborated in 13 "Future research agenda").

Findings from the Italian survey revealed that the overall implementation of the system is far from optimal and requires further investment. Surprisingly, the differences between industry and academia were not statistically significant. This outcome is attributed to the limited number of individuals who have received specific ISO GPS training in the industrial sector. Moreover, it is evident that the subject is not adequately covered at the academic level, resulting in a shift of ISO GPS education from academia to industry.

The study also unveiled that the responsibility for drafting geometric specifications primarily lies with the R&D/Design department, sidelining manufacturing and quality control. Simultaneously, the utilization of the system may be hindered by the limited knowledge of the readers. Therefore, investments in dedicated ISO GPS training for manufacturing and quality control personnel are necessary to streamline the overall management of geometric specifications.

Overall, the results are insufficient, given that the knowledge rating stood at 6.4/10 and the usage rating at 4.7/10. These figures are even lower when considering application-based results: the applied knowledge rating is 4.7/10, and the applied usage rating is 3.4/10.

The subsequent chapter will introduce and discuss a novel model for geometric specification management that aims to overcome the limitations of the current approach, wherein only designers are responsible for drafting geometric specifications. This work will further delve into methodologies and tools to facilitate the practical implementation of this geometric specification management model.

2 || A model for tolerance specification management²

"Lots of folks confuse bad management with destiny"

Kin Hubbard

As presented in the introduction to this manuscript, the information incorporated in the geometrical specification is shared between the departments involved in product development. This is independent of the medium used by a specific company/department. The traditional way is the use of 2D drawings. Alternatively, the Model-Based Definition (MBD) is a tool that allows the representation of technical product documentation contents, including the geometrical specification, directly in the 3D annotated CAD model [34,35]. Both are possible forms for Technical Product Documentations (TPDs) [36].

Within the ISO system on Geometrical Product Specifications (ISO GPS, managed by ISO/TC 213), an interesting yet not widely considered document is the ISO/TS 21619:2018, which lists the basic types of documents relating to geometrical product specifications: functional specification, manufacturing specification, and verification specification [37]. This document, a technical specification, inherits an ambiguous use for "specification" already existing in ISO publications. It is defined both as a "document stating requirement" [37], using the definition from ISO 9000:2015 [4], and as "expressing the field of permissible deviation of a characteristic of a workpiece as permissible limits" in ISO 17450-1:2011 [38]. Within ISO TPD (Technical Product Documentation, as managed by ISO/TC10), different types of specifications (e.g., general specification, performance specification, process specification, requirement specification, etc.) are considered as documents [36]. In the following, an analysis of the literature regarding the different types of specifications is presented. The final aim is to generate a management model for the coexistence of different types of specifications along the product life cycle.

² The context of this chapter is mainly derived from a pre-print already published by the author [164].

2.1 || State of the art

Dating back to Stanley Parker, the awareness of different needs from different departments is clear. Designers, manufacturers, and inspectors have different needs but need to communicate with each other to avoid misinterpretations [18]. Therefore, the separation between functionality, manufacturability, and inspection requirements is not a new concept in the field. However, the widespread use of integrated CAD tools has flattened the richness of detail that could have been captured by a multitude of different drawings that were necessary when the design and drawing phase was done only by hand.

In the following, an overview of the academic literature on the concepts of functional tolerancing, manufacturing tolerancing, and verification tolerancing is presented.

2.1.1 Functional tolerancing

The functional tolerancing activity is performed in the design phase and focuses on the product's functional needs: the result is the functional specification where the functional requirements are stated [37]. Many authors agree that interactions among parts and assemblability are important in functional tolerancing [39–42]. However, a clear and explicit definition for functional tolerancing was not found in the literature.

Nevertheless, many methodologies aiming to create a functional specification are described.

Mejbri et al. [39] proposed a recursive method to create a functional specification for complex mechanisms. For each geometrical functional requirement, a functional sub-assembly is defined and studied separately. The concept of blocks to indicate sub-assemblies needed for manufacturing and integration is presented. A further development [42] brought an approach for the identification and specification of key parts based on the study of both the parts' geometry and the interfaces between them. The methodology consists of a top-down decomposition of a geometric functional requirement for the whole mechanism into sub-assemblies and parts.

Ballu et al. [43] proposed a new design approach called GASAP (Geometric As Soon As Possible) that suggests starting with the CAD modeling of the product as soon as possible in the design phase to identify functional features and design parameters. It guarantees the link between the CAD model and the functional analysis.

Anselmetti [44] developed a semi-automatic system (CLIC, "Cotation en Localisation Avec Influence des Contacts") that creates a functional specification based on the interface between components. It automatically creates the datum reference frame on parts and provides specifications on contacting features. The designer still needs to express the other functional requirements. A clear distinction between the generation of the specification scheme and the tolerance synthesis is stated.

Hu J. and Peng Y. [45] developed a Computer-Aided Tolerancing (CAT) system to create a functional specification based on axiomatic design [46]. Two main phases are identified: the creation of the specification scheme based on rules and the allocation of values to every tolerance. In the second phase, manufacturing and cost-related influences are also considered.

Cao Y. et al. [47] defined a method to create a functional specification that starts by analyzing the assembly to identify the key part and key features. Then, an iterative procedure to create the specification on single parts is proposed.

Göhler et al. [48] proposed a methodological framework to decompose the functional requirement into sources of variation that will become the design parameters. This framework focuses on geometry plus other different parameters, e.g., materials, external factors, etc. The result is a clear link between the stated tolerance and the functional requirement.

2.1.2 Manufacturing tolerancing

The manufacturing tolerancing activity deals with the definition of the manufacturing process, containing all the relevant requirements [37]. If the actual manufacturing process involves multiple phases, each step needs its dedicated manufacturing specification.

Two original approaches in the manufacturing tolerancing field were proposed: one focused on a virtual “non-ideal surface model” [38] describing the part as built, and the other aims to determine the contribution of manufacturing deviations, step after step, in a bottom-up approach to define specifications for each manufacturing process step.

Bourdet et al. [49] proposed the Small Displacement Torsor (SDT), which can be used to describe the geometric deviations due to manufacturing processes.

Vignat and Villeneuve [50] proposed a simulation process that aims to create a representation of the manufactured part using the SDT concept, which allows describing the workpiece and tool relative position and the machining capabilities. The result describes a population of produced parts that can be compared to the functional specification. To perform this simulation, it is necessary to estimate both the parameters for positioning (fixturing) and the machining issues. A generic solution for the positioning (fixturing) problem was also given [51]. However, the determination of the SDT value for a given machining operation still needs to be assessed by experimental data.

Different methodologies that use the SDT to evaluate the machining process with respect to the functional specification using inequalities were also developed [52,53].

Anselmetti and Louati [54] proposed an iterative method that allows generating manufacturing specifications for every tooling step according to the ISO GPS language. The procedure is based on tolerance transfer that uses tolerance zones' vectorial description. Further development of this methodology led to a formal computing solution [55].

Ayadi et al. [56] developed a methodology to generate manufacturing specifications using the SDT concept and, at the same time, adopting the datum system definition given by ISO GPS standards.

Anselmetti [57] proposed the “analysis line method” to identify the relations between manufacturing steps to generate a tolerance stack-up analysis. This analysis leads to tolerance synthesis, which is a consequence of the specification generation described in [54].

Royer and Anselmetti [58] provided a methodology that allows both analysis and synthesis for the manufacturing specification using the ISO GPS language. The SDT is used to describe the deviations for the tolerance analysis. It was also proven that this methodology can be used even considering complex joining operations [59].

An integration between the tolerance transfer concept and a Computer-Aided Tolerancing (CAT) software, ANATOLE 3D, to automate the specification synthesis was also proposed [60].

2.1.3 Verification tolerancing

The verification tolerancing activity translates into metrological requirements/procedures, the functional/manufacturing specifications [37].

About “verification tolerancing” and/or “verification specification,” only a few contributions can be found in the literature, mainly focused on software testing. No dedicated contribution was found regarding geometric verification and inspection.

Woo [61] states that the verification specification can prevent the verification activity from diverging from the intended procedure and aim over time when carefully created. Then, if the requirement isn't met, it can be assessed whether the inspection wasn't appropriate or if the functional or manufacturing requirement needs to be updated.

In the aerospace sector, NASA defined a list of 18 items to be included in the verification procedure. It also listed 11 fields to be included in the verification report. Among others, information such as measuring equipment, calibration intervals, single operations sequence, data recording procedures, etc., can be found [62].

Morse [63] introduced the idea of “Design for Metrology” as a possible new concept that could be further divided into “Design for metrology,” “Design using metrology,” and “Metrology for manufacturing.” The possibility to share responsibility among different departments is also postulated.

It is evident that the field of verification tolerancing is the least explored among the three in the literature.

2.1.4 Relations in tolerancing

The functional, manufacturing, and verification tolerancing/specification were mainly considered separately in the literature. Only a few works show a clear link between functional and manufacturing specifications: Anselmetti and Louati [54] and Anselmetti [57] clearly state that the manufacturing process must be chosen by the manufacturing engineers to comply with the functional specification defined by the designer. In this framework, the manufacturing specification is used to describe the intermediate state between subsequent manufacturing phases.

Based on these findings, there is a lack of description of the relations among the different tolerancing activities/specifications. Therefore, this chapter aims to highlight the relations that occur among the different specification types and the relevant tolerancing activities. Moreover, it will analyze where and when such activities take place during the product design cycle, assigning the relevant responsibilities to the proper actors.

It is noteworthy to mention that, in the following, the analysis is focused on mechanical assemblies of industrial products for which interchangeable parts are required. The concept of interchangeable parts can be considered as the starting point for the development of the tolerancing field at the turn of the 19th century. During that period, especially in the military sector, the industry emphasized the need for more precise components that could be assembled interchangeably [64–67].

The assembly and parts geometries are described in the TPD, considered as the medium [36] (2D drawings or MBD). The term “specification” (or specification scheme) will refer to either a single or the whole information regarding the allowable deviations, specified according to the GPS language [38], and tolerancing will refer to the activity that generates a specification.

2.2 || Responsibilities in tolerancing management

In the current product design cycle, three different key actors can be identified: design, manufacturing and quality control departments.

2.2.1 Design department

In the context of this work, the design department (Fig. 2.1) has the responsibility to develop a geometric model for parts and assemblies that fulfills the functional requirements stated in the Product Requirements Document (PRD) [68].

However, the product geometry description is not limited to the nominal shape and architecture. In the design department, the functional tolerancing activity studies the assembly

relationships among the parts and therefore defines the allowable deviations from nominal geometry while still assuring the desired functionality. If needed, experimental tests or simulations may also be performed to assess the allowable deviations (i.e., dimensional and geometric tolerances).

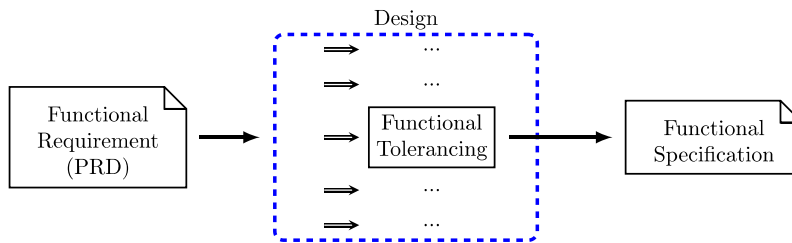


Fig. 2.1: Input/Output diagram that describes the functional tolerancing activity that takes place inside the design department. Other tasks performed by the design department are omitted.

2.2.2 Manufacturing department

The manufacturing department (Fig. 2.2) is responsible for producing parts and assemblies as defined in the TPD.

The input for this activity is the functional specification. The goal is to design and implement a manufacturing process capable of producing parts in conformity with the functional specifications.

Therefore, two sequential phases are needed: engineering and production.

The engineering phase aims to design and optimize the process. All the TPDs created in this phase convey manufacturing specifications that are based on the specific process characteristics and requirements. Usually, the manufacturing specification describes fixturing and/or tooling setup depending on the process planning. For example, in a particular manufacturing step, a Datum System change may be required because the functional datum features have not been produced yet, and the process considers different manufacturing datum features, as discussed in ISO/TS 8062-2:2013 [69].

The production phase deals with the actual fabrication of parts/assemblies according to the manufacturing specification, with the input being the manufacturing specification.

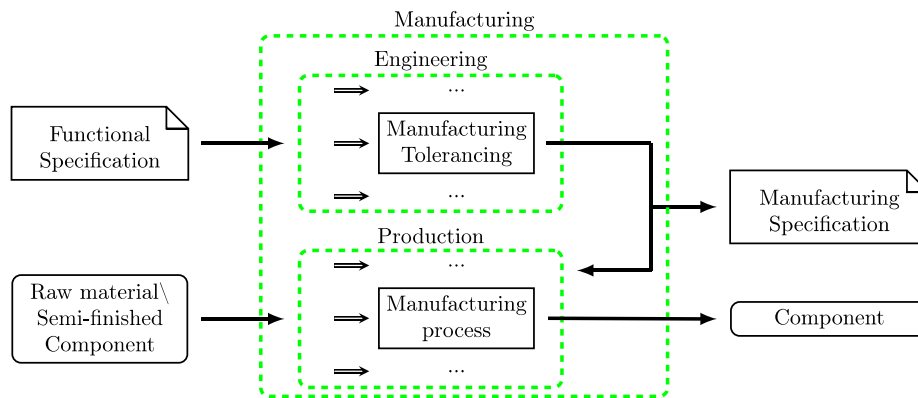


Fig. 2.2: Input/Output diagram that describes the manufacturing tolerancing activity taking place inside the manufacturing department. Other tasks performed by the manufacturing department are omitted.

2.2.3 The quality control department

The quality control department (Fig. 2.3) is primarily responsible for the acceptance or rejection of production batches and may also support the manufacturing department in statistical process control.

The inputs for this department are the produced parts and the functional and/or manufacturing specifications. The goal is to define and perform a metrological inspection procedure to assess conformance.

Two phases can be identified: inspection planning and the actual inspection.

Geometrical inspection can serve various purposes such as manufacturing process tuning, product certification or first batch approval, production process control, etc. These different aims may have varying time and cost requirements, and the number of items to be inspected can also vary greatly, ranging from a few tens to thousands per day. Moreover, the type of information (i.e., quantity) to be assessed can be different. Therefore, it is the responsibility of the quality control department to determine the appropriate measurement method and its implementation. A verification specification, which is represented within a TPD, may be generated if functional/manufacturing specifications need to be integrated to guide the verification procedure, reducing verification uncertainty and/or achieving agreement on measuring uncertainty statements.

Once the verification specification is defined, any qualified operator can perform the inspection by strictly following the specification itself, ensuring the estimated (budgeted) measurement uncertainty.

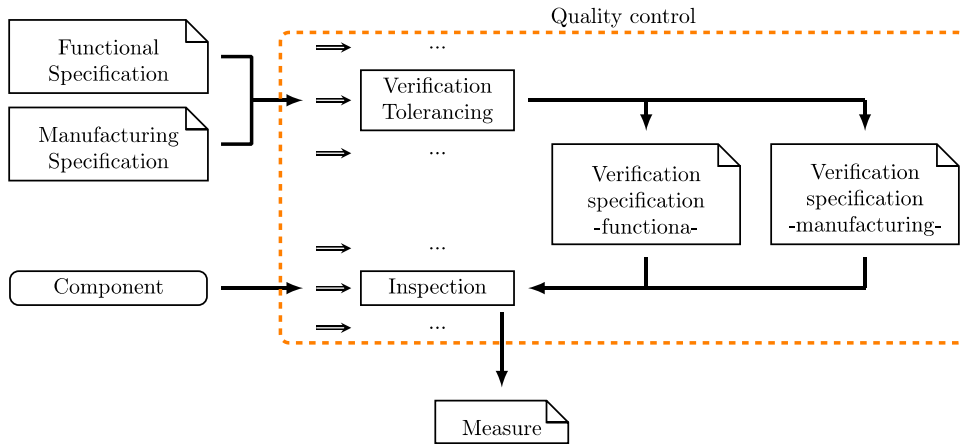


Fig. 2.3: Input/Output diagram that describes the verification tolerancing activity taking place inside the quality control department. Other tasks performed by the quality control department are omitted.

2.3 || Hierarchy in tolerancing

ISO/TS 21619 describes the types of documents/information and explicitly outlines the hierarchical relationships among the different specifications, as well as the activities described above. This approach has been further developed in Fig. 2.4.

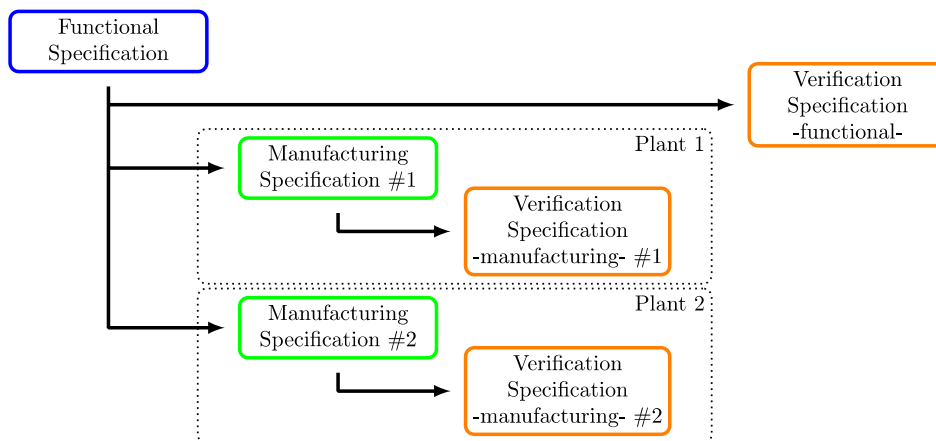


Fig. 2.4: Hierarchical relations (as described by the ISO/TS 21619) among different specifications: Functional, Manufacturing and Verification, inspired by [37].

To integrate this hierarchical structure with the previously described assignment of responsibilities, the relationships among the tolerancing activities of the three departments are highlighted (Fig. 2.5).

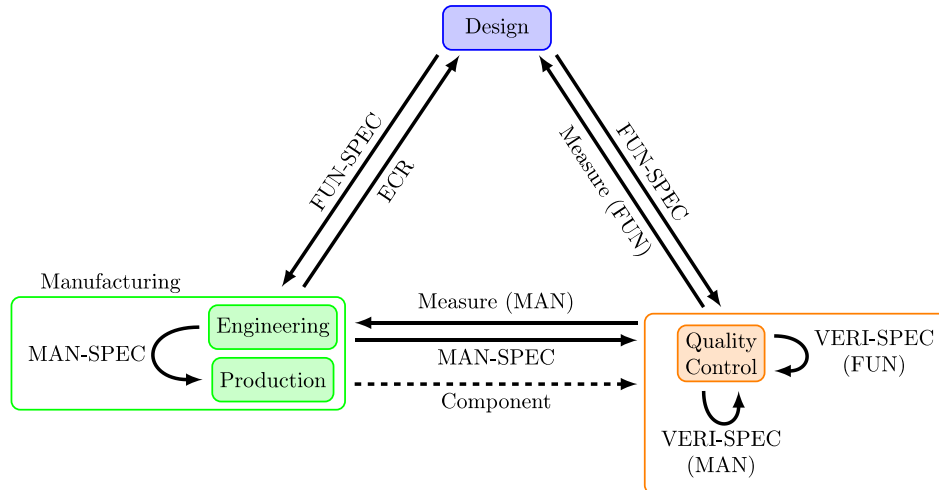


Fig. 2.5: The scheme represents the relations among the different departments involved in product development for what concern the tolerancing activities. Each department block is the zoom out from the diagrams represented in Fig. 2.1, Fig. 2.2 and Fig. 2.3, the solid arrows represent an information flow, while the dashed arrow the transfer of a physical entity. FUN-SPEC stands for Functional Specification, MAN-SPEC stands for Manufacturing Specification, VERI-SPEC stands for Verification Specification and ECR stands for Engineering Change Request.

The design department sends the functional specification to both the manufacturing and quality control departments. The quality control department provides measurement reports as feedback to the design department, allowing them to validate design assumptions and assess overall design quality.

The manufacturing department supplies components along with the manufacturing specification to the quality control department, which provides measurement feedback to fine-tune the manufacturing process. If tuning is not feasible, either a Manufacturing Change or an Engineering Change Request (ECR [70]) may be initiated. An ECR can be motivated by the quality control assessment.

The quality control department receives the functional specification from the design department and obtains the manufacturing specification and produced parts from the manufacturing department. Both specifications require a detailed verification specification, whether implicit or explicit, outlining the metrological checks. The verification specification derived from the functional specification is particularly important when the same inspection needs to be performed in different plants or in a customer-supplier relationship.

The relationships between the tolerancing activities (functional, manufacturing, and verification) are depicted in Fig. 2.5 when fully implemented. However, throughout the product development cycle, these activities undergo fine-tuning through iterative loops, which may involve a trial-and-error approach.

2.3.1 The supply chain

When considering the supply chain, the previously described framework introduces additional levels of complexity. Therefore, a more structured scheme is necessary to describe it (Fig. 2.6).

Fig. 2.6 illustrates the relationships between the different tolerancing activities across the supply chain, depicting the sub-departments involved in product development and the flow of relevant information.

The scheme in Fig. 2.6 expands upon the one-layer framework described in Fig. 2.5 to provide a company-wide view of the interrelated tolerancing activities.

Different layers can be identified, representing varying degrees of product decomposition from top to bottom. Each layer encompasses the design, manufacturing, and quality control functions as previously described. These layers represent different business units within the company (internal supply chain) or different companies (external supply chain).

The relationships analyzed in the one-layer framework (Fig. 2.5) exist within each layer in Fig. 2.6, but the relationships between layers must also be considered.

The uppermost layer represents the product level, considering the product in its “working” configuration. The product is then subdivided into different functional systems in the second level. Each system is further subdivided into subsystems in the third level, and the bottom level represents the processing of individual components.

The information flow among the levels is bi-directional. The functional specification from the upper level is handed over to the lower level, where the functional geometrical requirements are detailed into lower-level functional requirements. Consequently, the functional specification at any level must comply with the “parent” specification at the upper level to ensure consistency among all the specifications. At the end of the manufacturing process, the artifacts are transferred to the upper level for integration/assembly. Measurement reports assessed at any level can potentially be transferred to the upper level to implement quality traceability of the production batch.

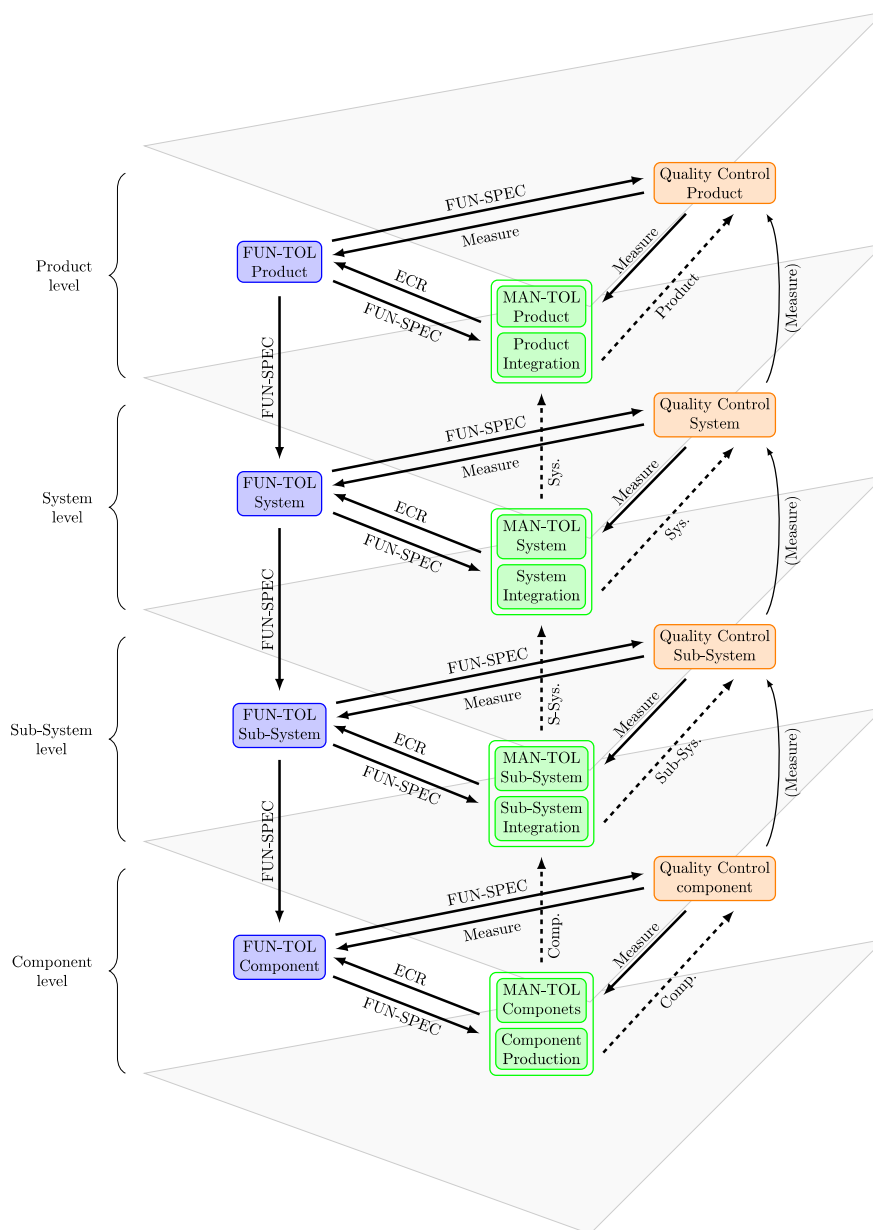


Fig. 2.6: The scheme represents the relations among different departments and different business units (or different companies) along the supply chain that are involved in the product development for what concern the tolerancing activities, each horizontal layer follows the scheme represented in Fig. 2.5.

2.4 || Consequences of the new model

According to the experience of different members of the Design Tools and Methods in Industrial Engineering Laboratory, many issues related to tolerancing activities can be attributed to

suboptimal allocation of tasks. The proposed scheme illustrates how the different tolerancing activities should be interconnected, providing each actor involved in the design cycle with the opportunity to apply their expertise and assume the corresponding responsibilities within the overall tolerancing process.

By considering the cause-effect relationship between specifications and assigning specific roles to each actor, improved management of the Technical Product Documentation (TPD) can be achieved. Any modifications made at any stage should be effectively and promptly communicated, ensuring that everyone is informed about relevant decisions made downstream in the development process. If the system at any point fails to meet the intended functionality, a direct link can be established from the functional requirements to their verification, through the manufacturing process, enabling potential solutions to be devised.

2.4.1 Tolerance hierarchy

It is important to emphasize that the scheme depicted in Fig. 2.6 illustrates the relationships between specifications for the production of a single component. However, a comprehensive product design entails a structured arrangement of multiple components. Additionally, a single component may be part of different functional subsystems simultaneously. Consequently, it inherits the functionalities from all the subsystems it is a part of.

It can be observed that both an intra-level tolerance hierarchy, as proposed in the ISO standard [37], and an inter-level hierarchy exist, as highlighted in Fig. 2.7. There is always a link between any specification and the corresponding functional specification at the product level.

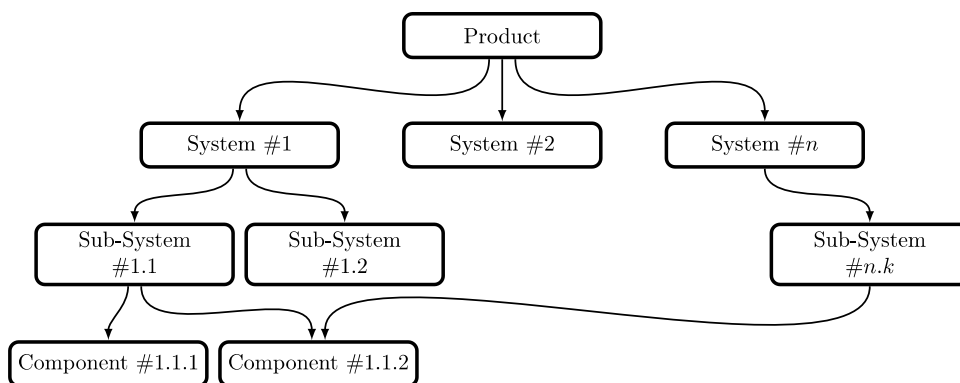


Fig. 2.7: The scheme represents the functional hierarchy among product, system, sub-system and component levels depicting a case in which one component inherit functionality from two distinct subsystems. It could represent a case of a standardized component used in different sub-systems or a complex component that is required for different functions (e.g., Structural and aerodynamic).

2.4.2 The relevance of functional specification

The product functions pertain to the assembly.

Functional tolerancing first addresses the product as a whole, and then transfers the functionality through systems and subsystems down to each individual part. At the part level, functional specifications describe the geometric requirements applied to the part and the working relations (fitting, position, orientation, etc.) among them. This definition is already established, at the standardization level, in the fields of system and software engineering [70] and information technology [71].

The proposed scheme (Fig. 2.6) assigns each tolerancing activity to the relevant department. Designers oversee the functional aspects, technologists handle process-related activities, and metrologists define inspection procedures. However, in industrial practice, it is often the case that neither the intra-level nor the inter-level hierarchy is followed. For example, all tolerancing activities may be assigned to a single actor. This results in a hybrid specification where all the different specifications (functional, manufacturing, and verification) are blended together. The outcome is a poor, partial, and incoherent specification with inconsistent information and narrower tolerances than necessary. Indeed, when there is a lack of coherent specification schemes and an abundance of non-organized datum systems, the tolerance values need to be assigned tighter in order to compensate for the lack of proper functional specification (see chapter 7 on page 179). This is necessary to fulfill functional requirements expressed in the form of Critical-To-Quality (CTQ) dimensions, customer critical dimensions, or Key Characteristics, to name a few terms found in the literature.

It is important to note that manufacturing and verification specifications are not intended to be transferred from one level to another. Only the functional specifications should be handed over since they represent the fundamental geometric requirements that guarantee the product's functionality and performance.

2.4.3 The V model as a key to understanding

The V-model approach can be applied to the proposed scheme to highlight the product development phases and timing within complex industrial organizations (Fig. 2.8). This approach emphasizes the top-down problem decomposition occurring in the design department, as well as the bottom-up integration and testing processes.

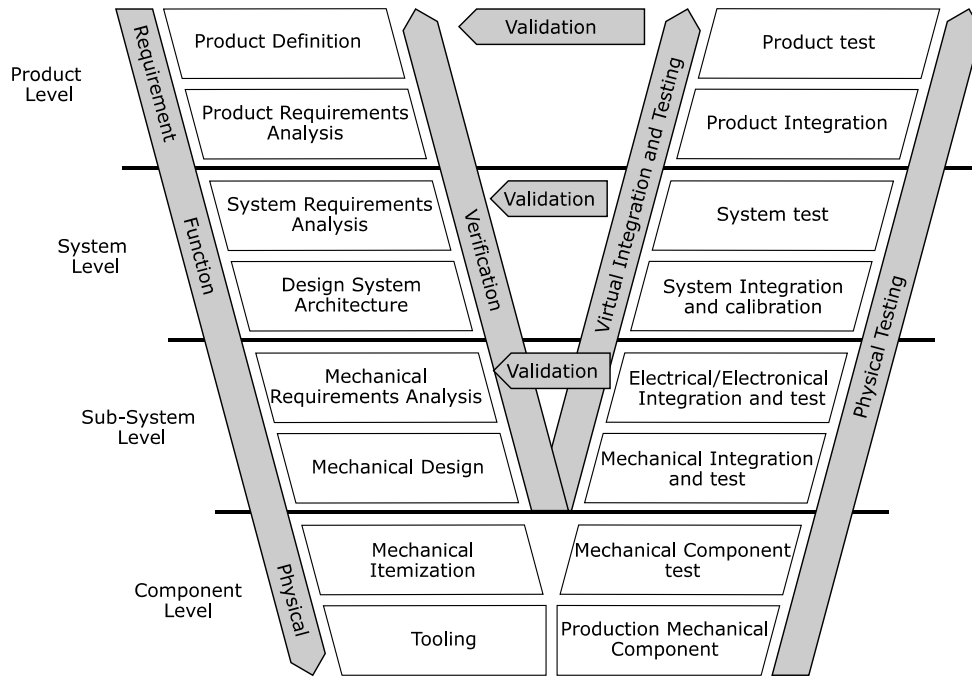


Fig. 2.8: A simplified V-Model framework used to describe the product development (Adapted from: [72]).

Functional tolerancing can be considered a top-down activity that is positioned on the descending side of the V-model. However, in practice, a bottom-up approach for functional tolerancing is often observed in industry. This means that upper-level specifications are constrained by lower-level requirements, resulting in a lack of coherence and control at the product level. To ensure the propagation of functional specifications, more design steps than necessary are often taken. Each additional step introduces uncertainties, particularly in the specification's ambiguity and the description of the function, as defined by ISO 17450-2:2012 [6]. These uncertainties consume a portion of the variability budget defined by the functional specifications at the product level, leading to a suboptimal specification scheme.

2.4.4 Clarifying Examples

In the following section, two examples are introduced to illustrate the “vertical” hierarchy of functional specifications and the distinctions among specification types in the “horizontal” hierarchy.

These examples are intended solely to clarify the concepts discussed in this chapter. Further investigations will be presented throughout the manuscript.

Submersible pump

The first example presents a simplified assembly of a submersible pump, focusing on the case and the impeller components. Fig. 2.9 illustrates a possible functional specification for the assembly, which encompasses both the case sub-system and the impeller envelope. The functional specification includes the primary datum [P-R], which represents the spinning axis that governs the mechanical dynamics of the pump, and the secondary datum [T], defined by the pump outlet. This datum system is established within the pump assembly since the datum features [73] are present in different parts. Additionally, other functional surfaces, controlled by surface profile tolerances, describe both the inner surface of the pump case and the impeller envelope, ensuring an appropriate functional gap.

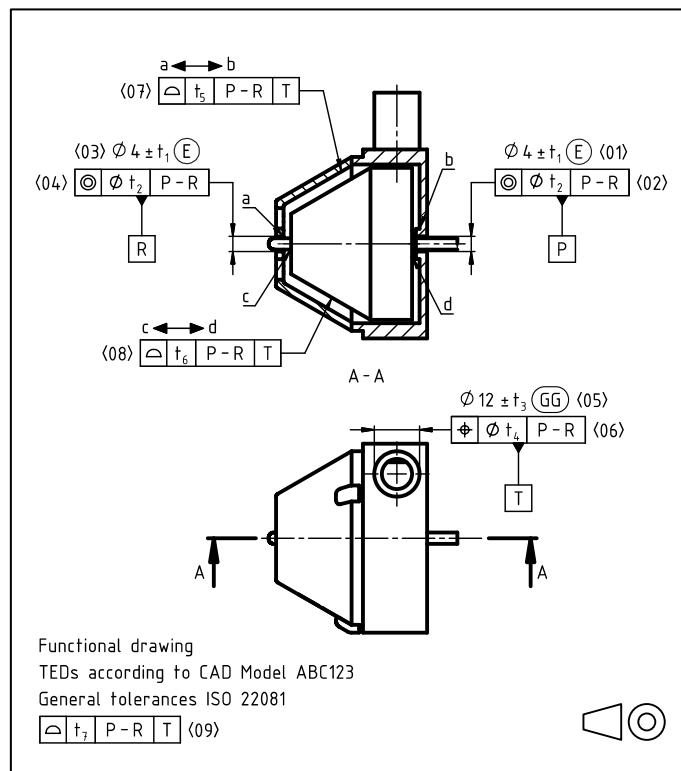


Fig. 2.9: Submersible pump assembly functional specification.

Fig. 2.10, Fig. 2.11, and Fig. 2.12 depict coherent functional specifications for the impeller, as well as the front and rear parts of the case sub-assembly. At the part specification level, the datum system defines the mating features of the assembly. This approach enables the establishment of direct and straightforward tolerance stack-ups, which in turn connect the parts' specifications to the corresponding functional specifications at the assembly level (see chapter 5 on page 135). Through these tolerance stack-ups, the “vertical” tolerance hierarchy can be implemented effectively.

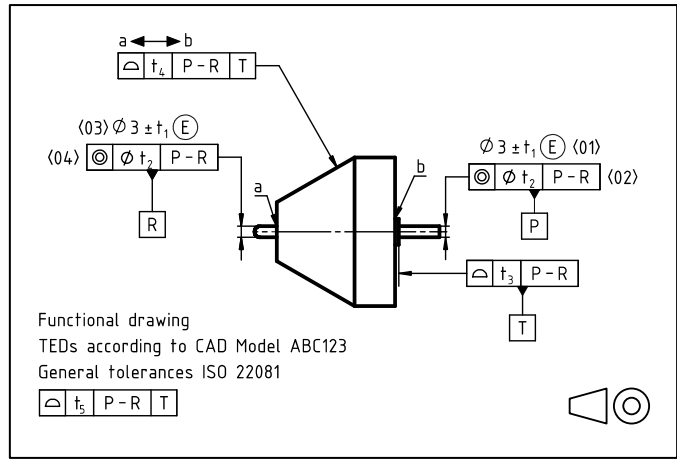


Fig. 2.10: Impeller functional specification.

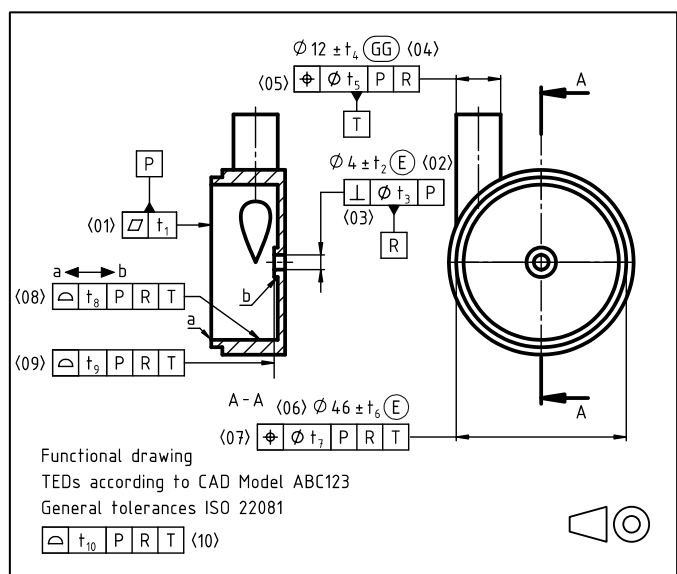


Fig. 2.11: Pump case base functional specification.

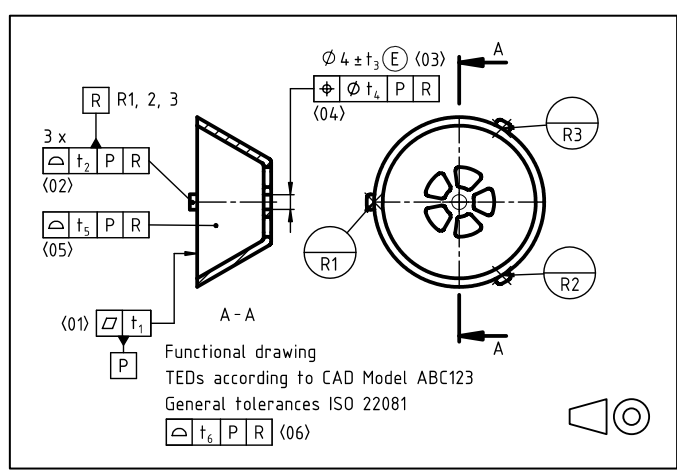


Fig. 2.12: Pump case functional specification.

Spacer plate

The second example focuses on a simple spacer used to adjust the distance between two parts. The spacer has a pattern of eight holes designed to accommodate through shafts.

Fig. 2.13 illustrates the functional specification for this component. The flange of the spacer has three symmetry planes, allowing it to be assembled in four different layouts. As a result, the primary datum is assigned to the median plane of the plate thickness. The holes are specified as a pattern according to ISO 5458:2018 [74], and they define the secondary datum, establishing a complete datum system. The challenge of creating a tolerance stack-up when a pattern defines the datum system is discussed in chapter 4. The remaining surfaces of the spacer do not interact with other parts in the assembly and are controlled by general tolerances based on ISO 22081:2021 [75].

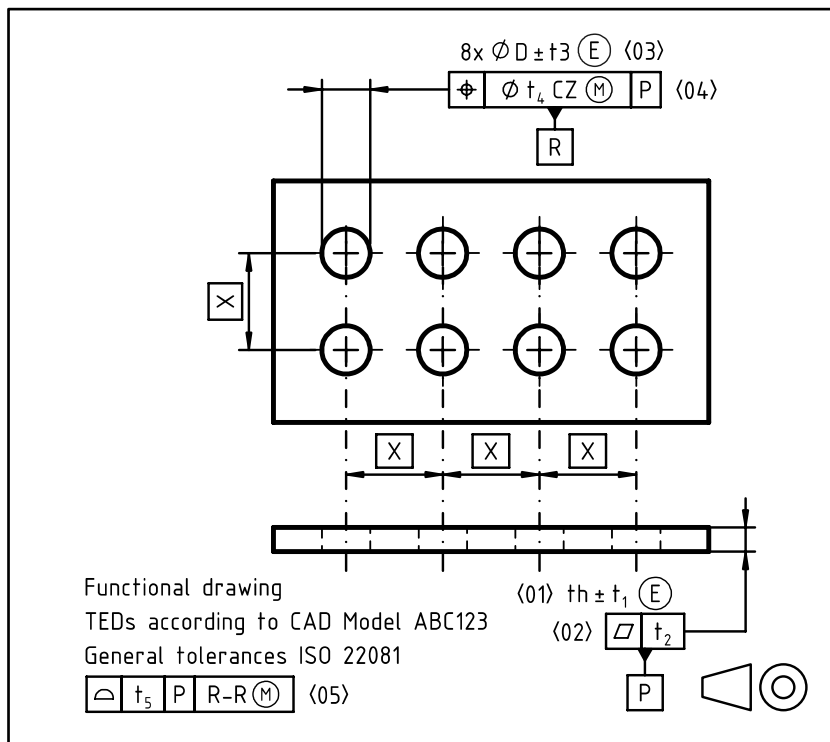


Fig. 2.13: Functional specification for a spacer plate.

One possible manufacturing specification is presented in Fig. 2.14. It is assumed that the part will be produced through machining, and the datum system is derived from the fixturing.

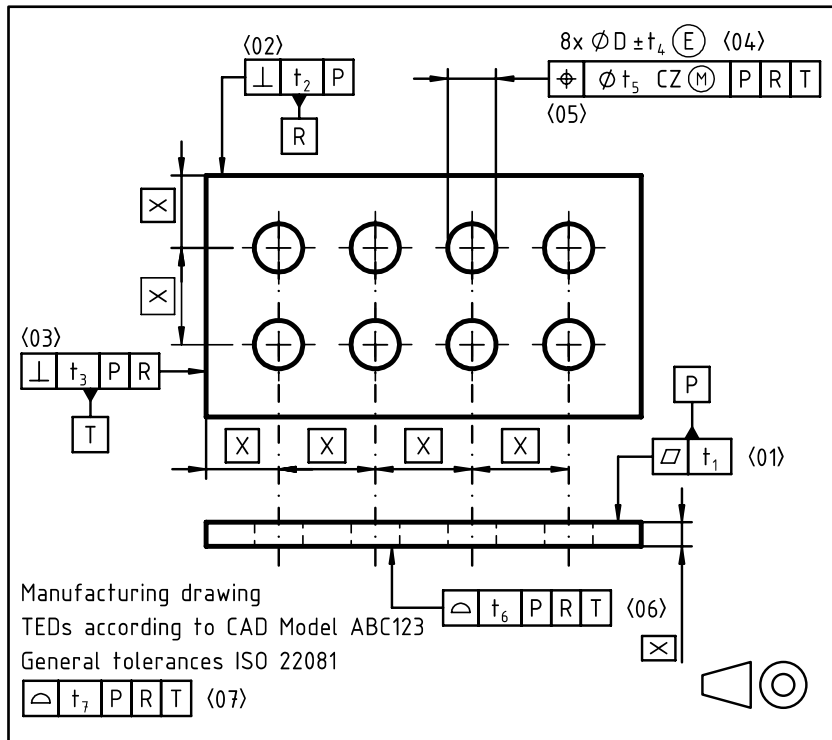


Fig. 2.14: Manufacturing specification for a spacer plate.

The functional and manufacturing specifications should be related through tolerance stack-ups, where the functional tolerances represent the critical dimension limits, and the manufacturing tolerances account for process-dependent variables. In the case of non-rigid parts, which only reach a stable configuration once assembled, the correlation should also consider deformability as presented in chapter 8.

By comparing the functional and manufacturing specifications proposed for the spacer, an interesting observation can be made. It is noticeable that the number of tolerances increases from the functional specification to the manufacturing specification, going from 5 to 7 tolerances. Additionally, in the functional specification, the tolerance t_2 (i.e., flatness of the median plane of the spacer) may be deemed irrelevant since the form is already controlled by the size tolerance with the envelope requirement.

The increase in tolerances, and consequently the increase in complexity, is attributed to the fact that the manufacturing specification includes additional requirements beyond those covered by the functional specification. While the functional specification focuses solely on ensuring functionality, the manufacturing specification must ensure functionality as well as address the specific requirements of the chosen manufacturing process.

Therefore, the manufacturing specification not only needs to consider the functional requirements but also incorporates the requirements associated with the manufacturing process, leading to a more wide-ranging set of tolerances.

2.4.5 Final remarks

It is crucial to distinguish between the act of tolerancing, the resulting information (specification or specification scheme), and the medium (as defined in ISO 10209:2012 [36]) that facilitates the transmission of information (TPD). The ISO/TS 21619:2018, as part of the ISO GPS, primarily focuses on the information (specification types) rather than the medium (TPD) and should be updated accordingly. Given the importance of hierarchically organizing the specification types as depicted in Fig. 2.4, it becomes evident to identify the key actors and their responsibilities, thereby expanding upon the “responsibility principle” outlined in ISO 8015:2011 [76].

At the industrial level, the implications of the hierarchical framework allow each department to take responsibility for managing the functional/manufacturing/verification specifications relevant to their respective expertise, while adhering to the constraints imposed by higher-level hierarchies.

2.5 || Research gaps

The proposed approach challenges the current critical modus operandi in the field of GPS and promotes a more efficient and effective management of tolerancing activities. The application of this model opens up several research gaps and research questions, which are summarized in Fig. 2.15.

Regarding the design department, the first issue is the creation of a pure functional specification, as in industry it is common to have hybrid specifications that merge functional and manufacturing requirements. The question is: Can we define a methodology that allows for the creation of a pure functional specification? Chapter 3 and 4 cover this point. In particular, chapter 3 looks at the identification and classification of functional features; chapter 4 looks at the actual creation of functional specifications as 2D drawings.

Once a functional specification has been developed, another question arises: How effective is the specification in describing functional requirements? The second research gap identified is the definition of specification efficiency. However, this research gap was not investigated within the PhD program and therefore is not covered in this manuscript. It will be addressed in future research.

Within the design department, isolated from interactions with other departments, the adoption of a top-down design and specification process raises the challenge of effectively managing tolerance stack-ups. Chapter 5 endeavors to present a methodology that integrates the top-down approach for handling tolerance stack-ups.

One specific type of feature to handle in functional specifications is patterns of fits. The question is: How can we compute the statistical rejection rate of patterns of fits when they serve as alignment features and therefore act as datum features? Chapter 6 will address this specific issue.

Pattern of Fits, or fits in general, are frequently employed for aligning parts. The most extreme instance is encountered when bolted connections are utilized to ensure alignment during assembly.

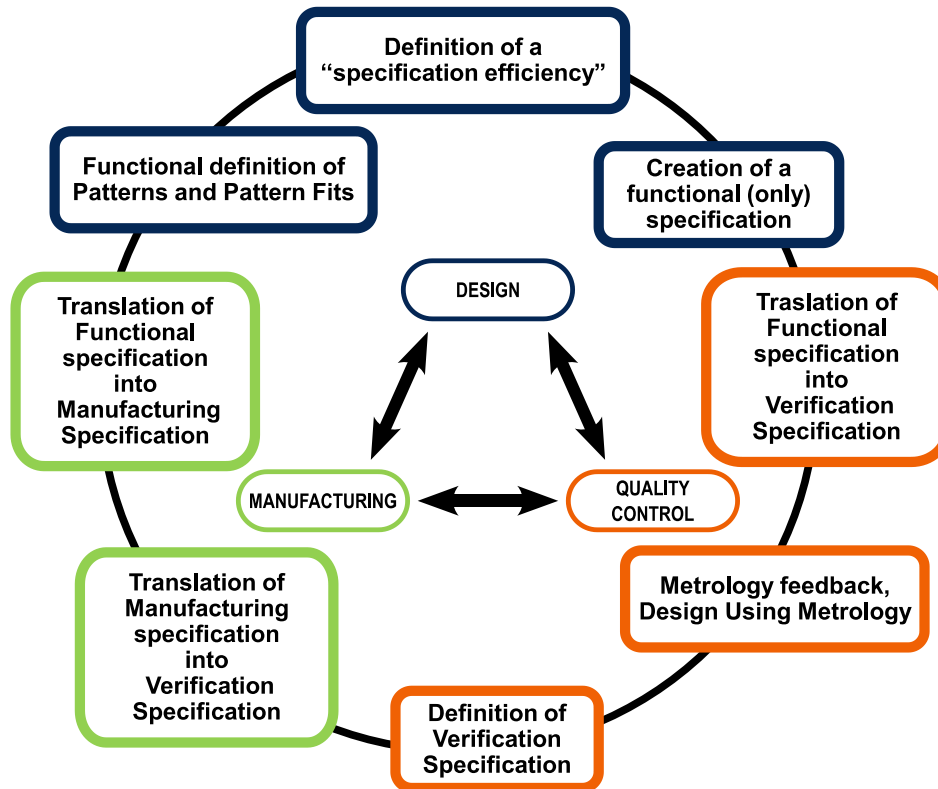


Fig. 2.15: graphical representation of the research gaps that were identified.

Clearance is unavoidable in such cases, which can lead to operational issues. Chapter 7 employs tolerance stack-up analysis to investigate the impact of various geometric specifications on the rejection rate. This analysis allows quantifying the effects of different design solutions, suggests when material conditions are appropriate, and demonstrates the positive effects of incorporating an explicit alignment feature.

In the manufacturing department, a key question arises: If functional, manufacturing, and verification specifications exist in separate forms, how can we handle the conversion of information from one specification to another? Chapter 8 will cover the correlation between functional and manufacturing specification in case of deformable assemblies.

In the quality control department, the first issue is the formal definition of what a verification specification should be. Although it is mentioned in the standards (ISO/TS 21619:2018), no practical definition or indication of its contents is provided. Chapter 9 will elaborate on this definition, proposing some applications that are compatible with the current ISO GPS system.

When actual distribution data obtained from quality control are employed as inputs for tolerance stack-ups, facilitating virtual assembly simulations, the challenge arises of how to appropriately configure the simulation. This is due to the fact that actual distributions may not always be Gaussian or centered. Chapter 10 explores different settings for tolerance stack-up analysis, utilizing Second Order Tolerance Analysis Methods (as implemented in CETOL 6sigma).

Lastly, in chapter 11, a potential industrial implementation of the proposed methodology is outlined. This section showcases some of the experience gained in collaboration with Electrolux Italia SpA, illustrating how the framework presented throughout this thesis can be practically applied in an industrial context.

3 || Classification of functional features

We classify things for the purpose of doing something to them. Any classification which does not assist manipulation is worse than useless.

Randolph Bourne

The Design Tools and Methods in Industrial Engineering Laboratory from the University of Padova, thanks to the experience gained over the years and as a result of collaborations with national and international companies, has developed a practical method for functional geometric specification that tries to bring together the goods from the two normative systems (languages), ISO GPS and ASME Y15.5 (GD&T).

The proposed method consists of three main phases:

- Phase 0: definition of functional requirements, including the definition of functional features and datum features.
- Phase 1: definition of the functional dimensioning scheme.
- Phase 2: addition of the functional specification (tolerances), both dimensional and geometrical.

Therefore, the first step for the creation of a functional specification is distinguish between what is functional and what is not in the component, or in other words, the definition of functional features/surfaces and its classification needed for a smooth operation during phase 1 and 2. This chapter focuses on phase 0, while the discussion on phase 1 and 2 can be found on the subsequent chapter.

3.1 || Phase 0: definition of functional requirements

In Phase 0, the functional requirements are discussed and defined. Everything start from the analysis of the assembly to which the component pertain. Functional requirement derives primarily from assembly constraint. There are really few product that are “single component products”. For the majority product are assemblies and their ability to serve a function lays behind the interaction

of each single component with its surrounding components within the assembly. A single misplaced screw can prevent an entire product to work properly. For this reason the functional requirements for sure collect together all assembly requirements [77]. A further refinement can reveal the existence of other functional requirements that does not directly derive from assembly requirement; this is the case of requirement deriving from the interaction of the part with the surrounding environment. An example may be the position of an aerodynamic surface that interact with the fluid flows. Nevertheless, these requirements, when they involve the location and or orientation of a feature, derive from assembly requirements: the misplacement or mis-assembly of the part prevent the correct functionality.

The assembly needs to be analyzed from a dynamic and cinematic point of view: the components does not “materialize” in position but they are place in position. Different strategies for this are followed on the two sides of the Atlantic ocean as quoted by Daniel Whitney in his book: “We [in the USA] like to let the parts fall into place by themselves. The Europeans want to overpower the parts and force them into shape” [77]; this difference can also be appreciated in the difference between the ISO GPS and ASME GD&T languages. This means that non only the contact surfaces/features are of interest but also the one that are used to guide the part in position.

The result of this phase is the definition and classification of all functional surfaces/features. From the experience gained so far, this is the most difficult phase since no methodological guidance has already been defined. Therefore, the discussion among designer may lead to entropy being generated and possibly divergences of functionality assumption. Indeed, many times, consideration coming from manufacturing requirements and/or verification requirements distract the designer and lead to the incorporation of information not relevant to functionality. To overcome this methodological constraint, in this chapter a formal methodology to complete phase 0 will be presented and discussed.

3.2 || A formal methodology for phase 0

Here the aim is to formalize Phase 0 of the Functional Geometric Specification Method. Its goal is to provide the designer with a step-by-step procedure for determining and cataloging the functional features resulting from the functional requirements.

Formalization is crucial to overcome critical issues encountered in many different industrial collaborations when performing the functional analysis of a part/subassembly. The comprehensive workflow of the proposed methodology is shown in Fig. 3.1. In the following, a top-level description of the workflow will be provided, followed by a detailed description of each step in the subsequent section.

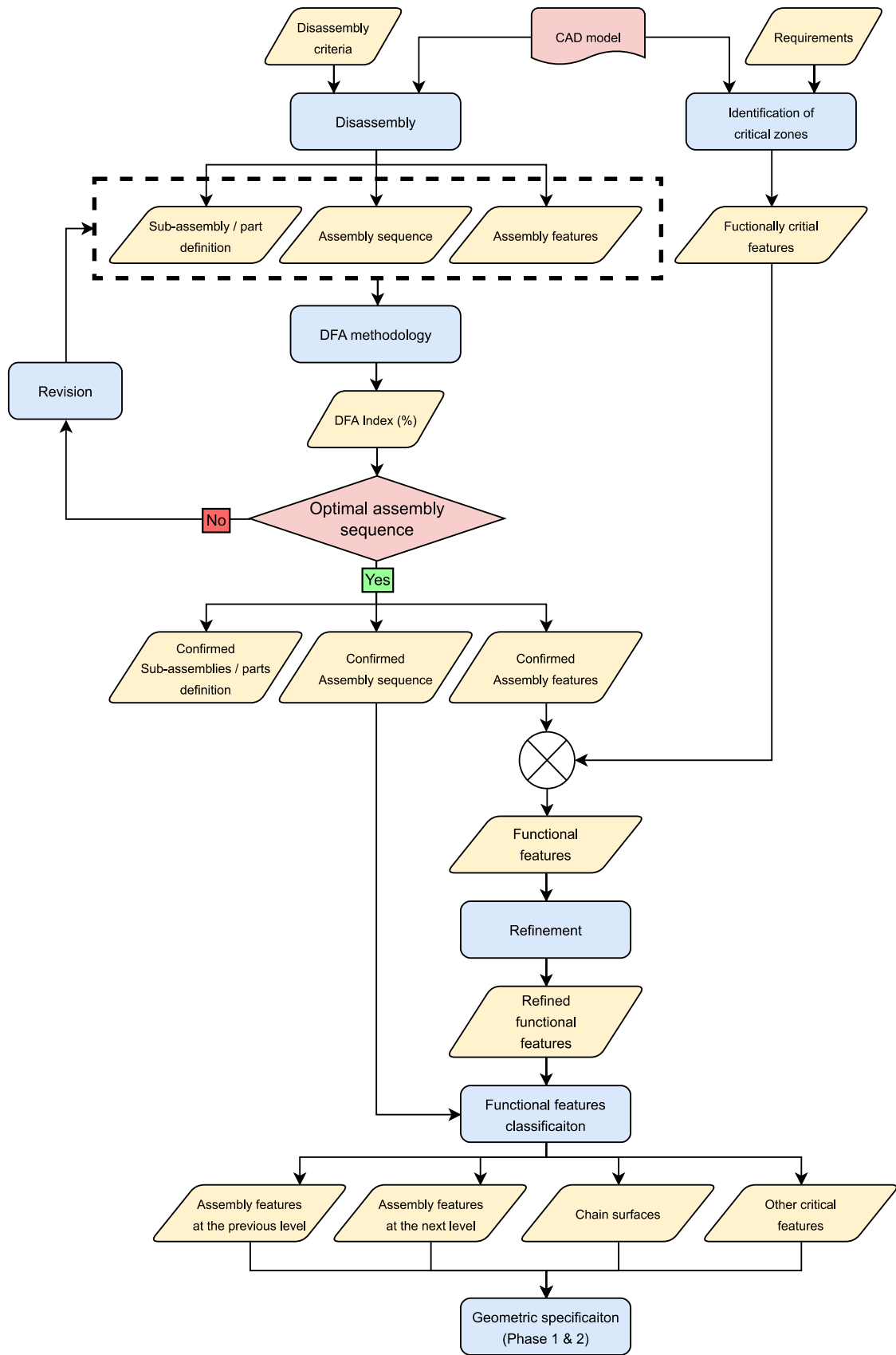


Fig. 3.1: Proposed workflow.

This flowchart is recursive, as it requires its application, starting from the top-level assembly, for each sub-assembly that is ideally disassembled, considering it as a new starting assembly. The recursive procedure somehow remaps the multilevel model for tolerance management presented in the previous chapter (Fig. 2.6). Initially, each sub-assembly is treated as an individual part, allowing for the creation of congruent sub-assembly drawings. In many industrial collaborations, the lack of proper assembly and sub-assembly drawings has been recorded. In many instances, assembly/sub-assembly drawings are used as bills of materials or as references for the assembly process, without providing actual specifications. Nonetheless, the functional specification at the assembly/sub-assembly level is crucial for the tolerance specification management framework presented in the previous chapter, as it explicitly assigns geometric variability to the relationships between parts that fulfill the functional requirements. For example, a nominal gap with a value of zero might need to be greater than zero to allow for assemblability, or in the opposite case, contact might be required between two specific surfaces. This type of information was already expressed in words in the work by Stanley Parker in the 1950s [18]. Unfortunately, it seems that the ISO GPS system has not evolved towards formalizing such requirements thus far. This issue may need to be addressed at the standardization level in order to provide standardized symbology to express these basic assembly requirements.

The workflow is divided into a series of operations that identify the main steps to follow:

- Critical zone identification.
- Disassembly.
- Application of DfA method.
- Refinement.
- Functional surface classification.
- Functional specification (Phase 1 and phase 2).

From Fig. 3.1, it can be observed that the first operation is the identification of critical zones: using the CAD model of the object and the functional requirements, the so-called “chain surfaces” and “other critical surfaces” can be identified. “Chain surfaces” refer to surfaces belonging to different components within the assembly that identify gaps, which may even be zero in the nominal case, that need to be controlled through tolerance stack-up. The “other functional surfaces” encompass surfaces critical for the assembly's operation due to their interface with the external world. Although they do not contribute to the definition of any tolerance chain, their misplacement at the assembly level could result in functional deficits. For example, a surface with aerodynamic characteristics can have a significant effect even if it doesn't define any critical gap.

With this information established by the operator recorded, the virtual disassembly of the product follows, resulting in sub-assemblies and/or individual parts. At this point, any sub-assemblies are considered as a whole part. The “assembly features” and a hypothetical assembly

sequence/procedure can be defined. The assembly features are the features that locate, orientate and lock the part in the assembly.

By applying the DfA method it is possible to estimate the assembly design's effectiveness in terms of assemblability. If the obtained value falls within the limits defined by the operator, the next phase can proceed; otherwise, the assembly sequences and/or identified sub-assemblies need to be revised. When the efficiency is satisfactory, the assembly procedure is frozen and confirmed. Consequently, the assembly surfaces are also confirmed. It is then possible to perform a "refinement" activity on the assembly surfaces: although an entire feature may have been defined as an assembly feature, the actual contact between the parts may occur in a restricted portion of it. By refining the assembly surfaces, the definition of Datum Targets is advanced, allowing for a better description of the functional condition related to assembly at the Datum System level. Then, the classification of functional features is carried out, identifying and naming the assembly feature to the previous level (i.e., the features through which the examined part/sub-assembly is assembled to what has already been assembled before) and the assembly feature to the next level (i.e., the features to which additional components or sub-assemblies will be assembled).

Completing the set of functional surfaces are the chain features and other critical features defined in the first step.

All this information is transferred to Phases 1 and 2 of the geometric specification method, where the defined functional information is converted into a proper functional geometric specification by means of the language define by the ISO GPS system.

3.3 || Approach validation

The presented method is applied to an exemplary case study. The product considered for the case study is a simple caster, composed of the following parts: Base, Risers (right and left), Bearings (right and left), Shaft, Wheel, and M10 Fastening Screws. A physical realization of the assembly is shown in Fig. 3.2 for reference. The model should look familiar to most since it is a typical case study used for training in 3D CAD modeling and other CAE applications. This particular model is far from optimized geometrically, which will allow the validation of the proposed methodology in a challenging yet very simple assembly.

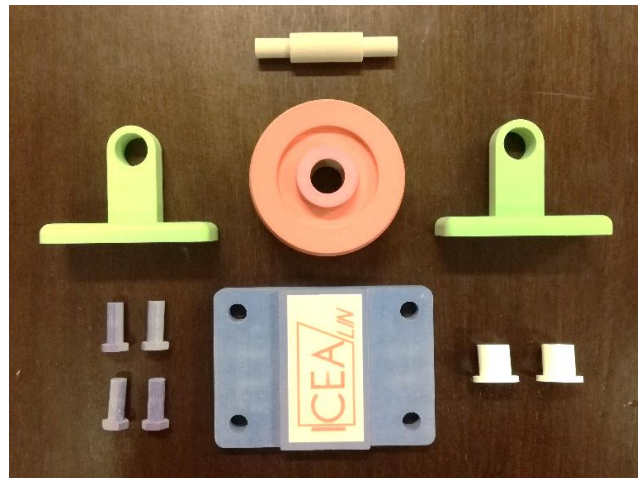


Fig. 3.2: The actual model used consists of the following components: the red Pulley component, the blue Base component, the two green Uprights, the white Bearings, the light gray Shaft, and the purple M10 Screws.

Having knowledge of the product's use is crucial for the operator to start the procedure. In this specific case, it was assumed that the rotating part (wheel) of this caster should be able to rotate freely to interact with an unseen belt, which must not interfere with any other component. Therefore, the caster act as a counterweight: it is a free standing assembly that does not have any fixed mounting on any other part/assembly. This last assumption will heavily influence the final result: a different assumption would have led to a significantly different result.

3.3.1 Identification of critical zones

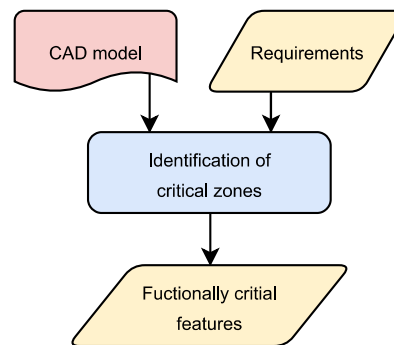


Fig. 3.3: Identification of critical zones.

Firstly, the CAD model of the assembly on which we intend to work needs to be analyzed. The objective is to identify functional features/surfaces that define critical areas, taking into account the functional requirements of the product. This observation must be carried out considering that we want to avoid problems at the assembly level. The product is considered already assembled, so it is not necessary to consider issues related to the assembly process itself. The focus is on gaps between the various parts that need to be present to allow for cinematic purposes or to guarantee specific contact points between parts. These are identified as “chain surfaces,” as previously defined. Other features/surfaces that interact with the external world and whose misplacement will impact performance need to be considered as well. For example, an aerodynamic surface may fit within this definition as its misplacement may significantly impact aerodynamic performance (e.g., drag, lift, power efficiency, etc.). Aesthetic surfaces may also fit within this category, as misplacement or misshaping of these surfaces may impact perceived quality by the customer and erode market share. It is noteworthy that in some instances, aesthetic surfaces may be considered as chain surfaces if a gap/alignment issue between two surfaces needs to be considered.

Clearly, the CAD model presents nominal dimensions, so any gaps may not be visible in the model as they have a nominally zero value. Nevertheless, to meet the functional requirements, the designer knows that the real model must have a positive gap (clearance) or a zero gap (contact). In the latter case, we no longer consider them as chain surfaces but as assembly surfaces.

Fig. 3.4 shows the identified areas for the case study.

The focus is on maintaining a predetermined distance (gap) between the components, which is essential for the functioning of the model according to the previously expressed functional requirements, specifically wheel rotation. At the same time, the gaps between the wheel and the bushing, as well as between the shaft and the bushings, should not exceed a predetermined value. Large gaps can induce vibrations, leading to decreased quality perception, noise, and increased wear. All of these considerations are even more relevant since we are dealing with a kinematic

assembly with one degree of freedom, which means that functionally, the assembly allows the wheel to move relative to the main structure.

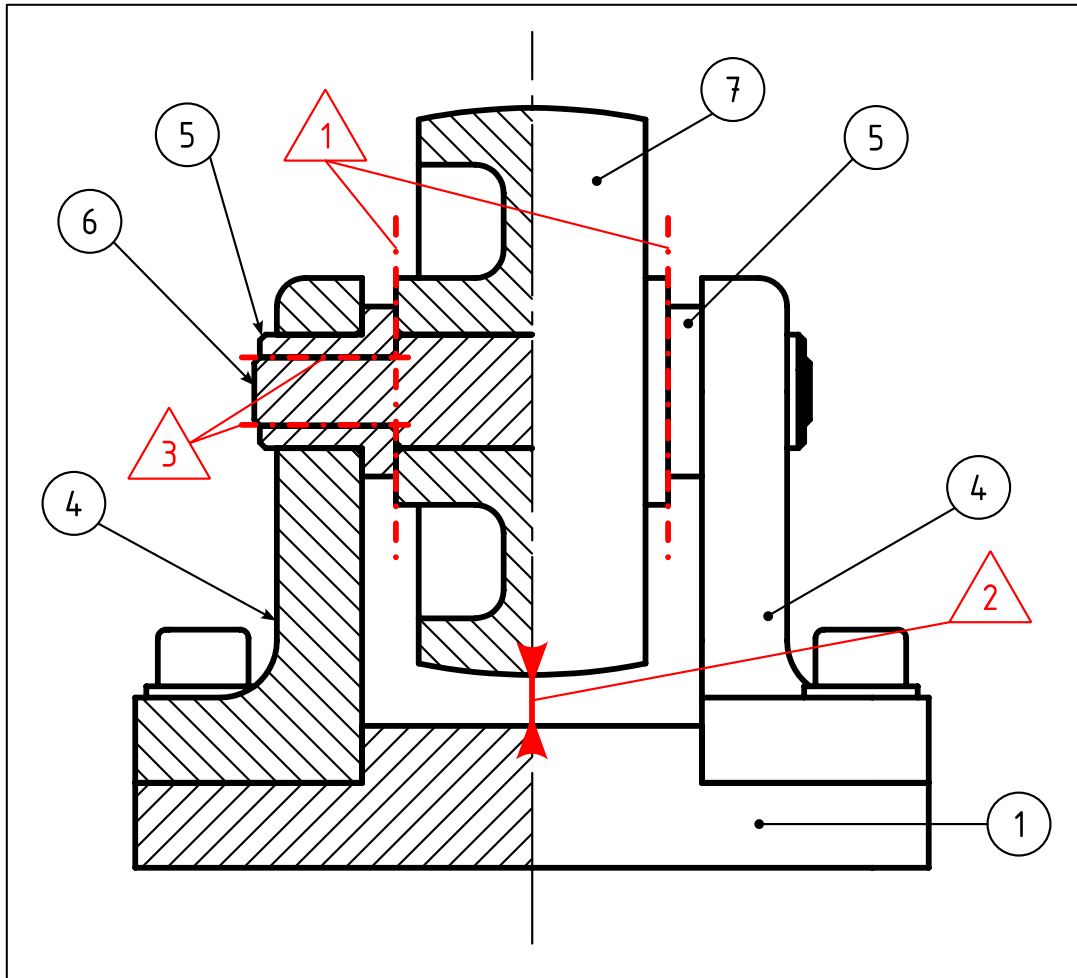


Fig. 3.4: The critical zones identified in the caster are as follows: Zone 1: Gap between the Bushings and Wheel. Zone 2: Gap between the Wheel and Base.

The geometric functional requirements for this assembly can be summarized as follows. In the lower area, between the surface of the wheel (component 7 in Fig. 3.4) and the surface of the Base (component 1 in Fig. 3.4), there must be a minimum distance to ensure the rotation of the wheel and provide sufficient space for the belt to pass through. Between the side surfaces of the wheel and the surfaces of the bushings, there should be a certain positive gap to prevent scraping between the components during their rotation, even though the nominal gap is zero. If the gap were negative, it would indicate interference that would prevent rotation. The shaft-hole coupling between both ends of the shaft and the bushings must have a close running fit.

These areas identify the initial functional surfaces of the model, which in this case include the chain surfaces and the clearance fit.

3.3.2 Disassembly

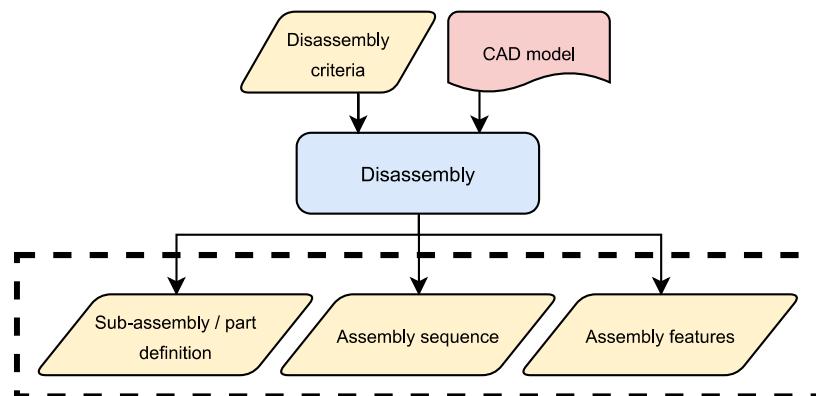


Fig. 3.5: Disassembly phase.

In this phase, the initial assembly is divided into multiple sub-assemblies and/or individual parts. The disassembly may be both physical, on a mockup or prototype, or digital considering the CAD model. If the disassembly is performed digitally, it is important to “think physically” meaning that the disassembly procedure should be possible in a physical context, indeed working on a CAD model it is possible to define disassembly procedure that are not physically possible. At this point it is important to stress that the disassembly is seen as an iterative process, as already mentioned throughout the first sections of this chapter. Each sub-assembly that is taken out from the product is treated as a separate part following a “Top-Down” approach. Once the workflow is followed till the end, each sub-assembly re-enters the workflow from the beginning. Referring to Fig. 2.6 in the previous chapter, the procedure is performed at each horizontal level to generate functional specifications. When the work at one level is done, the functional specification for a sub-assembly together with the CAD model is handed over to the lower level of the scheme and the workflow iterated. This approach should lead to better work management, even when dealing with large assemblies, as the sub-assemblies would be managed separately in subsequent phases of the work. This procedure can also be implemented independently from the type of supply chain involved (internal vs external). Indeed, each sub-assembly may represent a sub-assembly that is developed and produced by an external supplier.

When disassembling, it is necessary to establish a criterion for determining the sub-assemblies. Different strategies may lead to very different results and may depend on the company setup. In the context of this work, it has been decided to let this degree of freedom in the application of the framework. For the application of the framework in this work, it has been decided to define the sub-assemblies as “functional” to the assembly procedure. Therefore, ideally, a sub-assembly is an assembly of parts that would physically remain in the hands of an operator during a physical disassembly. In case this criterion is not satisfactory, other more elaborate criteria may be defined. As an example sub-assemblies may be defined considering relative motion, same material,

structural functions, etc. However, such an elaborate criterion has not been chosen due to the difficulties in generalizing a method that can be as general and widely applicable as possible, regardless of the assembly being considered. Nonetheless, it may be interesting to explore the variability of results due to different criteria.

Once the single sub-assembly and/or single parts are defined, the disassembly operations will lead to the identification of other functional feature, namely the “assembly features”, as well as the identification of hypothetical assembly sequences. In other words it is possible to know which surface/feature will be in contact and the order in which the contact occur.

In our case study, the disassembling immediately led to the identification of two main sub-assemblies and a single component:

- Sub-assembly named “wheel_asm,” containing the components Shaft and Wheel.
- Sub-assembly named “riser_asm,” containing the components Riser itself and Bushing (two units).
- Component “Base.”

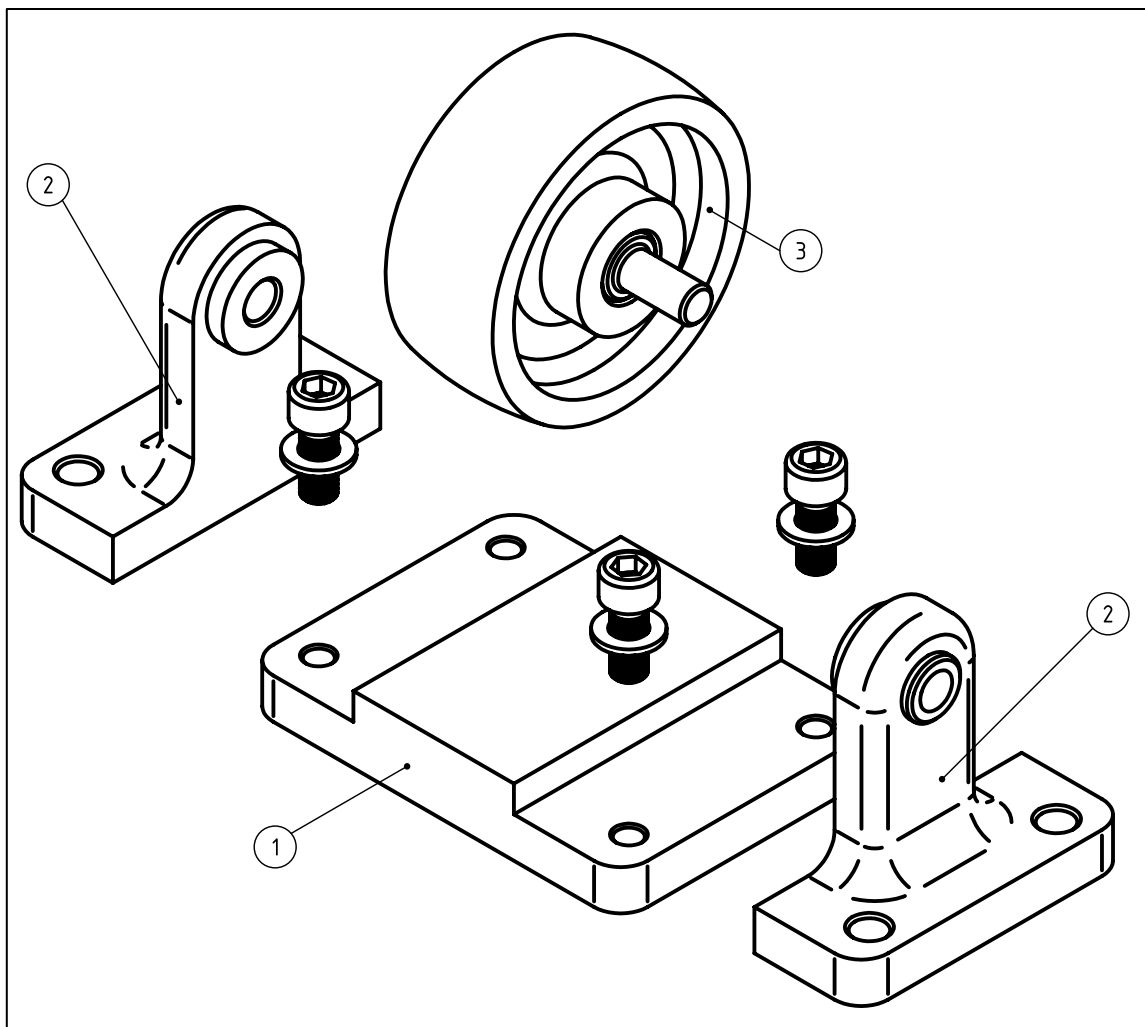


Fig. 3.6: Sub-assembly “wheel_asm” (3), “riser_asm” (2), and Base component (1).

The “wheel_asm” sub-assembly represents the components involved in the movement, while the “riser_asm” sub-assembly and the “base” component represents the statoric part of the assembly and gives rigidity to the structure (see Fig. 3.6 for the “wheel_asm,” “riser_asm,” and “base” sub-assemblies).

With the obtained sub-assemblies, individual parts, and information about the surfaces in mutual contact, it is possible to identify hypothetical assembly sequences. For the analyzed case, these sequences are detailed in the next sub-section.

3.3.3 DfA Methodology

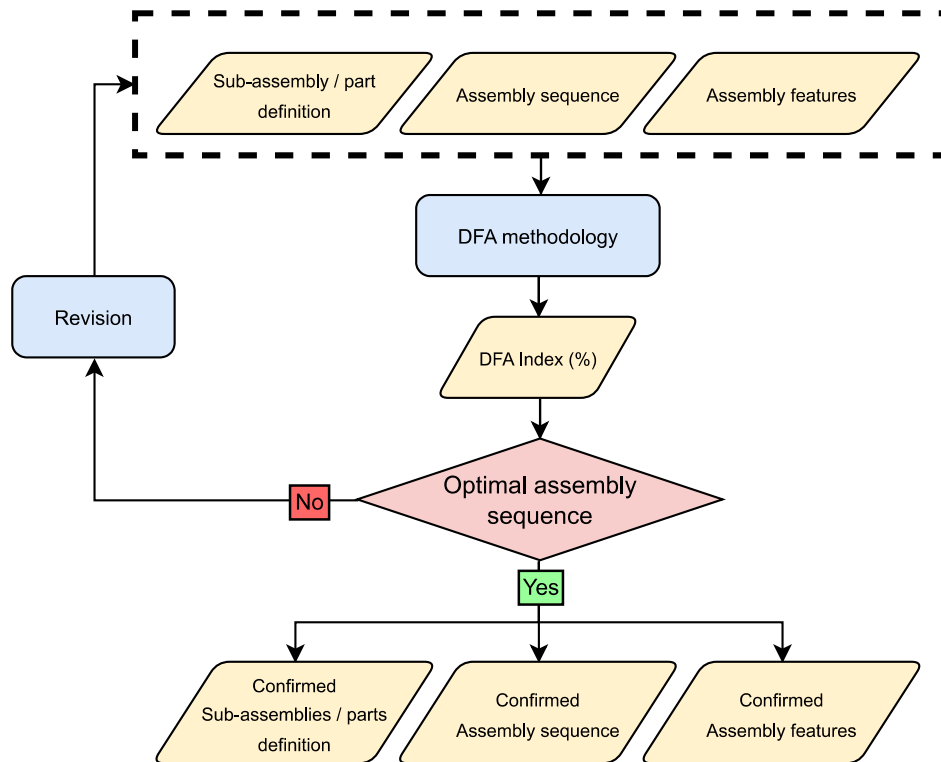


Fig. 3.7: DfA methodology phase.

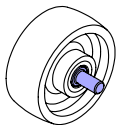
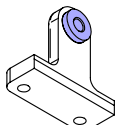
In this phase, considering the hypothesized assembly sequences, Design for Assembly (DfA) procedures can be applied, following the Boothroyd-Dewhurst method [78], to obtain the design efficiency. In this specific application, the efficiency value will be considered as an estimator of the quality of the assembly sequence associated with the 3D model, as the geometry of the components is considered fixed and non-negotiable. The goal is to define a functional geometric specification for the already defined geometry without the option to update the geometry of any part of the product. The subsequent phases can only proceed if the obtained efficiency is acceptable and

meets predefined criteria. Otherwise, a revision can be considered, as indicated by the loop in the diagram (Fig. 3.7). This revision will primarily be applied to the assembly sequences. In many instances, changing the assembly sequence can improve the result of the DfA analysis, for example, by allowing easier part insertion or eliminating restricted access issues. If no improvements are achieved, attention can be shifted to the definition of sub-assemblies and, consequently, the assembly surfaces.

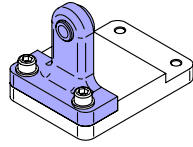
At this point, the analysis can be remade, and the results compared to the previous iteration. It is noteworthy to point out that, given the fact that the geometry cannot be changed (as hypothesis), the DfA result depends only on the assembly sequence and assembly hypothesis. Therefore, optimizing the DfA efficiency means identifying an optimal assembly sequence. In general, in accordance with the indication from Boothroyd-Dewhurst [78], the result from the DfA analysis can also be used to reiterate the design phase and update the nominal geometry accordingly.

Considering our case study, the caster, the assembly sequence remap backwards the disassembly procedure that has been described in the previous subsection. Therefore the assembly procedure requires the assembly of two preliminary sub-assembly: the “wheel_asm” and the “riser_asm” (two instances). The assembly of two preliminary sub-assembly requires interference. Once these three sub-assembly have been assemble the final assembly sequence can start. A summary of the assembly procedure is shown in Tab. 3.1. Initially, one instance of the “wheel_asm” sub-assembly is assembled by an interference fit between the shaft and the wheel; the sub-assembly is then put on hold. Two instances of the “riser_asm” need to be assembly, also in this case the assembly needs interference. These two identical sub-assemblies are put on hold too. At this point the base component is fixed in the fixture, and the first “riser_asm” is pre-assembled (screws are not tightened). The “wheel_asm” follows, and while it is manually maintained in position the second “riser_asm” is placed in position. At this point all screws are tightened and the caster is completely assembled.

Tab. 3.1: Assembly procedure with sub-assembly

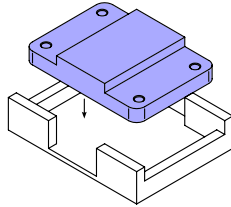
1		<p>The “riser_asm” is assembled by assembling together the riser and the bushing. Two sub-assemblies are needed.</p>
2		<p>The “wheel_asm” is assembled by assembling together the wheel and the shaft.</p>

3



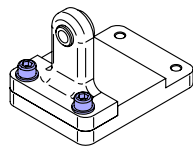
The base component is placed in the fixture.

4



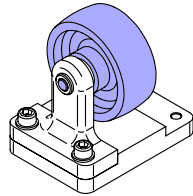
The first "riser_asm" is placed in its slot into the base.

5



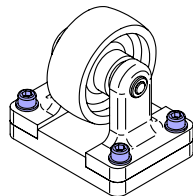
Two M10 screws are pre mounted to keep the first "riser_asm" in place.

6



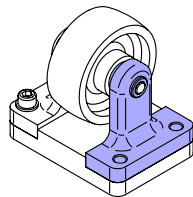
The "wheel_asm" is inserted into the bushing of the first "riser_asm".

7



The second "riser_asm" is assembled by inserting its bushing into the shaft and placing the riser in its slot into the base.

8



All the four M10 screws are tightened.

At this point, the Design for Assembly (DfA) methodology is applied. The DfA Index can be calculated for the procedure with individual components using the following formula:

$$DFA_{Index} = \frac{3 \cdot N_{min}}{Tot. Ass. Time}$$

where N_{min} refers to the total count of the minimum parts required for assembly (in this case, 6 components), 3 is a fixed value, and $Tot. Ass. Time$ refers to the total assembly time calculated as the sum of the times for each individual component.

In our case, the DfA index is:

$$DfA_{index} = \frac{3 \cdot 7}{119,04} = 0.17(17\%)$$

This result is considered as acceptable and the assembly procedure is confirmed. The detailed assembly procedure for the caster case study is presented below.

The first operation to be performed is the positioning of the Base component (Fig. 3.8) on a support and clamping plane to assemble the subsequent components in an organized and safe way. From Fig. 3.8, it can be observed that the Base is placed by inserting it along the Y-axis.

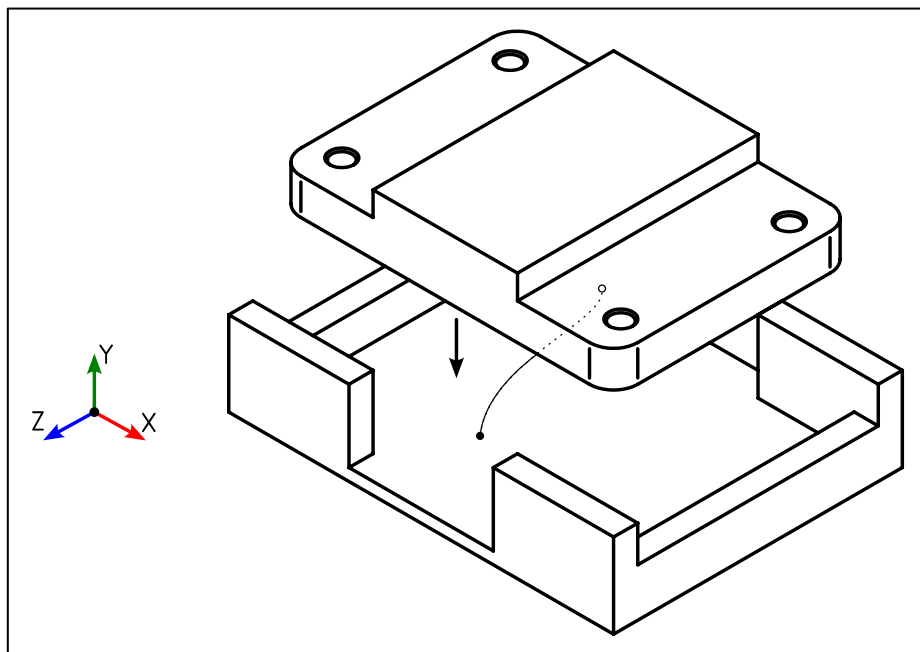


Fig. 3.8: Base posing on the fixturing base.

Fig. 3.9 illustrates how the sub-assemblies “riser_asm” and “wheel_asm” are assembled. In both cases, an interference fit is required between the components, namely riser + bushing and wheel + shaft, with the X-axis as the insertion direction of the components. The bushing stops when in contact with the riser along the X-axis, while the shaft and the wheel need to be aligned to create a single surface on both sides.

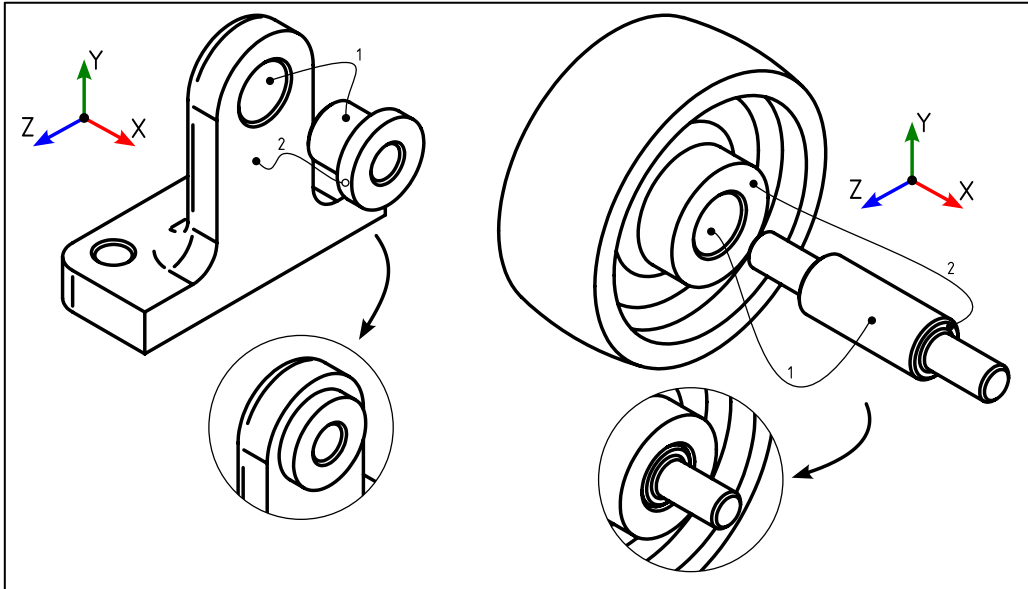


Fig. 3.9: assembly procedure to obtain the “riser_asm” and the “wheel_asm” sub-assemblies.

The next step is the pre-assembly of the “riser_asm” sub-assembly to the Base (Fig. 3.10) by placing the “riser_asm”, bringing it into contact with the vertical surface of the Base, and aligning the outer surfaces with those of the Base.

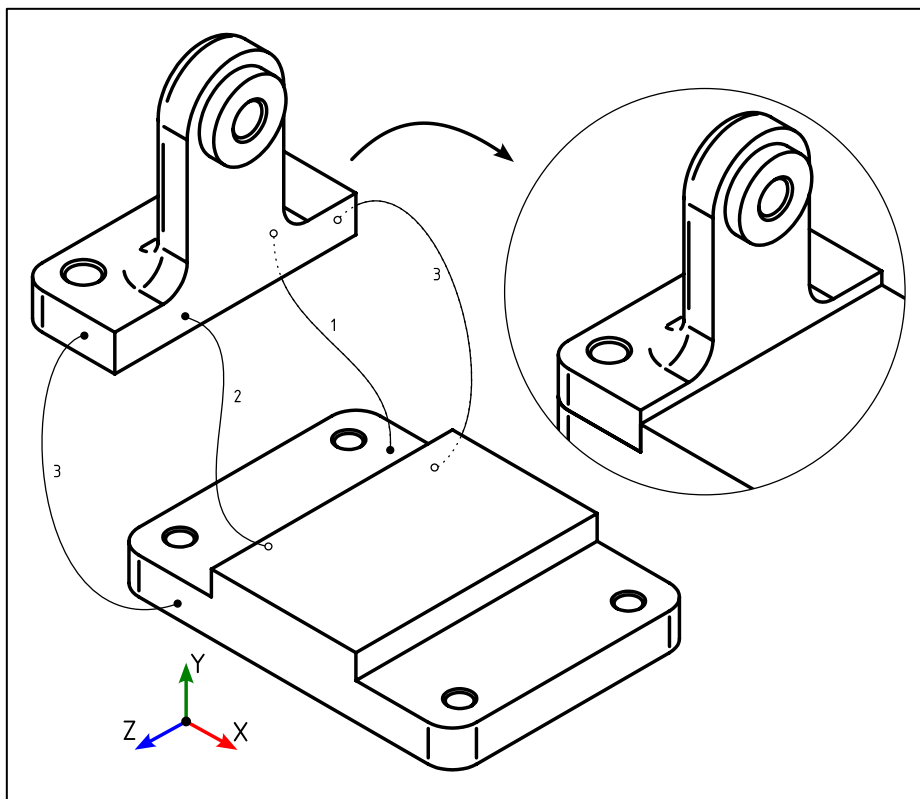


Fig. 3.10: “riser_asm” sub-assembly posing on the base component.

At this point, it is necessary to pre-assemble the two screws by lightly screwing them in for two simple reasons: the first is to free up the hand from holding the “riser_asm” sub-assembly in place (Fig. 3.11); the second reason is related to the correct insertion and positioning of the next sub-assembly. Since the “riser_asm” is not fully tightened, it will be possible to adjust its position to accommodate the “wheel_asm”.

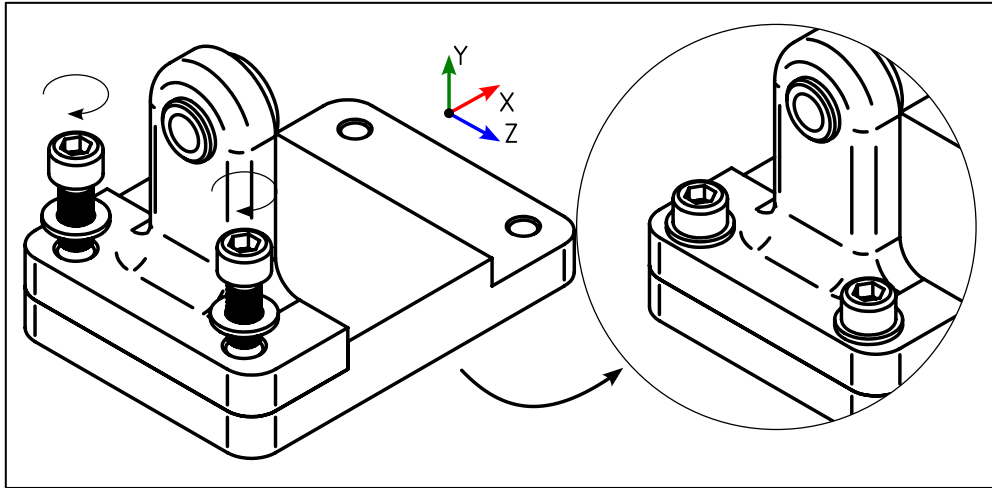


Fig. 3.11: Pre-mounting of M10 screws.

Now it is possible to insert the “wheel_asm” sub-assembly into the assembly already assembled so far, following the insertion direction along the X-axis (Fig. 3.12).

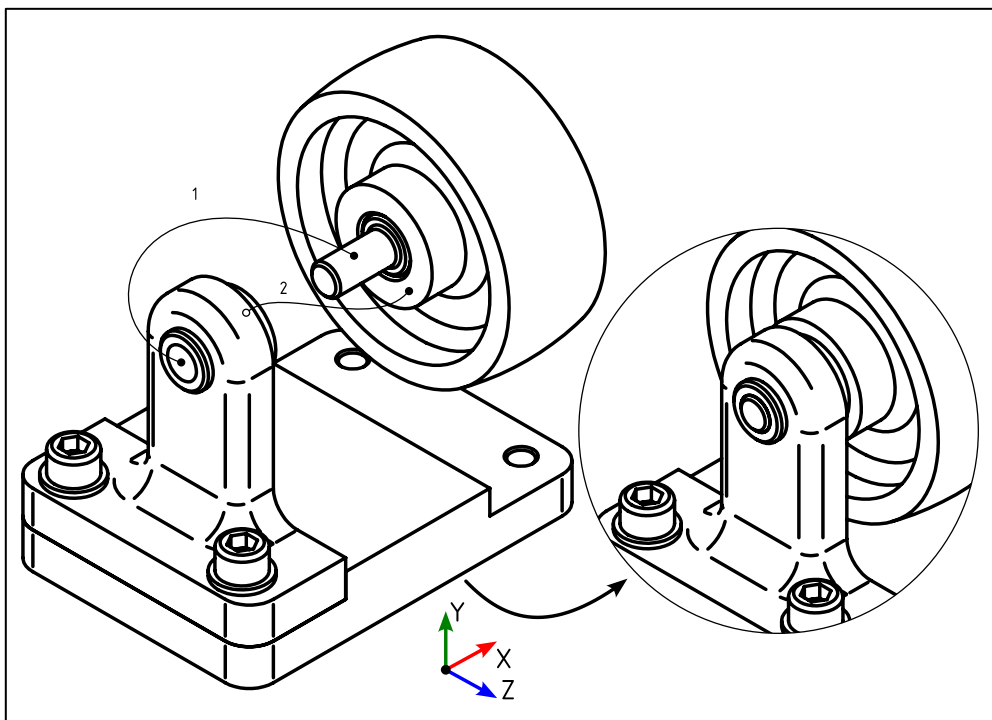


Fig. 3.12: “wheel_asm” insertion.

Next, proceed with the assembly of the second “riser_asm” sub-assembly (Fig. 3.13), following the same operations performed earlier, taking care to ensure that the shaft is properly seated inside the bushing.

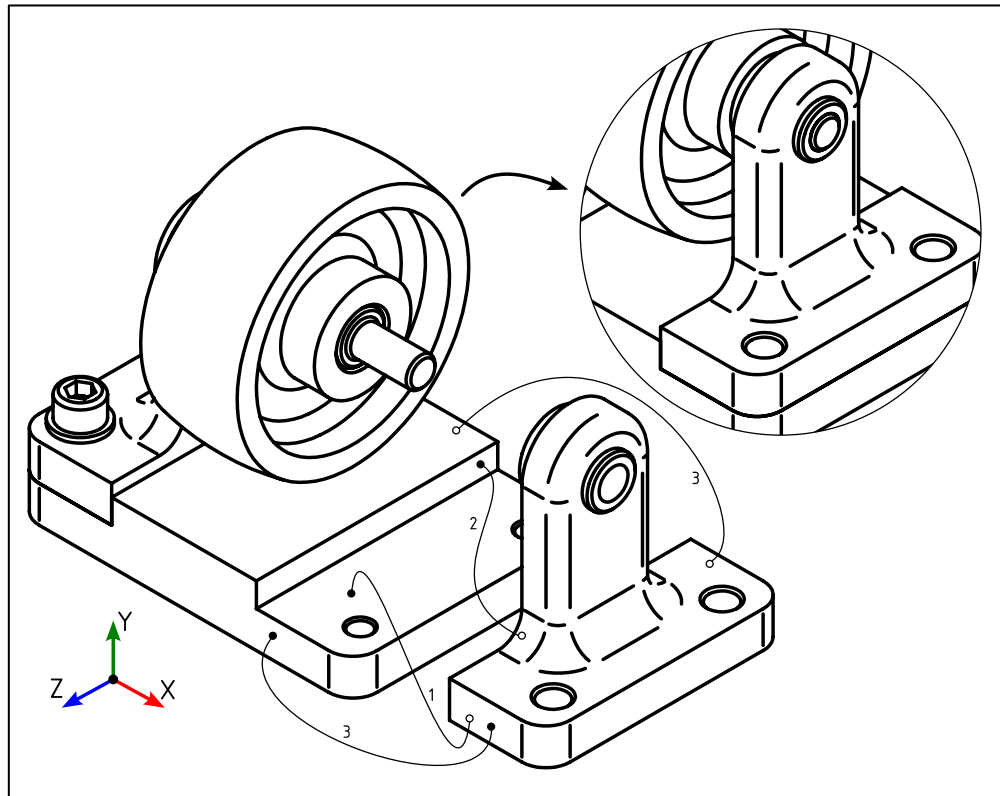


Fig. 3.13: assembly of the second “riser_asm” sub-assembly.

The remaining operation is the assembly of the 4 M10 screws (Fig. 3.14) that secure the complete object in place.

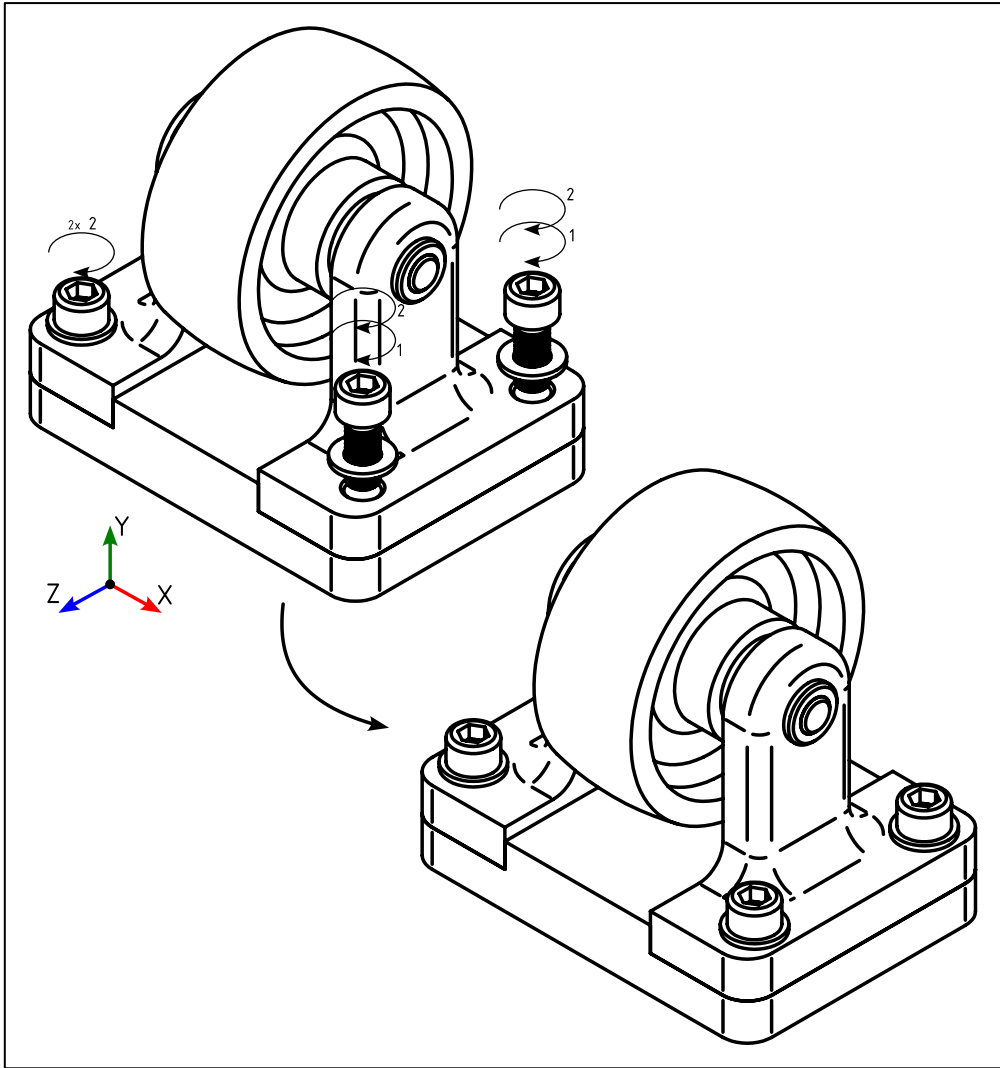


Fig. 3.14: tightening of all M10 screws.

3.3.4 Functional feature refinement

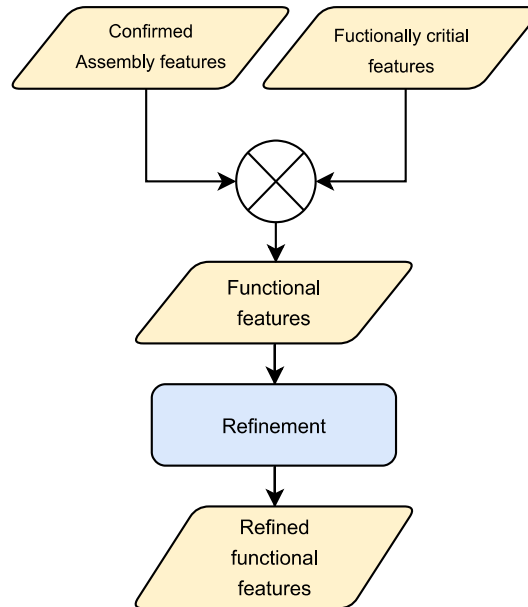


Fig. 3.15: Refinement of assembly surfaces phase.

In many cases, it is possible that the extension of a geometric feature classified as functional, according to the workflow, is much larger than the actual functional portion. For example, a planar surface may be classified as an assembly feature due to its contact with an adjacent part/sub-assembly, but the actual contact only occurs in a small portion of the surface.

If this is not addressed, in subsequent phases (functional specification), tolerances will be assigned to larger features than necessary. This would imply the use of more precise and accurate manufacturing processes than needed, resulting in increased production costs due to a poor functional description. A functional specification should strictly specify only the pure functional requirements, excluding functionality requirements that cannot be met. For instance, if a tight location tolerance is applied to a large planar surface because it is classified as an assembly surface, but the contact is limited to a small portion representing only 10% of the total surface area, then 90% of the surface controlled by the location tolerance is actually nonfunctional. This means that noncompliance in the nonfunctional area would lead to scrap a perfectly functional part.

Another peculiar case occurs when the same geometric feature serves two different functional needs. For example, the same planar surface may serve as an assembly feature to the previous level in one portion and as an assembly feature to the next level in another portion. Although they are both assembly requirements, according to phases 1 and 2 of the geometric specification methodology, the outcomes are very different. In the specification section, the

assembly features for the previous level will become datum features, while the assembly features for the next level will become controlled features. The refinement phase allows for the separation of contributions that define pure functional features, making it easier to create tolerance stack-ups. For example, if we assume the tolerance stack-up model proposed by Fischer [79], the ambiguity of integrating form tolerances into the stack-up is resolved. Paul Drake Jr.'s example of how to integrate form tolerances involved a geometric feature that is simultaneously an assembly feature for both the previous and subsequent levels [80]³.

For these reasons, it is crucial to refine the functional features for an effective functional description. This operation can be performed natively within the SolidWorks software, which was used throughout this case study. However, equivalent operations can be defined within each CAD tool.

To perform this operation, a "Top-Down" approach should be followed. The contact area between two components is identified by using the edges of the adjacent component's face. The geometric sketch is created in the part being refined, as a "converted entity" from the adjacent part. The shape of the geometric sketch depends on the shape of the adjacent part, while the sketch position depends on the assembly constraint in the assembly model. Any modifications to the parts or assembly constraint will impact the sketch accordingly. In some cases, the "convert entity" function may not work properly, especially when working with imported files. In such cases, it is up to the designer to properly remap the contact surface of the adjacent part, allowing for its parametrization.

Finally, to create the actual assembly feature, the sketch is used to "split" the surface. This can be achieved using the "Split Line" command in SolidWorks. The result of this process for our case study is shown in Fig. 3.16.

³ The example can be found in sub-section 9.3.1 and figure 9-10 of Paul Drake Jr.'s book [80].

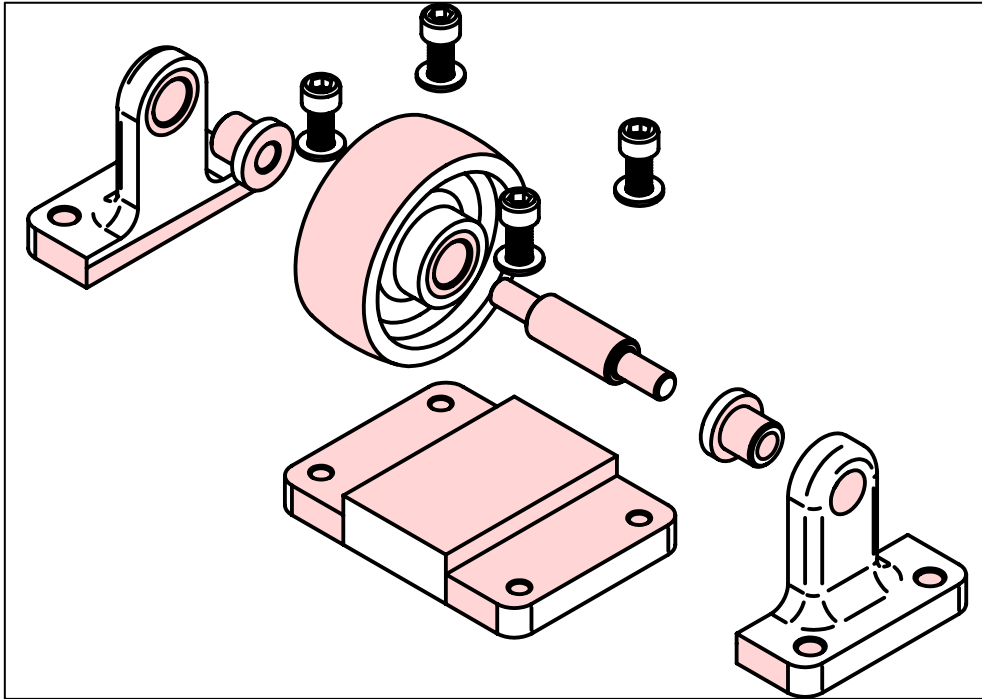


Fig. 3.16: Exploded view with all components where functional features are highlighted.

At this point, there is an interesting opportunity for visualizing the assembly, sub-assembly, or parts. A copy of the product containing only the functional surfaces can be generated, as shown in Fig. 3.17. The purpose is to “hide” all non-functional information that is not useful for the analysis, allowing the designer to focus solely on the functional surfaces/features.

In SolidWorks, this result is achieved using the “Offset Surface” command and selecting an offset distance of 0.00 mm . This creates a part file that includes both solid geometry (the modeled part) and a set of surfaces (the extracted surfaces). By hiding the solid model, the “surface model” can be viewed and studied. It is important to note that this result can be used as a baseline for generative design. With the interfaces and critical surfaces/features defined, a generative algorithm can optimize the material distribution, connecting these surfaces to withstand external loads and conditions.

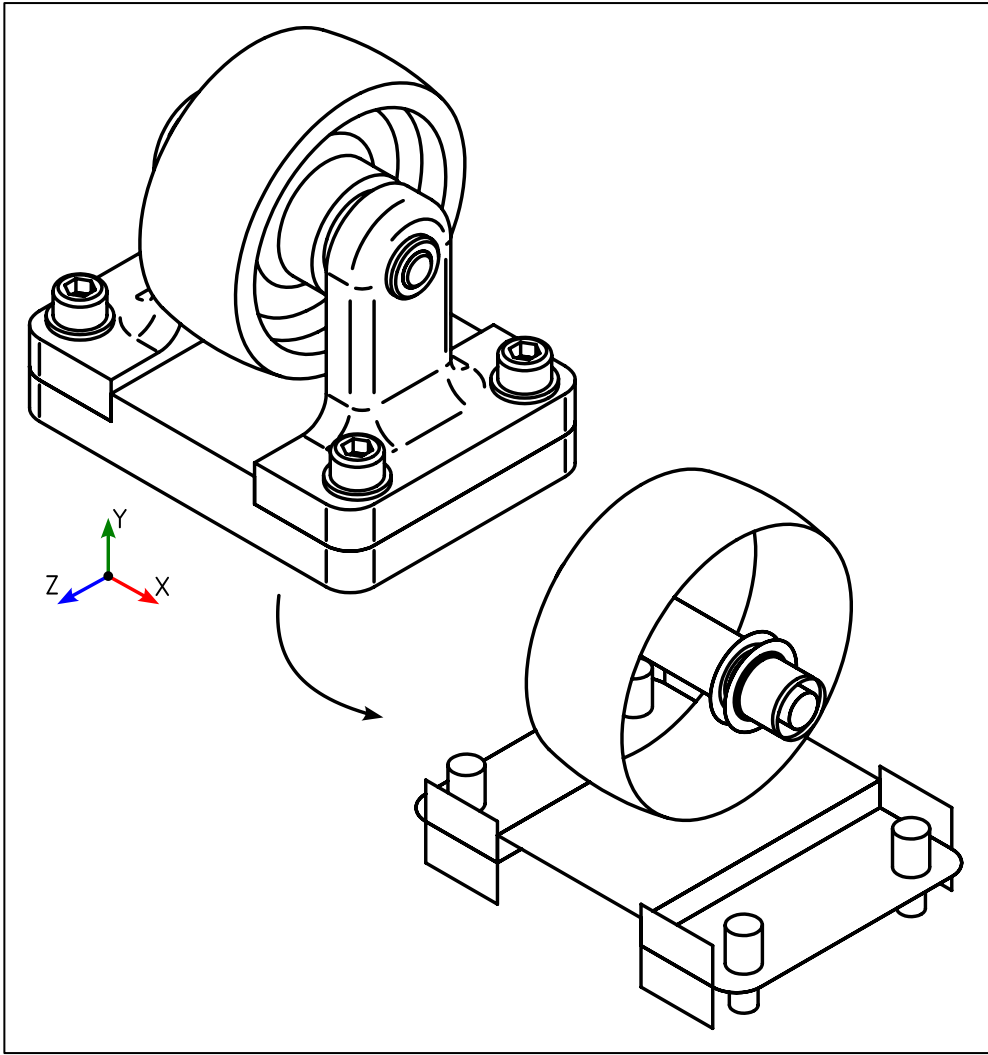


Fig. 3.17: Comparison between the solid model and the one with just the functional features.

3.3.5 Functional surfaces classification

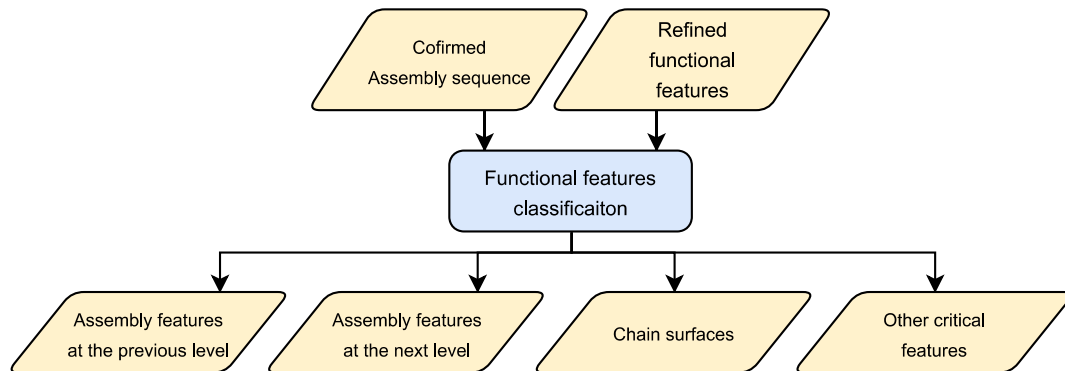


Fig. 3.18: Classification of functional features phase.

After analyzing the assembly procedure using the DfA analysis and confirming the optimal assembly procedure, a classification of all functional surfaces/features is performed. This classification is crucial for the subsequent phases as it allows for automated processing. During the initial stages of the method, at the assembly level, a collection of functional features, namely chain surfaces and other critical surfaces/features, were identified. With the help of the DfA analysis, the assembly surfaces are also identified. At this point, a formal classification for all functional surfaces can be as follows:

- Assembly surfaces/features:
 - At the previous level: surfaces and/or features used to assemble the part to what has already been assembled previously.
 - At the next level: surfaces and/or features used to assemble additional components or sub-assemblies to the part.
- Chain surfaces: surfaces that define gaps required for the proper functioning of the object and can be controlled through a tolerance stack-up.
- Other “critical” surfaces/features: all other surfaces/features that serve a functional need but do not contribute to the assembly or gaps controlled by tolerance stack-up.

Next, the results of the classification for each functional surface/feature in the case study (caster) are presented and discussed.

Examining the Base component (Fig. 3.19), we can identify two surfaces marked with the letter A, which represent a pattern of assembly surfaces at the next level. These surfaces will accommodate the “riser_asm” sub-assembly that will be assembled later. The letter B indicates a pattern of two vertical surfaces, which will serve as contact surfaces for the “riser_asm” sub-assembly, and are therefore classified as assembly surfaces at the next level. The letter C indicates

four features (threaded holes) that are categorized as surfaces with other functionalities. In this case, these features are not defined as assembly surfaces because, although they mate with four M10 screws and there is an actual assembly, the screws are considered off-the-shelf components. Their misplacement may make the assembly impossible but does not significantly affect the location of the parts in the final assembly. It is important to note that fastener elements should not be used for alignment purposes as they provide poor alignment compared to other solutions, see chapter 7. In fact, our focus is on the localization of these threaded holes with respect to the through holes in the “riser_asm”.

Surface D indicates a chain surface because it defines a required gap to prevent contact between the surface of the wheel and the Base. The four surfaces marked with the letter E identify small areas used for the alignment of the “riser_asm” sub-assembly. These areas represent the region used to align the “riser_asm” to the base. The alignment can be done manually (by the operator using their fingertips) or with the assistance of an external fixture (as supposed in this work). Therefore, these surfaces are classified as assembly surfaces at the next level.

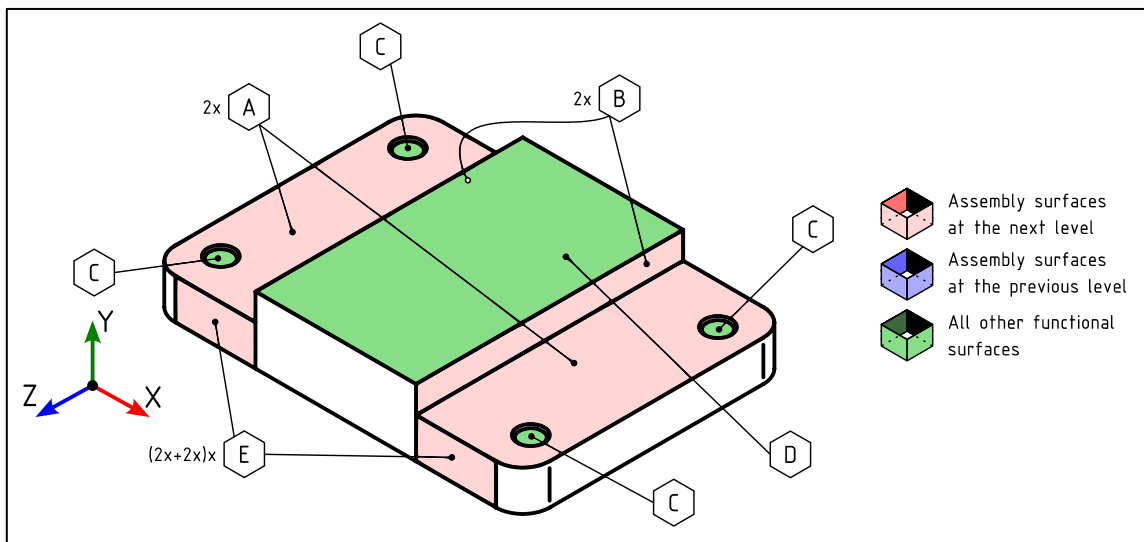


Fig. 3.19: Base component functional feature classification. A) Assembly features at the next level, B) Assembly features at the next level, C) Other functional features, D) Chain features, E) Other functional features.

Fig. 3.20 summarizes the functional surfaces visible when the “riser_asm” sub-assembly, consisting of the riser and bushing, is assembled. The two lateral surfaces indicated by the letter H are used for aligning the “riser_asm” with the Base, as mentioned earlier when discussing surfaces E on the Base (Fig. 3.19). In this case, these surfaces are classified as assembly surfaces at the previous level. Surfaces I and J come into contact with the Base component, and are therefore classified as assembly surfaces at the previous level. The two features identified by the letter K are the through holes through which M10 screws pass to secure the “riser_asm” to the base. Since we always want to maintain clearance between the holes and the screws, these are considered chain surfaces, as a minimum gap between each screw and hole is required. The surface indicated by

the letter L is also a chain surface, which is important for allowing the “wheel_asm” sub-assembly to rotate without experiencing friction. A gap should always be present between this surface and the “wheel_asm”. However, this same surface can also be considered an assembly surface at the next level, as it is nominally in contact with the “wheel_asm”. Lastly, feature M is an assembly surface at the next level, as the “wheel_asm” is assembled to it, creating a shaft-hole connection. It is important to note that this connection needs to be a clearance fit to allow for the free rotation of the “wheel_asm”.

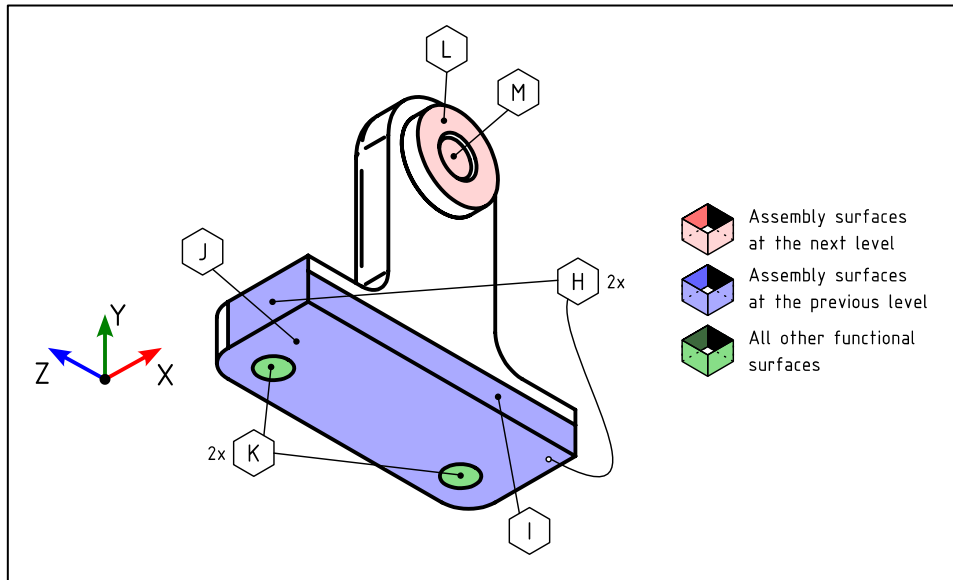


Fig. 3.20: “riser_asm” sub-assembly functional feature classification. H) Assembly features at the previous level, I) Assembly features at the previous level, J) Assembly features at the previous level, K) Other functional features, L) Chain features / Assembly features at the next level, M) Assembly features at the next level.

Analyzing the riser component in detail (Fig. 3.21), in addition to the surfaces mentioned in Fig. 3.20 (I, J, K, H), we observe the following: the feature (hole) indicated by the letter F, which represents an assembly surface at the next level where an interference fit between the riser and the bushing takes place; and the surface indicated by G, which refers to the surface that will be in contact with the bushing. Therefore, both the hole and the surface are considered assembly surfaces at the next level.

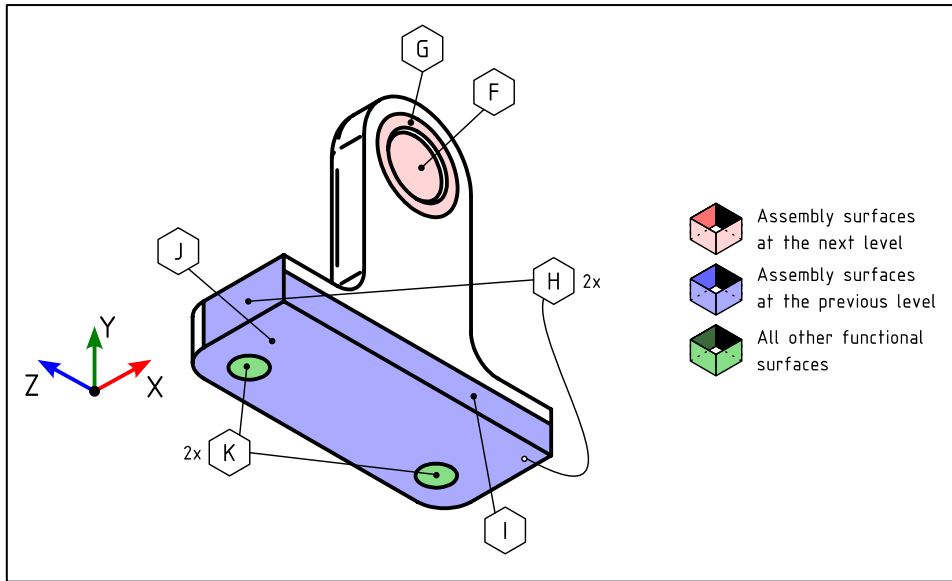


Fig. 3.21: Riser component functional feature classification. F) Assembly features at the next level, G) Assembly features at the next level, H) Assembly features at the previous level, I) Assembly features at the previous level, J) Assembly features at the previous level, K) Other functional features.

For the bushing component (Fig. 3.22), the features L and M were already analyzed at the sub-assembly level and their function does not change here at the component level. Besides these two, we can also highlight surface N, which comes into contact with the riser, and feature O, which mates with the riser through an interference fit. Therefore, both surface N and feature O are considered assembly surfaces/features at the previous level.

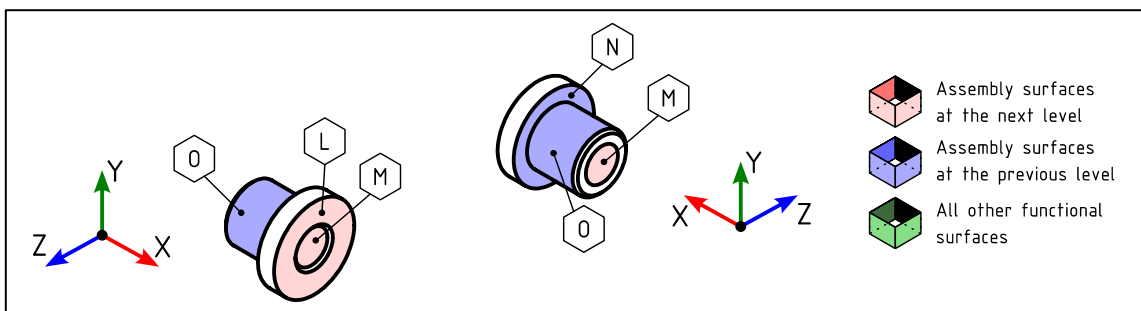


Fig. 3.22: Bushing component functional feature classification. L) Chain features / Assembly features at the next level, M) Assembly features at the next level, N) Assembly features at the previous level, O) Assembly features at the previous level.

Fig. 3.23, shows the classification of the functional surfaces after obtaining the sub-assembly "wheel_asm". The features indicated by the letter P refer to the features that have a clearance fit with the bushings, therefore they are classified as assembly surfaces at the previous level. The

surfaces labeled with the letters Q and S actually identify a single surface at the sub-assembly level and are classified as chain surfaces that oppose the surfaces of the bushing (indicated by the letter L in Fig. 3.22). Alternatively, these same surfaces can also be considered as assembly surfaces at the previous level. The surface labeled with the letter U is also a chain surface since it defines the gap with the base component that needs to be controlled.

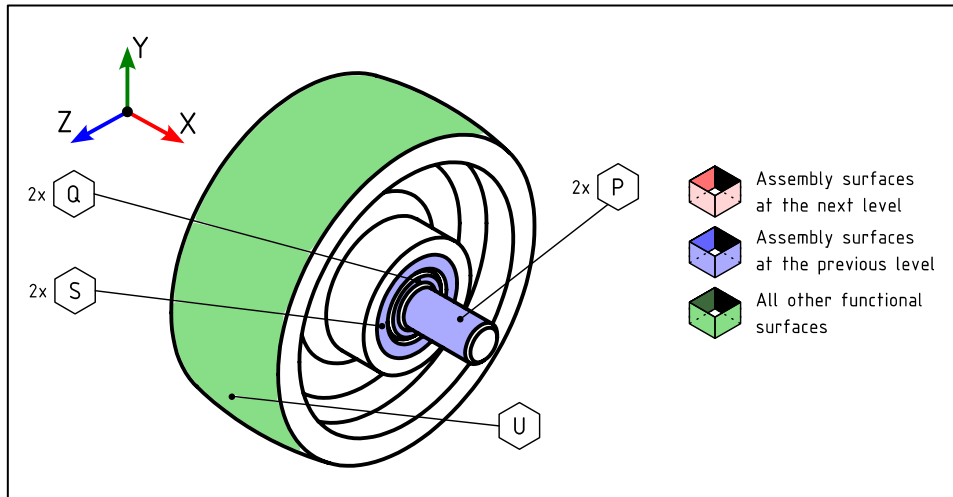


Fig. 3.23: – “wheel_asm” sub-assembly functional feature classification. P) Assembly features at the previous level, Q) Chain features / Assembly features at the previous level, S) Chain features / Assembly features at the previous level, U) Chain features.

Analyzing the Shaft component, in addition to the surfaces indicated by the letters P and Q, in Fig. 3.24, which were already analyzed at the sub-assembly level (Fig. 3.23), it is possible to identify the feature labeled by the letter R. This surface represents an assembly surface at the next level, as the wheel will be assembled with interference, ensuring rotation without slippage between the parts.

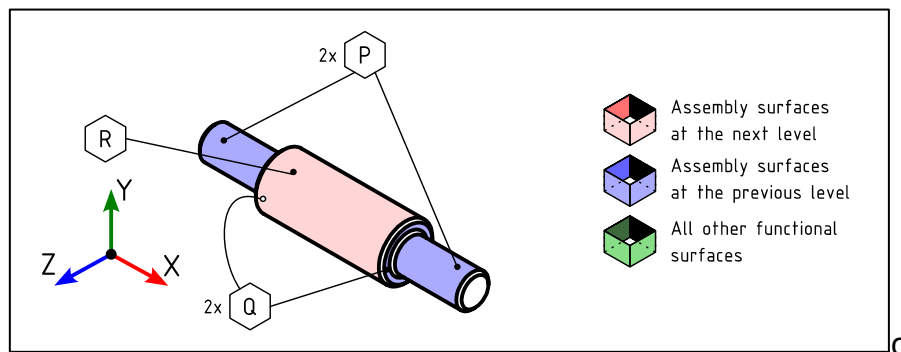


Fig. 3.24: Shaft component functional feature classification. P) Assembly features at the previous level, Q) Chain features / Assembly features at the previous level, R) Assembly features at the next level.

The wheel component (Fig. 3.25) also shows, in addition to surfaces S and U that were already analyzed at the sub-assembly level (Fig. 3.23), the surface indicated by the letter T. This surface serves as an assembly surface at the previous level, as it accommodates the interference fit with the shaft.

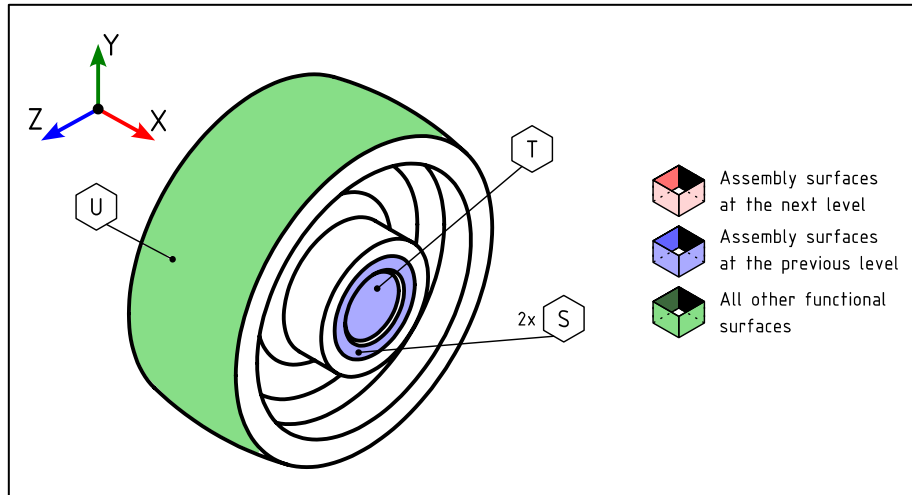


Fig. 3.25: Wheel component functional feature classification. S) Chain feature / Assembly features at the previous level, T) Assembly features at the previous level, U) Chain feature.

The final result, as carried out in our case study, is depicted in Fig. 3.26, where only functional surfaces are included in an “exploded” assembly. Functional surfaces with different purposes are distinguished by different colors: green for chain surfaces and surfaces with other functionalities, blue for assembly surfaces at previous level, and red for assembly surfaces at the next level.

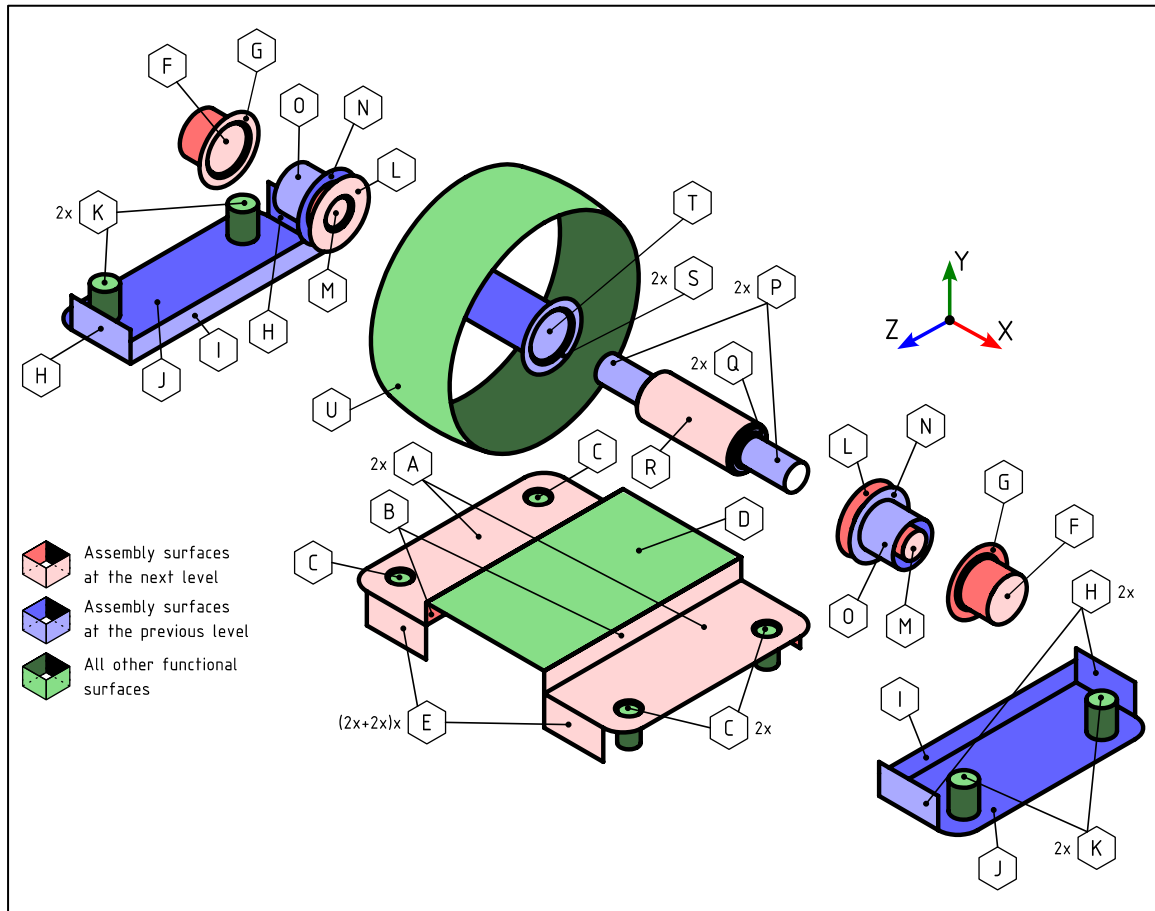


Fig. 3.26: Exploded view with all functional features highlighted.

3.3.6 Geometric specification

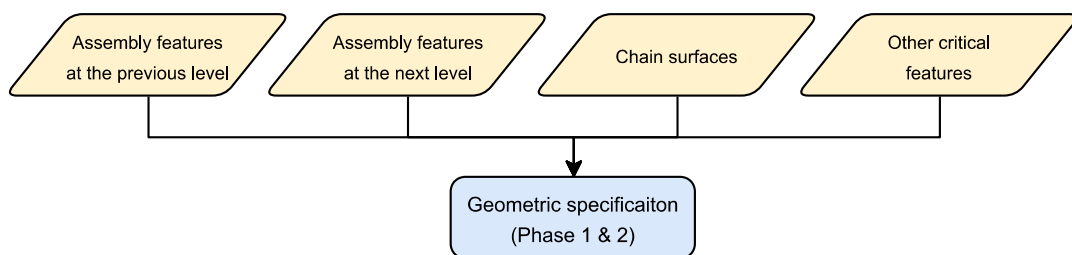


Fig. 3.27: Geometric specification phase.

In this final phase, we encompass phases 1 and 2 of the Functional Geometric Specification Method proposed by the Design Tools and Methods in Industrial Engineering Laboratory (referenced in the introductory section of this chapter) to obtain the functional geometric specification of the assembly/sub-assembly/parts we are dealing with.

The main characteristics that a quality geometric specification must adhere to are as follows:

- **Correctness:** There should be no formal errors in the specification (incorrect usage of symbology).
- **Coherence:** Different specifications should not contradict each other.
- **Completeness:** Each geometric element should be completely defined (all its degrees of freedom shall be controlled).
- **Essentiality:** The interrelation between different geometric elements should be as direct as possible, avoiding unnecessary information (e.g., avoiding the concatenation of Datum Systems within a part).
- **Effectiveness:** The specification should contain only the relevant information needed for functionality description.
- **Efficiency:** The specification should contain the least amount of information possible with the largest tolerances possible, requiring less time to be generated and resulting in lower production costs for the part.

Regarding this set of properties for a quality geometric specification, it is important to note that the first three points are mandatory, as the comprehension of the geometric specification is at risk without them. The last three points are “optional,” meaning that they are the properties that distinguish an outstanding geometric specification from a good one.

To achieve a quality geometric specification, it is advisable to anticipate the distinction between reference and referenced surfaces/features in phase zero. This involves distinguishing between the datum features and the controlled ones, or in other words, determining which surfaces/features will be included in the Datum System and in what hierarchical order.

The use of a model with pre-labeled surfaces, or even a model with only functional surfaces, helps to avoid ambiguity in this phase as the designer is not distracted by non-functional geometries. The refinement of functional surfaces also makes the process of identifying the Datum targets or restricted zones in which specific tolerances will be applied more intuitive.

As a general rule, the assembly surfaces/features to the previous level become datum features. These surfaces/features, which are used to position the part in the assembly, generally restrict all degrees of freedom and represent the interface of the part with the already established sub-assembly. Any misplacement of these surfaces will directly impact the placement of all other surfaces/features of the part. For these reasons, they are the best candidates to become the functional Datum System.

In cases where the part, when placed into the previous assembly, is not completely locked, meaning that a datum system based on the assembly features to the previous level cannot restrict all degrees of freedom, additional surfaces/features from the assembly level to the next level need to be included to achieve a completely defined datum system that locks all functional degrees of freedom. The selection of these surfaces/features from the assembly surfaces to the subsequent

level depends on the assembly order, and the hierarchical order between datum features is derived from the assembly order and sequence defined for the DfA analysis.

It is noteworthy that in order to define a completely defined Datum System, the functional degrees of freedom are invoked. We can differentiate between geometric degrees of freedom, which consider the full geometry of the part, and functional degrees of freedom, which only consider the functional features (see also Fig. 3.26). Therefore, even if a part is not axisymmetric due to non-functional features such as lightening holes, it can still be considered functionally axisymmetric.

Datum Features definition

In the following, a qualitative description of the Datum Systems for each sub-assembly and part of our case study will be provided. It should be noted that at this stage, the focus is on identifying the geometries that will compose the datum system and establishing the hierarchy among them, rather than assigning actual specifications.

For the Base component (Fig. 3.28), as it is the first in the assembly process, it does not have any assembly features to the previous level. Therefore, the datum features will be selected from the assembly surfaces to the subsequent level. Firstly, there is a primary Datum, which is defined by a common plane formed by the two horizontal surfaces where the risers are placed. This primary Datum locks the translation along the Y-axis and rotations around the X and Z axes. Secondly, there is a secondary Datum, which is defined by the collection of the two vertical surfaces where the risers stop in the X direction, creating a midplane. This midplane locks the translation along the X-axis and rotations around the Y-axis. Lastly, there is a tertiary Datum, which corresponds to the middle plane identified by the 2+2 lateral vertical surfaces used for the risers' alignment in the Z direction. This tertiary Datum restricts the remaining degree of freedom, namely the translation along the Z-axis. With these datum features in place, the datum system for the Base component is completely defined.

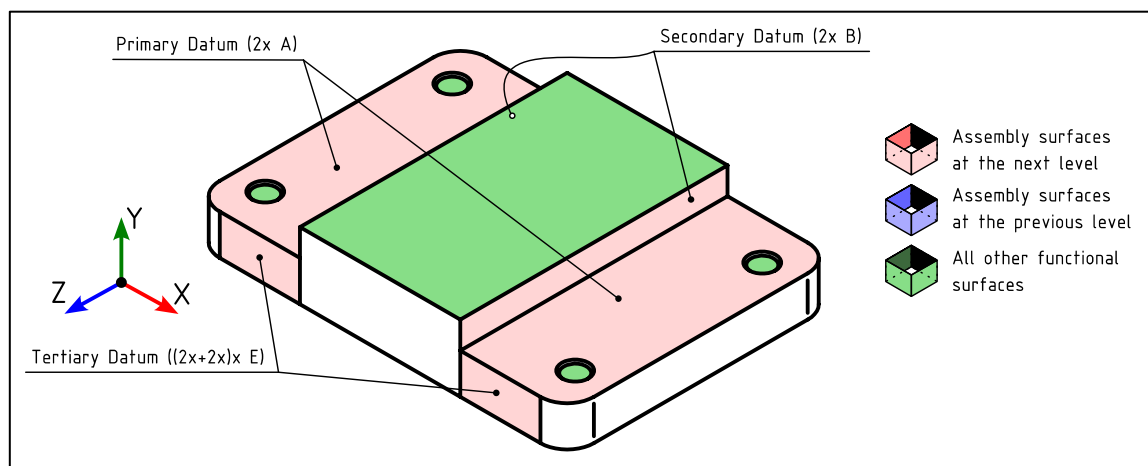


Fig. 3.28: Base component Datum System description.

Regarding the sub-assembly “riser_asm” (Fig. 3.29), the primary Datum chosen is the lower surface, which corresponds to the initial pose of the riser_asm on the Base. This plane locks the translation along the Y-axis and rotations around the X and Z axes. The vertical surface in contact with the Base has been identified as the secondary Datum, which locks the translation along the X-axis and rotation around the Y-axis. Additionally, the middle plane identified by the two lateral vertical surfaces will lock the translation along the Z-axis. It is evident that this Datum System aligns with the one declared for the Base component. The other functional surfaces, all located in the bushing component, will become referenced surfaces in the assembly.

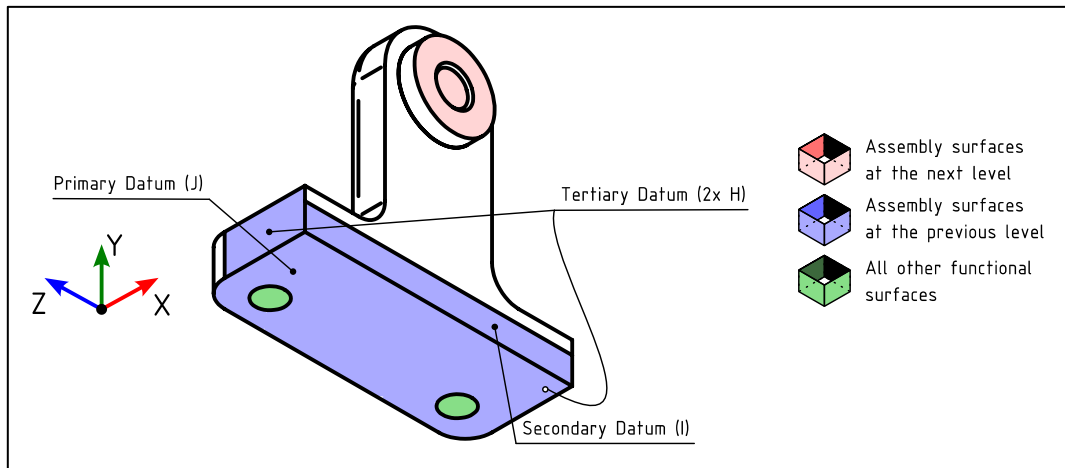


Fig. 3.29: “Riser_asm” Datum System description.

The riser component (Fig. 3.30) has the same Datum System as described in Fig. 3.29 for the sub-assembly “riser_asm.” This is possible because all the datum features at the sub-assembly level are from the same component, allowing for a direct transfer of the Datum System to the part level.

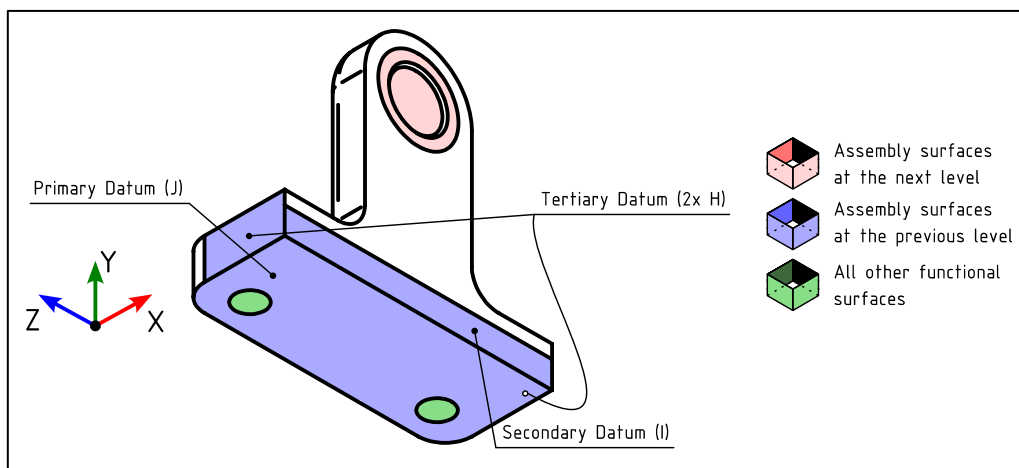


Fig. 3.30: Riser Datum System description.

The Datum System of the “bushing” (Fig. 3.31) includes, as the primary datum, the axis of the outer cylinder, the one mating with the riser. It locks both translations and rotations about the Y and Z axes. The secondary datum is identified by the vertical surface in contact with the riser, which locks translation along the X axis. By looking at the degrees of freedom locked by the datum system it is possible to realize that the rotation around the X-axis is still free therefore the datum system looks as it is not completely defined. Even though the datum system locks five degrees of freedom out of six it can be considered fully defined since the part is functionally and geometrically axisymmetric therefore the rotation around the X-axis cannot be lock in any case.

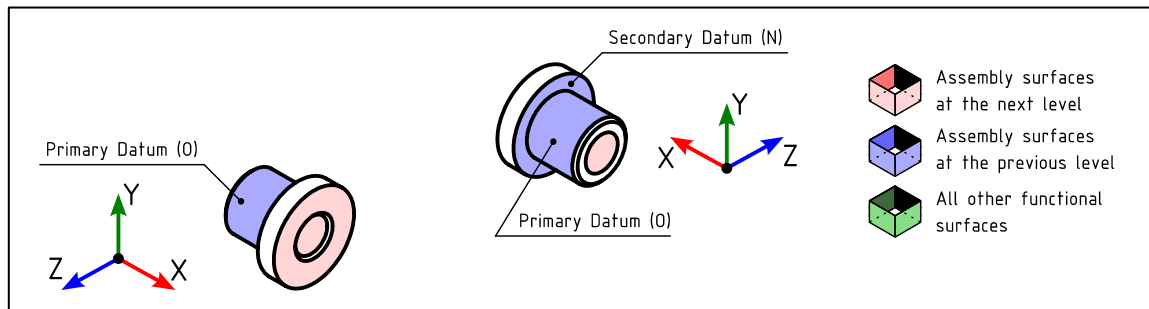


Fig. 3.31: Bushing Datum System description.

The Datum System for the sub-assembly “wheel_asm” (Fig. 3.32) includes the axis common to the two cylindrical features on the shaft that mate with the Bushings as the primary datum. This datum locks translations and rotations about the Y and Z axes. The secondary datum is identified by the collection of the two vertical side surfaces in common between the shaft and the wheel, forming a midplane that locks translation along the X-axis. Similarly to previous cases, the Datum System locks five out of six degrees of freedom, but since the sub-assembly is functionally axisymmetric, the rotation around the X-axis does not need to be locked.

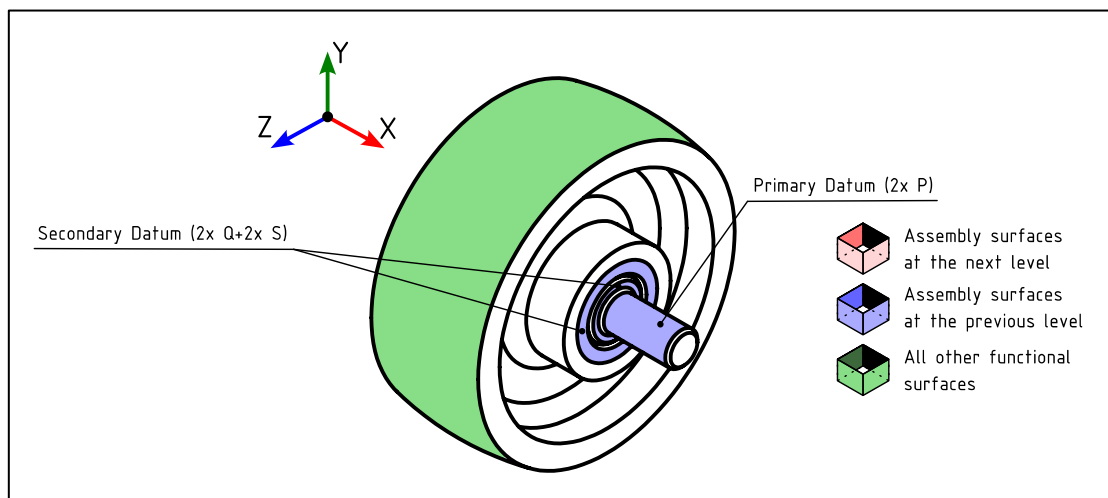


Fig. 3.32: “Wheel_asm” Datum System description.

For the Shaft component (Fig. 3.33), the primary datum corresponds to the datum identified in Fig. 3.32 for the “wheel_asm” sub-assembly. Similarly, the secondary datum corresponds to the portion of the secondary datum on the “wheel_asm” that pertains to the shaft, which includes the two vertical side surfaces. The resulting Datum System is very similar to that of the “wheel_asm,” and the same considerations can be made regarding its degrees of freedom.

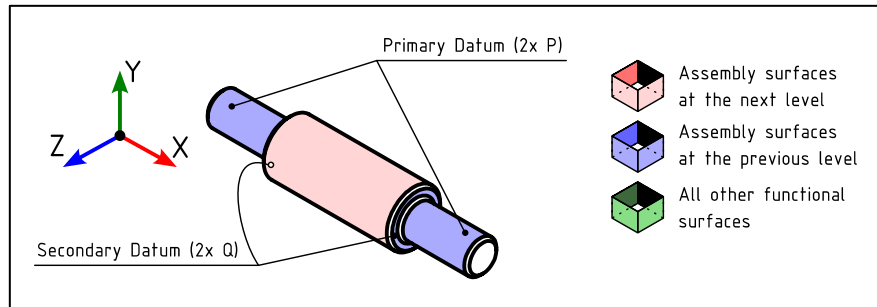


Fig. 3.33: Shaft Datum System description.

Regarding the wheel component, as shown in Fig. 3.34, the primary datum is identified by the axis derived from the through hole that mates with the shaft component. It locks translations and rotations about the Y and Z axes. The secondary datum coincides with the portion of the secondary datum on the “wheel_asm” that pertains to the wheel component, specifically the two side surfaces. This datum locks translation along the X-axis. Similarly to previous cases, we have a completely defined Datum System that does not lock rotations around the X-axis, as the part is axisymmetric.

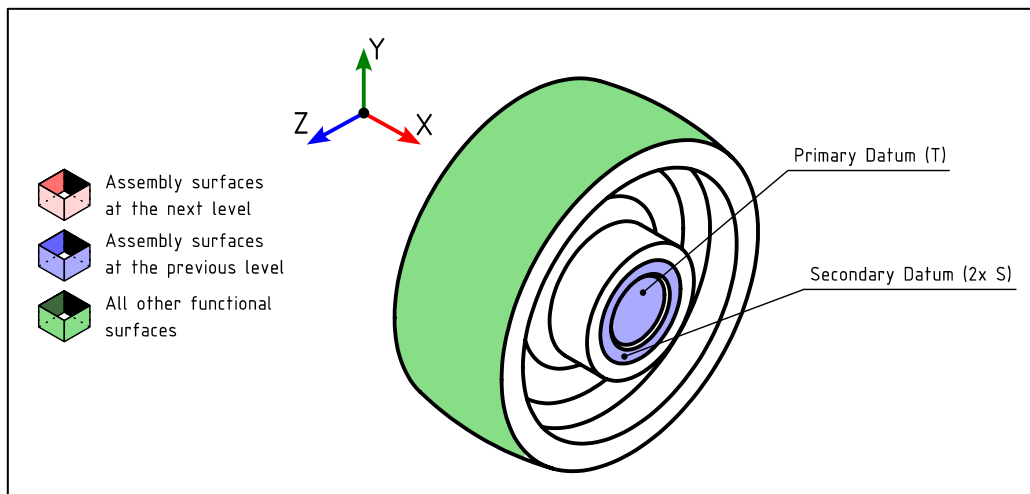


Fig. 3.34: Wheel Datum System description.

With this set of information in mind the actual phase of geometric specification can start leading to the creation of 2D drawings and/or MBD. For our case study 2D drawings will be presented in the next chapter.

3.4 || Conclusion

The objective of this chapter was to introduce a formal methodology suitable for the functional analysis of a product, leading to the identification of functional features. After this initial step, functional features are further categorized into different clusters, including assembly features at the previous and next levels, chain features, and other functional features. This categorization is essential to streamline the subsequent geometric specification process, which will be detailed in the following chapter.

The methodology is inherently top-down, seamlessly aligning with the framework outlined in Chapter 2. Moreover, the methodology itself, which requires a physical or virtual disassembly of the product, encourages designers to adopt a top-down approach, helping to overcome the deeply ingrained “Bottom-Up” approach often prevalent in industry. Additionally, identifying sub-assemblies for specification is crucial, as these sub-assemblies may represent products manufactured by external suppliers. Having a dedicated functional specification that includes assembly surfaces facilitates better coordination among different sub-assemblies.

The refinement of functional features, which essentially entails segmenting geometrical features to extract their functional portions, is a step that enables a more focused examination of the functionality of each geometry. However, its implementation may be influenced by the specific software in use. Different strategies can be applied using various software packages. Nevertheless, the segmentation procedure based on a top-down approach should be feasible with most major CAD tools available on the market, requiring only minimal adjustments to the procedure presented here.

Lastly, another notable aspect of this procedure is the integration of the Design for Assembly (DfA) process into the definition of functional features. This integration, apart from being crucial for identifying an optimal assembly procedure, has also proven effective in obtaining information about surfaces that can serve as Datum Targets for individual parts.

4 || Creation of functional specifications

Design must be functional, and functionality must be translated into visual aesthetics without any reliance on gimmicks that have to be explained.

Ferdinand Porsche

In this chapter, the description of the methodology developed by the Design Tools and Methods in Industrial Engineering Laboratory at the University of Padova for creating functional specifications will be concluded. The preceding chapter covered “phase 0,” detailing a formal methodology for conducting this phase, which was proposed and discussed. Here, the subsequent phases, namely “phase 1” and “phase 2,” will be presented. An illustrative overview of the comprehensive methodology is depicted in Fig. 4.1.

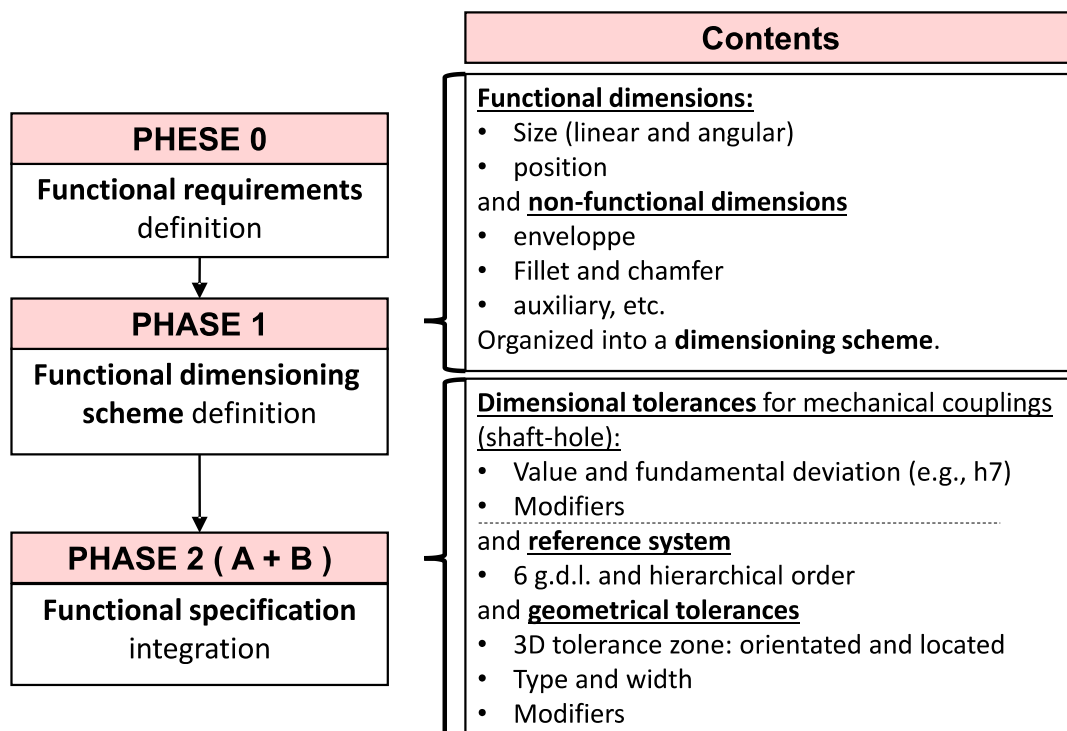


Fig. 4.1: Schematic view of the methodology to create functional specification.

At the conclusion of phase 0, as described in the previous chapter, all functional features/surfaces are identified and categorized. Additionally, the datum features and their hierarchical order have already been established, although their formal indication as datum features will be defined in phase 2.

In Phase 1, the functional dimensioning scheme is outlined. Each part (or sub-assembly, considered independently as a whole) can be broken down into fundamental geometric solids/elements (such as prisms, cones, pyramids, etc.) [81]. At this point, each geometric element can be dimensioned to define its “*bulk dimensions*” (e.g., the radius of a sphere or the side of a cube), and various basic solids can be spatially positioned in relation to one another, establishing their interrelationships. These relationships can be explicit through linear/angular dimensions referred to as “*distances*” or implicit through geometric constraints (e.g., collinearity, perpendicularity, symmetry, etc.). Initially, all these dimensions, necessary to characterize the dimensions of the basic solids and their relative arrangement, constitute the “geometric dimensioning scheme.” As the name implies, this dimensioning scheme holds a purely geometric significance and aligns with the set of dimensions and geometric relationships required to generate the CAD model.

Within these dimensions, it's essential to differentiate between “Functional dimensions” and “Non-Functional dimensions.” This differentiation traces its origins back to the standards of the 1960s [82,83]. As previously mentioned in this document, functionality pertains to the assembly. Consequently, it's not feasible to distinguish between functional and non-functional dimensions without an understanding of the assembly conditions between the part and its adjacent components. While the concept of functionality plays a pivotal role in this chapter and will be further explored later, for now, Functional Dimensions can be defined as encompassing all the essential dimensions and distances involving functional features. The identification of functional features is a part of Phase 0.

Within functional dimensions, two distinct categories of dimensions can be established:

- **Sizes:** These dimensions regulate the clearance or interference condition between two mating features. Only “bulk dimensions” can be classified as sizes.
- **Distances:** These dimensions determine the position of functional features. All distances in the “geometric dimensioning scheme” become “distances” within this context. “Bulk dimensions” may also be categorized as “distances,” such as the bulk dimension of a solid utilized for a Boolean subtraction.

This classification of dimensions diverges from the purely geometric meaning that is relevant to the so-called “geometric dimensioning scheme” and starts to integrate functionality requirements into its definition, thus evolving into the “functional dimensioning scheme.”

In Phase 2, specifications (tolerances) are introduced. While Phase 1 focuses on describing the fundamental geometry, Phase 2 considers permissible deviations from the nominal dimensions. It's essential to note that these specifications apply to the physical object (which can be described using a skin model) rather than the ideal one (nominal). Dimensional tolerances are defined for

sizes, and various modifiers can be added to these to refine the conveyed functional message. Furthermore, geometric tolerances are defined to manage the allowable deviation from the ideal geometry of actual integral or derived features.

Geometrically controlling these elements involves determining and defining the space (nominal geometry) within which the real feature must fit to ensure functional requirements are met (tolerance zones). To associate the real geometry with the nominal description of the tolerance zone, a datum system is employed, which formally outlines how to make this association. While this text does not aim to describe this procedure in detail, more information can be found in the relevant standards [73]. A datum system relies on a collection of datum features, which should inherently be functional features. All other functional features are located and/or oriented relative to the datum system.

Various types of geometric tolerances can be identified:

- Position tolerances: These tolerances determine the location of the feature in relation to the Datum System, resulting in a tolerance zone that is entirely constrained in all degrees of freedom. As the actual feature must fit within this tolerance zone, it also constrains orientation and form.
- Orientation tolerances: These tolerances govern the “inclination” of a feature with reference to the Datum System, leading to a tolerance zone constrained only in rotational degrees of freedom. This type of tolerance also restricts form deviations.
- Form tolerances: These tolerances control the shape of the feature in relation to its ideal shape. The tolerance zone is essentially free to move in relation to the datum system.

In the following sections, a description of the actions required within each phase will be presented. To illustrate the methodology, the riser component will be used as an example.

4.1 || Phase 1: functional dimensioning scheme

Phase 1 is subdivided into five distinct subphases that guide the designer in defining the functional dimensioning scheme:

- Phase 1.1: identification of size dimensions.
- Phase 1.2: identification of distance dimensions.
- Phase 1.3: identification of restricted feature dimensions.
- Phase 1.3: identification of non-functional dimensions.
- Phase 1.4: creation of the dimensioning scheme layout.

In the following subsections, each sub-phase will be analyzed. The process starts with a blank drawing featuring the basic geometry in orthogonal view, as shown in Fig. 4.2. In this drawing, the feature refinement is already outlined.

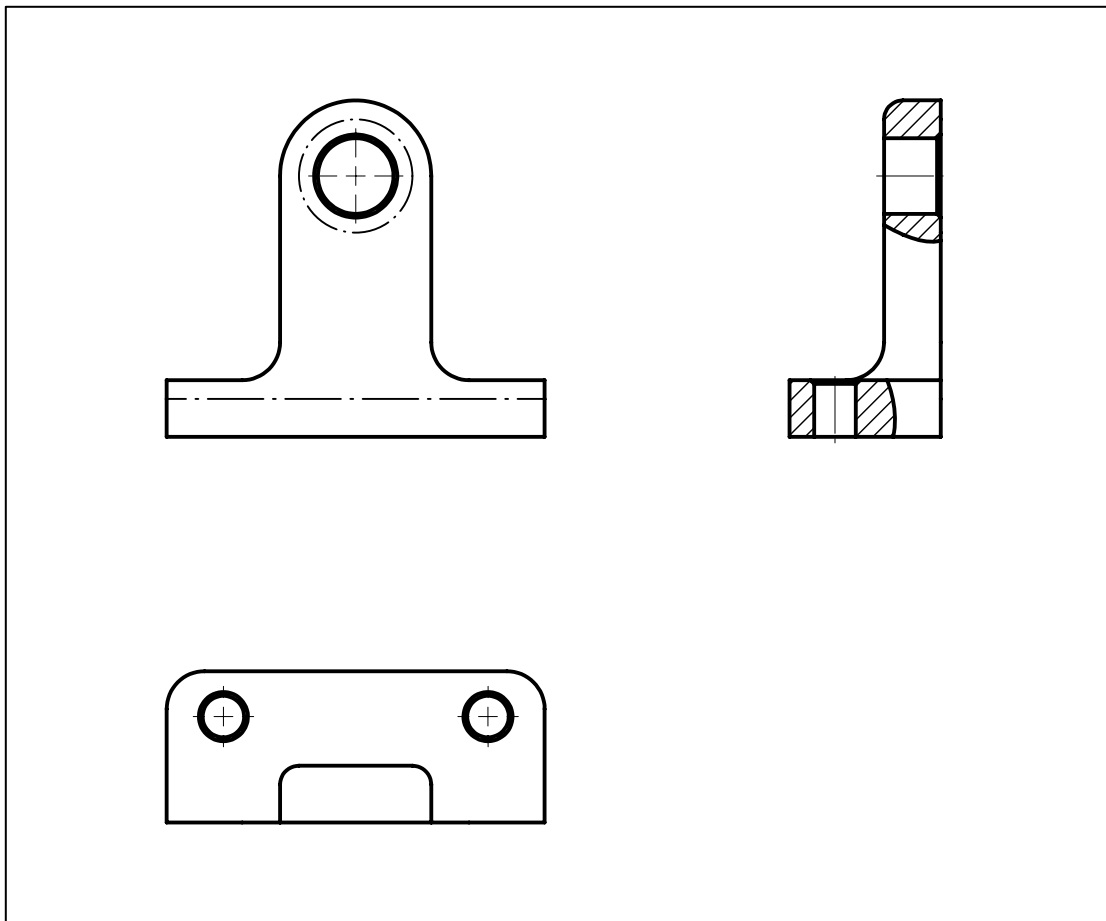


Fig. 4.2: orthogonal views of the risers.

4.1.1 Phase 1.1: Size dimensions

In Phase 1.1, the size dimensions are defined. Two distinct subpoints can be identified:

- Identification of mating features (features of size).
- Addition of mating features' nominal dimensions to the drawing.

Mating features can be found among the assembly features. Holes through which screws or shafts pass are always considered features of size, even if their classification can also be considered as a chain feature as discussed in the previous chapter.

For the riser, the features of size can be identified as follows: the two features “K” where two screws need to pass through, the feature “F” where the bushing is inserted with interference, and

the thickness identified by the two planar surfaces “H” that are simultaneously used to center the riser onto the base. The letters are the same as in Fig. 3.21. The identified features of size are highlighted in Fig. 4.3.

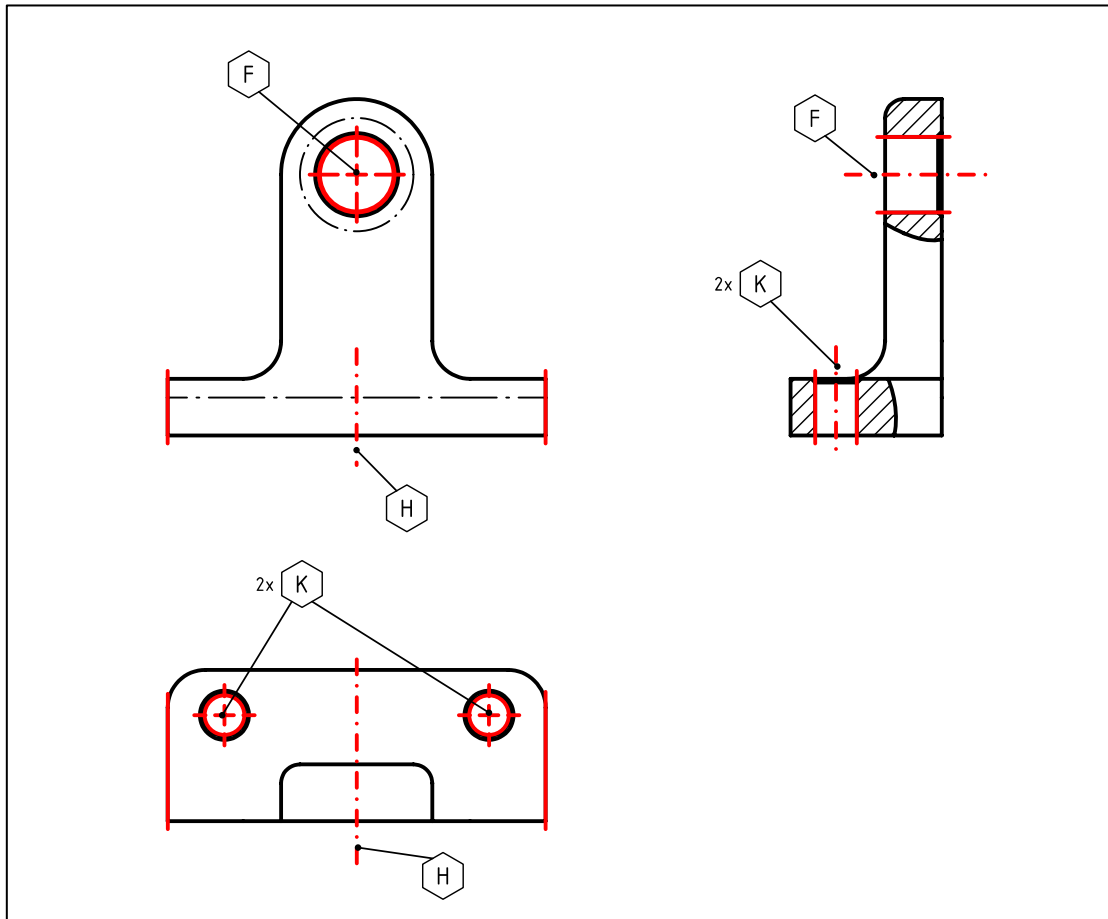


Fig. 4.3: orthogonal views of the risers with mating features (feature of size) highlighted.

A dimension is then added to the drawing for each of these features, as shown in Fig. 4.3

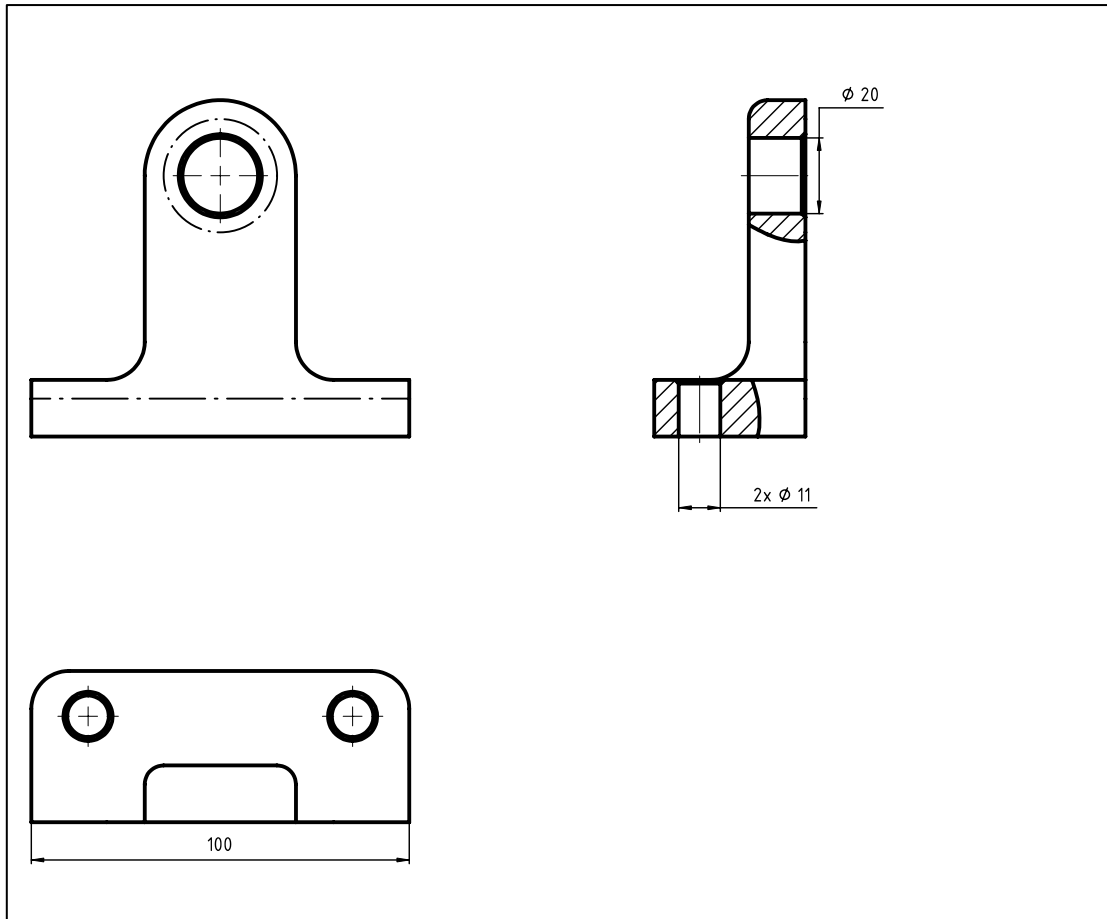


Fig. 4.4: orthogonal views of the risers with size dimension.

4.1.2 Phase 1.2: Distance dimension

Also in Phase 1.2, two distinct sub-phases can be identified:

- Identification of reference and referenced features.
- Addition of the nominal distance from the reference features to the referenced features on the drawing.

The reference features are the datum features that were classified during Phase 0: surface J as the primary datum, surface I as the secondary datum, and feature H (already defined as a feature of size) as the tertiary datum. All other functional features are referenced features: the two features of size K, the feature of size F, and the feature G. A summary of the reference and referenced features is shown in Fig. 4.5 : in red reference features, in green referenced features; it must be noted that for features of size, both the integral feature and the derived features are highlighted.

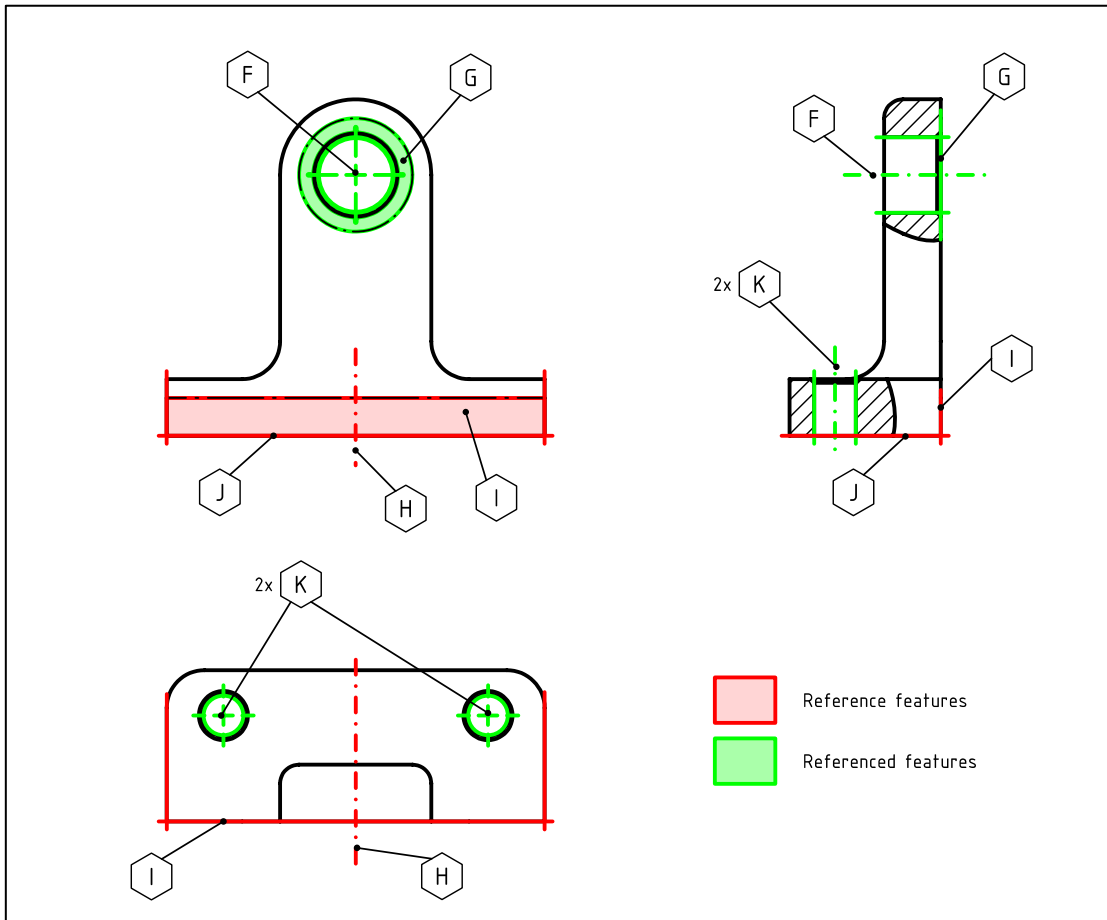


Fig. 4.5: orthogonal views of the risers with reference and referenced mating features highlighted.

A nominal dimension connecting each referenced feature to the relevant reference feature can now be added to the drawing. Symmetries are assumed implicitly, zero values linear and angular dimensions, and 90° or 180° angular dimensions are not explicitly added to the drawing. The result for the riser is shown in Fig. 4.6.

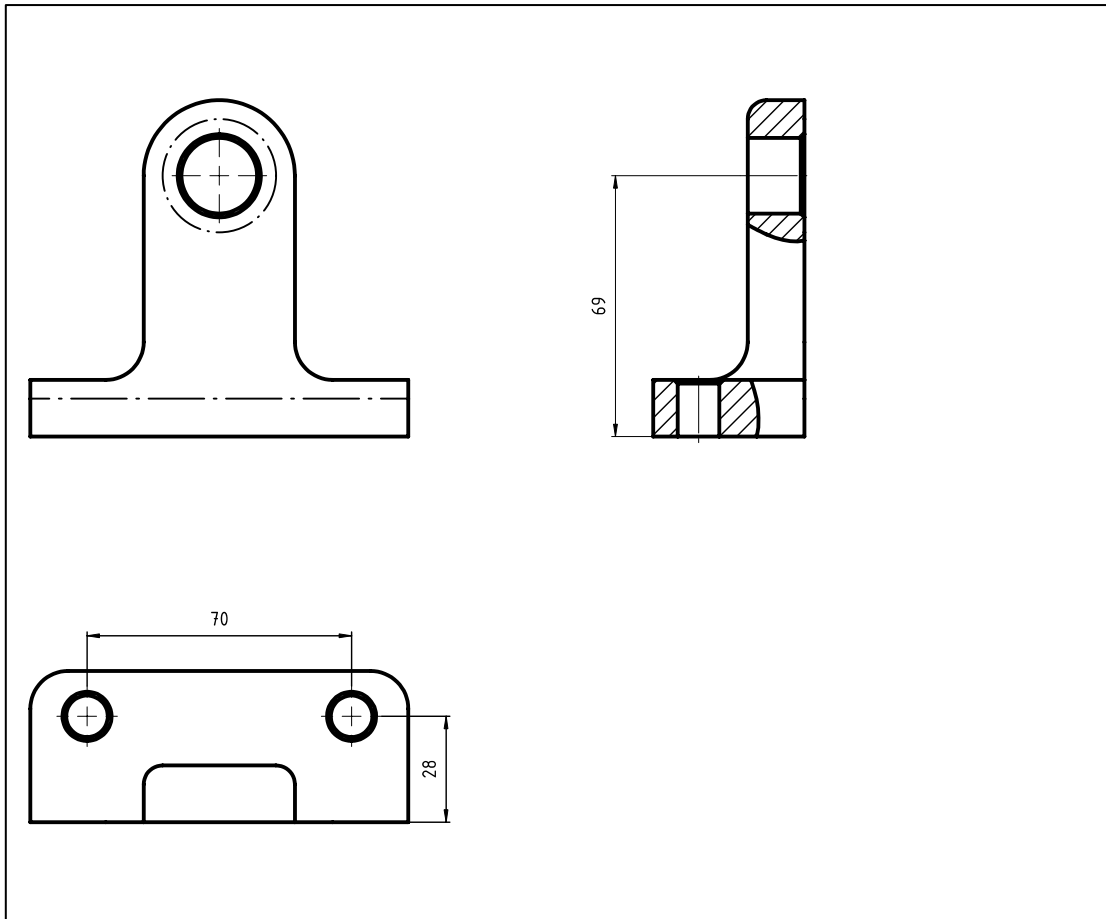


Fig. 4.6: orthogonal views of the risers with distance dimension.

4.1.3 Phase 1.3: restricted features dimensions

If, during the refinement phase (Phase 0), any of the integral features were partitioned, the subdivision needs to be formally defined. According to the ISO GPS system, a feature is naturally delimited by its borders (i.e., an edge); if the functional feature is delimited otherwise, dimensions specifying the actual extension of the functional features need to be added.

In the case of the riser, two functional features are “artificially” delimited: feature I and feature G. For these two specific dimensions, as shown in Fig. 4.7, are added.

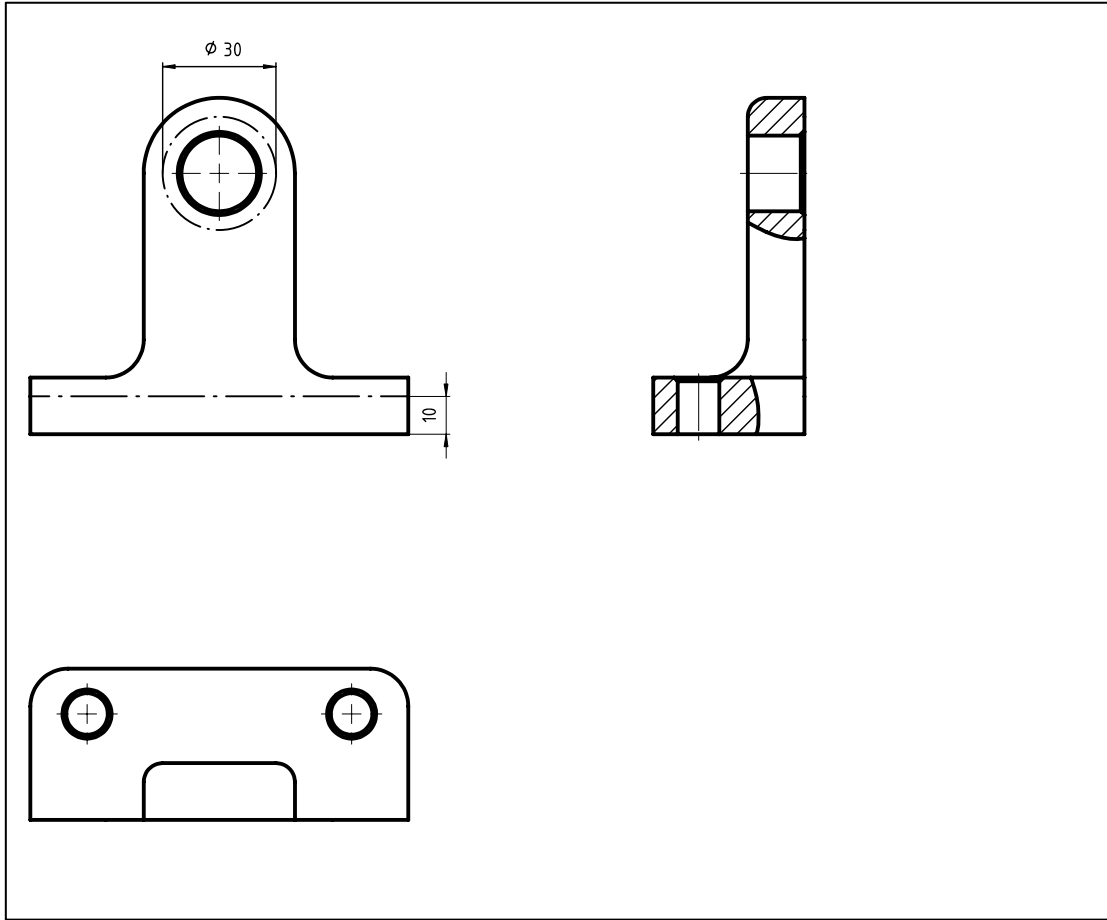


Fig. 4.7: orthogonal views of the risers with dimension to specified restricted features extension.

4.1.4 Phase 1.4: Non-functional dimension

All other dimensions needed to fully define the component geometry are non-functional and can be added to the drawing. Among these non-functional dimensions, we can identify chamfer and fillet dimensions, envelope dimensions, auxiliary dimensions, technological dimensions, etc.

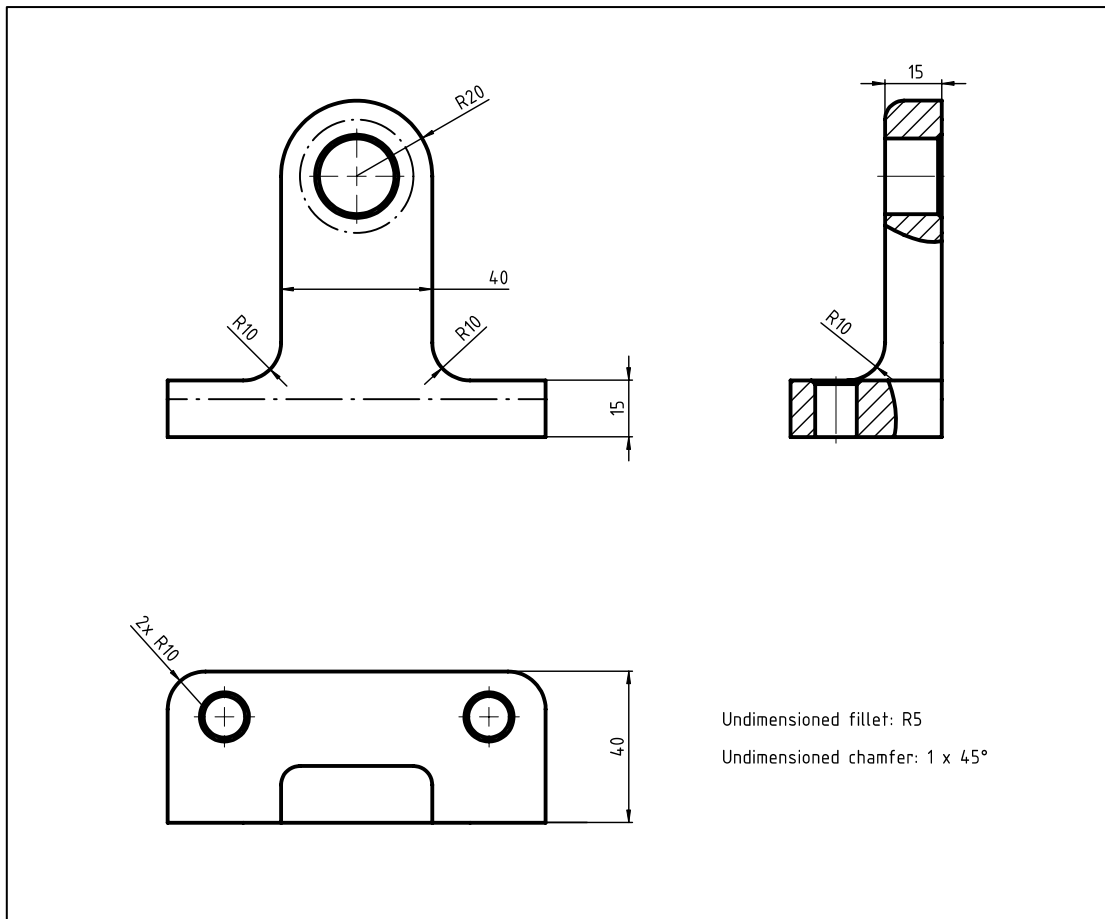


Fig. 4.8: orthogonal views of the risers with non-functional dimensions.

4.1.5 Phase 1.5: Dimensioning scheme layout

So far, four different dimensioning schemes have been separately created:

- The sizes dimensioning scheme.
- The distance dimensioning scheme.
- The restricted features dimensioning scheme.
- The non-functional dimensioning scheme.

Now, at the end of Phase 1, the four dimensioning schemes need to be merged together. By doing so, the distance dimensioning scheme can be optimized without limitation, choosing between parallel and series dimensions, since during Phase 2, these dimensions will become theoretically exact dimensions (TEDs), and therefore tolerance accumulation is not an issue.

To help with subsequent phases, each layer of dimensions can be labeled in a different way to aid identification later on. The use of layer may represents a valid option.

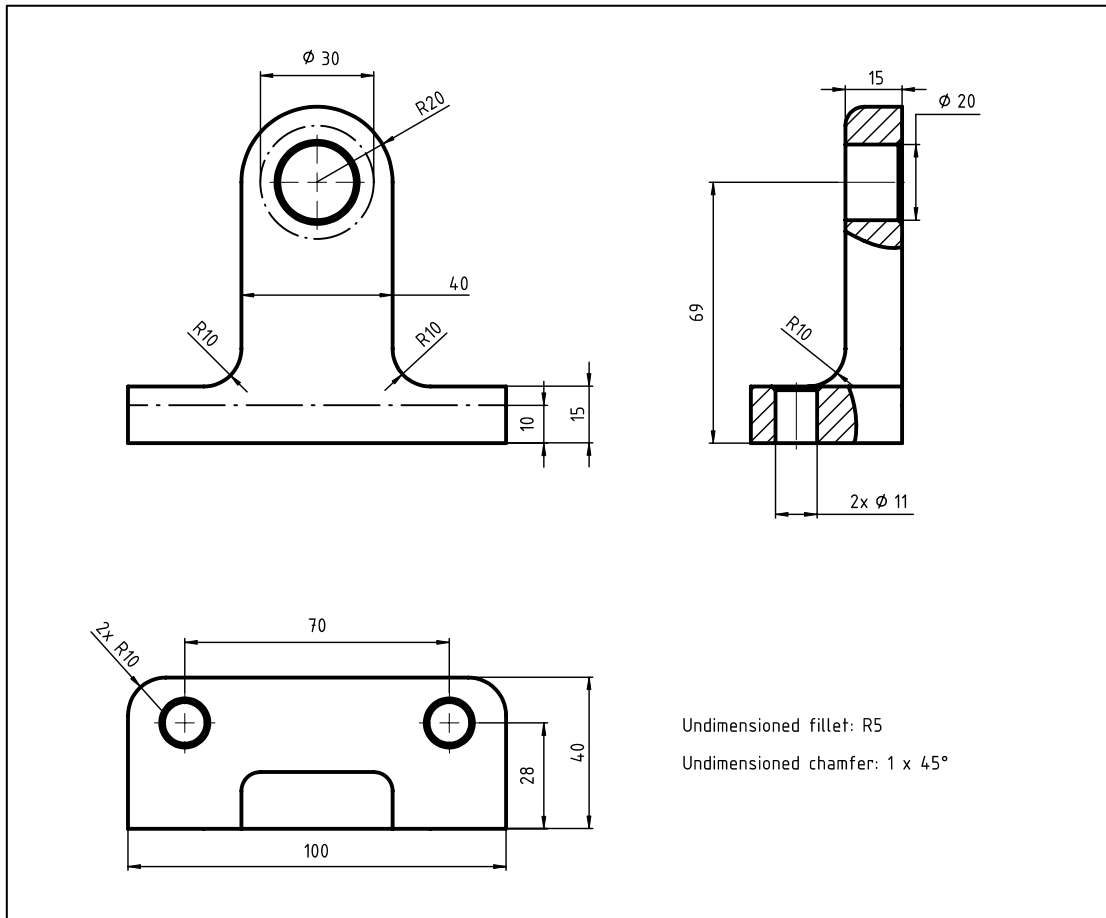


Fig. 4.9: Functional dimensioning scheme at the end of phase 1.

4.2 || Phase 2

Phase 2 is subdivided into two main sub-phases that cover:

- Phase 2.A: size tolerances.
- Phase 2.B: geometric tolerances.

In the following subsections, each sub-phase will be analyzed. At this point, the evolution of the geometric specification is incremental and starts from the results of the previous phase.

4.2.1 Phase 2.A: Size tolerances

Phase 2.A is subdivided into two sub-phases that cover:

- Phase 2.A.1: size variability.
- Phase 2.A.2: size modifiers.

In the following subsections, each sub-phase will be analyzed. The starting point is the set of orthogonal views with size dimensions, as shown in Fig. 4.4.

Phase 2.A.1: Sizes variability

First, the size variability is considered and specified. The variability can be expressed as a deviation from nominal or using the ISO system for limits and fits (ISO 286-1:2010 [11]). The latter is useful as it allows choosing classes of tolerances directly linked to functional requirements. For instance, by referring to Tab. 4.1 and based on the specific application, it is possible to determine the required amount of clearance or interference. Similarly, consulting Tab. 4.2 enables the translation of this requirement into a specific tolerance class according to the ISO system.

Tab. 4.1: Fits requirements based on application, from [84].

Type	Description	Application
Clearance	Loose	Where accuracy is not essential, such as in building and mining equipment.
	Free	In rotating journals with speeds of 600 rpm or greater, such as in engines and some automotive parts.
	Medium	In rotating journals with speed under 600 rpm, such as in precision machine tools and precise automotive parts.
	Snug	Where small clearance is permissible and where matins parts are not intended to move freely under load.
Interference	Wringing	Where light tapping with harmer is necessary to assemble the parts.
	Tight	In semipermanent assemblies suitable for drive or shrink fits on light sections.
	Medium	Where considerable pressure is required for assembly and for shrink fits of medium sections; suitable for press fit on generator and motor armatures and for automotive wheels.
	Heavy force or shrink	Where considerable bonding between surfaces is required, such as locomotive wheels and heavy crankshaft disks of large engines.

Tab. 4.2: Usual Fit tolerances table, from [85].

Type	Description	Hole Basis	Shaft Basis	Application
Clearance Fits	Loose Running	H11/c11	C11/h11	Wide commercial tolerances or allowances on external members.
	Free Running	H9/d9	D9/h9	Large temperature variations, high running speed, or heavy journal pressure, but accuracy is not essential.
	Close Running	H8/f8	F8/h8	Accurate machines and for accurate locations at moderate speeds.
	Sliding	H7/g6	G7/h6	Not intended to run freely, but move and turn freely and locate accurately.
	Location Clearance	H7/h6	-	Snug fit for locating stationary parts that can be freely assemble and disassembled.
Transition Fits	Similar	H7/k6	K7/h6	For accurate locations.
	Fixed	H7/n6	N7/h6	For more accurate locations where great interference is permissible.
Interference Fits	Press	H7/p6	P7/h6	For part requiring rigidity and alignment with prime accuracy of location but without special bore-pressure requirements.
	Driving	H7/s6	S7/h6	For ordinary steel parts or shrink fits on light sections. (The tightest usable fit for cast iron)
	Forced	H7/u6	U7/h6	For part that can be highly stressed or for shrink fits where the heavy pressing forces required are impractical.

In cases of bolted connections where the nominal dimensions are already different between the hole and shaft, there is no need to use the ISO system, and the tolerances can be assigned as limits of variation, which will be subsequently defined using the boundary condition design criterion (see chapter 6 and 7).

For the riser, four features of size were identified during the previous phase: two through holes (features K) where screws need to pass, the hole where the bushing needs to be mounted with interference (feature F), and the width of the riser (feature H).

For the first two holes (feature K), the size variation can be assigned as an upper and lower tolerance since there is no specific clearance requirement, and tolerance values can be defined through calculation. For the width of the riser (feature H), assuming a specific tool is used for alignment, the ISO system is used to guarantee a precise alignment with location clearance (referencing Tab. 4.2); therefore, a class of tolerance H/h is assumed, and being a shaft-like feature, a tolerance of class h is assigned.

Finally, for the hole where the bushing is mounted (feature F), interference is needed. In this case (referencing Tab. 4.1), a tight interference can be assumed to avoid manual disassembly while allowing the bushing to be disassembled if needed. Therefore, referencing Tab. 4.2, a press interference can be assumed using an H/p class of tolerance; being a hole, a tolerance of class H is assigned, and a tolerance of class p will be assigned to the bushing. The tolerance grade (tolerance value) is still a free parametric variable and can be optimized based on the capability of the manufacturing process.

The result of phase 2.A.1 is shown in Fig. 4.10.

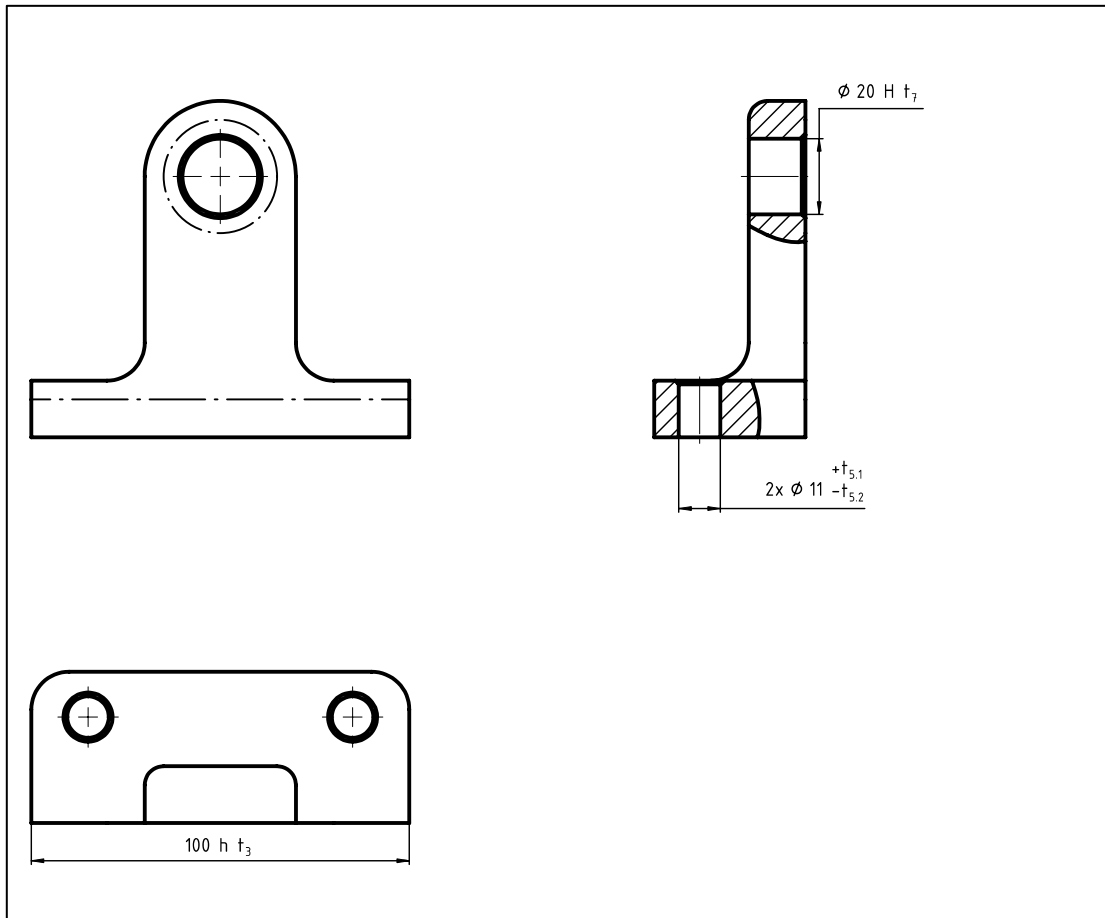


Fig. 4.10: orthogonal views of the risers with size dimension and their variability.

Phase 2.1.1: Sizes modifiers

Once the variability for the sizes has been set, eventual modifiers may be applied to refine the functional description. Within the ISO system in ISO 14405-1:2016 [20], sixteen different modifiers are defined, as seen in Tab. 4.3. These modifiers indicate the characteristics of the feature that need to be compared to the tolerance values. The characteristics can be clustered into Local Sizes, Global Sizes, Calculated Sizes, and Statistical Sizes.

Local sizes represent values that can be defined locally, such as a two-point size that equals the value that could be measured with a standard caliper. Local sizes of an actual feature are potentially infinite (an actual feature of size has an infinite section, and each section has infinite two-point sizes), and all of them need to fall within tolerance limits.

Global sizes represent a single value associated with the feature; they are obtained by associating a perfect geometry to the actual one. An example is the Gaussian size that, for a cylinder, gives the diameter of a perfect cylinder associated with the actual data using the Gaussian best fit.

Calculated sizes represent a value that is calculated starting from another quantity, such as the circumference diameter, which is derived by first measuring the circumference and dividing it by π .

Finally, statistical sizes define a selection criterion to choose, among a subset of measurements, a single value. For instance, the average size when associated with a local size defines the average among the infinite local sizes.

The standard also gives the possibility to change the behavior of a global size into a local size (section by section) using the additional indication "ACS" (Any Cross Section) and the option to define different modifiers for upper and lower limits.

Tab. 4.3: Size modifiers according to ISO 14405-1:2016.

Local sizes	(LP)	Two-point size
	(LS)	Local size define by a sphere
Global sizes	(GG)	Least-square association criteria
	(GX)	Maximum inscribed association criteria
	(GN)	Minimum circumscribed association criteria
	(GC)	Minmax (Chebyshev) association criteria
Calculated sizes	(CC)	Circumference diameter
	(CA)	Area diameter
	(CV)	Volume diameter
Statistical sizes	(SX)	Maximum size
	(SN)	Minimum size
	(SA)	Average size
	(SM)	Median size
	(SD)	Mid-range size
	(SR)	Range of sizes
	(SQ)	Standard deviation of sizes
	(E)	Envelope requirement

This description of different modifiers is not intended to be exhaustive, as it falls outside the scope of this chapter, which is presenting the methodology.

In the ISO system, the default modifier is the two-point size, indicated by the modifier (LP) [Local Point], which, for the definition of size provided in this work, is not particularly useful. From a functional standpoint, if an assemblability requirement is to be adhered to, the functional requirement is always defined by a combination of two different modifiers applied to the upper and lower limits. In the case of an external feature of size (i.e., a shaft), the upper limit has to be specified with the (GN) modifier, defining as characteristic the Minimum Circumscribed Feature, while the lower limit is specified with the (LP) modifier, which, as already discussed, indicates the two-point size. For an internal feature (i.e., a hole), the upper limit has to be specified with the (LP) modifier, and the lower limit with the (GX) modifier, defining as characteristic the Maximum Inscribed Feature.

Considering the definition of size previously given – “dimensions that control the clearance or interference state between two mating features” – assemblability is crucial, especially when clearance is required. Consequently, this type of indication is commonly used in a geometric specification. To address this, the standard introduces an additional modifier, the Envelope requirement (E), which allows for the avoidance of the double modifier indication.

Simultaneously, the standard offers the opportunity to overwrite the default by stating the new default in the drawing notes. This is helpful to prevent the need to use the (E) modifier every time. The notation for the notes is: “Linear size ISO 14405 (E)”; this notation is recommended in accordance with this methodology and is employed in Fig. 4.11.

Different modifiers will be defined on a case-by-case basis, as needed. For instance, when interference is required, the Gaussian size (GG) might be of interest since the focus is on the “average” interference. If describing a connection between a rigid part and an elastic part, an appropriate choice might be the circumference diameter (CC), as it directly controls the tightness of the connection when an elastic part is involved.

In our case, the default has already been modified to the Envelope requirement. Therefore, for feature K and H, no additional modifiers need to be added, as the envelope requirement aligns with our intentions in these cases. For feature F, as an interference fit is needed, the (GG) modifier is added.

The final result is depicted in Fig. 4.11.

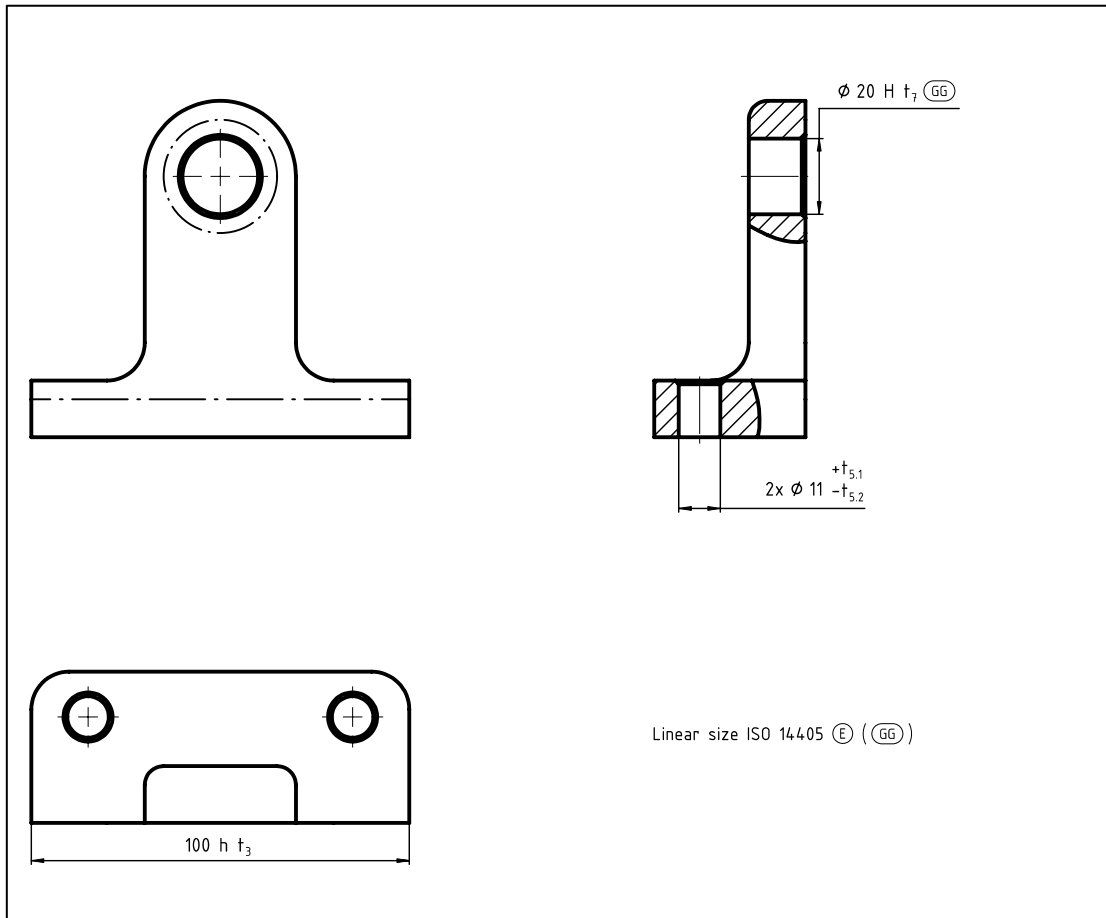


Fig. 4.11: orthogonal views of the risers with size dimension and their variability and modifiers.

4.2.2 Phase 2.B: Geometric tolerances

Phase 2.B is subdivided into seven sub-phases that cover:

- Phase 2.B.1: datum feature tolerances.
- Phase 2.B.2: datum feature tolerances modifiers.
- Phase 2.B.3: position tolerances.
- Phase 2.B.4: position tolerance modifiers.
- Phase 2.B.5: orientation tolerances.
- Phase 2.B.6: form tolerances.
- Phase 2.B.7: general tolerances.

In the following sub-section, each sub-phase will be analyzed. But before beginning with Phase 2.B.1, the Geometrical Tolerance Hierarchical Matrix (H-Matrix) will be presented.

Geometrical tolerance hierarchical matrix (H-Matrix)

The H-Matrix is a tool that helps the designer determine the correct tolerance that needs to be applied to each feature. From a methodological point of view, the first step is to assess the tolerance zone geometry and its constraints without considering the “name” of the tolerance itself. With the tolerance zone identified, it is possible to use the H-Matrix, shown in Fig. 4.12, to determine the correct tolerance to apply.

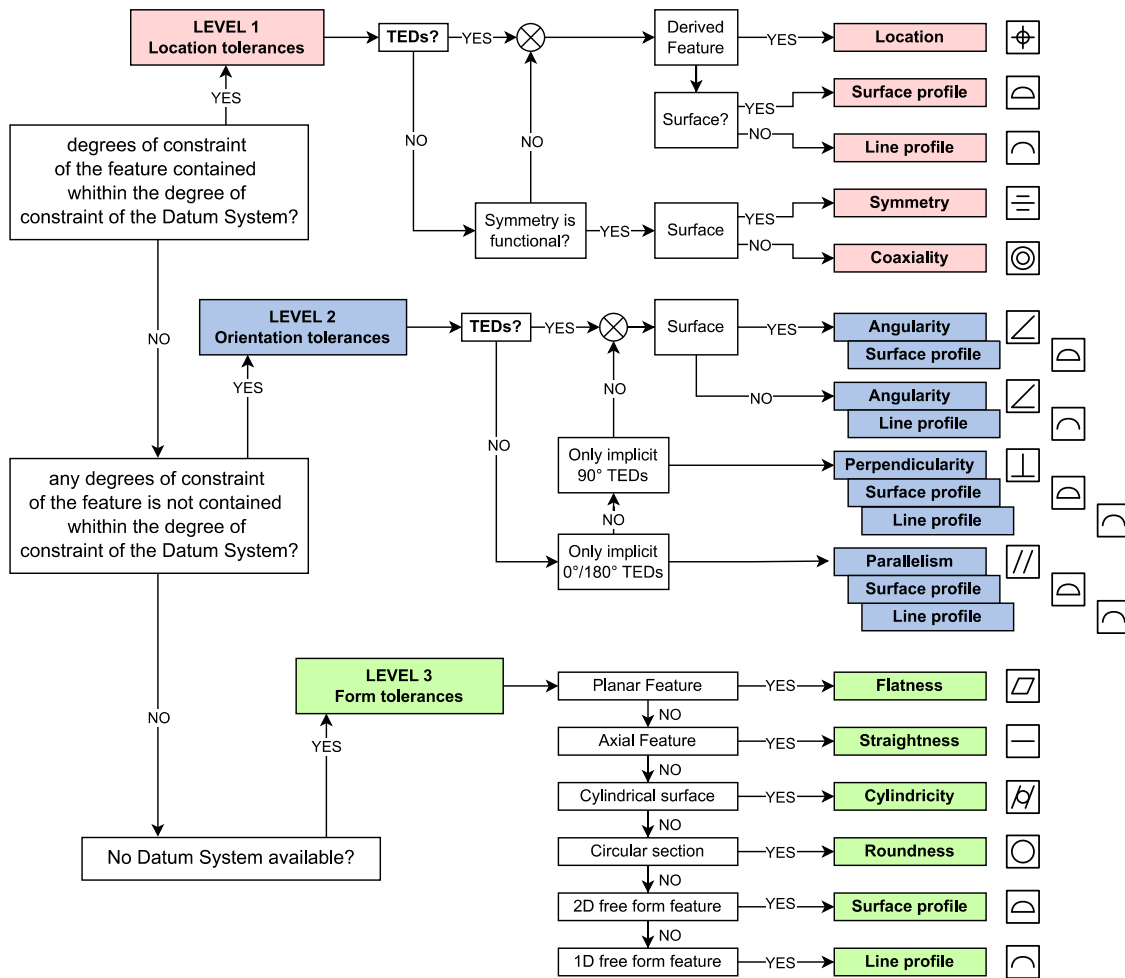


Fig. 4.12: H-Matrix, Geometrical tolerance hierarchical matrix.

While determining the type of tolerance to assign to a feature, the following considerations need to be taken into account: first, we need to consider the invariance degree of the feature and its degrees of constraint. The degrees of constraint are complementary to the invariance degree. The invariance degrees according to the ISO system are defined in ISO 17450-1:2011 [38]. Secondly, we need to establish the datum system that will be used to control the feature. For a referenced feature, the full datum system is used. For datum features, a datum defined by previously established datum/datum features is used. In each case, the degrees of constraint of

the datum system need to be defined, consisting of the union of the degrees of constraint of the datum features.

The first step in using the H-Matrix is to compare the degrees of constraint of the feature we want to specify with the degrees of constraint of the datum system.

If the degrees of constraint of the feature are contained within the degrees of constraint of the datum system, we enter level 1: position tolerances.

If any of the degrees of constraint of the feature is not contained within the degrees of constraint of the datum system, we enter level 2: orientation tolerances.

If no datum system is available, we enter level 3: form tolerances.

When the feature to be controlled is part of a pattern and any of the degrees of constraint of the feature is not contained within the degrees of constraint of the datum system, we might consider entering level 1 to emphasize the mutual position between each feature of the pattern. Moreover, for common datums, each datum feature enters level 1 and the datum use is the common datum itself.

Once we have entered the correct level, if there is an explicit dimension locating or orienting the feature, we proceed horizontally in the matrix; if there is not, we move down and select the proper tolerance based on the feature's geometry (plane, line, complex surface, complex line).

The application of the H-Matrix will be presented in the following paragraphs.

Phase 2.B.1: Datum Features tolerances

The first step involves examining the datum features that were already defined during phase 0 for the riser: surface J as the primary datum, surface I as the secondary datum, and feature H (already defined as a feature of size) as the tertiary datum. If a feature of size is involved, the datum feature is the derived element and not the integral feature.

At this point, each datum feature can be formally defined by assigning a name to each of them, as shown in Fig. 4.13. If a feature of size is a datum feature, the indication of the datum needs to be placed in line with the dimension. At this point, a tolerance frame is added for the actual specification of the datum features, but it is left empty.

A reference system can be associated with the datum system, which is useful to define degrees of constraint in an unambiguous way.

The tolerance zone is topologically defined by the nominal geometry, often referred to as Theoretical Exact Feature (TEF). For a plane, the tolerance zone is the space between two planes; for a straight line (axis), it is the space within a cylinder; for a complex surface, it is the space between two surfaces defined as an offset from the nominal one. In general, the tolerance zone is the portion of space that is swept by a sphere whose diameter is the same as the tolerance values and whose center lays on the nominal surface (TEF) or its offset if a UZ (Unequally disposed tolerance zone) modifier is used.

From the distance dimension scheme (Fig. 4.6) and the restricted features extension dimensioning scheme (Fig. 4.7), we need to check whether there are explicit dimensions describing

the mutual position of the datum features or specifying the tolerance zone extension. In case these dimensions exist, they need to be extracted and converted into Theoretically Exact Dimensions (TEDs). In our case, we need to record the dimension of 10 mm , which specifies the vertical extension of the secondary datum feature's tolerance zone. In Fig. 4.13, the tolerance zones for the datum features are indicated.

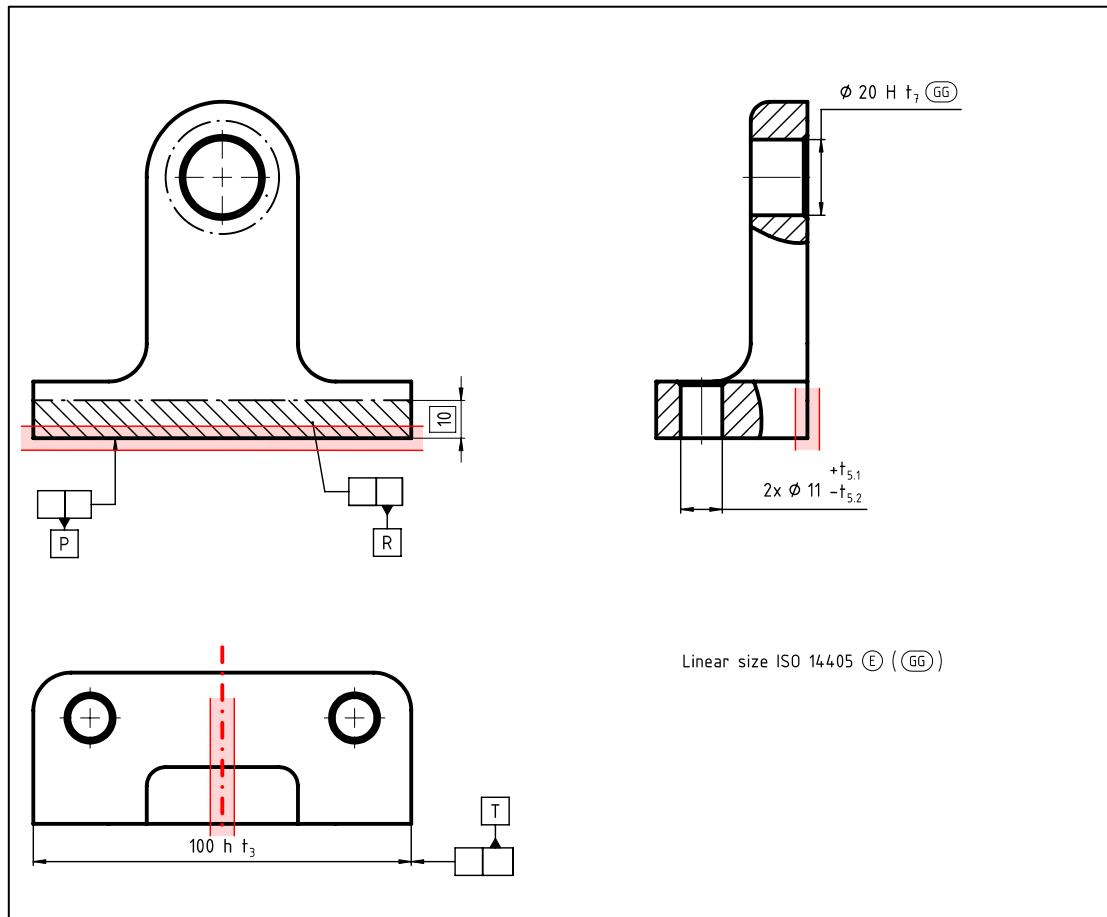


Fig. 4.13: orthogonal views of the risers with datum features tolerance zone and datum features naming.

For the primary datum (feature J), no previously defined datum features are associated, therefore no datum needs to be added to its tolerance frame; the datum is simply given the name [P]. The tolerance zone for a plane is the space between two planes, thus we can parametrically add the tolerance value to the tolerance frame. If the tolerance zone were cylindrical or spherical, the diameter or the spherical diameter symbol, respectively, would need to be included before the tolerance value. Since no datum applies to this tolerance, we enter level 3 of the H-Matrix; given that the feature is a plane, the tolerance is a flatness.

For the secondary datum (feature I), the datum [P] has already been defined, so it is added to the tolerance frame; the secondary datum is named [R]. Similarly, the tolerance zone for a plane is added parametrically. The degrees of constraint (referencing to Fig. 3.30 at page 94 for the

reference system associated to the part) for feature I are T_x , R_y , and R_z , while the datum system (P) has degrees of constraint T_z , R_y , and R_x . Since T_x and R_z are not constrained by the datum system, we enter level 2 of the H-Matrix; as no explicit angular dimension is given and the nominal angle between feature J and feature I is 90° , the appropriate tolerance is perpendicularity.

For the tertiary datum (feature H), both datum [P] (primary) and datum [R] (secondary) have already been defined, and together they form the datum [P|R], which is added to the tolerance frame; the tertiary datum is named [T]. The tolerance zone is still the space between two planes, and its parametrical value is included. The degrees of constraint for feature H are T_y , R_x , and R_z , whereas the datum system (P|R) has degrees of constraint T_x , T_z , R_x , R_y , and R_z . Because T_y is not constrained by the datum system, we enter level 2 of the H-Matrix; likewise, as no explicit angular dimension exists and feature H is mutually perpendicular to both feature J and feature I, the appropriate tolerance is perpendicularity.

The complete datum system becomes [P|R|T], effectively constraining all degrees of freedom. The outcome of the specification for the datum system can be found in Fig. 4.14.

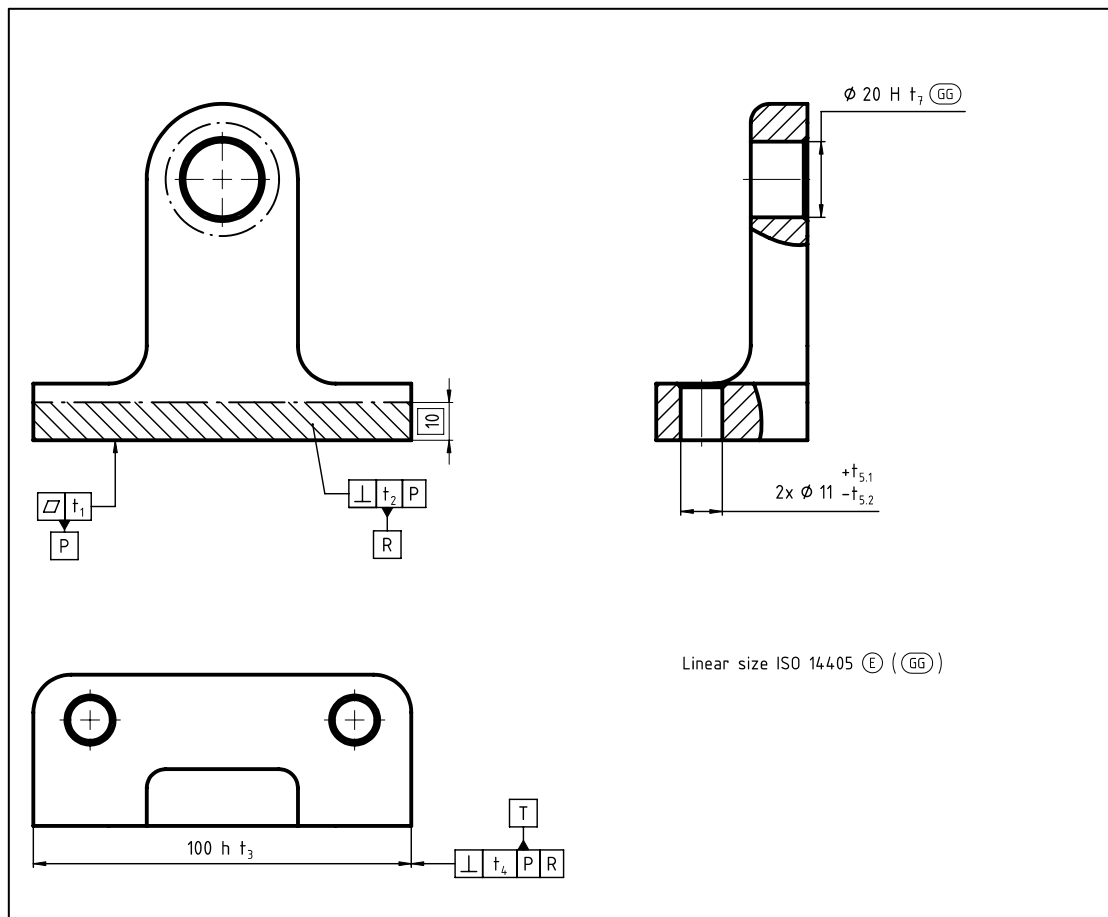


Fig. 4.14: orthogonal views of the risers with datum features geometric specification.

Phase 2.B.2: Datum Features tolerances modifiers

Once the geometric tolerance for the datum features has been applied, any potential modifiers need to be evaluated.

If a datum feature is part of a pattern, the use of the CZ (combined zone) is needed to ensure that the tolerance zone of each feature in the pattern is constrained together.

If a datum feature is a feature of size, the application of the Maximum Material Requirement (MMR) to both the tolerance of the datum feature and to each reference of the datum in the tolerance frames permits the description of cases where assembly clearance might result in shifts between parts.

In the case of the riser, no pattern is used as a datum feature, thus no CZ is required. Datum [T] is a feature of size. Whether to apply the material requirement depends on the assembly procedure. Functionally, if manual alignment is performed, the operator's hand touches the part, resulting in no clearance and making the material condition irrelevant to assembly conditions. If a tool is used for alignment, the clearance between the tool and the riser can cause shifting during assembly, making the material condition necessary to describe assembly conditions.

In our assumed scenario of using a tool for alignment, the material condition is added. Consequently, the complete datum system becomes [P|R|T(M)]. The final geometric specification for the riser can be observed in Fig. 4.15.

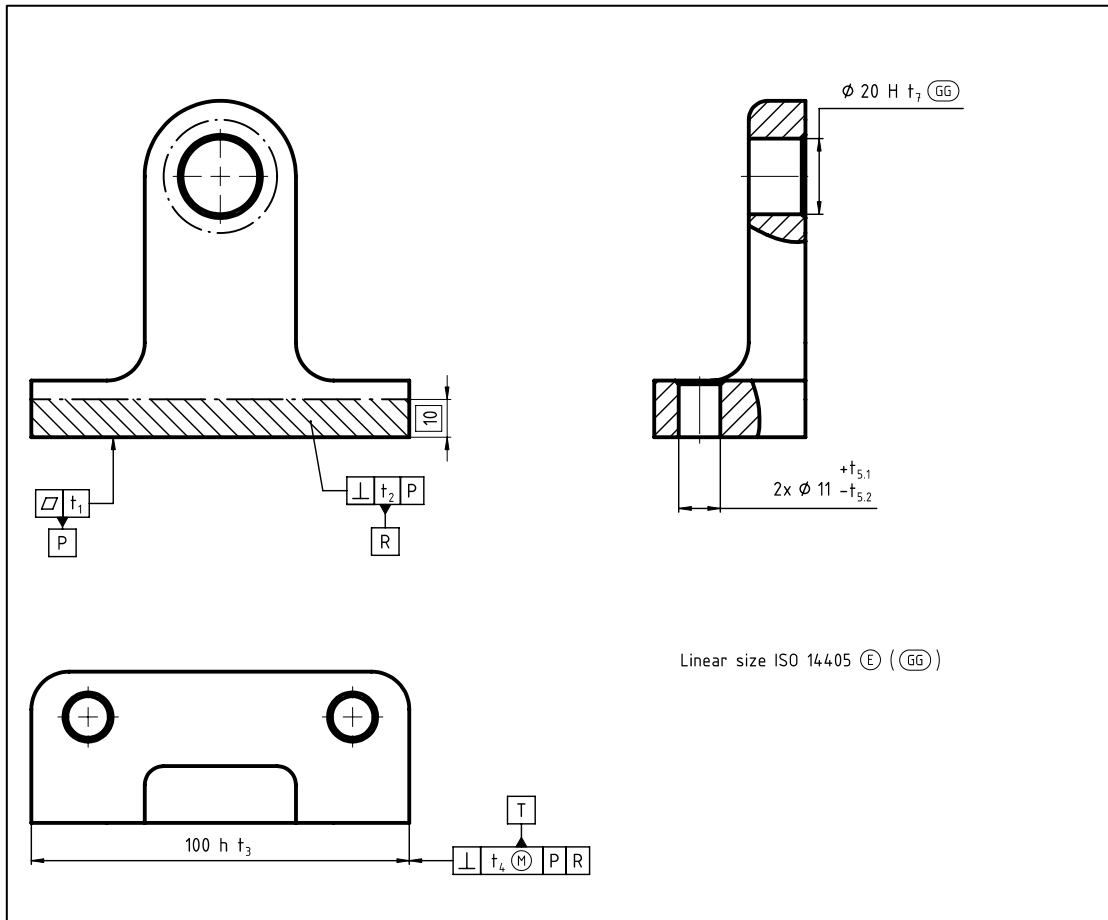


Fig. 4.15: orthogonal views of the risers with datum features geometric specification with modifiers.

Phase 2.B.3: Position Tolerance

At this point, the datum system is fully defined and specified, intended to lock all degrees of freedom of the part. As already discussed in subsection 3.3.6, exceptions are possible for functionally axisymmetric components where not all six degrees of freedom are locked, but all the degrees of constraint of functional features are locked.

In this context, when dealing with referenced features, the first aspect to consider is position tolerances, which corresponds to level one of the H-matrix. Similar to datum features, the initial step involves defining the topology of the tolerance zone, following the same guidelines provided for datum features. In our case, the referenced features include hole F, shoulder G, and the two holes K. Since holes F and K were previously defined as features of size, it's important to remember that the referenced feature is the derived element, namely the axes. As a result, the tolerance zone for these elements is the space within a cylinder. On the other hand, for feature G, being a plane, the

tolerance zone corresponds to the space between two nominal planes. Fig. 4.16 illustrates the tolerance zones for the referenced features.

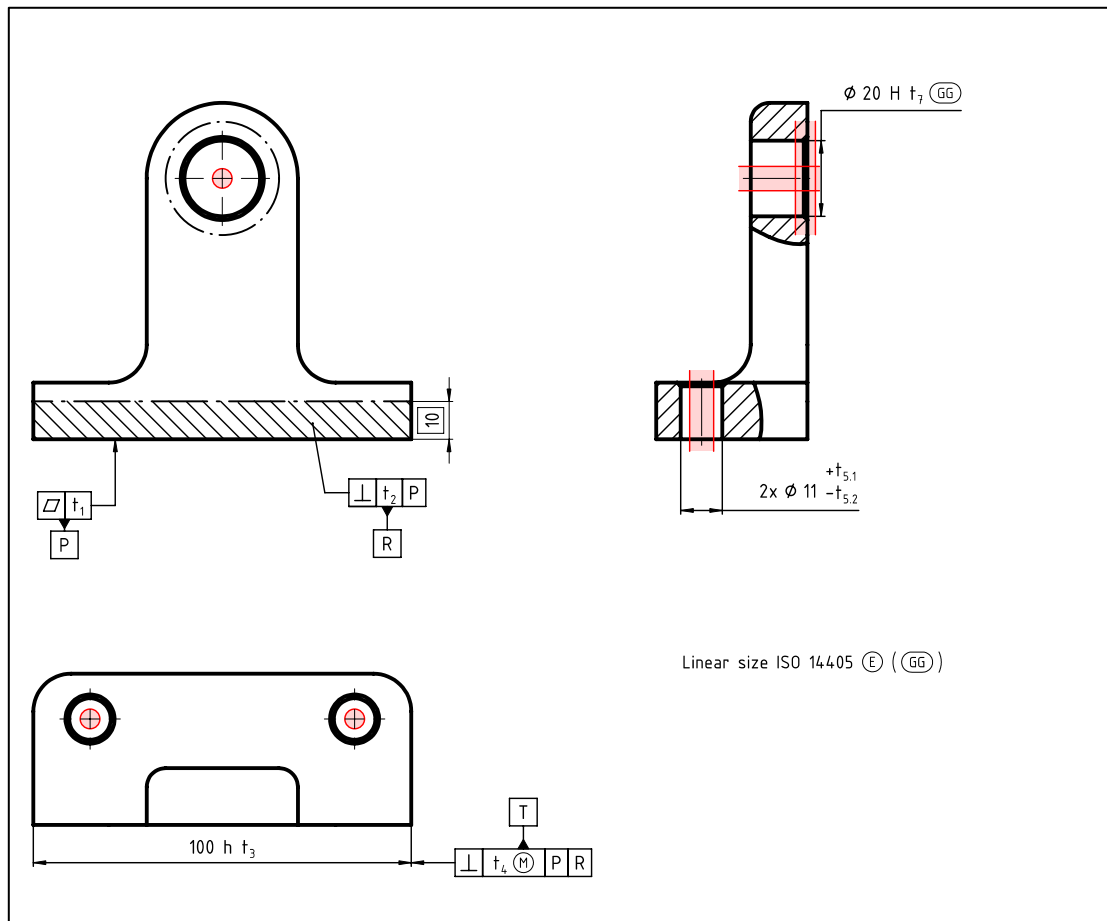


Fig. 4.16: orthogonal views of the risers with referenced features tolerance zone.

Each of these tolerance zones needs to be located from the full datum system and, if required, defined in terms of extension. Referring to the distance dimensioning scheme (Fig. 4.6) and the restricted features extension dimensioning scheme (Fig. 4.7), all the dimensions that are used to establish the nominal position of the nominal features and the dimensions used to specify tolerance zone extensions need to be extracted and converted into Theoretically Exact Dimensions (TEDs): “squared” dimensions. If phase zero was carried out accurately, all dimensions in Fig. 4.6 and Fig. 4.7 should be converted into TEDs. The outcome is depicted in Fig. 4.17.

At this juncture, it becomes possible to describe the position and orientation of each tolerance zone in a clear and unambiguous manner.

For feature F, the axis of the tolerance zone is perfectly parallel to the primary datum of the full datum system, perfectly perpendicular to the secondary datum, it coincides with the tertiary datum, and is located 69 mm from the primary datum.

Concerning feature G, the tolerance zone is entirely perpendicular to both the primary and tertiary datums of the full datum system, while its median plane rests on the secondary datum. Its

radial extension spans 15 mm ($\phi 30\text{ mm}$) from a point coinciding with the intersection between the secondary datum and the axis of the tolerance zone for feature F.

As for features K, both axes are perfectly perpendicular to the primary datum of the full datum system and are parallel to both secondary and tertiary datums. They are each positioned 28 mm away from the secondary datum and 35 mm away from the tertiary datum in opposite directions.

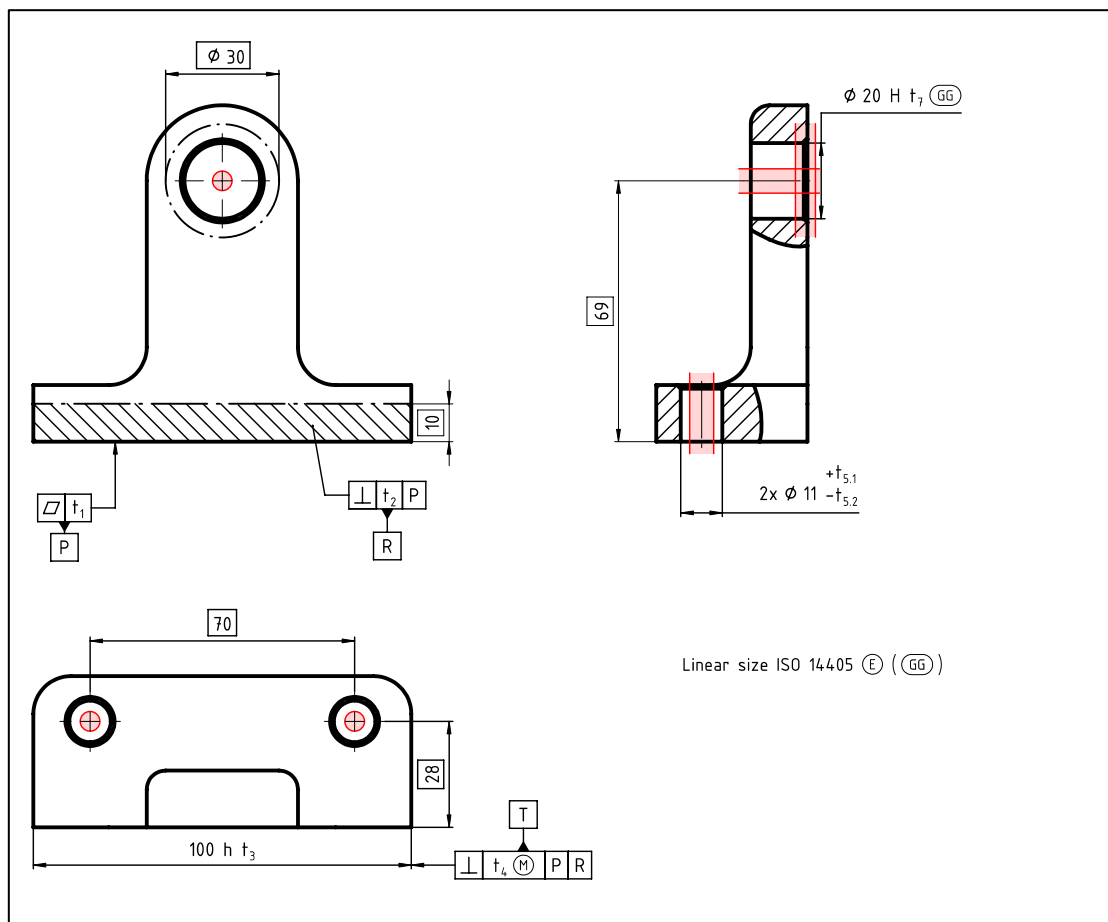


Fig. 4.17: orthogonal views of the risers with referenced features tolerance zone and TEDs.

Now, for each referenced feature, the appropriate type of tolerance to be applied needs to be determined using the H-matrix. Here, only level one is relevant since we are focusing on location tolerances.

For feature F, we enter level one; as there is an explicit TED, we proceed horizontally. Given that it's a derived feature, the required tolerance is a position tolerance.

Concerning feature G, we enter level one. As there isn't an explicit TED, we move down the matrix. Since the feature has no functional symmetries with respect to the Datum System, we move up. As it's an integral feature, the appropriate tolerance is a surface profile.

For features K, we enter level one. As there is an explicit TED, we proceed horizontally. Given that they are derived features, the necessary tolerance is a position tolerance.

The outcome for the specification of referenced features can be observed in Fig. 4.18.

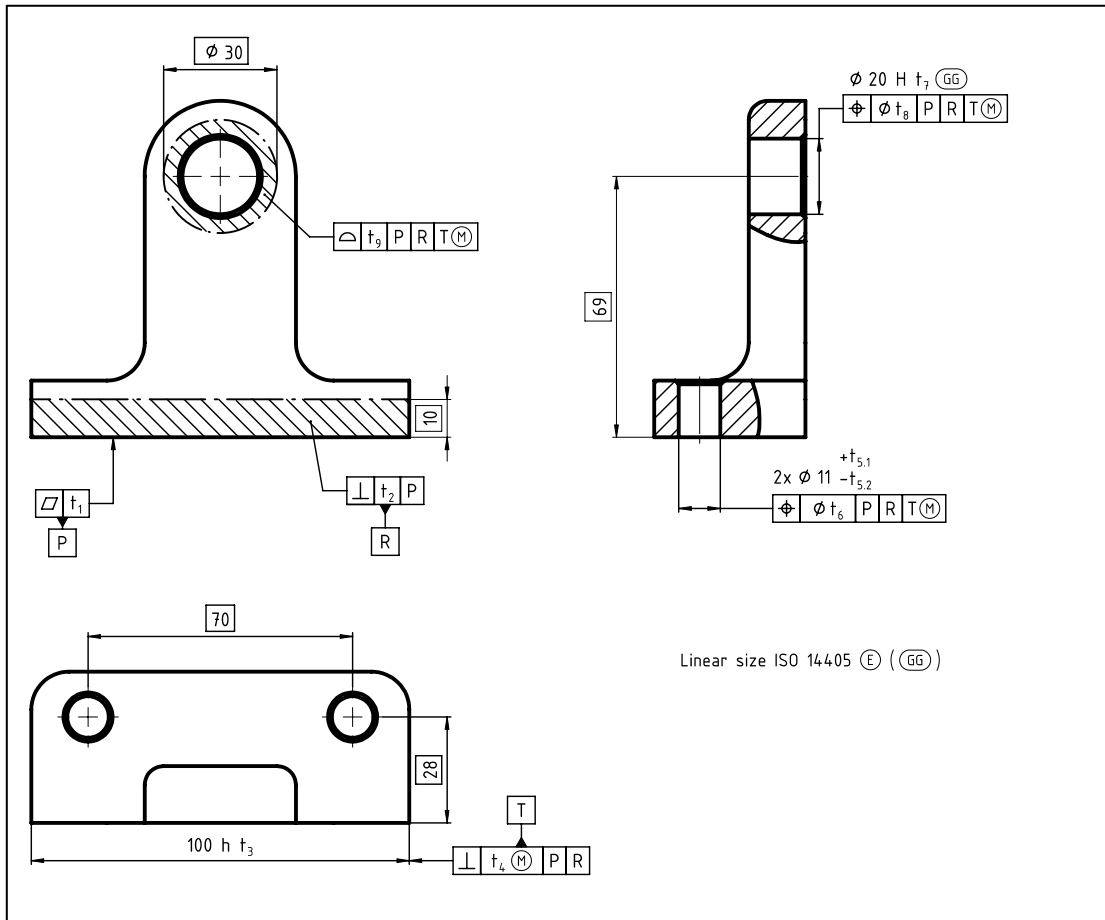


Fig. 4.18: orthogonal views of the risers with referenced features specification.

Phase 2.B.4: Position Tolerance modifiers

Once the geometric tolerance for the referenced features has been applied, any potential modifiers need to be evaluated.

Whenever a referenced feature is part of a pattern, the CZ modifier may be added to emphasize the pattern behavior. In this context, the CZ modifier doesn't alter the behavior of the tolerance zone. As per the proposed methodology, it is suggested to use the CZ modifier whenever a pattern is invoked, particularly if the feature functionally constitutes a pattern (not solely geometrically, where the same geometry repeats, but each repetition functions independently without interaction). Applying the CZ modifier when it has no impact doesn't change the functional description of the part. However, not using the CZ modifier when it's needed can significantly alter the functional description.

In cases where a referenced feature is a feature of size, the application of the Maximum Material Requirement should be considered. The Maximum Material Requirement is to be employed whenever a clearance fit is necessary. However, it might not be suitable for an

interference fit and should never be utilized when the feature of size is employed for alignment. A detailed discussion on the impact of material condition when the feature of size is used for alignment can be found in chapter 7, on page 179.

Regarding the riser, both features K are part of a pattern; therefore, the CZ modifier is added. Additionally, as they are features of size where clearance is necessary, the Maximum Material Requirement is also included. The other feature of size is feature F, and since an interference fit is required, the material requirement is not applied in this instance. The final outcome is depicted in Fig. 4.19.

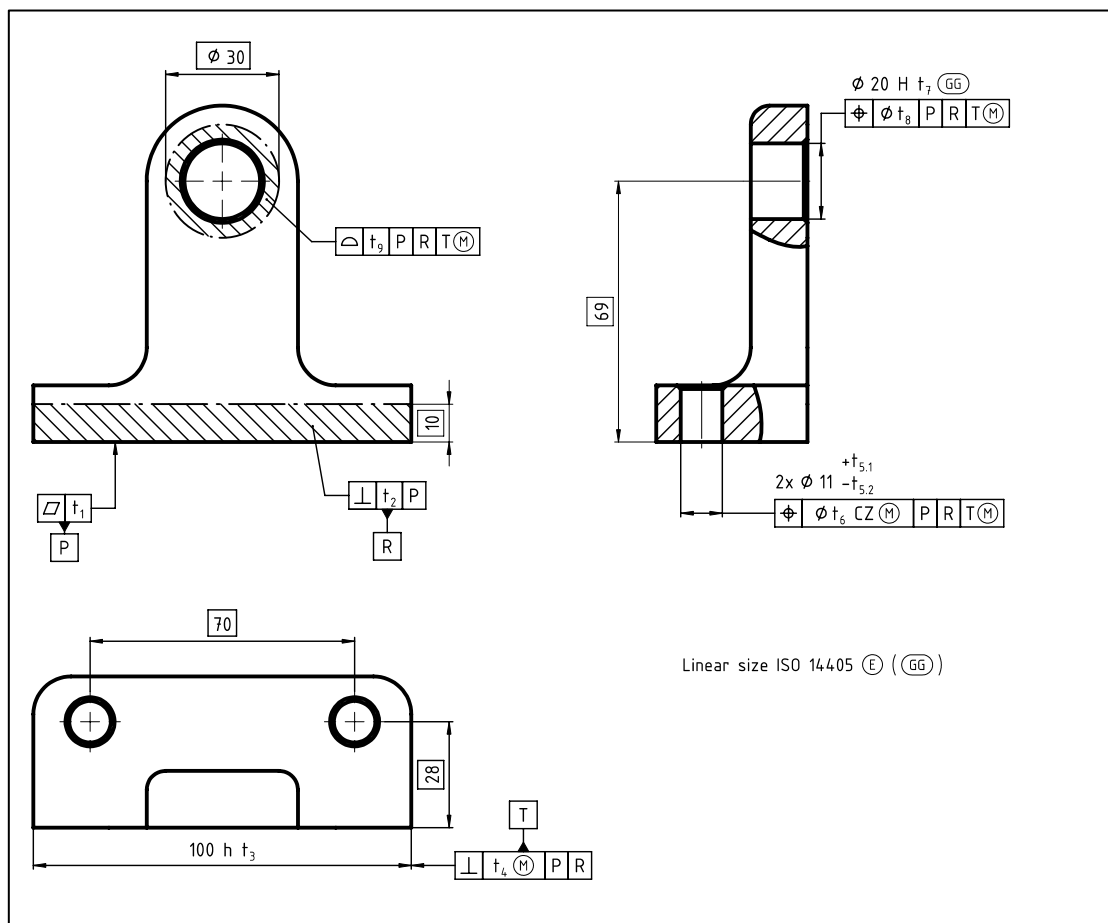


Fig. 4.19: orthogonal views of the risers with referenced feature full geometric specification.

Phase 2.B.5/6: Orientation and Form tolerances

The geometric specification developed thus far comprehensively controls all the functional features of the component. In many cases, this type of functional description might suffice. However, there are instances where the need arises to enhance the functional description by introducing additional constraints to referenced features. Location tolerances inherently regulate orientation and form as well. The degree to which orientation and form are controlled might not always be adequate. An illustrative example is a table's geometric specification. While the location

tolerance for the table's top surface might be relatively large, even on the order of 1 cm, insufficient orientation control could lead to round objects sliding off the table. In such scenarios, an added orientation tolerance is necessary to more precisely define the functional requirements. The same consideration applies to form tolerances.

It's important to note that each new tolerance increment increases manufacturing costs and thus should be carefully evaluated. For each additional tolerance, the steps include defining the tolerance zone's topology, determining the datum system (which might potentially be a local one), specifying the appropriate tolerance to apply, and evaluating any necessary modifiers.

Regarding the riser, there is no requirement to introduce any additional tolerances beyond those already defined.

Phase 2.B.7: General tolerances

After all the functional features have been fully specified and any necessary refinements have been added, the last consideration is addressing non-functional features. As the name suggests, non-functional features aren't critical for the functional specification. Therefore, these features are controlled using general tolerances.

In Phase 1, the non-functional dimensioning scheme was defined. At this stage, variability for all these dimensions needs to be established. Formerly, the practice involved using general tolerances according to ISO 2768, encompassing both parts one and two. Part one addresses linear dimensions, while part two addresses geometric tolerances. A recent development in the ISO GPS system led to ISO 22081:2021 [75], which suspended ISO 2768-2 and overlaps with ISO 2768-1.

Given the definition provided so far, linear dimensions are classified as size dimensions, which are intrinsically functional as they pertain to matings. Therefore, all non-functional dimensions cannot be categorized as size dimensions. Consequently, from a methodological standpoint, all non-functional dimensions should become TEDs (Theoretically Exact Dimensions), and non-functional features should be controlled using a surface profile tolerance as indicated in ISO 22081.

However, ISO 22081 allows for the indication of linear size general tolerances using custom values, tables, or even referencing ISO 2768-1. Yet, based on the approach proposed thus far, and for functional considerations, there ideally shouldn't be a need to do so.

At this point, one might consider not displaying non-functional TEDs to achieve a cleaner drawing, replacing them with a note such as "TEDs according to CAD model" alongside the general tolerances. While this note generally allows for omitting TEDs, it's recommended to explicitly include TEDs that locate functional elements in a functional specification.

The general tolerance for our specific case can be observed in Fig. 4.20, where the complete geometric specification is presented.

4.2.3 Final geometric specifications

By consolidating all the intermediate results that have been defined thus far, we arrive at the final geometric specification for the riser, as depicted in Fig. 4.20.

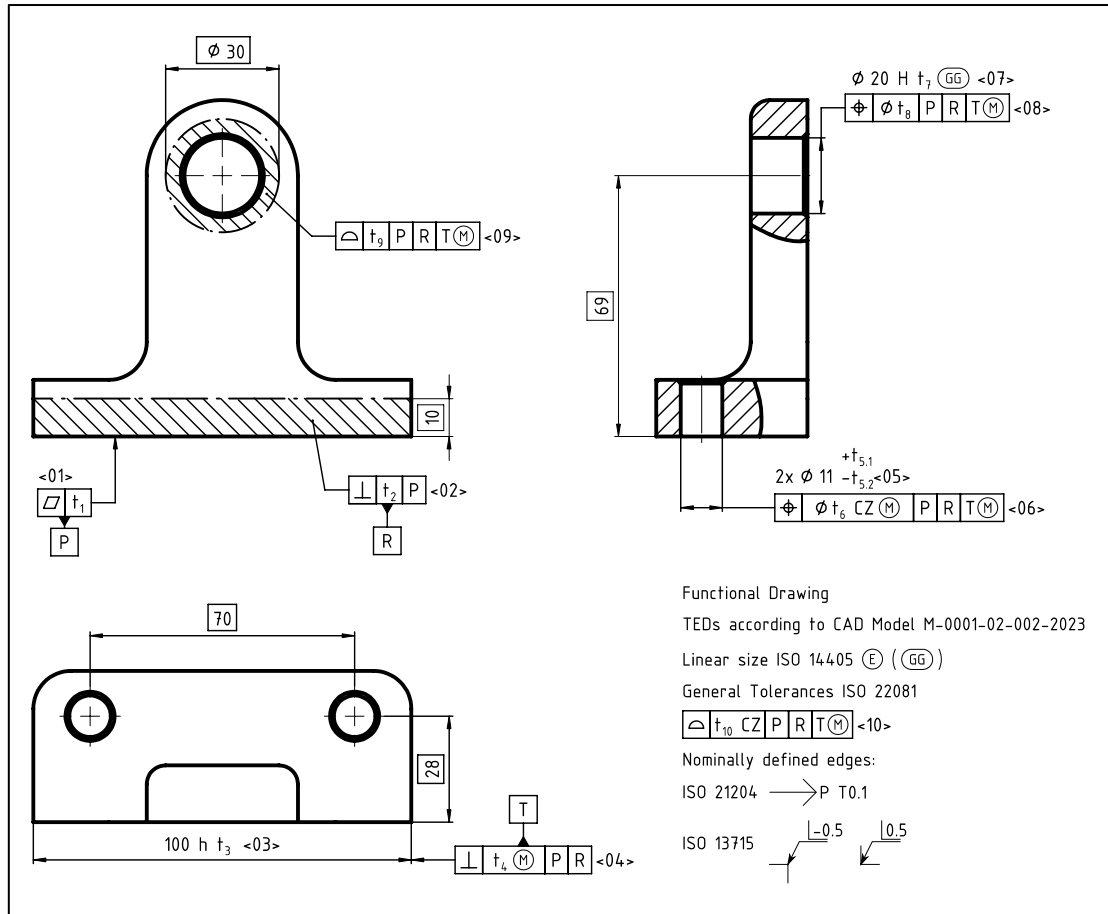


Fig. 4.20: orthogonal views of the risers with full geometric specification.

4.3 || Results

In this section, we will present the results of the geometric specification for the case study. We will provide an extract from each 2D drawing and discuss it. The full 2D drawings can be found in Appendix A on page 277.

In the drawings, tolerance values are assigned parametrically, including both geometric and dimensional tolerances. However, the actual tolerance values are not included in this chapter as they will be assigned later during the “tolerance synthesis” phase. This phase may involve the use of calculation and simulation tools such as tolerance chains. The specification scheme determines the type of tolerance to be assigned to the functional surfaces/features, but not their specific values.

4.3.1 Assembly drawing

In this subsection, the 2D drawing relevant to the full assembly will be presented.

In Fig. 4.21 an extract from the actual drawing is shown. Functional requirements are specified, beginning with the maximum and minimum clearance necessary for the rotation of the wheel. Additionally, the minimum gap required between the wheel and the base is indicated as a minimum distance. Lastly, the necessary mating between the shaft and the bushing is outlined.

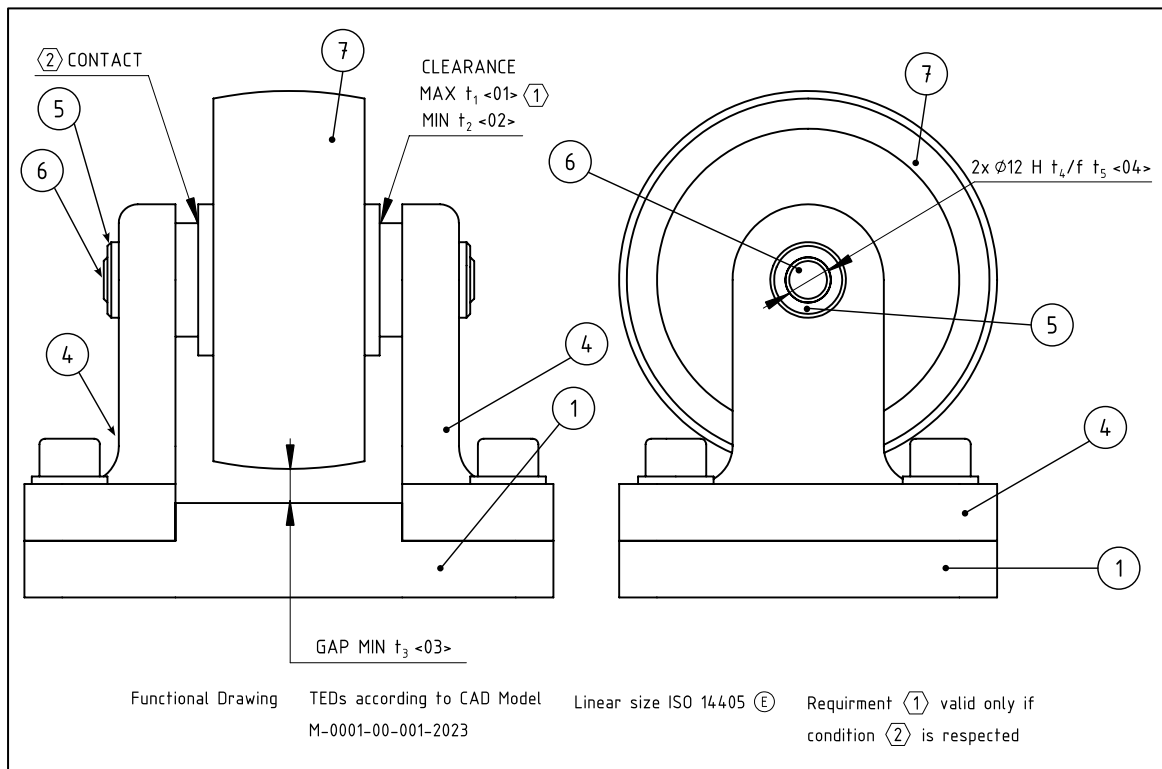


Fig. 4.21: Extract from the full assembly 2D drawing.

4.3.2 Sub-assembly drawings

In this subsection, the results relevant to the sub-assemblies will be presented.

Starting from the “riser_asm” sub-assembly, as shown in Fig. 4.22. The 2D drawing conveys the functional geometric specification for this sub-assembly. The complete datum system is [P|R|T(M)], as indicated in the general tolerances. The geometric specification is straightforward: for the primary datum feature (a plane), a flatness tolerance is allocated; for the secondary datum feature (also a plane), a perpendicularity tolerance with respect to the primary datum is applied; and for the tertiary datum feature (a feature of size, representing a median plane), a perpendicularity

tolerance with respect to both the primary and secondary datum is assigned with maximum material requirement.

According to the notes on the drawing, it is important to mention that the envelope principle applies to all sizes unless otherwise specified. This principle is applicable to all the drawings that will be presented.

All other functional surfaces are controlled by location tolerances. The hole that mates with the shaft has a Maximum Material Requirement (MMR) specified, indicating a mating requirement. The two holes where the screw passes through are defined as a pattern with the CZ modifier, emphasizing their functional behavior as a pattern. The MMR is also used in this case to describe the assemblability requirement.

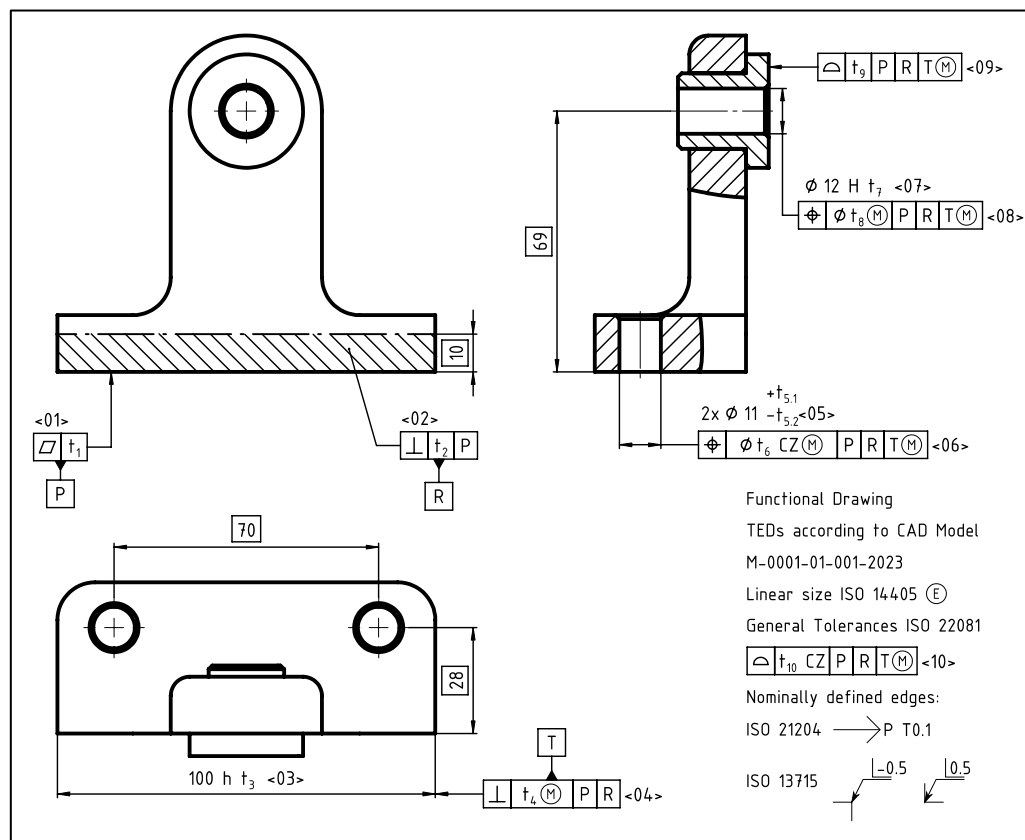


Fig. 4.22: Extract form the “riser_asm” 2D drawing.

In Fig. 4.23, it is presented the 2D drawing for the “wheel_asm” sub-assembly. The primary datum [P-Q] is defined based on the two ends of the shaft. Each individual datum feature [P] and [R] is characterized by a coaxiality tolerance relative to the axis derived from their two individual axes, which represents the axis the “wheel_asm” actually rotates around. The secondary datum [T(M)] is defined by the feature of size that identifies the width of the wheel. The complete datum system for this sub-assembly is [P-R|T(M)].

The outer surface of the wheel is located using a surface profile tolerance with respect to the complete datum system.

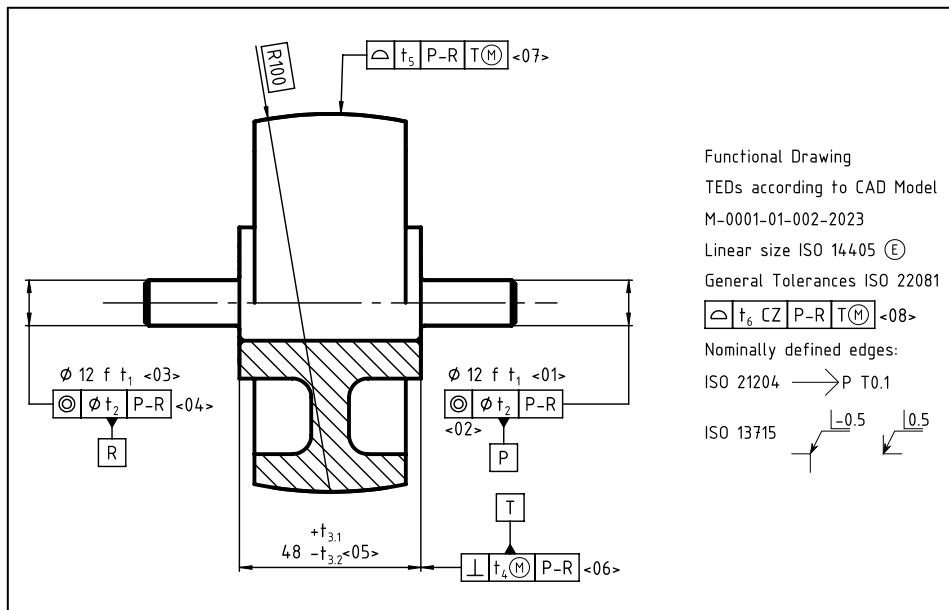


Fig. 4.23: Extract from the “wheel_asm” 2D drawing.

4.3.3 Part drawings

In this subsection, the 2D drawings relevant to the individual parts will be presented.

In Fig. 4.24, it is shown an extract from the Base component drawing. We can observe the presence of multiple surface patterns. The primary datum [P] is specified with a planarity tolerance over the pattern of two planar surfaces discussed in the previous chapter. The CZ modifier is essential in this case to align the individual tolerance zones and consider them as a single plane. The secondary datum [R] is defined as the pattern of the two vertical surfaces, as discussed earlier. In this case, the datum feature is the collection of the two integral planar features, and it is not a feature of size since full contact is always present on both surfaces. Therefore, it does not represent a mechanical fit. Its specification uses a location tolerance (surface profile) with respect to the primary datum. The CZ modifier is applied to align the two individual tolerance zones at the specified distance (60 mm) defined by the TED. The use of a surface profile tolerance, instead of a perpendicularity tolerance, emphasizes the importance of the mutual distance between the two integral features. The tertiary datum [T(M)] is defined as a feature of size describing the width of the component, implying that the datum is the median plane. The Maximum material condition is added since it is supposed to use a fixture for the assembly procedure. The use of datum targets (four square zones) allows us to consider only the relevant portions used during the alignment of the “riser_asm”. The median plane is controlled by an orientation tolerance with reference to the primary

and secondary datum. The complete datum system is therefore defined as [P|R|T(M)]. The top surface is located with reference to the complete datum system to control the gap with the wheel. The four M10 holes are defined as a pattern, with the CZ modifier emphasizing their role as a pattern. The maximum material requirement (MMR) is not applied since the dimensional tolerance is negligible for threaded elements. The projected tolerance zone is used, as the actual assembly requirement is determined by the interaction between the screw and the “riser_asm”, not solely by the hole itself.

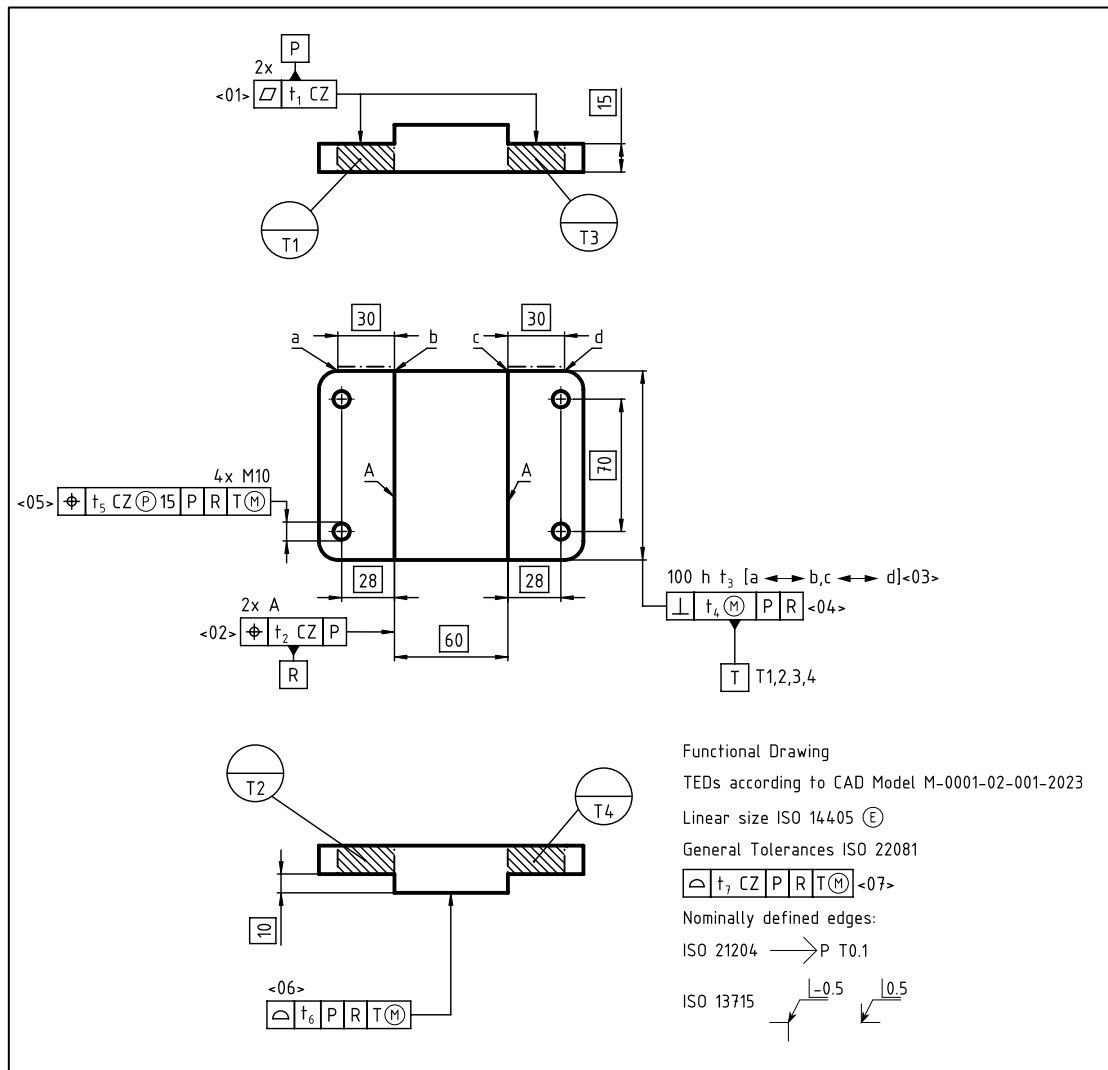


Fig. 4.24: Extract from the base component 2D drawing.

The 2D drawing for the riser, shown in Fig. 4.25, is quite similar to the one previously defined for the “riser_asm” (Fig. 4.22). The description of the datum system remains the same, and the same considerations for the two holes where the screws are inserted apply. The other functional features are the ones where the bushing is mounted. The hole dimension is specified with the (GG) modifier (Global Gaussian size) since an interference fit is required. Therefore, we are interested in

the “average” dimension that mates with the bushing. It is also located with respect to the complete datum system, without the MMR, due to the interference fit.

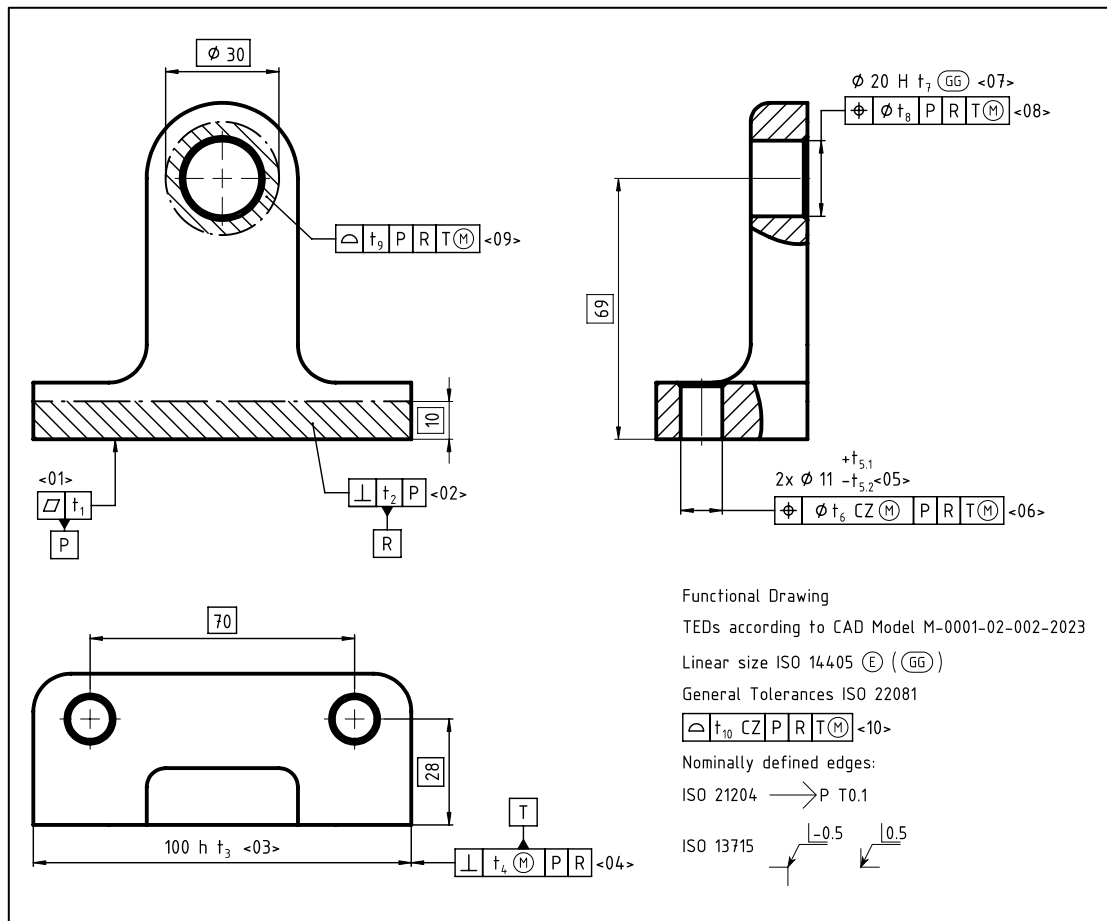


Fig. 4.25: Extract form the riser component 2D drawing.

In Fig. 4.26, the 2D drawing for the bushing component is shown. The primary datum [P] is defined by the feature of size describing the outer cylinder of the bushing, and the datum is derived from the axis of the cylinder. The dimension of the feature of size is specified with the GG modifier (similar to the mating hole in the riser) since an interference fit is required. The axis is controlled with a linearity tolerance. The secondary datum [R] is controlled with a perpendicularity tolerance with reference to the primary datum, and it is defined over the shoulder where the bushing stops against the riser. The complete datum system is therefore [P|R]. From the complete datum system, the “external” vertical surface that interacts with the wheel is located. The internal hole that mates with the shafts is located only with respect to the primary datum to allow the use of a coaxiality tolerance. The MMR is used since an assemblability requirement (clearance fit) is needed.

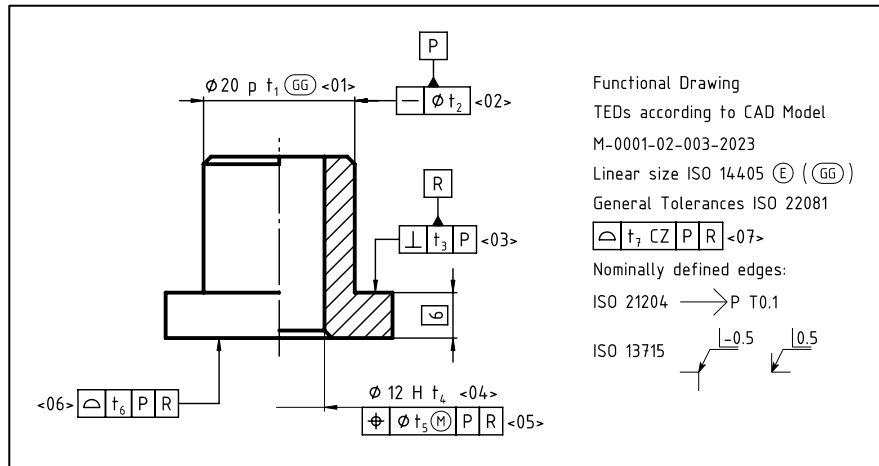


Fig. 4.26: Extract from the bushing 2D drawing.

For the shaft component, an extract from the 2D drawing is shown in Fig. 4.27. The datum description is analogous to the one given for the “wheel_asm” (Fig. 4.23). The only other functional feature is the cylinder that mates with the wheel. The dimension is specified with the (GG) modifier because of the interference fit that is required to hold the wheel once mounted. It is also located with respect to the primary datum using a coaxiality tolerance.

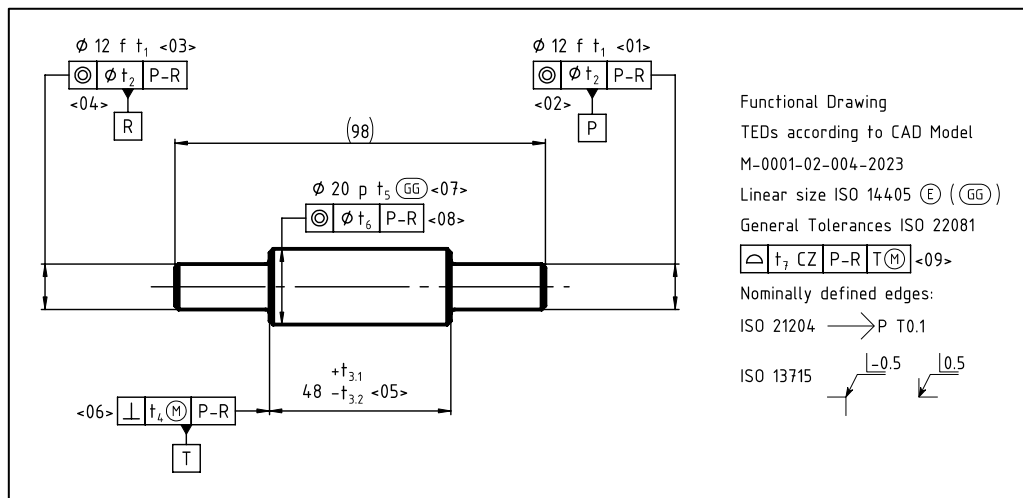


Fig. 4.27: Extract from the shaft component 2D drawing.

The 2D drawing for the last component, the wheel, is shown in Fig. 4.28. The primary datum [P] is defined over the hole that mates with the shaft. Dimensionally, it is defined using the (GG) modifier because of the interference fit, and geometrically, a linearity tolerance is applied to the axis. The secondary datum [R(M)] corresponds to the secondary datum assigned to the “wheel_asm” (Figure 4.36). The outer surface of the wheel is then located (surface profile tolerance) with respect to the complete datum system [P|R(M)].

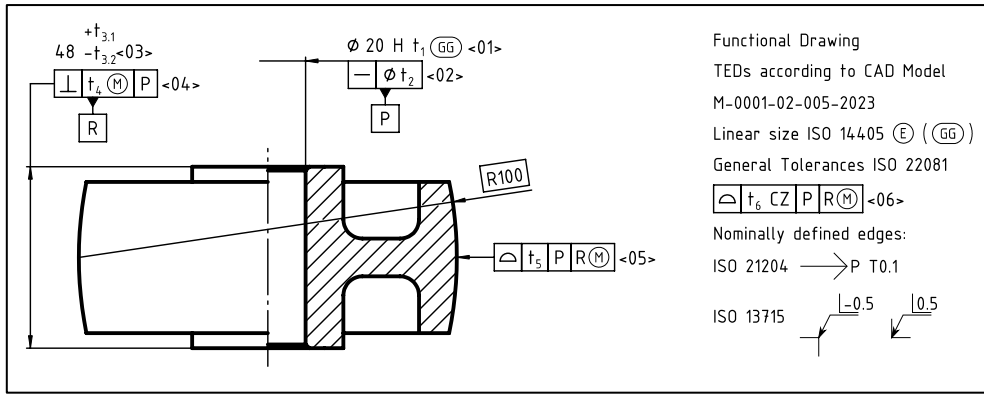


Fig. 4.28: Extract from the wheel component 2D drawing.

5 || A top down approach for tolerance synthesis using tolerance stack-up

A top-down view reveals patterns that a bottom-up approach may never see.

Anonymous

In the previous two chapters, a methodology for creating functional specifications has been presented. Firstly, the definition and cataloging of functional features were introduced in Chapter 3. Secondly, it was demonstrated how the information collected through the cataloging of functional features can lead to the definition of a functional geometric specification. At this point, we have a geometric specification without tolerance values, meaning that dimensional and/or geometric tolerances have not been applied to the assembly/sub-assembly/part features.

Now, the focus is on formalizing the value of each tolerance through a process referred to as “tolerance synthesis” or “tolerance allocation.” Tolerance synthesis or allocation is the process through which an optimal set of tolerance values can be assigned to a geometric specification. A product is typically composed of different components assembled together [77]. The assembly process brings into relation the single parts, and the geometric deviations of each part are mechanically transferred to the subsequent part in a sort of mechanical chain, spreading the effect of each deviation throughout the product. The interrelation of these deviations can build up and potentially affect the functionality of the final product.

At the product level, a set of functional requirements can be defined, expressed as a set of geometric constraints in the form of gaps and/or angles between features pertaining to different parts of the assembly. Each of these geometric functional requirements can be assigned a functional range. The simplest version of this can be identified in a gap required to be positive to allow assemblability. These functional requirements can be referred to as Key Characteristics (KC), Significant Characteristics, Key Product Characteristics, Critical-to-Function (CTF), Critical-to-Quality (CTQ), Customer Critical Dimension, etc [77,86].

The problem now translates into finding appropriate values for each tolerance on each part that allow the actual KC to be within functional limits; this can be achieved through tolerance stack-up. Tolerance stack-up allows for the simulation/estimation of the value of a KC based on the

tolerance values assigned in the geometric specification. The estimation can be based on both worst-case or statistical simulation. In either case, it is possible to see the estimated value and/or distribution for the KC as a function of all the tolerances. If we invert the equation aiming to find tolerance values that allow us to respect the functional requirement, there are more variables than constraints, therefore, infinite combinations of tolerance values can be found.

Among the infinite combinations, an optimal set can be defined through a process of optimization. The definition of an optimal set is still lacking, as different function loss definitions can lead to different solutions. Usually, the optimization problem consist in defining the set of tolerances that minimize manufacturing cost, requiring a tolerance-cost model, or maximize the overall tolerance value while respecting a given quality (e.g., max rejection rate). Many examples of applications using different strategies can be found in the literature [87–93].

All these approaches look at the final product as made of single parts assembled together, and therefore, the optimization involves all the parts at once. While this might be a good way to distribute the geometric variability throughout the entire product, eventually based on the manufacturing process capabilities for each part, it requires that all the responsibility is taken by the top-level design (see chapter 2). Furthermore, the use of a tolerance-cost model is intimately linked to the manufacturing process, making it closely related to tolerance synthesis for manufacturing specifications. In the field of synthesis of functional specifications, this chapter proposes a top-down approach for tolerance synthesis, taking into consideration the sub-assembly definition, where the result of each synthesis step becomes the requirement for the subsequent step up to the part level.

5.1 || What’s the meaning of tolerance stack-up

Before starting to use tolerance stack-up for the purpose of tolerance synthesis, it is crucial to define the meaning of performing a tolerance stack-up. In many industrial cases, as observed during the industrial collaboration gained by the Design and Tools in Industrial Engineering Laboratory, tolerance stack-ups were used in a “non-conventional” way. Instead of defining Key Characteristic (KC) limits first, these limits were set through tolerance stack-up: the natural tolerances of the manufacturing process, meaning the tolerance limits that enclose the geometric errors found during the inspection of pre-production batches, are imposed on all tolerances, and the variability of the KC is simulated to define its limits. This is an example of “open-loop” tolerance stack-up, and its real benefit is unclear: a bottom-up approach is used, and everyone hopes for the best. Luckily, in many conventional industrial applications, the manufacturing process capabilities are better than actually needed (functionally). No real optimization is possible since a pure snapshot of the manufacturing process capability is taken.

Performing a tolerance stack-up is indeed a simulation. As with any type of simulation (Mechanical, Fluid dynamics, multibody, etc.), there is a fixed set of inputs, an output (result), and

an evaluation criteria that is used to evaluate the result. As input, it is almost always possible to define the geometry, the properties, and the boundary conditions, as depicted in Fig. 5.1.

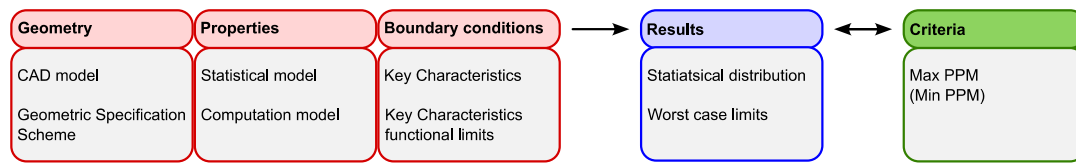


Fig. 5.1: Input-output relation for tolerance stack-up simulation.

For a tolerance stack-up analysis, the geometry is described by the CAD model, and its allowable geometric variation is described in the geometric specification. When referring to the geometric specification, both the specification scheme and tolerance values are included. The properties are the statistical model used to generate statistical distributions based on the geometric specification and the computation model. If a worst-case analysis is performed, there is actually no need for a statistical model. However, since worst-case computation is usually not economically convenient, there is a need to generate statistical distributions from the geometric specification. In the design phase, where little to no knowledge of the manufacturing process is available, the common assumption is to fit a Gaussian distribution centered at the tolerance midpoint with a standard deviation (σ) equal to one-sixth of the tolerance value, meaning that the tolerance limits are at 3σ from the mean value. The result is a distribution that allows 0.3% of samples out of the tolerance zone. It is noteworthy to mention that Gaussian distributions are usually a good approximation of geometric deviations due to manufacturing processes but are not suitable for deviations due to clearances within the assembly; in this case, a uniform distribution better describes the actual behavior of the assembly. The boundary conditions are the Key Characteristics (KC) themselves, meaning their definition and their functional limits.

With this set of input, the tolerance stack-up can be performed, and the result is the estimated statistical distribution for the KC (or the estimated Worst case limits).

This result can now be compared to the KC functional limits, and a formal evaluation can be made. For instance, if the maximum number of scrap is defined as the evaluation criteria, this value can be compared to the simulated one, and a decision can be taken.

The two main decisions that can be made are to validate the design (geometric specification included) or to take action and review the design. Three different instances can occur, and if we still consider the evaluation criteria as the maximum number of scrap:

- The simulated value of scrap is slightly lower than the requirement.
- The simulated value of scrap is well below the requirement.
- The simulated value of scrap is above the requirement.

The distinction between the first two cases is not absolute, and a decision rule should be defined beforehand, including a minimum number of scrap, or a maximum C_p and/or C_{pk} .

In the first case, the design can be considered validated since the result is conformal to the requirement and it is not “oversized.” Yet, optimization of the single tolerance value can be performed.

In the second case, we have an “oversized” design, meaning that tolerance values are tighter than needed (functionally). This may lead to higher manufacturing costs with no real benefit (no increased value for the product). For this reason, tolerance values should be relaxed to meet the quality requirement at the lower cost possible.

In the third case, the quality requirement is not met, therefore action should be taken to fix the design. In this case, there is no single solution, but various paths can be theoretically chosen, each with different implementation costs since changes can be made at any input level.

The first option is to act on the geometry. The geometric specification can be updated, meaning that tolerance values can be decreased. This comes, generally, with a higher manufacturing cost, but no re-design is needed. If this approach is not feasible because the tolerances are already at the limit of the manufacturing process or too expensive, another solution is to change the nominal geometry to decrease leverage factors. In this case, a re-design is needed, and the associated cost shall be considered. Another extreme solution is to opt for selective assembly strategies, considering that every part needs to be inspected to be properly clustered.

The second option is to act on the property of the simulation. For instance, based on the knowledge of the manufacturing process, the statistical model can be updated so that more accurate statistical distributions can be used. Even though this is a viable solution, it is not advisable to do it since any decision may be based on biased data coming from preliminary production batches that do not reflect the long-term variability of the production process.

The third option is to act on the boundary conditions. In this case, the limit for the KC needs to be updated. One way to do it is to decrease the correlation uncertainty, allowing for a better definition of the geometrical limits that fulfill functional requirements. Simulations shall be performed to increase the knowledge of the correlation between function and geometric deviation. Another way is to return back to the drawing board to rethink the entire design, enabling larger variability on the KC. Of course, this type of change requires a significant investment of resources and may not be convenient.

A final option is to change the requirement on the evaluation criteria, allowing, for instance, a larger number of scraps. Economic loss due to the larger number of scraps needs to be quantified and evaluated.

5.1.1 Responsibility in Tolerance stack-up

Many times, tolerance stack-ups are performed during the design phase or the engineering phase when the manufacturing process needs to be set up. For this reason, the responsibility for the simulation and its results is given to the design department, even though, as presented so far, there are inputs coming from manufacturing or quality. It is noteworthy to point out that the quality department does not coincide with the quality control department: the quality department is responsible for setting the quality standards for a company (legislator), while the quality control department is responsible for checking conformity to the specifications according to the quality standards (judge).

Therefore, it is important to define the responsibility in tolerance stack-ups to allow all the actors to be informed and to give proper inputs to get the most out of the simulation.

Regarding the geometry used for the simulation, the responsibility lies with the design department since they are the ones responsible for creating the CAD model. No changes to the 3D model shall be done without the designer's approval and supervision.

The specification scheme/geometric specification, as presented in chapter 2, can be divided into functional specification, manufacturing specification, and verification specification; the responsibility for these three different types of specifications pertains respectively to the design department, the manufacturing department, and the quality control department. For tolerance stack-ups, only functional and manufacturing specifications can be used. The responsibility over the specification, when it regards tolerance stack-ups, pertains to the specification owner.

The property of the simulation, namely the statistical model and the computation methods, shall be controlled by the quality department/management and shall be used coherently within a company. A designer shall never be allowed to change these properties without permission from the quality department/management.

The boundary conditions, therefore the KCs and their variabilities, are set at the assembly level, and the responsibility for their definition lies with the designer at the "upper level" (refers to Fig. 2.6 at page 51).

Lastly, the evaluation criteria are under the responsibility of the quality/management and shall be used consistently. A summary of the considerations presented here can be found in Tab. 5.1.

Tab. 5.1: Responsibilities in tolerance stack-up.

Parameters	Responsible
Geometry:	
CAD model	Designer
Geometric Specification	Specification Owner
Parameters:	
Statistical model	Quality
Computation model	Quality
Boundary conditions:	
KC definition	Assembly (Upper level) designer
KC limits	Assembly (Upper level) designer
Evaluation criteria:	
Maximum PPM (or others)	Quality

5.2 || Updated mono-dimensional Excel model for tolerance stack-up

To perform tolerance stack-up analysis many different model can be found in the literature. The vector-loop approach uses a kinematic model to represent the product variability [94,95]. The variational approach represents the deviations from nominal and assembly constraints using a set of mathematical equations [96]. The matrix approach uses a matrix to describe the small displacement of a feature in its tolerance zone or the gaps between parts [97]. An approach based on the Jacobian uses virtual joints associated with functional elements to simulate small displacements in terms of translations and rotations around a point of interest. Functional elements are collected in pairs creating a kinematic chain, both internal pairs, to describe part variation, and external pairs, describing the link between parts in contact, are possible [98,99]. The torsor approach assumes that the feature deviation within its tolerance zone can be described using small linear and angular dispersions that are described using the small displacement torsor [49,52]. The approach based on Jacobian is used in conjunction with the torsor approach in the unified Jacobian-torsor model, the first one is used for tolerance propagation, the second is used to describe features variability [100]. The use of Tolerance-Map®, or T-Map®, to describe the multiple degrees of freedom controlled by each tolerance zone brings an approach that allows deriving stack-up equations: the Minkowski sum is used to combine different T-Maps to find the result on a target feature [101].

Based on these models, different commercial CAT (Computer Aided Tolerancing) software solutions were developed, e.g., 3DCS by Dimensional Control Systems®, CETOL6sigma by Sigmetrix, VisVSA by Siemens®, and many more.

For the sake of this chapter, none of the above have been used, nor specific CAT tools. Instead, an Excel tool based on the one developed by Fischer [79] is used. The reason behind this choice is that an Excel tool allows for quick and simple customization for different applications and its widespread usage in industry. The Excel tool implements the worst-case analysis, the RSS analysis, and the Adjusted RSS as defined in [79].

Several add-ons have been incorporated into the model by Fischer to enhance efficiency and flexibility, and an integrated graphical representation of the results has been developed. The updated worksheet now internally calculates a new nominal value and symmetric tolerance limits when asymmetric limits are assigned. It also allows for the explicit assignment of the coverage factor k , which is used to convert the tolerance limit into terms of standard deviation, for each row.

The worksheet has been modified to include the capability of setting the sensitivity coefficient ($|s_i|$) using an adapted version of the formulas described by Cox [102,103].

The output mean and variance are determined using the following equations:

$$\mu_{OUT} = \sum_{i=1}^n |s_i| \cdot \mu_i \quad (5-1)$$

$$\sigma_{OUT}^2 = \sum_{i=1}^n (|s_i|)^2 \cdot \sigma_i^2 \quad (5-2)$$

It is important to note that when computing the mean of the output (μ_{OUT}), each input mean (μ_i) should be used with their positive or negative value, according to the convention described in [79], which allows for considering the absolute value of the sensitivity.

Once the output mean and variance are known, the rejection rate can be easily determined by integrating the Gaussian probability density function:

$$r = \int_{-\infty}^{LSL} \frac{1}{\sqrt{2\pi\sigma_{OUT}^2}} \exp\left\{-0.5 \frac{(x-\mu_{OUT})^2}{\sigma_{OUT}^2}\right\} \partial x + \int_{USL}^{+\infty} \frac{1}{\sqrt{2\pi\sigma_{OUT}^2}} \exp\left\{-0.5 \frac{(x-\mu_{OUT})^2}{\sigma_{OUT}^2}\right\} \partial x \quad (5-3)$$

Where LSL and USL are the lower and upper specification limits respectively.

The Excel tool has two tabs, one for input (Fig. 5.2) and one for the results (outputs) (Fig. 5.3).

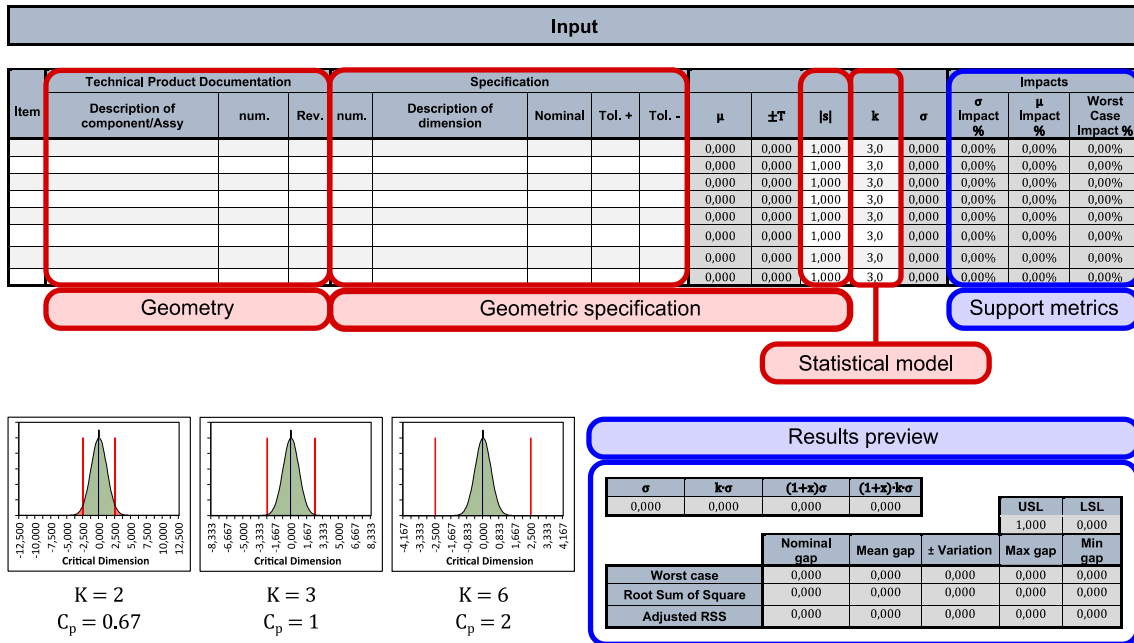


Fig. 5.2: Input tab for the Excel tool.

In the input tab, the geometry and simulation parameters are set. The Key Characteristic (KC) is implicitly defined by constructing the stack-up, and its functional limits are set in the output tab. Each tolerance input to the stack-up is covered in one or more rows. As shown in Fig. 5.2, a section is dedicated to describing the nominal geometry. In each row, it is possible to state the name of the component from which the input tolerance is taken, along with the drawing (or MBD model) number and revision to ensure traceability of the information.

In a second section, information about the specifications is added. A numerical identifier and a description can be included for each tolerance to ensure traceability, followed by the numerical values. The nominal dimension is added following the Fischer convention [79]. The tolerance values are added as upper and lower limits, and the mean value and symmetric tolerance are computed automatically. Additionally, the sensitivity can be defined, with the default value being 1. If a different value is manually input, the cell is highlighted in yellow to notify the user.

In addition to these inputs, this tab also provides a preview of the results, which may be useful during tolerance synthesis, and some support metrics, namely the statistical impact on the output variance, the impact on the output mean shift, and the worst-case contribution for each row.

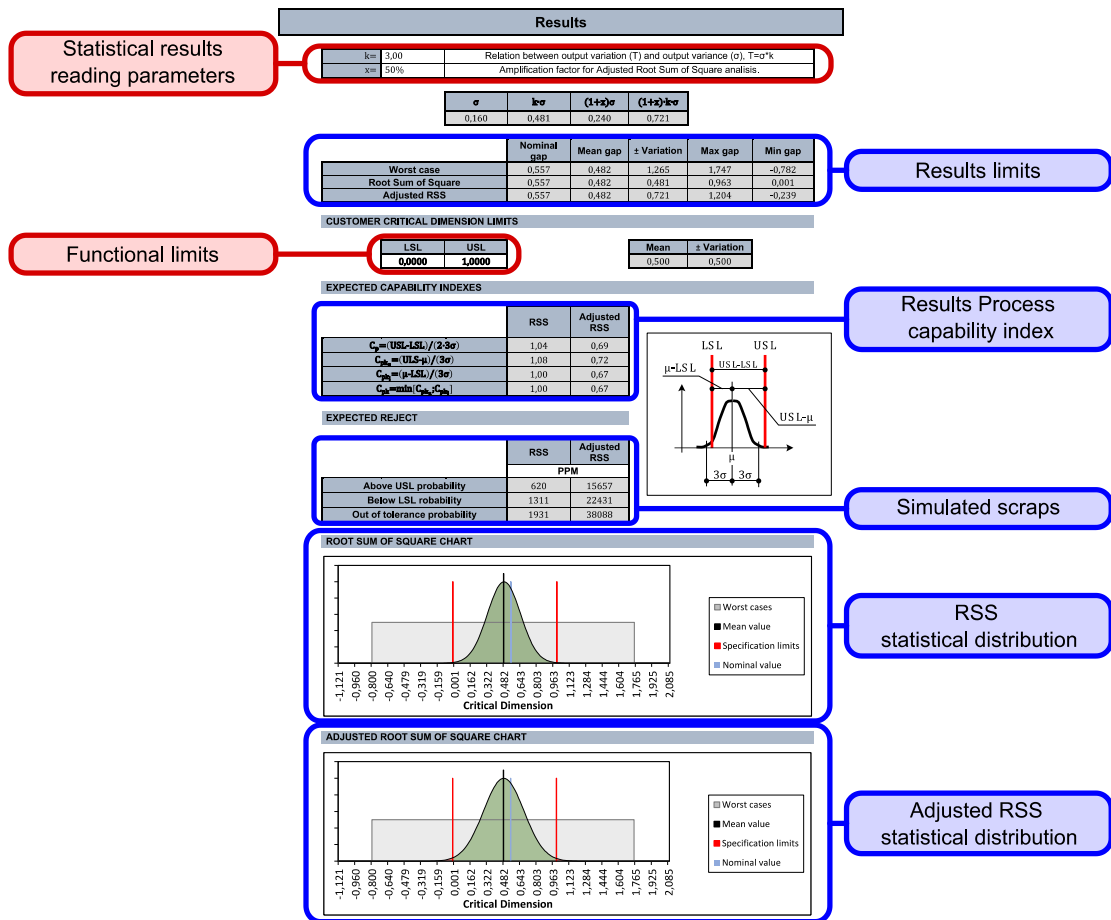


Fig. 5.3: Output tab for the excel tool.

In the output tab, the functional limits on the Key Characteristic (KC) need to be set. There is also the option to set the parameter k for the definition of statistical limits. Since the Gaussian distribution is defined from negative infinity to positive infinity, there is no actual maximum dimension according to the statistical distribution. To define a maximum and minimum dimension based on the statistical distribution, the limit is set at k times the standard deviation (σ) from the mean. Furthermore, it is possible to manually set the parameter that defines the Adjusted RSS computation method.

The first set of results in the output includes the KC limits according to the three computation models that are implemented. The second result is relevant to the statistical computation model only; the commonly used C_p and C_{pk} parameters are estimated for the KC, and then the expected number of scrap is quantified.

Lastly, a graphical representation is provided for both the RSS and Adjusted RSS: the statistical distribution is plotted against the functional limits, and the worst-case limits are also displayed. To provide an immediate graphical feedback, the distribution is shown in green between the functional limits and in red outside them.

5.2.1 Tool general hypothesis

When using this tool, it is important to remember and check whether the general hypotheses used to build the model are met. These hypotheses include.

- **Linear tolerance stack-up:** It is possible to define an unambiguous linear geometric relation between each input and output.
- **Mono-dimensional tolerance stack-up:** All the dimensions (both input and outputs) act on the same line of action (projections are always possible to align the contributions).
- **Rigid assembly:** All components in the assembly are considered as perfectly rigid.
- **Isostatic assembly:** There are no components that are constrained iperstatically.
- **Central distribution:** The statistical distributions are considered centered to the tolerance midpoint and fill all the tolerance zone.

If any of these hypotheses are not met, the result of the tolerance stack-up may not be correct.

5.2.2 Compiling examples

In this section, some examples of how to use the Excel tool will be provided. The main types of tolerances involved in the creation of the tolerance stack-up are sizes, location tolerances (location, symmetry, concentricity), and surface/line profile tolerances. For each of these three categories, different types of information are needed. In Fig. 5.4 the template with mandatory and optional information is presented. Optional information depends on specific modifiers.

Description of dimension	Nominal	Tol. +	Tol. -
Size			
Location/symmetry/concentricity tolerances			
Bonus M/L			
Datum Feature Shift (DFS)			
TED			
Surface/Line profile			
UZ shift			
Datum Feature Shift (DFS)			
TED			

Mandatory

Optional

$200 \begin{matrix} +t_{36} \\ -t_{37} \end{matrix} \textcircled{E} <01>$

$8x \varnothing D \pm t_4 \textcircled{E} <04>$

$\oplus \varnothing t_5 \textcircled{CZ} \textcircled{M} \textcircled{P} \textcircled{R} \textcircled{T}$
 (05)

$<04>$

$\ominus t_{20} \textcircled{UZ+u_3} \textcircled{P} \textcircled{R} \textcircled{T}$

Fig. 5.4: Template for input quantities based on the type of tolerance.

Sizes are the easiest items to manage in the Excel tool, as they only need one single line. The nominal value is always mandatory, while the tolerance values are optional. If the feature of size is located with a Material Condition, the contribution of the size variability needs to be added as a “Bonus” in the location tolerance, and the nominal value needs to be changed to the minimum material size if Maximum Material Condition is applied to the location tolerance, or the maximum material size if Minimum Material Condition is used instead. The full description of these rules can be found in [79].

Location tolerances require four lines: tolerance, Bonus, Datum Feature Shift, and the Theoretically Exact Dimension (TED). The first line is dedicated to the tolerance itself, and the tolerance limits are mandatory. The second line is used for the Bonus coming from the application of a material condition, and the tolerance limits are optional, used if a material condition is applied. The third line is used if the datum system is specified using a material condition, and the datum feature shift needs to be calculated according to the equations given by Fischer, and is added in the tolerance limits. Lastly, the fourth row is dedicated to the TED, where the nominal value is mandatory, but it might also be zero.

Surface/line profile tolerances are similar to location tolerances, as they also need four lines, and three of them are identical to the previous case: tolerance, Datum Feature Shift, and TED lines. The difference is that the Bonus line is not present, since no material condition can be applied to this class of tolerances, but the UZ shift line is added. The UZ is a modifier that allows the tolerance zone to be translated from the nominal value by a given amount, positive if the shift is outside the part, and negative if it is inside the part. The actual result is the same as changing the nominal value

(TED), as the numerical value is added to the nominal column. Particular attention shall be given to the sign of the UZ. Methodological examples are provided in the next sections.

5.3 || Traditional approach

In order to appreciate the differences in the proposed top-down approach, a simple case study is presented, starting with a “traditional” tolerance synthesis. In the next section, the top-down approach will be presented.

The assembly drawing for the case study can be seen in Fig. 5.5. The assembly is actually composed of a slot (part D) that mates with a sub-assembly (parts A1, B1, C1, A2, B2, and C2 pre-assembled together); this sub-assembly is created by assembling two sub-assemblies, the first one consisting of parts A1, B1, and C1, and the second one consisting of parts A2, B2, and C2. The requirement in this example is given by the pure assembly requirement, where the gap between the cave and the “shaft” (higher-level sub-assembly) needs to be positive, while also being lower than a given value of 1 mm to avoid excessive wobbling. The requirement is stated in the assembly drawing, as shown in the book by Stanley Parker [18].

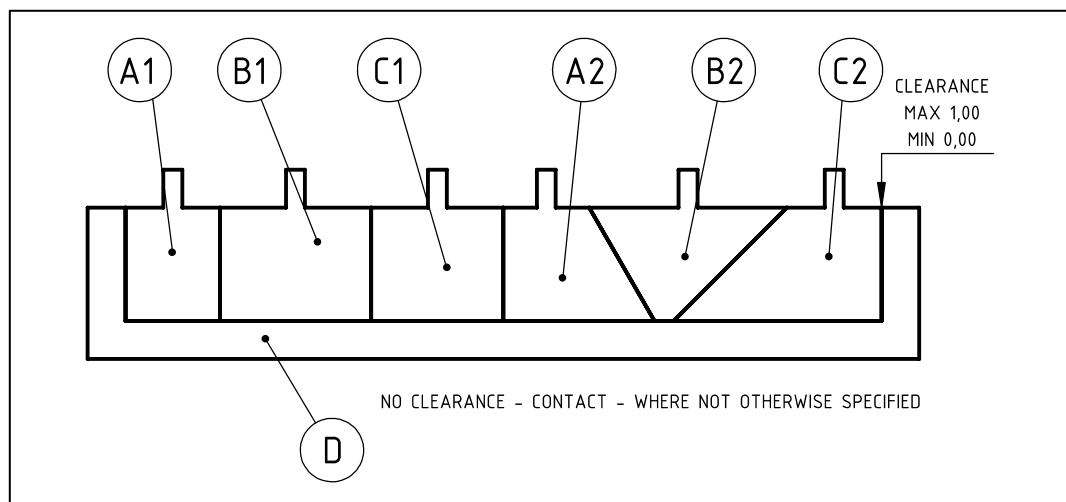


Fig. 5.5: Case study assembly 2D drawing.

In the standard practice, when it comes to tolerance synthesis, the sub-assembly definition is not taken into account. The tolerance stack-up is, therefore, based on the single parts' geometric specifications. Here follows an extract of the 2D drawings of each part, from Fig. 5.6 to Fig. 5.12.

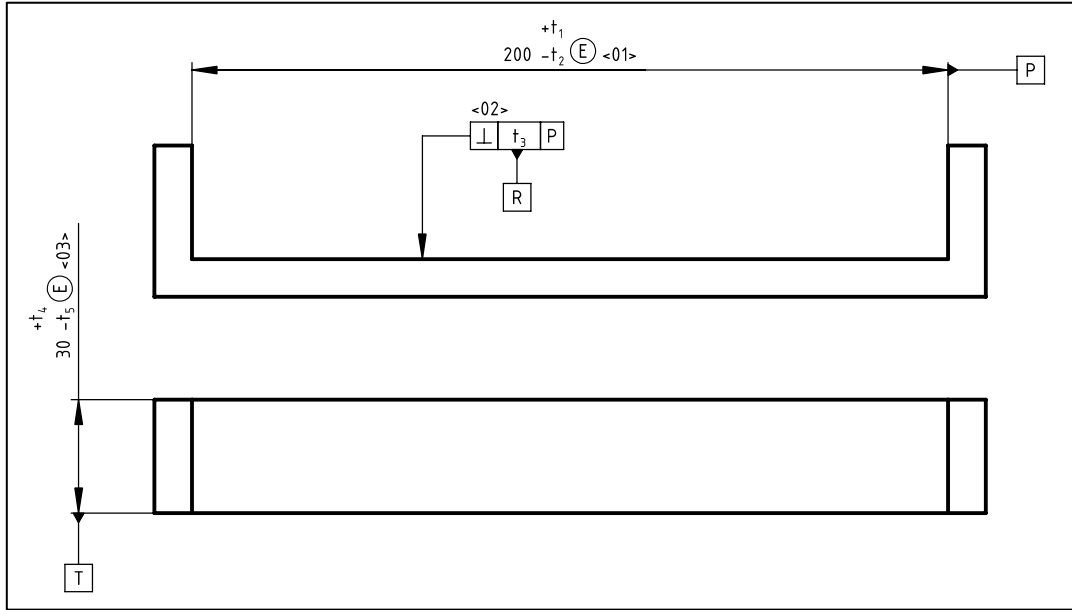


Fig. 5.6: Slot geometric specification.

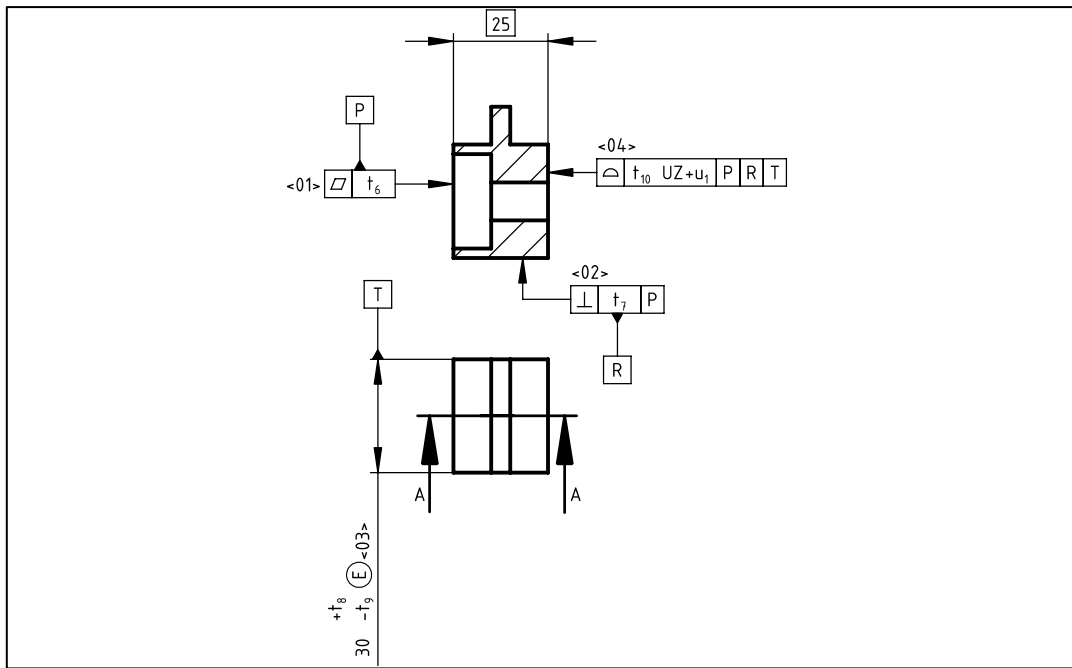


Fig. 5.7: Component A1 geometric specification.

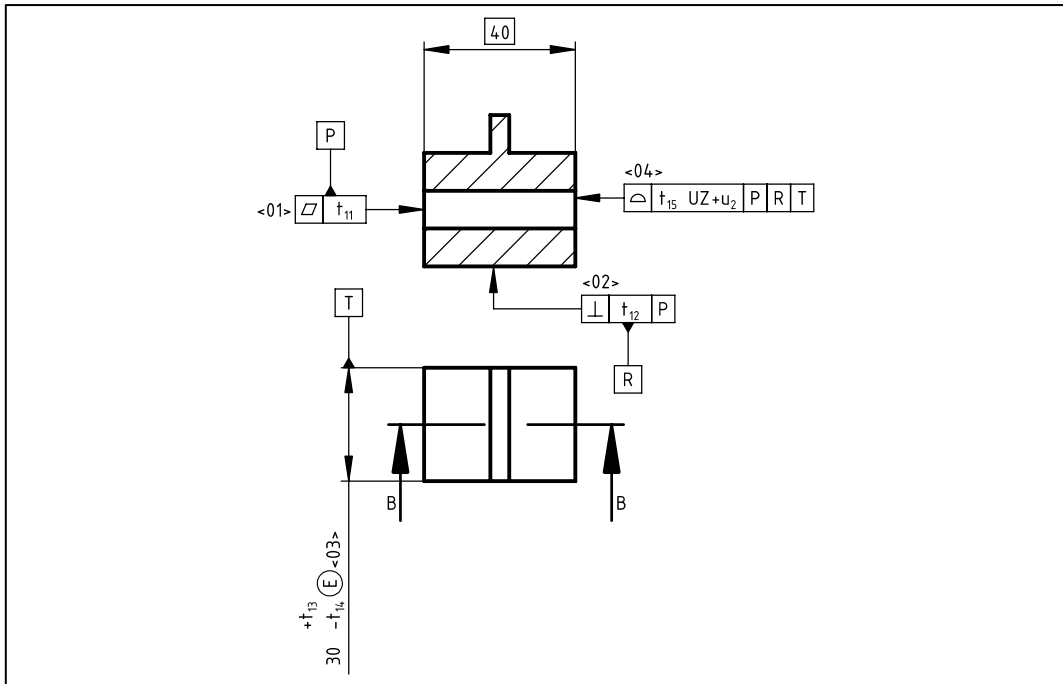


Fig. 5.8: Component B1 geometric specification.

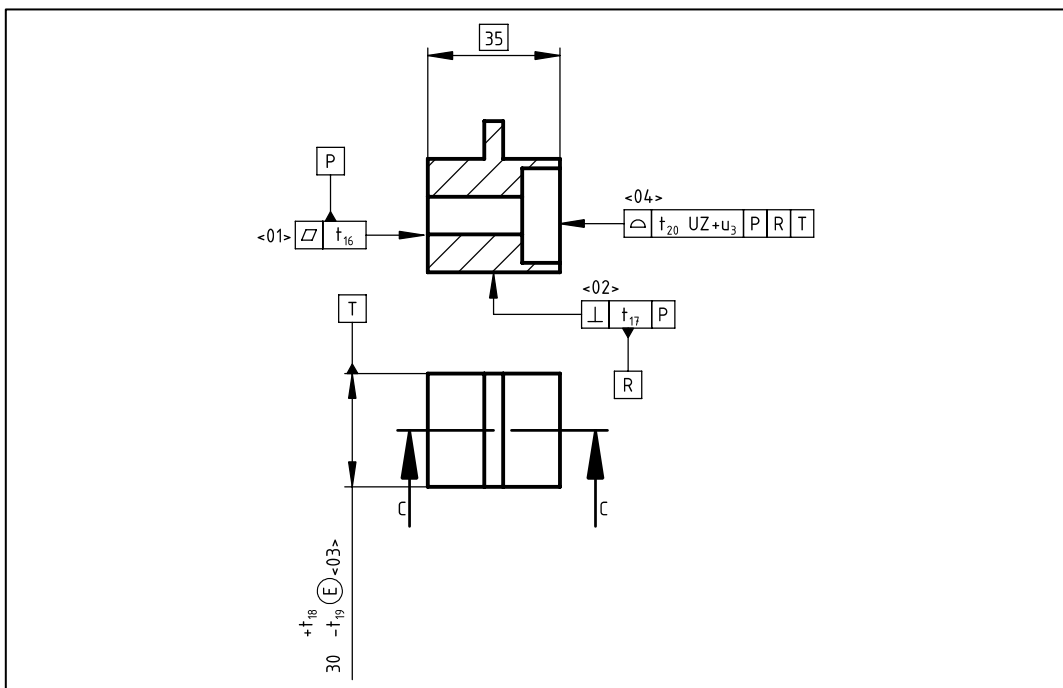


Fig. 5.9: Component C1 geometric specification.

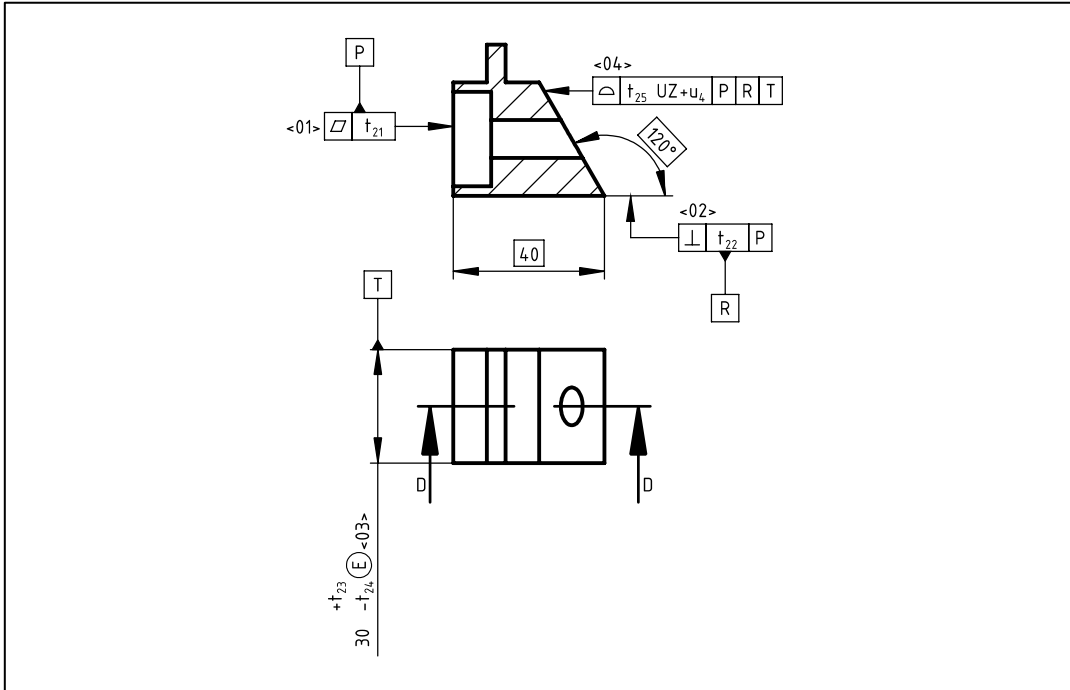


Fig. 5.10: Component A2 geometric specification.

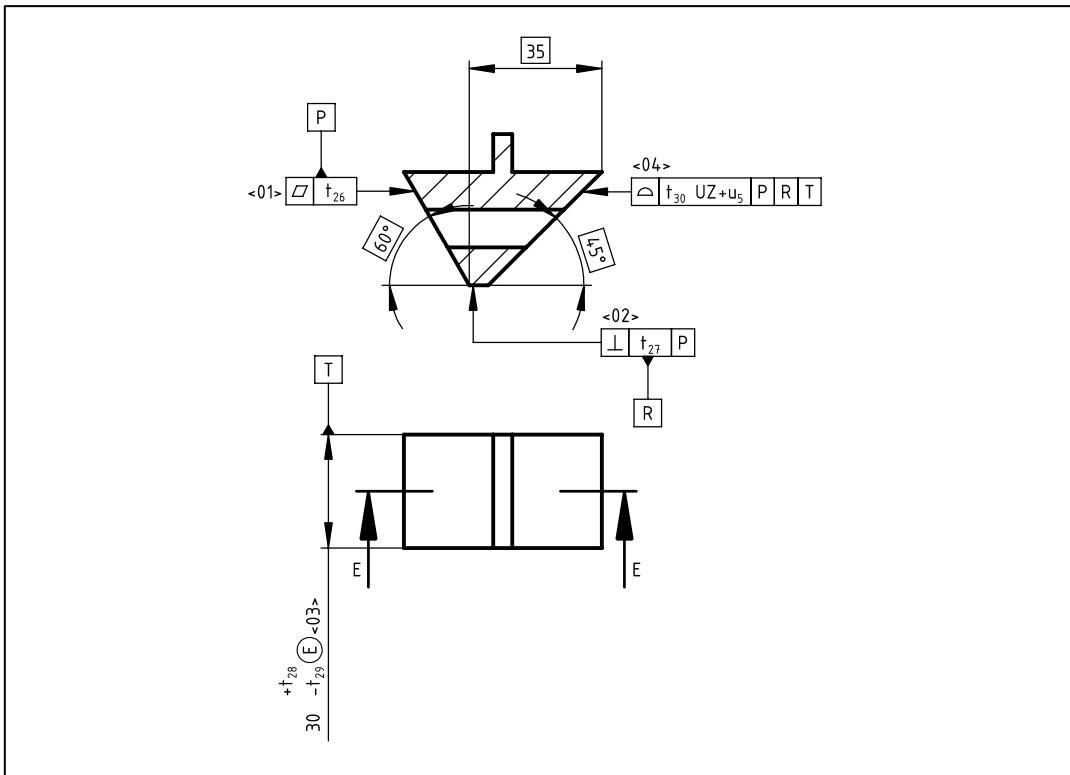


Fig. 5.11: Component B2 geometric specification.

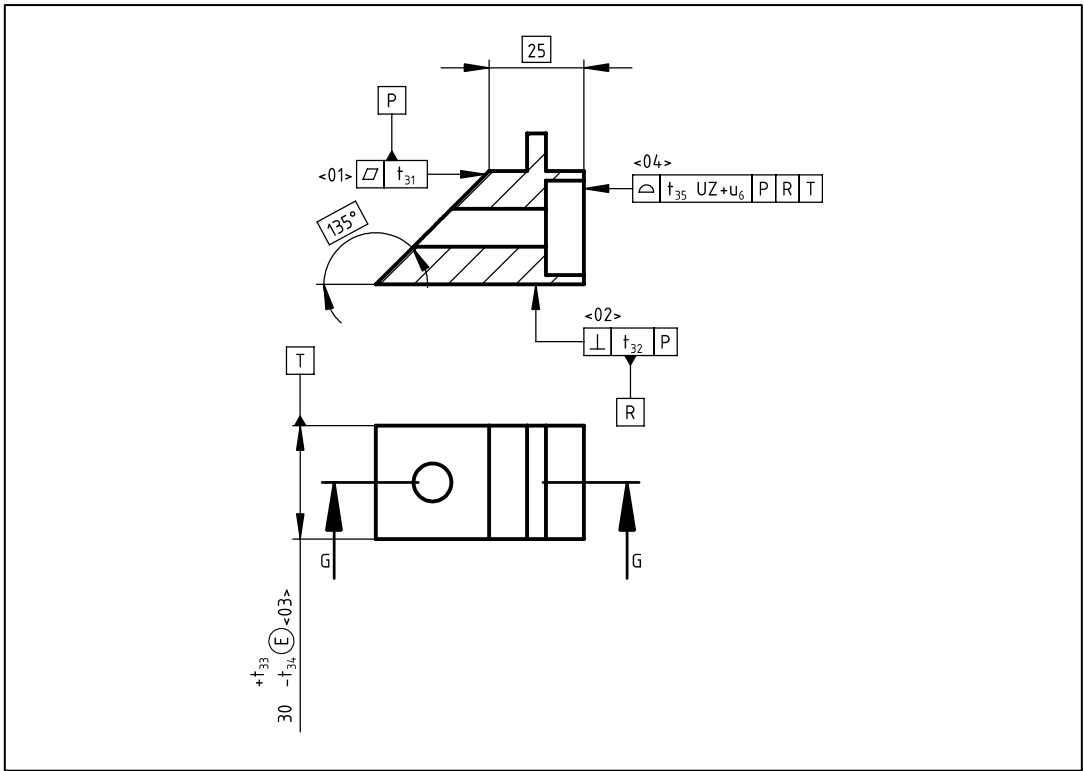


Fig. 5.12: Component C2 geometric specification.

At this point, no actual values are assigned to any tolerance value; the ASME rule on the usage of location tolerance and surface profile, respectively for derived features and integral features, is followed. This distinction is indeed very useful since it allows using the UZ modifier to control asymmetry in tolerance zones. In full generality, the UZ modifier is applied to all surface profile tolerances since it represents a value that can be used during synthesis/optimization.

At this point, the stack-up “scheme” can be drafted. In Fig. 5.13 the first iteration of the scheme can be seen. At this point, the UZ contribution is neglected, and the actual position of each feature involved along the stack-up direction is drafted as a vertical line. The Gap vector is added; starting from the initial point of the gap vector, the vector loop following all parts can be traced. The positive direction needs to be in the same orientation as the gap vector to have a positive gap with clearance, a negative one with interference.

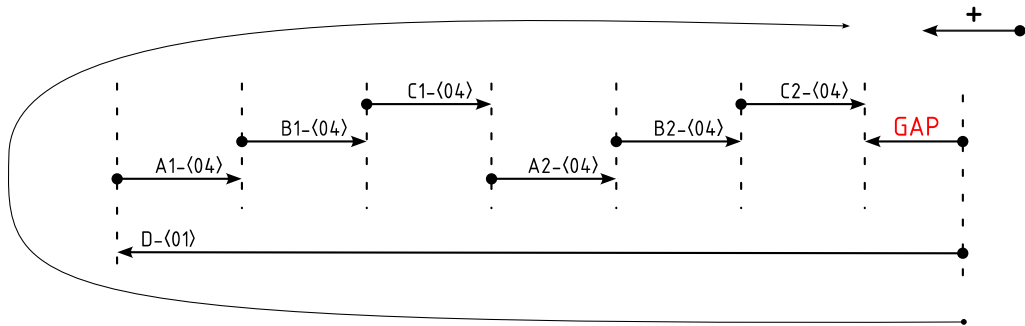


Fig. 5.13: Stack-up scheme, still not displaying UZ contribution.

Using this scheme, it is not really easy to interpret the sign of the UZ values. To easily consider the UZ values in each interface where a UZ modifier is applied, a new vertical line needs to be traced on the sign of positive UZ. A small vector linking the old line to the new one can be added. The direction of this vector gives the sign that needs to be used before the UZ value. In Fig. 5.14, the final result can be seen; this scheme can be used to insert information in the input tab of the Excel tool.

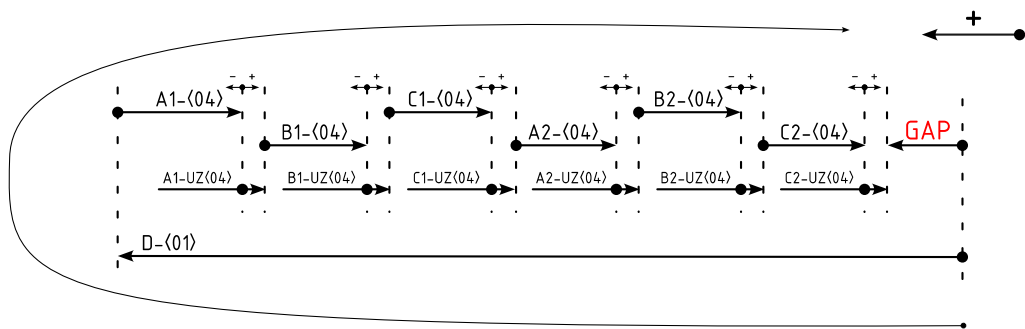


Fig. 5.14: Stack-up scheme, displaying UZ contribution.

When sloped surfaces are involved, it is possible to choose any height to determine the nominal dimensions, and the variability contributions are scaled using the sensitivity coefficient $|s| = \cos(\alpha)$ where α is the first quadrant angle between the stack-up direction and the surface normal.

Using the parameters assigned to each tolerance value in Fig. 5.6 to Fig. 5.12, the stack-up inputs can be seen in Fig. 5.15.

Item	Technical Product Documentation			Specification					s	k
	Description of component/Assy	num.	Rev.	num.	Description of dimension	Nominal	Tol. +	Tol. -		
									1,00	3,0
01	slot, component D	D	01	<01>	Size slot	200,00	t_1	$-t_2$	1,00	3,0
									1,00	3,0
02	component A1	A1	01	<04>	surface profile		$t_{10}/2$	$-t_{10}/2$	1,00	3,0
					UZ shift	$-u_1$			1,00	3,0
					Datum Feature Shift (DFS)				1,00	3,0
					TED	-25,00			1,00	3,0
									1,00	3,0
03	component B1	B1	01	<04>	surface profile		$t_{15}/2$	$-t_{15}/2$	1,00	3,0
					UZ shift	$-u_2$			1,00	3,0
					Datum Feature Shift (DFS)				1,00	3,0
					TED	-40,00			1,00	3,0
									1,00	3,0
04	component C1	C1	01	<04>	surface profile		$t_{20}/2$	$-t_{20}/2$	1,00	3,0
					UZ shift	$-u_3$			1,00	3,0
					Datum Feature Shift (DFS)				1,00	3,0
					TED	-35,00			1,00	3,0
									1,00	3,0
05	component A2	A2	01	<04>	surface profile		$t_{25}/2$	$-t_{25}/2$	$\cos(30^\circ)$	3,0
					UZ shift	$-u_4$			$\cos(30^\circ)$	3,0
					Datum Feature Shift (DFS)				1,00	3,0
					TED	-40,00			1,00	3,0
									1,00	3,0
06	component B2	B2	01	<04>	surface profile		$t_{30}/2$	$-t_{30}/2$	$\cos(45^\circ)$	3,0
					UZ shift	$-u_5$			$\cos(45^\circ)$	3,0
					Datum Feature Shift (DFS)				1,00	3,0
					TED	-5,00			1,00	3,0
									1,00	3,0
07	component C2	C2	01	<04>	surface profile		$t_{35}/2$	$-t_{35}/2$	1,00	3,0
					UZ shift	$-u_6$			1,00	3,0
					Datum Feature Shift (DFS)				1,00	3,0
					TED	-55,00			1,00	3,0

Fig. 5.15: Extract from the input tab of the Excel tool.

Assuming that the requirement is to have the KC with both C_p and C_{pk} greater than 1, meaning a maximum scrap of 0.3 %, the procedure can be divided into two steps. First, we assign a tentative value to all tolerances based on previous experience and assume all UZ values to be equal to 0. Looking at the result, if C_p is lower than 1, the tolerance values need to be decreased; if C_p is much greater than 1, tolerances might need to be enlarged. Iteratively, we can reach the point where C_p is equal to 1 or slightly above. It is noteworthy that a change in tolerance values for tilted surfaces has a lower effect on the KC.

Once C_p is within specification, attention shifts to C_{pk} . In this particular case, C_{pk} will be very small since the nominal gap is 0. The statistical distribution needs to be shifted; to do so, it is possible to make size tolerances asymmetrical and/or change the UZ values. Changing these

values does not change manufacturing cost since the effect is a shift in the “nominal” (mean) value. Iteratively, we can reach a point where Cpk requirements are respected.

In our case study, this is achieved for the values in Tab. 5.2; the values for tolerances that are not used in the stack-up are omitted. These values are not actually optimized, as no optimization routine was implemented; nonetheless, it might be implemented in future iterations.

Tab. 5.2: Tolerance values after traditional tolerance synthesis.

Component	Tolerance	Value (mm)
D	$t_1 =$	0.10
	$t_2 =$	0.25
A1	$t_{10} =$	0.35
	$u_1 =$	-0.10
B1	$t_{15} =$	0.40
	$u_2 =$	-0.10
C1	$t_{20} =$	0.40
	$u_3 =$	-0.10
A2	$t_{25} =$	0.40
	$u_4 =$	-0.10
B2	$t_{30} =$	0.40
	$u_5 =$	-0.10
C2	$t_{35} =$	0.40
	$u_6 =$	-0.10

The result using these values is shown in Fig. 5.16.

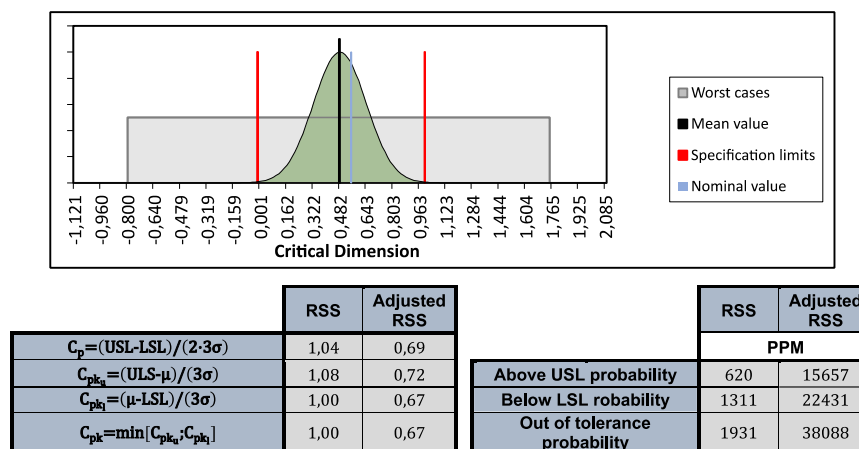


Fig. 5.16: Tolerance stack-up result after tolerance synthesis.

5.4 || Top-Down approach

A top-down approach for tolerance synthesis is now presented. In order to proceed in this way, sub-assembly geometric specifications need to be defined; an extract of the 2D drawings can be seen in Fig. 5.17, Fig. 5.18, and Fig. 5.19.

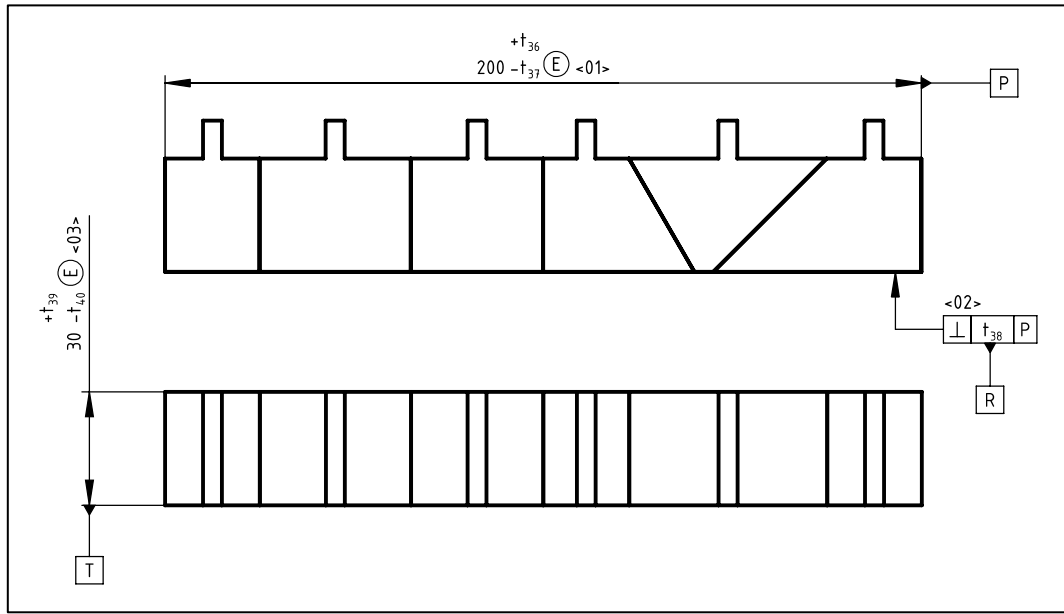


Fig. 5.17: Sub-assembly 1+2 geometric specification.

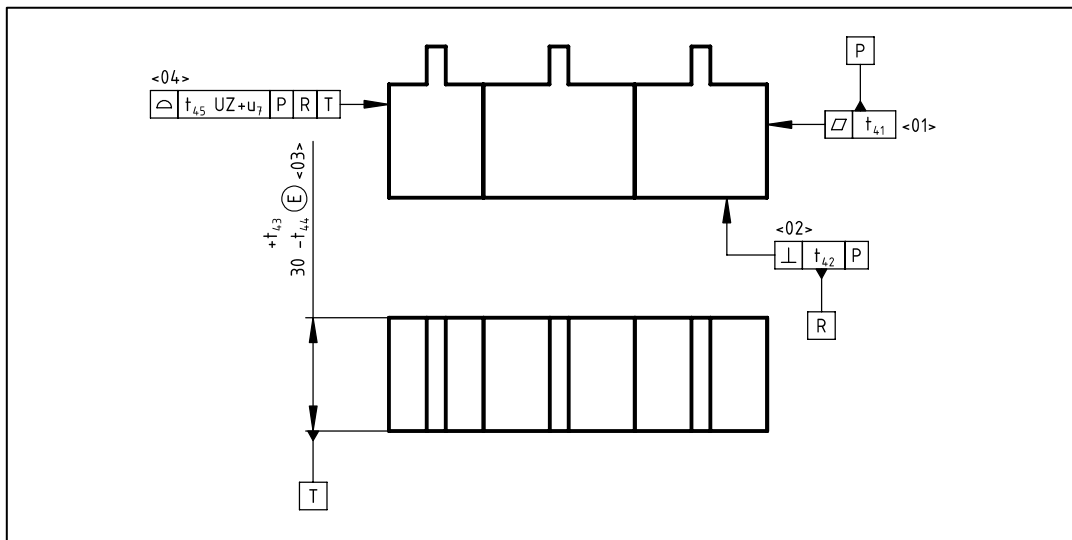


Fig. 5.18: Sub-assembly 1 geometric specification.

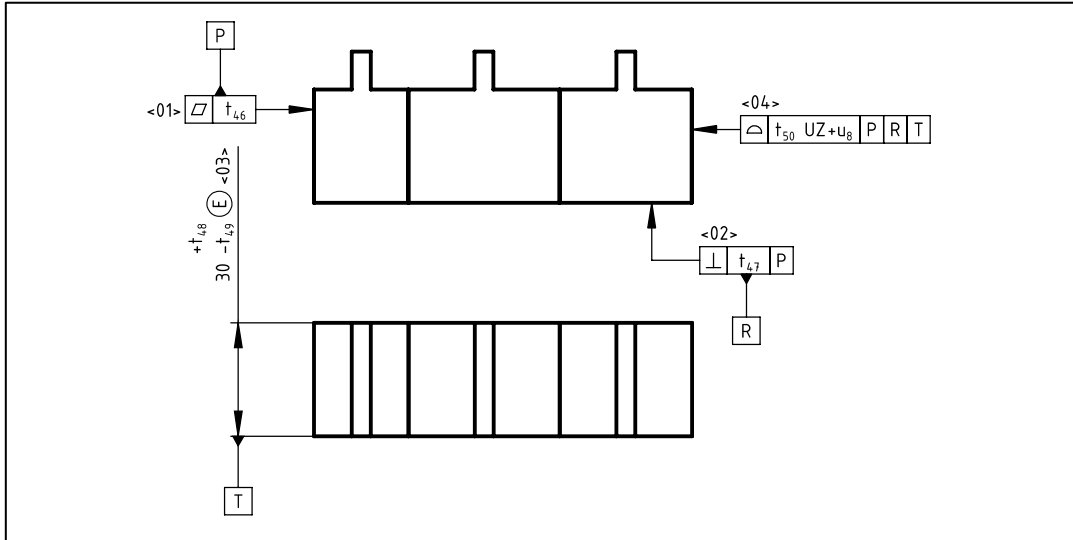


Fig. 5.19: Sub-assembly 2 geometric specification.

The geometric specifications for the single parts can be seen in Fig. 5.6 to Fig. 5.12. Following the top-down approach, four different stack-ups can be defined. The first one looks at the mating between component D (Fig. 5.6) and the sub-assembly 1+2 (Fig. 5.17), and the requirement can be seen in the full assembly geometric specification (Fig. 5.5). The second one looks at the mating between sub-assembly 1 and 2 (Fig. 5.18, and Fig. 5.19), and the requirement is stated in the sub-assembly 1+2 geometric specification (Fig. 5.17). The third one looks at the assembly of components A1, B1, and C1 (Fig. 5.7, Fig. 5.8, and Fig. 5.9), and the requirement comes from the assembly 1 geometric specification (Fig. 5.18). The fourth and last stack-up looks at the assembly of components A2, B2, and C2 (Fig. 5.10, Fig. 5.11, and Fig. 5.12), and the requirement comes from the assembly 2 geometric specification (Fig. 5.19). It can be easily seen that a hierarchical structure is defined, and the inputs at the higher level become the requirements at the lower one. Therefore, the tolerance stack-up can be clustered together and automatically linked.

The first stack-up becomes really simple and might be solved even without any specific tool since it represents the difference between two sizes. The KC is the gap between the two components, and its limits can be seen in Fig. 5.5. The resulting tolerance stack-up, using the parametric values defined in the geometric specifications presented so far, is shown in Fig. 5.20.

Item	Technical Product Documentation			Specification					s	k
	Description of component/Assy	num.	Rev.	num.	Description of dimension	Nominal	Tol. +	Tol. -		
									1,00	3,0
01	slot, component D	D	01	$\langle 01 \rangle$	Size slot	200,00	t_1	$-t_2$	1,00	3,0
									1,00	3,0
02	shaft, sub-assembly 1+2	1+2	01	$\langle 01 \rangle$	Size shaft	-200,00	t_{36}	$-t_{37}$	1,00	3,0

Fig. 5.20: Extract from the input tab of the Excel tool for the highest level (product).

At the lower level, which can be considered as the system level from Fig. 2.6, a quite simple stack-up can be defined too. Here, two sub-assemblies are assembled together, and the end surfaces are located from the datum system that describes the assembly features. This time, the KC is the total length of the sub-assembly; therefore, its functional limits actually coincide with the values $l + t_{36}$ and $l - t_{37}$ (where l is the nominal length), which can be seen as inputs at the higher level stack-up (Fig. 5.20). Since UZ modifiers are used, it is essential to have the tolerance stack-up scheme to properly assign the sign of each contribution, as shown in Fig. 5.21.

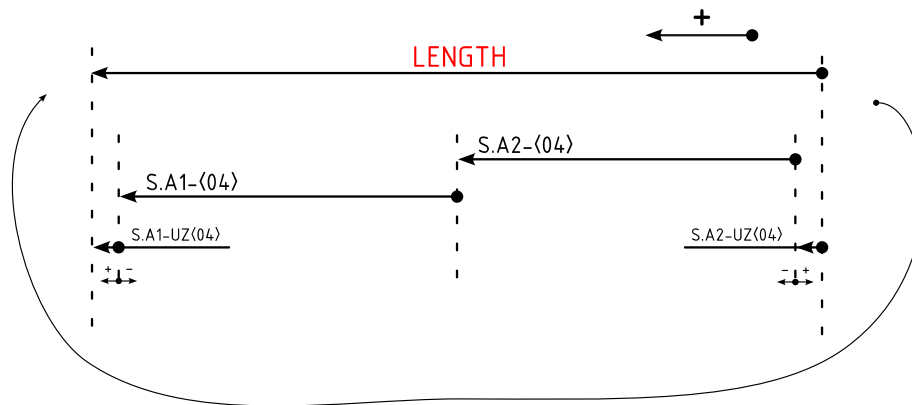


Fig. 5.21: Tolerance stack-up scheme for the second level (system).

The parametric inputs to the stack up can be seen in Fig. 5.22.

Item	Technical Product Documentation			Specification					s	k
	Description of component/Assy	num.	Rev.	num.	Description of dimension	Nominal	Tol. +	Tol. -		
									1,00	3,0
01	Sub-assembly 1	1	01	{04}	Surface profile		$t_{45}/2$	$-t_{45}/2$	1,00	3,0
					UZ shift		$+u_7$		1,00	3,0
					Datum Feature Shift (DFS)				1,00	3,0
					TED	100,00			1,00	3,0
									1,00	3,0
									1,00	3,0
02	Sub-assembly 2	2	01	{04}	Surface profile		$t_{50}/2$	$-t_{50}/2$	1,00	3,0
					UZ shift		$+u_8$		1,00	3,0
					Datum Feature Shift (DFS)				1,00	3,0
					TED	100,00			1,00	3,0

Fig. 5.22: Extract from the input tab of the Excel tool for the second level (system).

Finally, the last two stack-ups are at the sub-system level and involve the assembly between single parts. The first of these looks at sub-assembly 1, where components A1, B1, and C1 are assembled together. The KC is the length; therefore, the functional limits are derived from the stack-up at the system level and coincide with value $l + u_7 + t_{45}/2$ and $l + u_7 - t_{45}/2$, as shown in Fig.

5.22. The stack-up scheme is presented in Fig. 5.23, while the parametric inputs can be seen in Fig. 5.24.

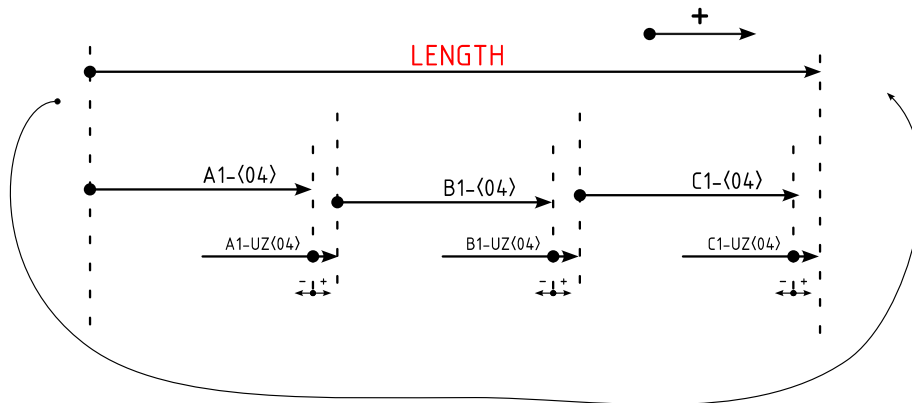


Fig. 5.23: Tolerance stack-up scheme for the third level (sub-system 1).

Item	Technical Product Documentation			Specification					s	k
	Description of component/Assy	num.	Rev.	num.	Description of dimension	Nominal	Tol. +	Tol. -		
									1,00	3,0
01	Component A1	A1	01	⟨04⟩	Surface profile		$t_{10}/2$	$-t_{10}/2$	1,00	3,0
					UZ shift	u_1			1,00	3,0
					Datum Feature Shift (DFS)				1,00	3,0
					TED	25,00			1,00	3,0
									1,00	3,0
									1,00	3,0
02	Component B1	B1	01	⟨04⟩	Surface profile		$t_{15}/2$	$-t_{15}/2$	1,00	3,0
					UZ shift	u_2			1,00	3,0
					Datum Feature Shift (DFS)				1,00	3,0
					TED	40,00			1,00	3,0
									1,00	3,0
									1,00	3,0
03	Component C1	C1	01	⟨04⟩	Surface profile		$t_{20}/2$	$-t_{20}/2$	1,00	3,0
					UZ shift	u_3			1,00	3,0
					Datum Feature Shift (DFS)				1,00	3,0
					TED	35,00			1,00	3,0

Fig. 5.24: Extract from the input tab of the Excel tool for the third level (sub-system 1).

The last stack-up looks at sub-assembly 2 where components A2, B2, and C2 are assembled together. The KC is also the total length in this case, and its functional limits can be derived from the stack-up at the system level, coinciding with values $l + u_8 + t_{50}/2$ and $l + u_8 - t_{50}/2$, as shown in Fig. 5.22. The stack-up scheme is presented in Fig. 5.25, while the parametric inputs can be seen in Fig. 5.26.

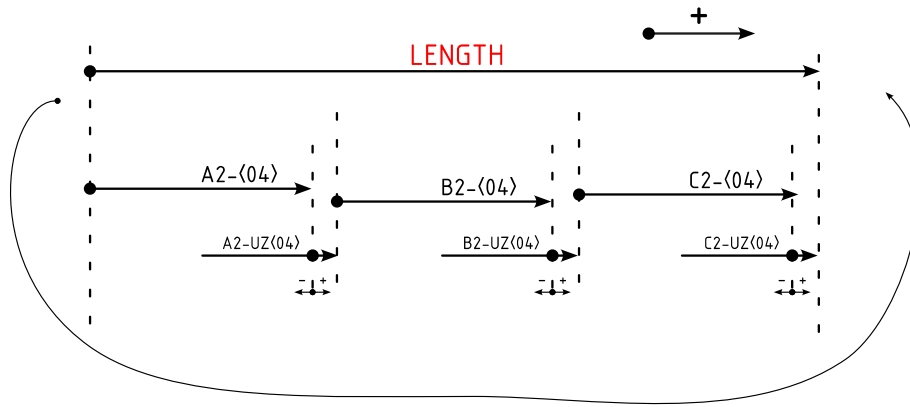


Fig. 5.25: Tolerance stack-up scheme for the third level (sub-system 2).

Item	Technical Product Documentation			Specification					s	k
	Description of component/Assy	num.	Rev.	num.	Description of dimension	Nominal	Tol. +	Tol. -		
									1,00	3,0
01	Component A2	A2	01	{04}	Surface profile		$t_{25}/2$	$-t_{25}/2$	$\cos(30^\circ)$	3,0
					UZ shift	u_4			$\cos(30^\circ)$	3,0
					Datum Feature Shift (DFS)				1,00	3,0
					TED	-40,00			1,00	3,0
									1,00	3,0
									1,00	3,0
02	Component B2	B2	01	{04}	Surface profile		$t_{30}/2$	$-t_{30}/2$	$\cos(45^\circ)$	3,0
					UZ shift	u_5			$\cos(45^\circ)$	3,0
					Datum Feature Shift (DFS)				1,00	3,0
					TED	5,00			1,00	3,0
									1,00	3,0
									1,00	3,0
03	Component C2	C2	01	{04}	Surface profile		$t_{35}/2$	$-t_{35}/2$	1,00	3,0
					UZ shift	u_6			1,00	3,0
					Datum Feature Shift (DFS)				1,00	3,0
					TED	55,00			1,00	3,0

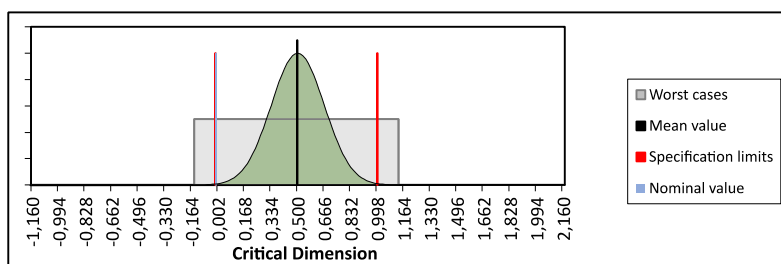
Fig. 5.26: Extract from the input tab of the Excel tool for the third level (sub-system 2).

Using this top-down approach, a possible solution can be found in Tab. 5.3 for both components and sub-assemblies. The tolerances that are not involved in the stack-up are omitted. As with the traditional synthesis, these values are not optimized since no optimization routine has been used.

Using these values, the statistical distribution and the other statistical metrics obtained for each tolerance stack-up can be seen in Fig. 5.27 to Fig. 5.30.

Tab. 5.3: Tolerance values after traditional tolerance synthesis.

Component	Tolerance	Value (mm)
D	$t_1 =$	0.30
	$t_2 =$	0.00
A1	$t_{10} =$	0.40
	$u_1 =$	-0.05
B1	$t_{15} =$	0.40
	$u_2 =$	-0.05
C1	$t_{20} =$	0.40
	$u_3 =$	-0.05
A2	$t_{25} =$	0.40
	$u_4 =$	-0.035
B2	$t_{30} =$	0.40
	$u_5 =$	-0.10
C2	$t_{35} =$	0.40
	$u_6 =$	-0.10
Sub. 1	$t_{35} =$	0.70
	$u_6 =$	-0.15
Sub. 2	$t_{35} =$	0.60
	$u_6 =$	-0.20
Sub. 1+2	$t_{36} =$	0.125
	$t_{37} =$	0.825



	RSS	Adjusted RSS		RSS	Adjusted RSS
$C_p = (USL - LSL) / (2 \cdot 3\sigma)$	1,00	0,67			
$C_{pk_1} = (USL - \mu) / (3\sigma)$	1,00	0,67			
$C_{pk_2} = (\mu - LSL) / (3\sigma)$	1,00	0,67			
$C_{pk} = \min[C_{pk_1}, C_{pk_2}]$	1,00	0,67			
			PPM		
			Above USL probability	1301	22346
			Below LSL probability	1301	22346
			Out of tolerance probability	2601	44692

Fig. 5.27: Result for the highest level stack-up (product).

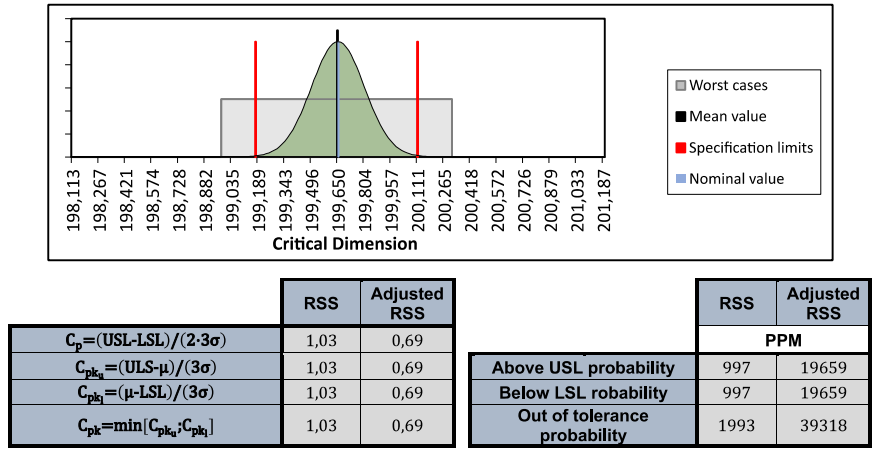


Fig. 5.28: Result for the second level stack-up (system).

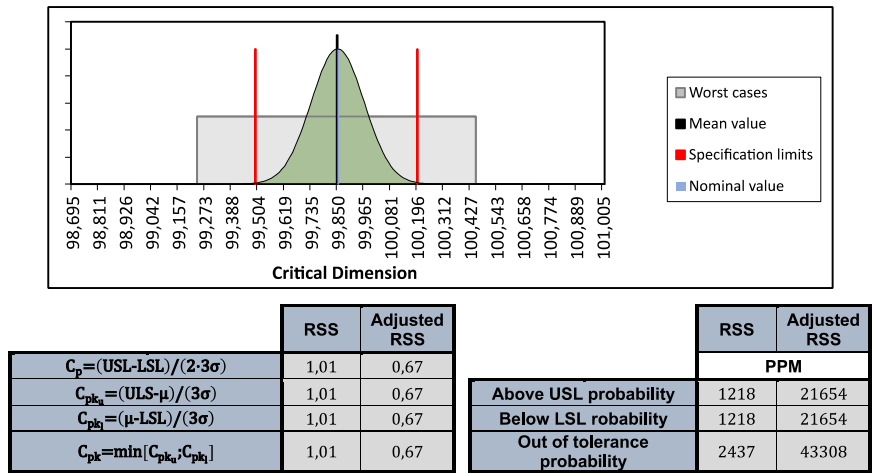


Fig. 5.29: Result for the second third stack-up (sub-system 1).

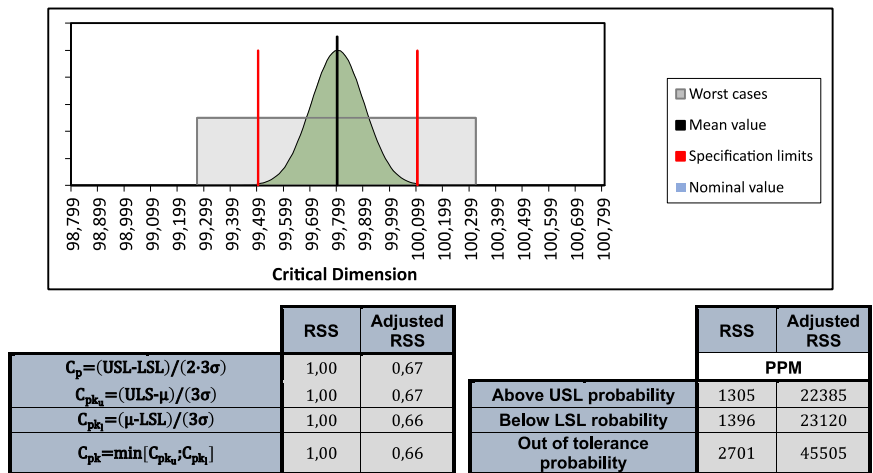


Fig. 5.30: Result for the second third stack-up (sub-system 2).

As it can be seen, the requirement of C_p and C_{pk} greater than or equal to one is always respected. In two cases, at the product level in Fig. 5.28, and sub-system 2 in Fig. 5.30, both C_p and C_{pk} are exactly equal to 1, meaning that larger tolerances are not possible. Optimization in this case would only act on the distribution of the contributions from one part/sub-assembly to the other. In the other two cases, Fig. 5.28 and Fig. 5.29, both C_p and C_{pk} are slightly above one. Even though it is always possible to obtain a result exactly equal to one, this would come with tolerance values that require more significant digits than can actually be measured, therefore there is no benefit in increasing the resolution of the result. In this case, the resolution for tolerance values was chosen to be $5 \mu\text{m}$.

5.5 || Discussion

In the previous two sections, the standard and top-down tolerance synthesis were presented. The tolerance values that were assigned are shown in Tab. 5.2 and Tab. 5.3. Upon examining the values, it is possible to see that there are no significant differences; the final values are quite similar, with the maximum difference being 0.05 mm for two tolerances. However, significant differences can be seen for the UZ values since the decision taken at the first step of the top-down approach guides the overall design. This difference does not result in a real difference in production cost, as discussed previously.

From an operational perspective, the top-down approach is much more labor-intensive since it requires creating four different stack-ups; however, it allows the implementation of the responsibility principle as presented in Chapter 2. On the other hand, the standard approach is viable in case of fully internalized design and manufacturing, as optimization can be spread over the totality of parts. However, in cases of an external supply chain where entire subsystems are designed and manufactured by external companies, or in cases of an internal supply chain where different departments are involved, the standard approach fails to give all the designers the possibility to design the variability of their part/sub-assembly. In such cases, the top-down approach is the only way to unlock the stack-up potentiality and allow optimization. Indeed, these are the cases in which, most of the time, an open-loop bottom-up approach is used in the industry, where no real requirements are set at the beginning, and suppliers define the quality of the final product.

The top-down approach proposed here is considered crucial for a proper implementation of the expanded responsibility principle, where each actor/professional is given the possibility to contribute to the final quality of the product, bringing in their own expertise.

6 || Functional definition of Pattern of fits⁴

"Pay attention to the intricate patterns of your existence that you take for granted."

Doug Dillon

Shaft-hole pattern fits are commonly used in mechanical assemblies for various purposes such as bolting of plates or flanges and accurate alignment with dowel pins. Describing these fits functionally can be challenging, especially when they provide alignment.

To assign size and location tolerances to the pattern features, the Boundary Condition design criterion can be used. This criterion, described in Appendix B "Formulas for positional tolerancing" of ASME Y14.5-2018 [5], helps in assigning tolerance zones that satisfy the worst-case scenario, ensuring a 100% acceptability rate. The Boundary Condition is determined by the collective effect of the Feature of Size (FoS) at its Maximum Material Size (MMS) and the location tolerance. Its value is used to determine clearance between parts and/or gage sizes [5].

However, it is worth noting that the Worst Case approach, based on the Boundary Condition design criterion, may not always be desirable. If the C_p (process capability index) is equal to or greater than one, tolerance allocation based on statistical approaches may be more economical. Additionally, choosing a tighter nominal fit regardless of location and size tolerances may be necessary to prevent wobbling, vibrations, and to meet customer expectations of quality [104].

In all these situations, the resulting fit may deviate from the Boundary Condition design criterion, leading to a certain amount of scrap. Therefore, it is important to statistically quantify the acceptability rate or other relevant metrics.

In cases where the geometric specification of the pattern includes the Maximum Material Requirement (MMR) or Least Material Requirement (LMR) modifier [7,40,105], establishing a relationship between location and size tolerances for each FoS adds complexity but reduces the number of non-conforming, yet still functional, parts [106].

When a pattern of fits is located with reference to an External datum system (see Fig. 6.1), ensuring functional alignment of mating parts, the assembly equation is straightforward. In this

⁴ The context of this chapter is mainly derived from a paper already published by the author [150].

case, a tolerance stack-up analysis can be performed to compute the statistical metrics for each fit of the pattern. Each fit is independent of one another, allowing for a simple mono-dimensional tolerance stack-up analysis. Fischer [79] presents such a model that can also be used when material requirements (MMR or LMR) are involved. Commercial CAT (Computer Aided Tolerancing) software like CETOL 6 σ [™] and 3DCS[™] can be employed when material requirements are applied to a Feature of Size (FoS).

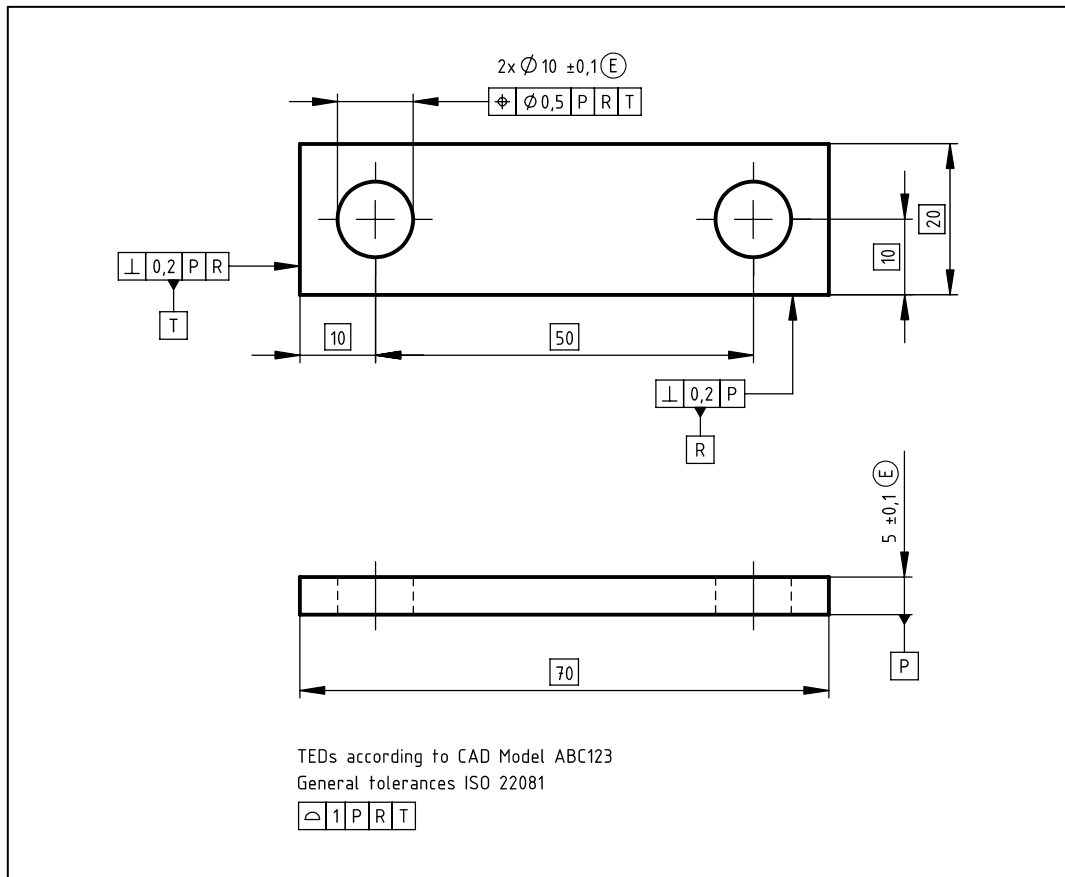


Fig. 6.1: External Datum System for a spacer.

However, when the pattern itself is the datum feature and serves as the alignment geometry (see Fig. 6.2), the situation becomes more complex. Each feature within the pattern is located with respect to the best fit of the pattern, which can be considered as the centroid of the actual pattern. In this case, the actual contacts between mating parts depend on the actual geometry of both parts, making it impossible to predict in advance which individual fit will make contact. Multiple assembly configurations are possible, and different assembly functions should be studied. Creating a tolerance stack-up and quantifying statistical metrics becomes non-trivial because a unique, explicit, or implicit assembly function cannot be defined.

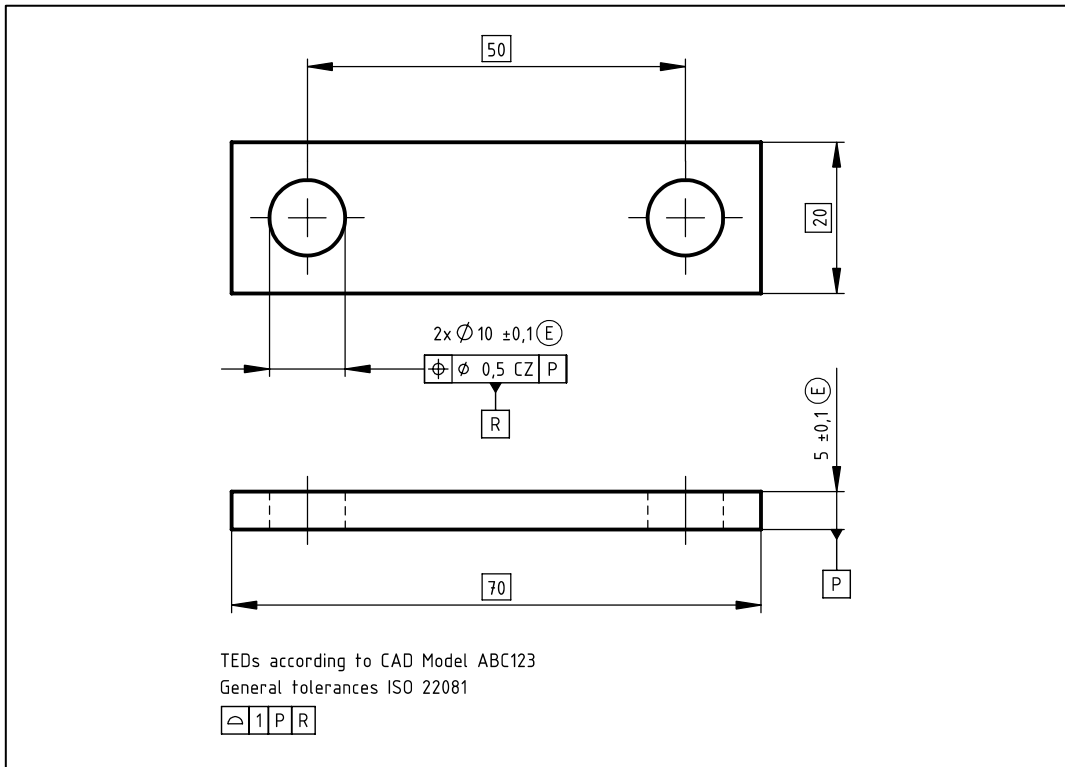


Fig. 6.2: Intrinsic Datum System for a spacer.

Scholz [107] discusses the riveting problem as an example where two holes need to match and a pin needs to enter both holes simultaneously (floating fastener). Assuming negligible hole and pin size variability and true position part alignment, Scholz shows that the position mismatch increases on the order of $\sqrt{\log(n)}$. However, this assumes “true alignment,” which is essentially adopting an external datum system. Scholz points out that considering the relative adjustment between the parts, which arises when “best alignment” is considered, introduces “dependency complications.”

In this chapter, these dependency complications will be addressed. The primary focus is on the “2x” pattern, exploring different methodologies that can be applied to create a tolerance analysis when the pattern of Features of Size (FoS) itself serves as the alignment feature (i.e., datum feature). The differences and implications of the two different datum systems will be discussed, and a general procedure to express the variability observed from the centroid in an external arbitrary Cartesian reference frame will be presented.

An analytical procedure will be developed and presented for estimating the rejection rate based on Root Sum of Squares (RSS) tolerance analysis. This procedure will be compared to Monte Carlo Simulation. It is important to note that the proposed method is relevant in the functional design phase, as it allows the designer to simulate the impact of their design intent regardless of subsequent manufacturing decisions.

Additionally, a case derived from an actual industrial study will be presented and discussed, focusing on a pattern of two shaft-hole fits. The holes are punched into sheet metal, and the shafts protrude from a plastic injection molded part. In the assembly, the alignment is determined by the fit itself. Two configurations will be studied: one assuming manual assembly (Intrinsic datum), and the other considering automated assembly with location tolerances determined by a robotic arm (External datum).

6.1 || Methodology development

The methodology is based on the tolerance stack-up tool presented in the previous chapter. In brief, it follows the model introduced by Fischer [79] and is implemented in Excel with an add-on that enables the use of sensitivity coefficients, automatic computation of symmetric tolerance limits, and updated graphical results.

6.1.1 General Hypothesis

The general assumptions used in the model are as follows:

- tol_{pos} refers to the location tolerance, and the associated bilateral tolerance is half its value ($\pm tol_{pos}/2$).
- The coverage factor k is assumed to be equal to 3 for all input variables, i.e., $\sigma = \frac{tol}{3}$.
- The location variability is known from the datum system used in the specification.
- All the sizes are non-correlated.
- Feature locations are non-correlated if seen from an External datum system; correlated if seen from the Intrinsic datum system.

6.2 || External vs Intrinsic datum system

When the pattern of FoS is located with reference to an external and independent datum system, as shown in Fig. 6.1, each element is not correlated with the others, regardless of the multiplicity. Therefore, the actual location of each element does not impose any limitation on the position of the others. The covariance is null, and the variance is the same for each element.

In the case of a pattern with multiple features, considering the i -th and j -th elements, the variance of the mutual distance (σ_L^2) can be expressed as follows.

$$\sigma_L^2 = \text{var}(L) = \text{var}(x_j - x_i) = \sigma_j^2 + \sigma_i^2 - 2\sigma_{ij} = 2\sigma^2 \quad (6-1)$$

Regardless of pattern multiplicity, the statistical representation of the actual mutual distance between any two axes (i.e., derived features) of the fits can be written as follows:

$$L = L_{\text{nom}} \pm \sqrt{2} \cdot \frac{\text{tol}_{\text{pos}}}{2} \quad (6-2)$$

When the pattern is specified with the CZ indication and is designated as a datum feature, as shown in Fig. 6.2, the origin of the datum system can be assumed to be the centroid of the pattern. In this reference system, the centroid remains fixed, meaning that $x_G = 0$ and $\sigma_G = 0$.

For a “nX” pattern, the variance of the centroid can be expressed as follows:

$$\sigma_G^2 = 0 = \sum_{i=1}^n \frac{\sigma_i^2}{n^2} + \frac{2}{n^2} \sum_{i>j} \sigma_{ij} \quad (6-3)$$

From the last equation, assuming the same variance for all pattern elements and the same covariance for each pair of elements, the covariance can be determined:

$$\sigma_{ij} = -\frac{1}{n-1} \sigma_i^2 \quad (6-4)$$

Using this result, the variance for the mutual distance of any pair in an “nX” linear pattern can be determined.

$$\sigma_L^2 = 2 \frac{n}{n-1} \sigma_i^2 \quad (6-5)$$

It is noteworthy that for an infinite pattern, the result coincides with the one found for an External datum system. This means that the covariance decreases as the number of elements increases. At the infinite limit, there is no more correlation and dependency.

The mutual distance between two fits located from the centroid can be written as follows:

$$L = L_{\text{nom}} \pm \sqrt{2 \frac{n}{n-1}} \cdot \frac{\text{tol}_{\text{pos}}}{2} \quad (6-6)$$

It can be noted that the use of the Intrinsic datum system has an impact on the variability of the mutual distance between two elements of the pattern.

6.2.1 Datum system transformation

To perform a Monte Carlo simulation when dealing with an Intrinsic datum system, due to the dependency between the reference system and the actual pattern situation, it is not possible to directly sample the location of the pattern. It is necessary to base the sampling on an independent reference system.

If σ is the variability (expressed as standard deviation) seen from the centroid reference system and $\tilde{\sigma}$ is the variability seen from any external fixed reference system, the following relation can be found.

$$\frac{\tilde{\sigma}}{\sigma} = \sqrt{\frac{n}{n-1}} \quad (6-7)$$

To prove equation (6-7) a Monte Carlo simulation has been performed for a “2x” and a “3x” patterns. Given a fixed value for the standard deviation seen from the external reference system, 500'000 samples have been simulated. For each sample, the pattern location from the centroid is computed, and statistical metrics are calculated and compared to those seen from the External datum system. The results are presented in Tab. 6.1 and Tab. 6.2.

Tab. 6.1: Monte Carlo simulation results for 2x pattern.

External Reference System		Intrinsic Reference System				Comparison	
X_1	X_2	x_1	x_2				
\bar{X}_1 0.000	\bar{X}_2 80.000	\bar{x}_1 -40.000	\bar{x}_2 40.000	Theoretical	$\sqrt{\frac{n}{n-1}}$	1.414	
$\tilde{\sigma}_1$ 0.067	$\tilde{\sigma}_2$ 0.067	σ_1 0.047	σ_2 0.047	Experimental	$\frac{\tilde{\sigma}}{\sigma}$	1.416	

Tab. 6.2: Monte Carlo simulation results for 3x pattern.

External Reference System			Intrinsic Reference System			Comparison	
X_1	X_2	X_3	x_1	x_2	x_3		
\bar{X}_1 0.000	\bar{X}_2 80.000	\bar{X}_3 160.000	\bar{x}_1 -80.000	\bar{x}_2 0.000	\bar{x}_3 80.000	Theoretical	$\sqrt{\frac{n}{n-1}}$ 1.225
$\tilde{\sigma}_1$ 0.067	$\tilde{\sigma}_2$ 0.067	$\tilde{\sigma}_3$ 0.067	σ_1 0.054	σ_2 0.054	σ_3 0.054	Experimental	$\frac{\tilde{\sigma}}{\sigma}$ 1.225

The results of the simulation confirm the accuracy of the transformation formula, with the error being well below 1% in both cases. Skewness and Kurtosis, although not displayed, also confirm that in both cases, the distribution seen from the centroid tends to approach normality as expected.

6.3 || 2x Patterns stack-up

In this section, various methodologies for creating a tolerance stack-up when the reference system is based on the centroid are presented. The geometric specification for the shaft can be seen in Fig. 6.3, the specification for the holes in Fig. 6.2. The Boundary Condition for holes is $9.9 - 0.5 = 9.4$ mm, while for shafts is $10 + 1 = 11$ mm, therefore no 100% fit is allowed, and the resulting rejection rate must be estimated.

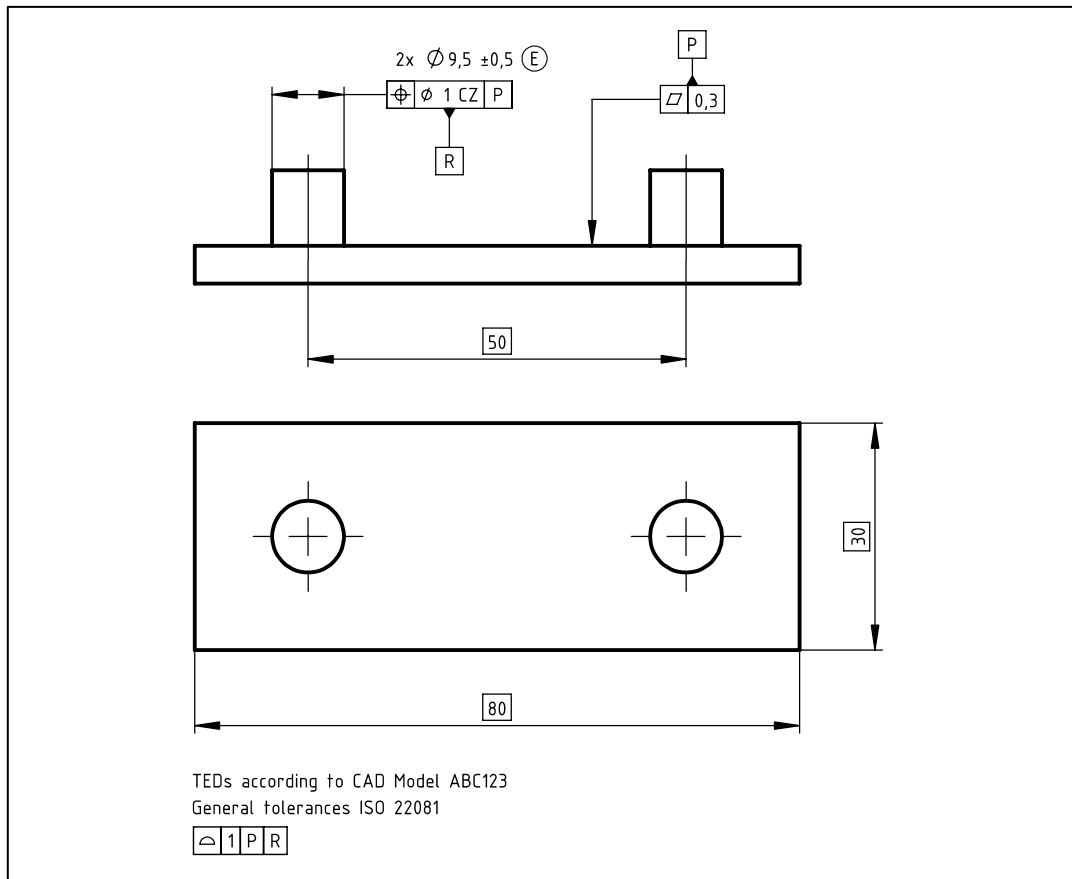


Fig. 6.3: Geometric specification for a two shafts cap.

6.3.1 Stack-up by cases

For a “2x” pattern, one element can be considered as the master, and the gap can be evaluated on the second one. In this case, two different assembly equations can be found, and for each one, a unilateral gap can be analyzed, as shown in Fig. 6.4.

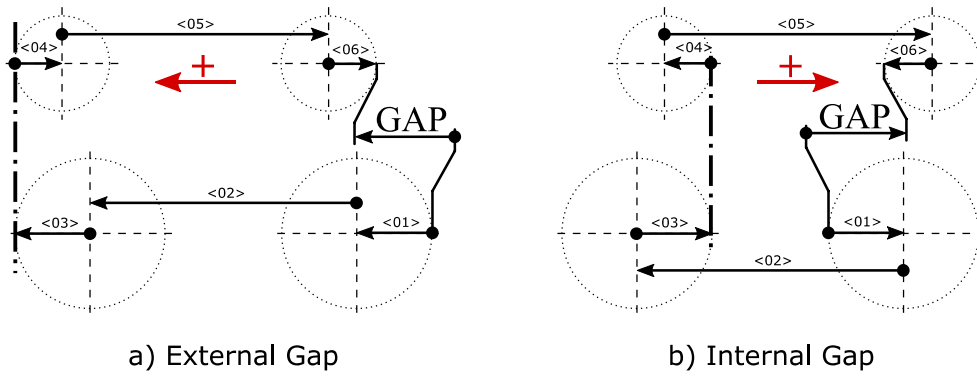


Fig. 6.4: Stack-up scheme.

With the first case, it is possible to compute the rejection rate for overshoot, while the second case gives the rejection rate for undershoot, as shown in Fig. 6.5. The overall rejection rate is the sum of the two.

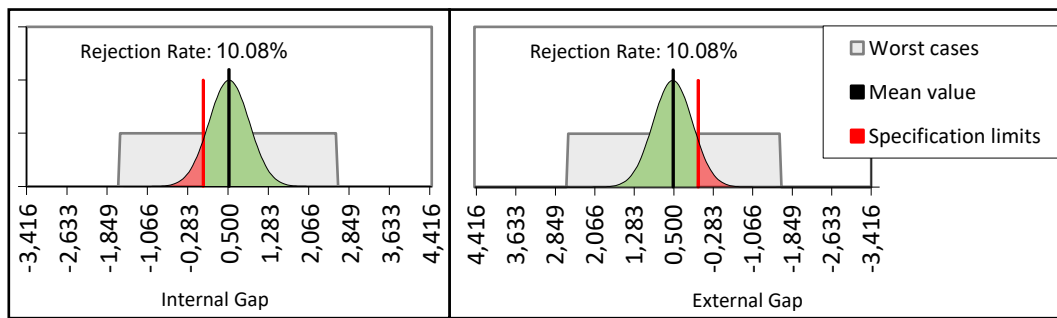


Fig. 6.5: External and Internal gap distribution and rejection rate, stack-up by cases.

A generalized gap, capable of considering both internal and external gaps simultaneously, can be defined by applying a dummy upper limit equal to twice the mean gap. The rejection rate and other statistical metrics can be directly found in the worksheet, as shown in Fig. 6.6.

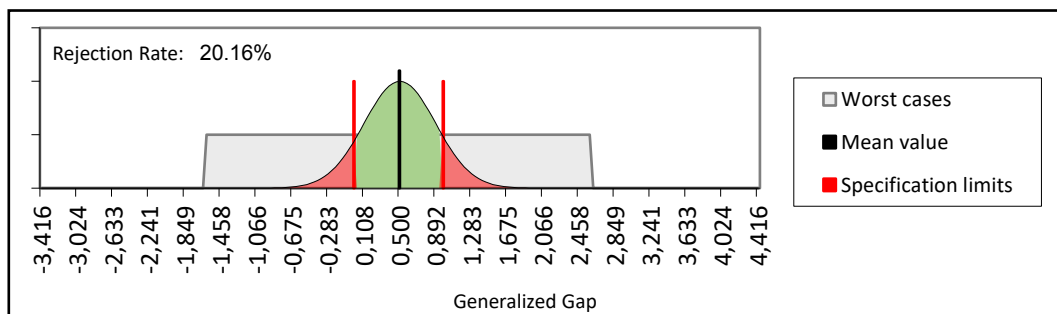


Fig. 6.6: Generalized Gap distribution and Rejection Rate, stack-up by cases.

This method, excluding the generalized gap, is a straightforward application of the model as described by Fischer [79], and although consistent, it does not use a rigorous definition of the datum system. In the following sections, alternative methods are proposed, and their effectiveness is discussed.

6.3.2 Symmetric stack-up

Considering that the pattern is symmetric with respect to the datum system, the tolerance stack-up can be centered by aligning the datum systems of the mating parts. Consequently, one single fit can be studied. Two distinct unilateral gaps can be defined, as shown in Fig. 6.7.a).

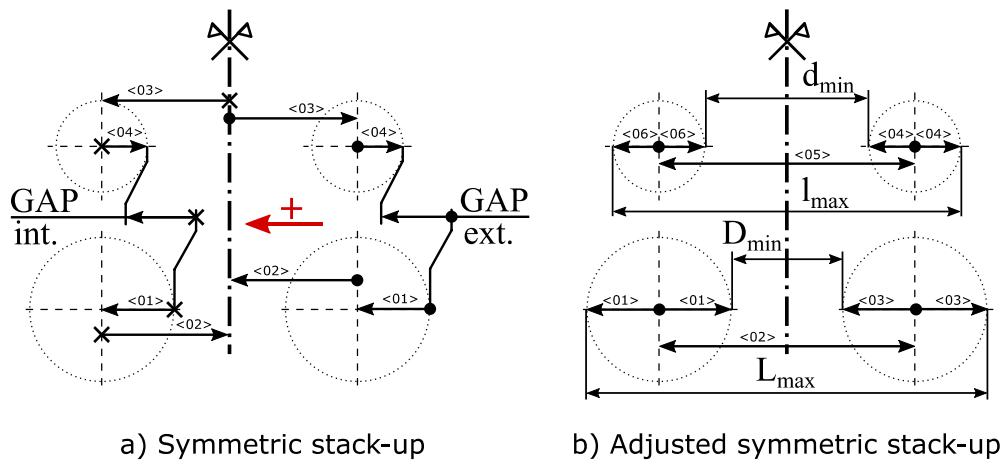


Fig. 6.7: Stack-up scheme for all symmetric cases: a) Internal and external gaps for the symmetric stack-up; b) Elements use in the symmetric adjusted stack-up.

Similar to the previous case, a generalized gap can be defined, and statistical metrics can be computed accordingly. The result is shown in Fig. 6.8.

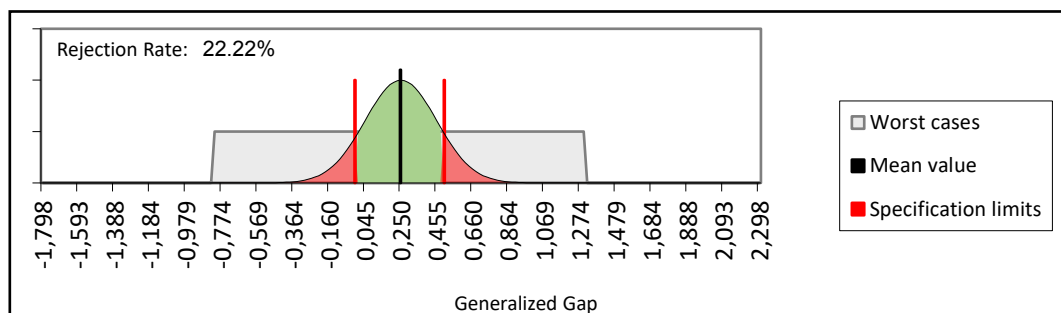


Fig. 6.8: Generalized Gap distribution and Rejection Rate, symmetric stack-up.

The rejection rate obtained using this method is higher compared to the previous method. This is because in this case, the true position alignment is considered and the sizes of the two features of size are correlated.

6.3.3 Symmetric adjusted stack up

To overcome the limitation mentioned in the previous section, an adjustment can be made to the model. Instead of studying only half of the pattern, the entire pattern is considered. The distance from the datum system of the second feature of size is correlated to the first one, so it cannot be simply added. Instead, the half distance needs to be duplicated using a sensitivity coefficient of 2. This results in four gaps that need to be considered, but they can be grouped into two pairs that are symmetrical. By considering the gaps resulting from the differences $L_{\max} - l_{\max}$ (Sum of the external gaps) e $d_{\min} - D_{\min}$ (Sum of the internal gaps), two unilateral gaps can be studied, as shown in Fig. 6.7.b.

A generalized gap can also be defined by adding a dummy upper limit, similar to the previous cases, as shown in Fig. 6.9.

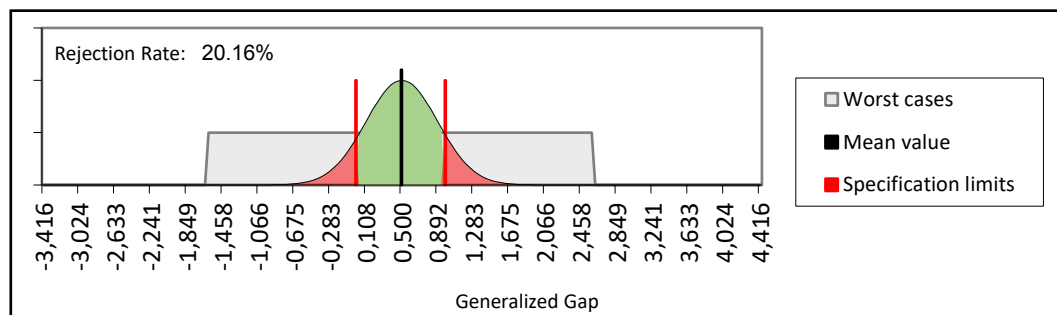


Fig. 6.9: Generalized Gap distribution and Rejection Rate, symmetric adjusted stack-up.

In this case, the rejection rate is equal to the one found with the first method, meaning it can account for the non-linearities caused by the contact points. Additionally, since it starts from the datum system, the material condition can be taken into account.

6.3.4 Symmetric optimized stack up

The model can be further optimized by neglecting the contribution of the TED (Theoretically Exact Dimension), as it does not affect the gap. Additionally, the FoS contribution can be added once by using a sensitivity of 1 and scaling the tolerance by a factor of $1/\sqrt{2}$ to account for the independence between the sizes of the two elements. However, this approach does not allow for consideration of the material conditions.

6.3.5 Monte Carlo Verification

To verify the results of the proposed method, a Monte Carlo simulation is conducted. The standard deviation associated with the localization of the FoS is “corrected” using the relation given by equation (6-7). A total of 500'000 combinations for the eight variables are generated, and both the external and internal gaps are calculated. If both gaps are positive, the assembly is accepted.

The variability seen from the centroid and its normality are checked.

After performing the simulation over twenty re-computations, the average rejection rate is found to be 20.15% with a standard deviation of 0.06%, which closely matches the analytical value of 20.16%.

Based on these results, the analytical model is considered to be verified.

6.4 || Path towards generalization

To generalize the proposed method to a “ $n \times$ ” linear pattern it is first possible to define $n - 1$ independent pairs of FoS in the pattern.

For each independent pair, the method can be applied considering the location variability seen from the centroid of the pair that can be found equal to half of the variability of the mutual distance. The rejection rate (r_i) for any pair can be determined, and the probability that the assembly is successful ($P = P(i) = 1 - r_i$) as well. If each pair is considered stochastically independent $P(j|i) = P(j) \forall j, i$, the probability that both the j -th and the i -th pairs can be assembled is $P(j \cap i) = P(j)P(i) = P^2$.

It can be easily derived that for a “ $n \times$ ” pattern the probability to assemble the pattern, according to the given hypothesis, is $P_n = P^{n-1}$. The rejection rate accordingly becomes $r_n = 1 - [1 - r]^{n-1}$.

Through Monte Carlo simulation, this equation was not verified: the probability of assembling a further pair of the pattern is less than the previous ones since the relative adjustment between the mating FoS depends on the actual situation of the previous pairs.

A more general equation for the rejection rate is proposed:

$$R(n) = 1 - [1 - \beta \cdot r]^{n-1} \quad (6-8)$$

Where $\beta \geq 1$ is a coefficient that needs to be experimentally determined and whose dependencies need to be determined too.

Another possibility is given by the definition of a general interpolation equation that can fit the rejection rate curves as a function of n . Considering that $R(n)$ is a limited function ($r \leq R(n) \leq 1$)

whose limit for $n \rightarrow \infty$ is 1, an exponential function can be employed. With proper variable definitions, the interpolation function takes the form:

$$R(n) = 1 - [1 - r]e^{-\frac{1}{\theta_1}(n-2)} \quad (6-9)$$

Here, θ_1 , represents a time constant that needs to be determined experimentally. Investigating these potential analytical generalization holds promise for future research, as discussed in chapter 13.

At the time of writing, a Design of Experiment approach to establish a model for equations (6-8) and (6-9) is under consideration and study.

In addition to analytical solutions, a numerical generalization could also be explored, as detailed in chapter 13. In this scenario, the actual geometry of the pattern and the precise contact points among different fits could be taken into account, along with the necessary rotational and translational movements for the pattern's assembly. This approach would involve generating patterns (holes and shafts) randomly using Monte Carlo simulation, accounting for both size variability and location variability (in 2D). Maximum interference would be computed vectorially. Subsequently, a virtual assembly routine would need to be defined to determine whether a mutual position of the two patterns allowing for assembly exists.

6.5 || The case study

The geometric specification for the case study, derived from an actual industrial case, is depicted in Fig. 6.10. The dimensions and tolerances have been modified while maintaining the same general proportions.

Using the method proposed in section 6.3.3, the estimated rejection rate under “best alignment” (manual assembly) is 24.16%.

To simulate the automated assembly, two additional terms need to be considered. Firstly, the model presented in section 6.3.2 should be used to exclude the possible adjustment between parts during assembly. Secondly, two additional terms should be added: one for the sheet metal part to describe the variability between the centroid of the pattern and the alignment features used by the robotic arm (not specified), and another for the cap side to account for the precision of the robotic arm.

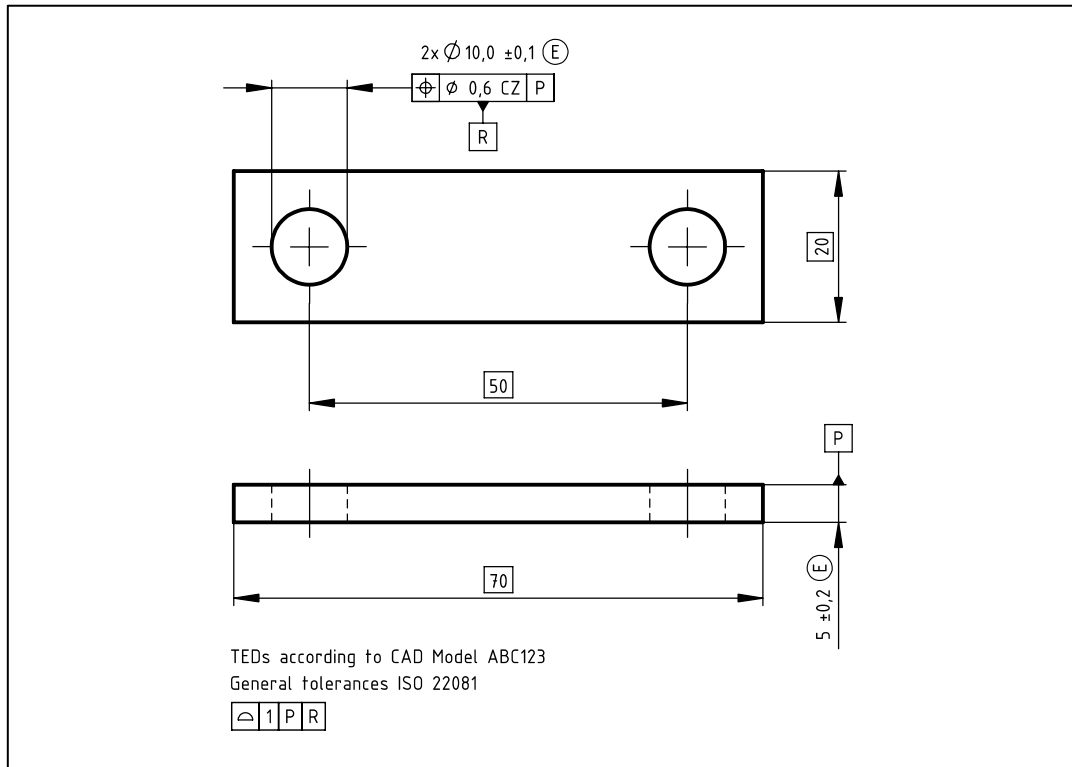


Fig. 6.10: Case study geometric specification for the spacer.

In the stack-up, the first term is assumed to have a tolerance of $\pm 0.3\text{mm}$, while the second term has a tolerance of $\pm 0.1\text{mm}$.

With these considerations, the estimated rejection rate increases to 32.72%. The difference of 8.56% represents the fraction of parts that cannot be assembled using the specific chosen assembly process. This value can potentially be reduced by exploring alternative automated assembly processes, taking into account their associated costs.

It is important to note that automated assembly introduces additional uncertainty to the stack-up. The functional specification for pattern fits should include assemblability as a necessary requirement for mating parts. The case study highlights that the assemblability of the pattern fit depends on the actual assembly process. Therefore, it is crucial to differentiate between functional and manufacturing specifications. The manufacturing specification should consider each step of the production, including assembly, and may tighten tolerance values accordingly. The functional specification, on the other hand, represents the non-negotiable boundary that ensures functionality and should not be exceeded.

Overall, the case study emphasizes the need to carefully consider both functional and manufacturing specifications, with the latter being used to optimize the process while maintaining functionality based on the entire manufacturing chain.

A practical case, derived from an industrial study, has been presented and resolved. This case facilitated the simulation of differences between manual and automated assembly methods.

Equation (6-8) and (6-9) hold potential as analytical generalizations for an “ n ” linear pattern. However, further investigations are warranted to comprehensively define the β parameter or the time constant θ_1 .

The analytical definition of a pattern fit might introduce a new type of kinematic constraint for use in stack-up analyses. Presently, the conventional practice involves defining a primary and secondary fit to establish kinematic constraints between mating parts.

Furthermore, this approach could be applied for formal computations involving “ n ” dowel pins, wherein more than two pins with greater clearance emulate the behavior of two tighter pins.

7 || Tolerance stack-up: yet another proof for alignment design rules and design for maintenance

A well-aligned machine whispers its brilliance; a misaligned one shouts its flaws.

Anonymous

In chapter 5, the use of tolerance stack-up for tolerance synthesis is presented, and both the standard approach and the top-down approach enabling the expanded responsibility principle are discussed. Tolerance stack-ups are not limited to tolerance synthesis or computing the number of scraps; they are also valuable for making design decisions.

One commonly forgotten design rule advises against using bolts to guarantee alignment between parts. The reason is simple and was partially discussed in the previous chapter. Bolted connections often rely on a large difference in nominal size between the screw and the holes to avoid interference during assembly. The boundary condition design criterion can be used to define dimensional and location tolerances for this purpose [5]; the obvious result is that clearance is always expected, therefore accurate alignment cannot be guaranteed. Despite the simplicity of this explanation, many industrial practices continue to use bolted connections (or shaft hole connections, more generally) to align different parts. While automated assembly lines may solve the alignment problem using robotic arms, the design still lacks robustness, especially from a design-for-disassembly and design-for-maintenance perspective. The product may be assembled on the automated line, but during service or maintenance, it becomes challenging to reassemble it correctly.

Tolerance stack-up can be used to evaluate such design decisions: whether to use a dedicated alignment feature or not. The simulation outcome can suggest whether both solutions are viable or not.

Another significant design question concerns material conditions. Designers are often told that Maximum Material Condition should always be used to describe the assemblability requirements in shaft hole connections. While the worst-case explanation is straightforward to derive, it is much more difficult to appreciate the effect on the statistical distribution. This effect can be better understood and described by analyzing a tolerance stack-up.

In [79], it is also advised not to use Maximum Material Condition if the feature is used to guarantee alignment. However, no real rationale (metric) behind this statement is provided.

This chapter aims to address all these questions. The impact of a dedicated alignment feature will be explored, and the effect of material conditions will be analyzed. To achieve this, a simple assembly between two parts, bolted together, will be considered. The effect of different specifications, both functional (as defined in chapter 3 and 4) and non-functional will be assessed.

7.1 || Functional requirements

The functional requirements for the case study are shown in Fig. 7.1. The assembly needs to have a total length of $50 \pm 0.5 \text{ mm}$, and a M5 bolt is required for assembly. The first requirement is simply stated using a size dimension on the total length. The second one asks for a perfect cylinder of diameter 5 mm to pass through, so a size dimension is specified using the global maximum inscribed feature.

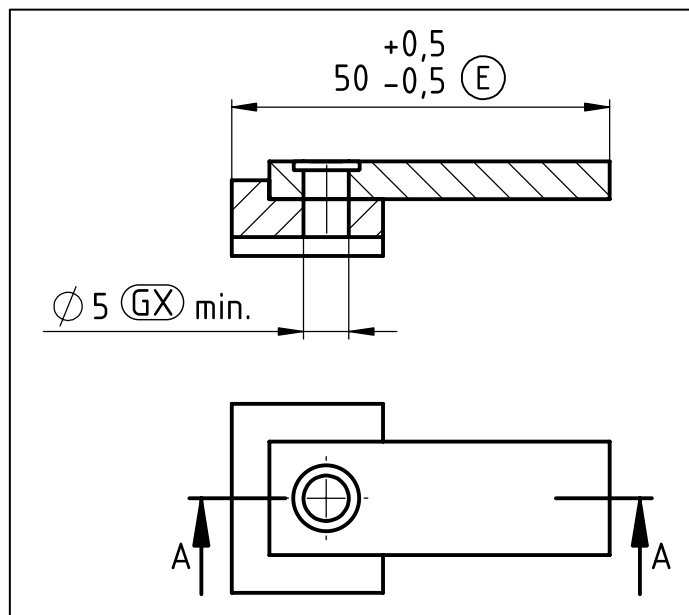


Fig. 7.1: Case study functional requirements.

These functional requirements are independent of the assembly conditions, with or without the explicit alignment features. In Fig. 7.1, the assembly conditions using the explicit alignment feature are proposed.

7.2 || Explicit alignment feature

The first case to be analyzed is the one using an explicit alignment feature, a plane. The bolt does not provide alignment; the through holes need to be aligned to let the bolt be assembled. A possible functional specification, considering the assembly condition for both parts, is shown in Fig. 7.2.

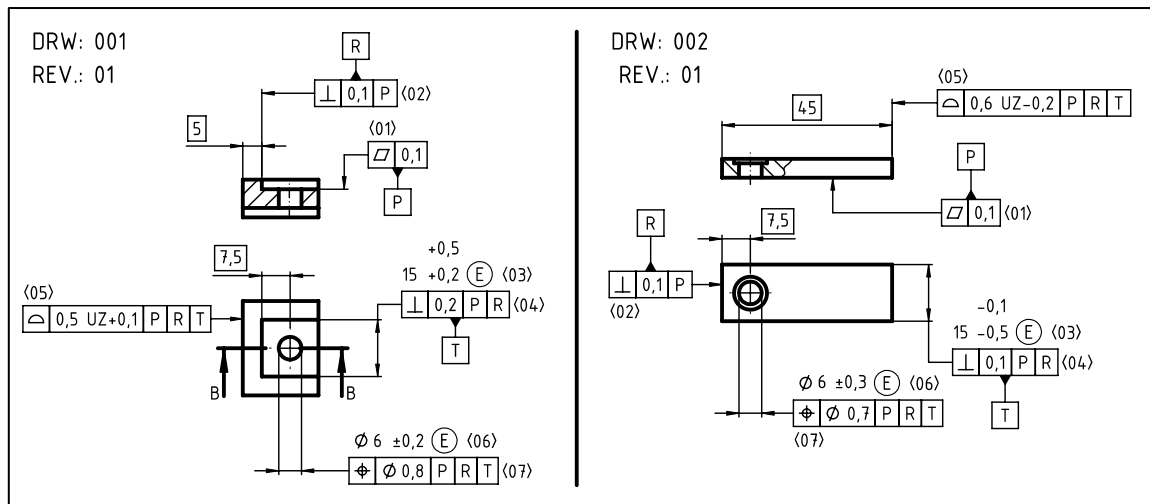


Fig. 7.2: Functional specification for both parts considering the alignment feature without material conditions.

The functional geometric specification is coherent with the procedure for functional specification presented in chapters 3 and 4. In both parts, the datum system is based on the mutual assembly features. All other functional features are located with respect to the functional datum system. In this first design iteration, material conditions are not used.

Looking at the tolerances assigned to the holes, it is possible to see that the boundary condition design criterion applies. In this case, we have a floating fastener, and the equation to assign location tolerances is:

$$POS = HOLE_{MMC} - SHAFT_{MMC} \quad (7-1)$$

Where POS is the location tolerance value, $HOLE_{MMC}$ is the minimum hole diameter, and $SHAFT_{MMC}$ is the maximum shaft diameter. Since the shaft is a screw, the tolerance on the diameter is negligible.

Therefore, for the “base” part we obtain:

$$POS = 5.8 - 5 = 0.8 \text{ mm}$$

For the “plate” part:

$$POS=5.7 - 5 = 0.7 \text{ mm}$$

Since location tolerances are congruent to the boundary condition design criterion, we already know that 100% assemblability will always be guaranteed, and no tolerance stack-ups are required. Nonetheless, to examine the contribution of material condition to the statistical distribution, the tolerance stack-up for the holes alignment will be addressed in the next sections.

In Fig. 7.3, the same design including material conditions is shown.

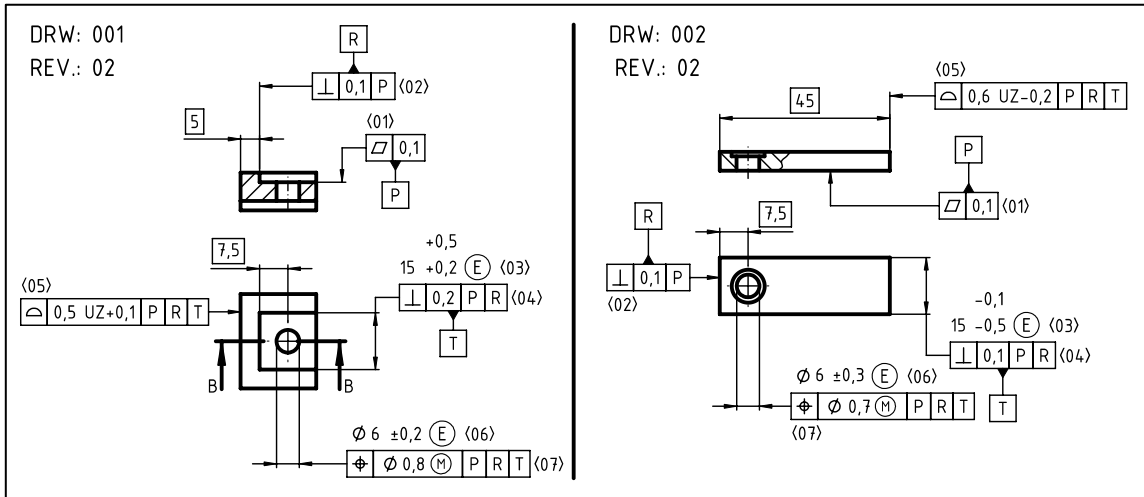


Fig. 7.3: Functional specification for both parts considering the alignment feature with material conditions.

In this case, since the requirement is assemblability, the Maximum Material Condition is applied to the location tolerances of the holes.

7.2.1 Total length stack-up with external alignment feature

The total length stack-up is not influenced by the material condition, as the hole features do not have any contribution to the stack-up. In Fig. 7.4, the scheme for the stack is shown.

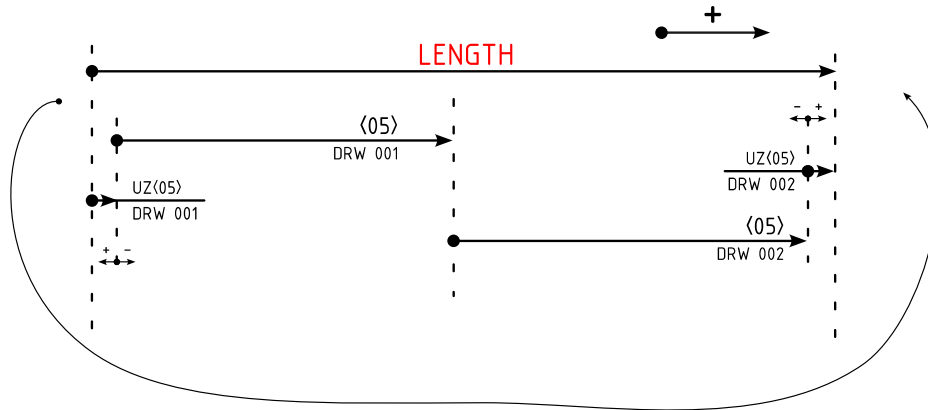
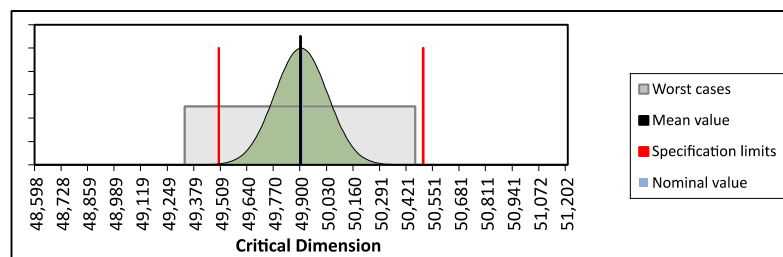


Fig. 7.4: Total length stack up scheme using an explicit alignment feature.

Using this scheme, it is possible to create the tolerance stack-up. An extract of both the inputs and outputs tab is shown in Fig. 7.5.

Item	Technical Product Documentation			Specification				s	k	
	Description of component/Assy	num.	Rev.	num.	Description of dimension	Nominal	Tol. +			Tol. -
01	base	001	01	<05>	Surface profile		0,250	-0,250	1,00	3,0
					UZ shift	0,10			1,00	3,0
					Datum Feature Shift (DFS)				1,00	3,0
					TED	5,00			1,00	3,0
02	plate	002	01	<05>	Surface profile		0,300	-0,300	1,00	3,0
					UZ shift	-0,20			1,00	3,0
					Datum Feature Shift (DFS)				1,00	3,0
					TED	45,00			1,00	3,0



	RSS	Adjusted RSS
$C_p = (USL - LSL) / (2 \cdot 3\sigma)$	1,28	0,85
$C_{pk_u} = (USL - \mu) / (3\sigma)$	1,54	1,02
$C_{pk_l} = (\mu - LSL) / (3\sigma)$	1,02	0,68
$C_{pk} = \min[C_{pk_u}; C_{pk_l}]$	1,02	0,68

	RSS	Adjusted RSS
PPM		
Above USL probability	2	1060
Below LSL probability	1060	20251
Out of tolerance probability	1062	21311

Fig. 7.5: Extract from the input and output for the total length tolerance stack-up.

It is possible to see that with the proposed specification, the KC (total length) is well within requirements if we look for both C_p and C_{pk} greater or equal to 1 with the RSS computation method. The upper limit is not reached even with the worst-case analysis.

Therefore, even if the geometric specification presented in Fig. 7.2 and Fig. 7.3 is not optimized, it respects the requirement for the total length.

7.2.2 Hole alignment stack-up without material condition

As already presented, since the location tolerance for the holes respects the boundary condition design criterion, the assemblability requirement is always respected. The tolerance stack-up is shown to highlight the effect of the material condition. In this first case, the material condition is not considered, and therefore the geometric specification shown in Fig. 7.2 is used.

For hole alignment, it is possible to define two distinct stack-ups since two distinct gaps can be identified: referring to Fig. 7.2, the first gap is between the left side of the hole on the plate and the right side on the base, the second gap between the right side of the hole on the plate and the left side on the base. The results for the two gaps are actually the same; therefore, only one can be analyzed.

The direct requirement for the KC is a minimum dimension of 5 mm; however, a maximum KC can be derived assuming the minimum gap occurs on the other possible gap, and both holes are at Least Material Conditions:

$$\begin{aligned} KC_{MAX} &= (HOLE_{LMC} - 5)_{base} + 5 + (HOLE_{LMC} - 5)_{plate} = \\ &= (6.2 - 5) + 5 + (6.3 - 5) = 7.5mm \end{aligned}$$

If the KC exceeds the value of 7.5 mm, it means that the other possible gap is below 5 mm; therefore, the assembly is not possible.

The stack-up scheme is shown in Fig. 7.6, and the extract from the inputs and outputs tab of the tolerance stack-up is shown in Fig. 7.7.

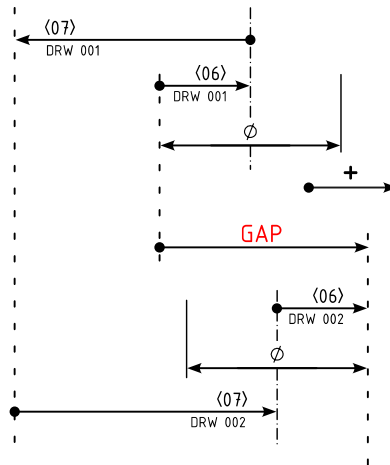
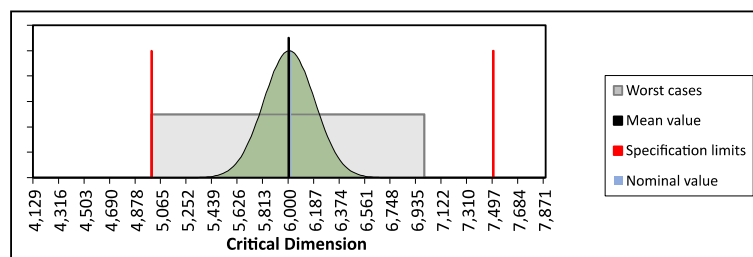


Fig. 7.6: Hole alignment without material condition stack-up scheme using an explicit alignment feature.

Item	Technical Product Documentation			Specification					s	k
	Description of component/Assy	num.	Rev.	num.	Description of dimension	Nominal	Tol. +	Tol. -		
									1,00	3,0
01	base	001	01	(06)	size	6,00	0,200	-0,200	0,50	3,0
									1,00	3,0
02	base	001	01	(07)	location		0,400	-0,400	1,00	3,0
					Bonus M/L				1,00	3,0
					Datum Feature Shift (DFS)				1,00	3,0
					TED	-7,50			1,00	3,0
									1,00	3,0
03	plate	002	01	(07)	location		0,350	-0,350	1,00	3,0
					Bonus M/L				1,00	3,0
					Datum Feature Shift (DFS)				1,00	3,0
					TED	7,50			1,00	3,0
									1,00	3,0
04	plate	002	01	(06)	size	6,00	0,300	-0,300	0,50	3,0



	RSS	Adjusted RSS
$C_p = (USL - LSL) / (2 \cdot 3\sigma)$	2,23	1,48
$C_{pk_u} = (USL - \mu) / (3\sigma)$	2,67	1,78
$C_{pk_l} = (\mu - LSL) / (3\sigma)$	1,78	1,19
$C_{pk} = \min[C_{pk_u}, C_{pk_l}]$	1,78	1,19

	RSS	Adjusted RSS
		PPM
Above USL probability	0	0
Below LSL probability	0	183
Out of tolerance probability	0	183

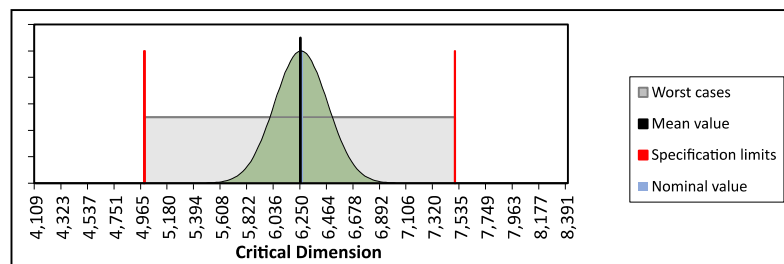
Fig. 7.7: Extract from the input and output for the Hole alignment without material condition tolerances stack-up.

As predicted, the worst case coincides with the lower limit; however, the upper limit is never reached. This means that there is a possibility of allowing more variability while still ensuring functional requirements are met. The solution is the application of the maximum material condition to the hole features.

7.2.3 Hole alignment stack-up with material condition

If the same stack-up is now iterated using the geometric specification in Fig. 7.3, where the maximum material requirement is assigned to hole features, the extract from the inputs and outputs tab is shown in Fig. 7.8.

Item	Technical Product Documentation			Specification					s	k
	Description of component/Assy	num.	Rev.	num.	Description of dimension	Nominal	Tol. +	Tol. -		
									1,00	3,0
01	base	001	02	(06)	size	6,20			0,50	3,0
									1,00	3,0
02	base	001	02	(07)	location		0,400	-0,400	1,00	3,0
					Bonus M/L		0,200	-0,200	1,00	3,0
					Datum Feature Shift (DFS)				1,00	3,0
					TED	-7,50			1,00	3,0
									1,00	3,0
03	plate	002	02	(07)	location		0,350	-0,350	1,00	3,0
					Bonus M/L		0,300	-0,300	1,00	3,0
					Datum Feature Shift (DFS)				1,00	3,0
					TED	7,50			1,00	3,0
									1,00	3,0
04	plate	002	02	(06)	size	6,30			0,50	3,0



	RSS	Adjusted RSS
$C_p = (USL - LSL) / (2 \cdot 3\sigma)$	1,95	1,30
$C_{pkq} = (USL - \mu) / (3\sigma)$	1,95	1,30
$C_{pkl} = (\mu - LSL) / (3\sigma)$	1,95	1,30
$C_{pk} = \min[C_{pkq}, C_{pkl}]$	1,95	1,30

	RSS	Adjusted RSS
PPM		
Above USL probability	0	50
Below LSL probability	0	50
Out of tolerance probability	0	99

Fig. 7.8: Extract from the input and output for the Hole alignment with material condition tolerances stack-up.

The rule for considering material condition as explained in [79] is followed, where the size variability is moved to the bonus line of the location tolerance, and the nominal size is inserted as the Least Material Size.

Looking at the statistical distribution, it is evident that the KC variability is increased, indicating that more variation during manufacturing can be allowed. The statistical distribution stretches towards the upper limit and does not change towards the lower limit. As a result, the statistical distribution is now perfectly centered within the requirement limits, and the worst-case scenario perfectly fits inside the requirement limits.

7.2.4 Maximum Material Condition vs Regardless of Feature size

In Fig. 7.9, the statistical distribution for the KC derived from the assemblability requirement is compared both without and with the material requirement. It is evident that the application of the maximum material requirement increased the expected variability of the KC. Another observation is that this increased variability does not influence the output quality; instead, the variability is maximized to fit within the space allowed by the requirements.

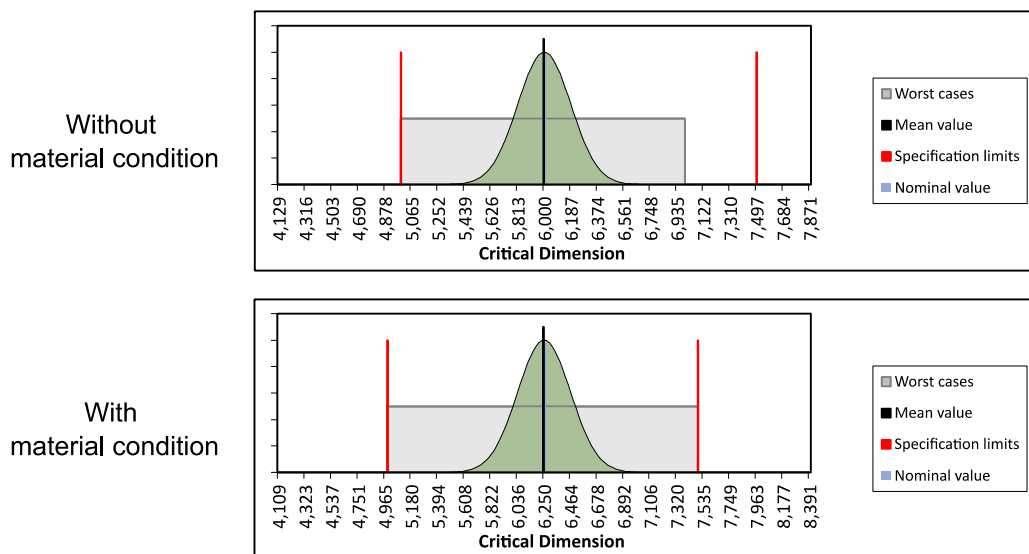


Fig. 7.9: Tolerance stack-up output statistical distribution comparison between the case without and with material condition.

Therefore, the use of material requirements is always advisable when an external alignment feature is used since it allows greater variability during the manufacturing phase.

7.3 || Alignment through the fastener

Now we consider new assembly conditions: there is no dedicated alignment feature, and therefore the alignment relies on the bolt. The functional requirements do not change and can be seen in Fig. 7.10. In this case, the hole alignment stack-up is irrelevant since the assemblability requirement is respected if the holes at Least Material Size have diameters above 5 mm. Therefore, the only tolerance stack-up that will be analyzed is the one relevant to the total length.

First, the total length will be analyzed using the previously defined specification both without and with material condition, using a non-functional geometric specification (not describing assembling conditions).

Secondly, a functional specification will be defined, both without and with material condition, and the tolerance stack-up will be updated. The functional geometric specification, looking at the new assembly condition, will retain the same tolerance values for referenced features to maintain a similar production cost to the one analyzed so far.

The results of the tolerance stack-up will be compared to see the implications of the different geometric specifications.

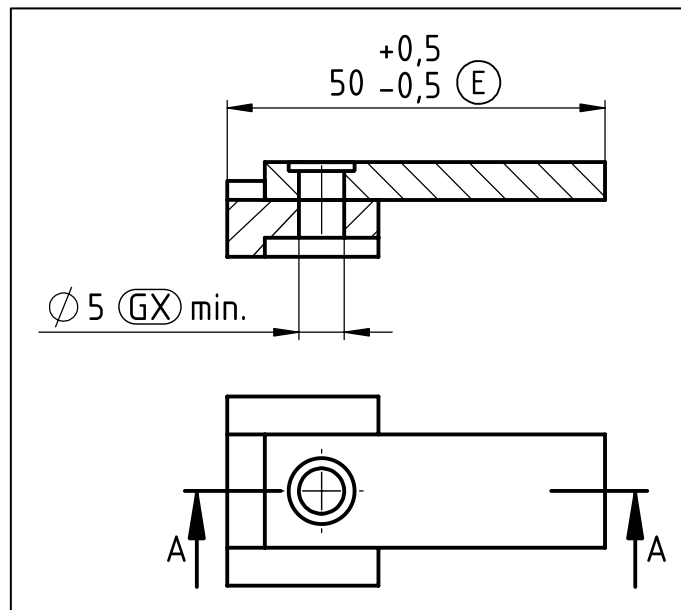


Fig. 7.10: Case study functional requirements.

7.3.1 Total length stack-up without external alignment feature and non-functional specification without material condition

For this first iteration, the geometric specification considering the assembly condition derived from the existence of an external alignment feature will be used. Therefore, the geometric

specification cannot be considered as functional according to the definition that has been given throughout this work.

Since the alignment is given by the bolts and the geometric specification is non-functional, the stack-up scheme (Fig. 7.11) becomes quite complex. First, for each component considered in the stack-up, a direct relation between the assembly feature and the controlled feature cannot be found, and a “double jump” needs to be made, passing through the datum feature. Second, the alignment through the bolt initiates the “assembly shift,” which describes the fact that the axes of the holes can shift with respect to the axis of the screw. The assembly shift is defined by the following equation:

$$ASM_{Shift} = \pm(HOLE_{LMC} - SHAFT_{LMC})/2$$

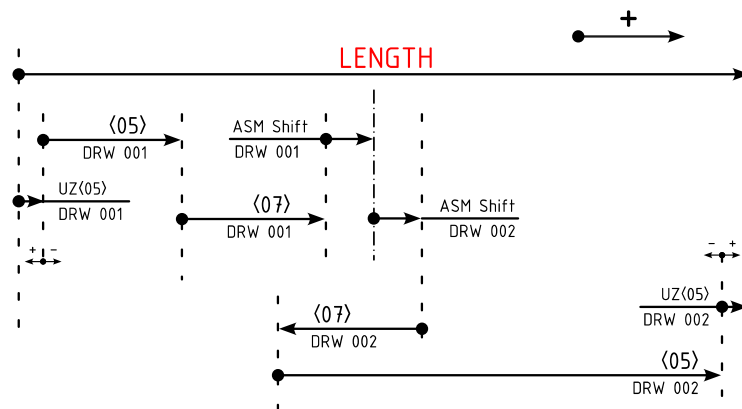


Fig. 7.11: Total length stack-up scheme using the bolt as alignment with non-functional specification.

The extract from the inputs tab of the tolerance stack-up is shown in Fig. 7.12. It can be noted that the assembly shift appears twice since the shift is possible both between the screw and the base and between the screw and the plate. For the base component, the assembly shift becomes:

$$ASM_{Shift} = \pm(HOLE_{LMC} - SHAFT_{LMC})/2 = \pm(6.2 - 5)/2 = \pm 0.60 \text{ mm}$$

For the plate component:

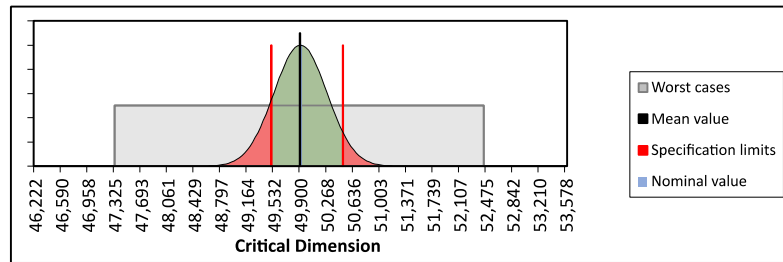
$$ASM_{Shift} = \pm(HOLE_{LMC} - SHAFT_{LMC})/2 = \pm(6.3 - 5)/2 = \pm 0.65 \text{ mm}$$

Item	Technical Product Documentation			Specification					s	k
	Description of component/Assy	num.	Rev.	num.	Description of dimension	Nominal	Tol. +	Tol. -		
									1,00	3,0
01	base	001	01	{05}	Surface profile		0,250	-0,250	1,00	3,0
					UZ shift	0,10			1,00	3,0
					Datum Feature Shift (DFS)				1,00	3,0
					TED	5,00			1,00	3,0
									1,00	3,0
02	base	001	01	{07}	Location		0,400	-0,400	1,00	3,0
					Bonus M/L				1,00	3,0
					Datum Feature Shift (DFS)				1,00	3,0
					TED	7,50			1,00	3,0
									1,00	3,0
03	base	001	01	{06}	Assembly shift, screw 5mm		0,600	-0,600	1,00	3,0
									1,00	3,0
04	plate	002	01	{06}	Assembly shift, screw 5mm		0,650	-0,650	1,00	3,0
									1,00	3,0
05	plate	002	01	{07}	Location		0,350	-0,350	1,00	3,0
					Bonus M/L				1,00	3,0
					Datum Feature Shift (DFS)				1,00	3,0
					TED	-7,50			1,00	3,0
									1,00	3,0
06	plate	002	01	{05}	Surface profile		0,300	-0,300	1,00	3,0
					UZ shift	-0,20			1,00	3,0
					Datum Feature Shift (DFS)				1,0	3,0
					TED	45,00			1,00	3,0

Fig. 7.12: Extract from the input for the total length stack-up using the bolt as alignment without material condition and non-functional specification.

It is important to note that, according to our model, statistical distributions are considered as normal. However, the assembly shift distribution may not conform well to a normal distribution since it comes from a free play in the assembly prior to the bolt being fastened. A better statistical distribution for this case would be a uniform distribution or a “U shape” distribution. The first option assumes that there is no bias during assembly, while the second one assumes that during assembly, the components will stop in a position where they both touch the screw. The actual statistical distribution depends on the specific assembly procedure and may be influenced by the operator's actions. The Gaussian distribution may represent the outcome from an automated assembly line. Nonetheless, the impact of any of the aforementioned distributions, when compared to the Gaussian one, is that the output variability increases. Therefore, using a Gaussian distribution for the assembly shift may be considered a best-case scenario.

The output of this tolerance stack-up is shown in Fig. 7.13. It is possible to see that the statistical distribution is spread out, and the number of scraps increases considerably compared to the solution with the explicit alignment feature. Both C_p and C_{pk} are almost divided by a factor of three.



	RSS	Adjusted RSS
$C_p = (USL - LSL) / (2 \cdot 3\sigma)$	0,45	0,30
$C_{pk_u} = (USL - \mu) / (3\sigma)$	0,54	0,36
$C_{pk_l} = (\mu - LSL) / (3\sigma)$	0,36	0,24
$C_{pk} = \min[C_{pk_u}; C_{pk_l}]$	0,36	0,24

	RSS	Adjusted RSS
PPM		
Above USL probability	51412	138398
Below LSL probability	138398	234217
Out of tolerance probability	189810	372615

Fig. 7.13: Extract from the output for the total length stack-up using the bolt as alignment without material condition and non-functional specification.

7.3.2 Total length stack-up without external alignment feature and non-functional specification with material condition

For this second iteration, the same non-functional specification will be used. However, the material conditions, namely the Maximum Material Condition on the holes, will now be applied. In the previous case, using the material condition in the presence of an explicit alignment feature was beneficial since it did not influence the total length and increased the variability of the holes while still ensuring the assemblability requirements.

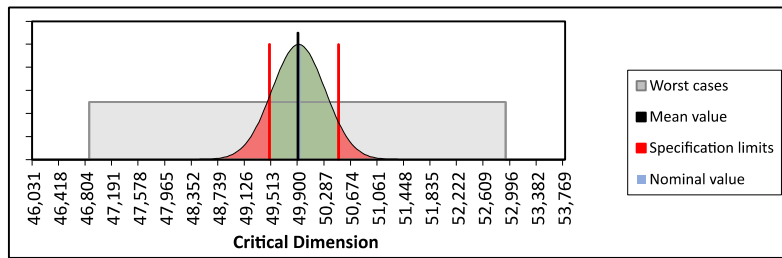
Now, the aim is to analyze the effect of the material condition when the holes are used for alignment. The stack-up scheme remains the same as the previous scheme (Fig. 7.11) since the application of a material condition does not influence the scheme itself.

The extract from the inputs tab is shown in Fig. 7.14. With respect to the previous case, the only difference is the appearance of the bonus on hole location tolerances.

Item	Technical Product Documentation				Specification				s	k
	Description of component/Assy	num.	Rev.	num.	Description of dimension	Nominal	Tol. +	Tol. -		
									1,00	3,0
01	base	001	02	(05)	Surface profile		0,250	-0,250	1,00	3,0
					UZ shift	0,10			1,00	3,0
					Datum Feature Shift (DFS)				1,00	3,0
					TED	5,00			1,00	3,0
									1,00	3,0
02	base	001	02	(07)	Location		0,400	-0,400	1,00	3,0
					Bonus M/L		0,200	-0,200	1,00	3,0
					Datum Feature Shift (DFS)				1,00	3,0
					TED	7,50			1,00	3,0
									1,00	3,0
03	base	001	02	(06)	Assembly shift, screw 5mm		0,600	-0,600	1,00	3,0
									1,00	3,0
04	plate	002	02	(06)	Assembly shift, screw 5mm		0,650	-0,650	1,00	3,0
									1,00	3,0
05	plate	002	02	(07)	Location		0,350	-0,350	1,00	3,0
					Bonus M/L		0,300	-0,300	1,00	3,0
					Datum Feature Shift (DFS)				1,00	3,0
					TED	-7,50			1,00	3,0
									1,00	3,0
06	plate	002	02	(05)	Surface profile		0,300	-0,300	1,00	3,0
					UZ shift	-0,20			1,00	3,0
					Datum Feature Shift (DFS)				1,00	3,0
					TED	45,00			1,00	3,0

Fig. 7.14: Extract from the input for the total length stack-up using the bolt as alignment with material condition and non-functional specification.

The result is that the variability increases compared to the previous case, as shown in Fig. 7.15. Therefore, the application of material conditions when the holes are used for alignment is not advisable since it increases the output variability, which goes against the alignment requirement.



	RSS	Adjusted RSS
$C_p = (USL - LSL) / (2 \cdot 3\sigma)$	0,43	0,29
$C_{pk_u} = (USL - \mu) / (3\sigma)$	0,52	0,34
$C_{pk_l} = (\mu - LSL) / (3\sigma)$	0,34	0,23
$C_{pk} = \min[C_{pk_u}; C_{pk_l}]$	0,34	0,23

	RSS	Adjusted RSS
PPM		
Above USL probability	60495	150626
Below LSL probability	150626	245359
Out of tolerance probability	211121	395984

Fig. 7.15: Extract from the output for the total length stack-up using the bolt as alignment with material condition and non-functional specification.

7.3.3 Total length stack-up without external alignment feature and functional specification without material condition

Now, a functional specification considering the assembly condition given by the alignment by the bolt is considered. The functional specification without material condition is shown in Fig. 7.16. The datum system now considers the holes as datum features; tolerance values for controlled features are the same as in the previous case, therefore the manufacturing cost is comparable.

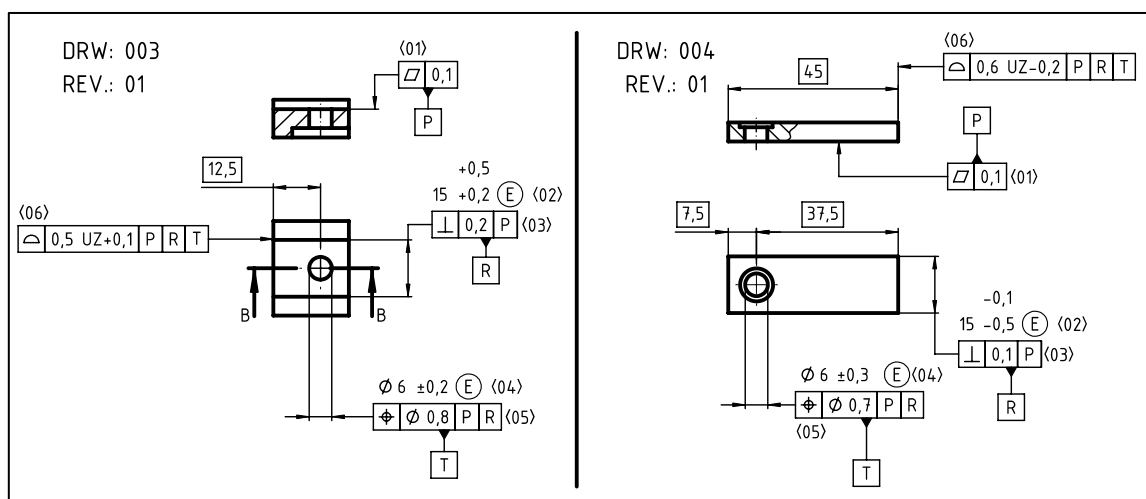


Fig. 7.16: Functional specification for both parts considering the alignment through the bolt without material condition.

The stack-up scheme for this case is shown in Fig. 7.17. It can be noted that compared to the previous case where the non-functional specification was used, the stack-up is “shorter,” therefore fewer contributions need to be considered. The assembly shift is still present.

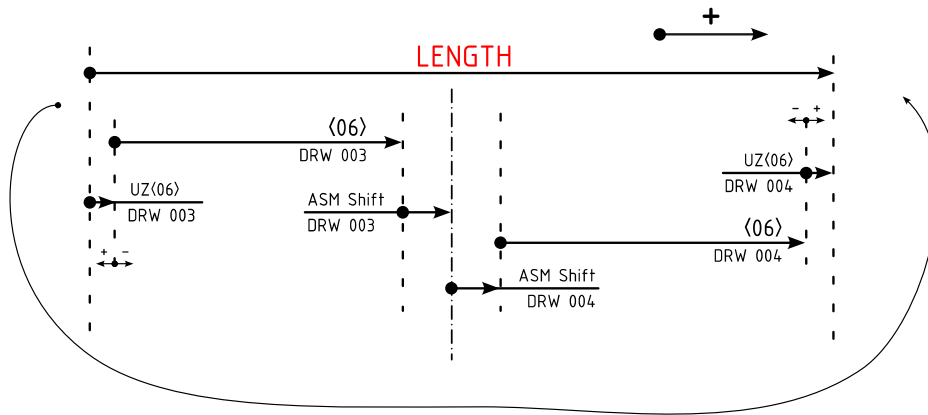
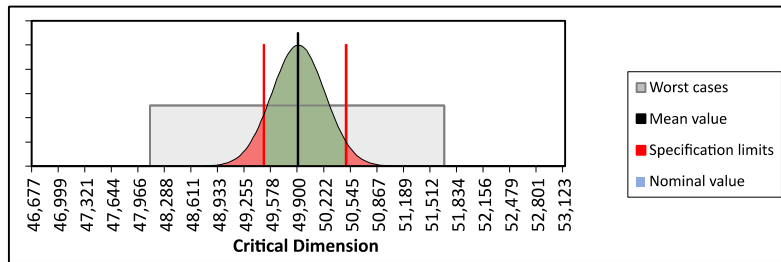


Fig. 7.17: Total length stack-up scheme using the bolt as alignment with functional specification.

The extract from the input tab is shown in Fig. 7.18; while an extract from the outputs tab is shown in Fig. 7.19.

Item	Technical Product Documentation			Specification					s	k
	Description of component/Assy	num.	Rev.	num.	Description of dimension	Nominal	Tol. +	Tol. -		
									1,00	3,0
01	base	003	01	<05>	Surface profile		0,250	-0,250	1,00	3,0
					UZ shift	0,10			1,00	3,0
					Datum Feature Shift (DFS)				1,00	3,0
					TED	12,50			1,00	3,0
									1,00	3,0
02	base	003	01	<06>	Assembly shift, screw 5mm		0,600	-0,600	1,00	3,0
									1,00	3,0
03	plate	004	01	<06>	Assembly shift, screw 5mm		0,650	-0,650	1,00	3,0
									1,00	3,0
04	plate	004	01	<05>	Surface profile		0,300	-0,300	1,00	3,0
					UZ shift	-0,20			1,00	3,0
					Datum Feature Shift (DFS)				1,00	3,0
					TED	37,50			1,00	3,0

Fig. 7.18: Extract from the input for the total length stack-up using the bolt as alignment without material condition and functional specification.



	RSS	Adjusted RSS
$C_p = (USL - LSL) / (2 \cdot 3\sigma)$	0,52	0,34
$C_{pk_u} = (USL - \mu) / (3\sigma)$	0,62	0,41
$C_{pk_l} = (\mu - LSL) / (3\sigma)$	0,41	0,28
$C_{pk} = \min[C_{pk_u}, C_{pk_l}]$	0,41	0,28

	RSS	Adjusted RSS
PPM		
Above USL probability	31336	107301
Below LSL probability	107301	204022
Out of tolerance probability	138637	311323

Fig. 7.19: Extract from the outputs for the total length stack-up using the bolt as alignment without material condition and functional specification.

It can be seen that the output variability decreased when compared to the previous two cases where a non-functional specification was used. Nonetheless, the variability is still almost double compared to the one found using an explicit alignment feature.

7.3.4 Total length stack-up without external alignment feature and functional specification with material condition

In this last iteration, the total length stack-up when the holes are used as alignment features is based on a functional specification with the use of material condition. The functional specification for this case is shown in Fig. 7.20.

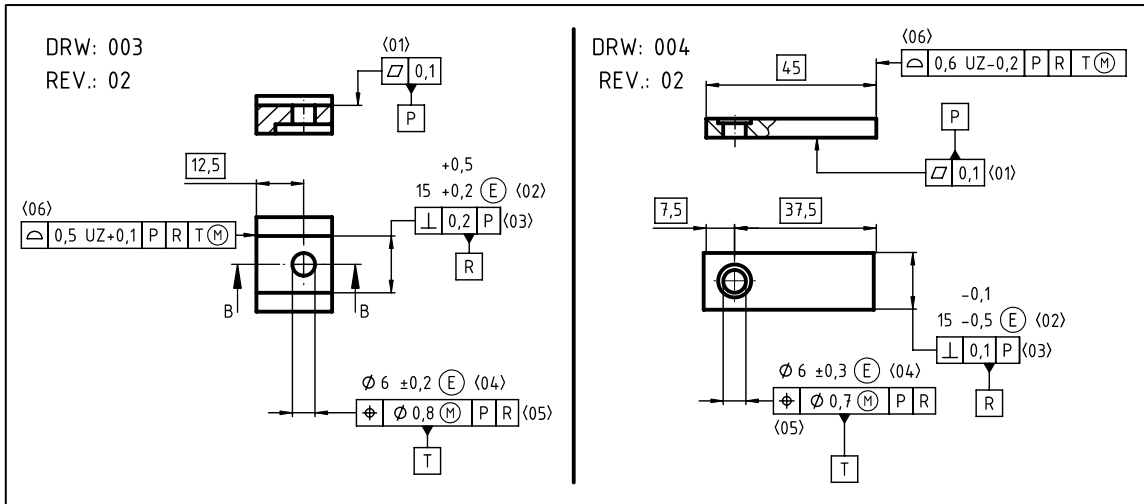


Fig. 7.20: Functional specification for both parts considering the alignment through the bolt with material condition.

The stack-up scheme is still the same as in the previous case (Fig. 7.17).

The inputs tab for this case is shown in Fig. 7.21. In this case, we have both the assembly shift and the datum feature shift since the datum feature is specified with a maximum material condition. The Datum Feature Shift is given by the following equation:

$$DFS = \pm |(FEATURE_{LMC} - FEATURE_{MMC}) / 2|$$

Therefore, for the base component:

$$DFS = \pm |(FEATURE_{LMC} - FEATURE_{MMC}) / 2| = \pm |(6.2 - 5.8) / 2| = \pm 0.2$$

While for the plate component:

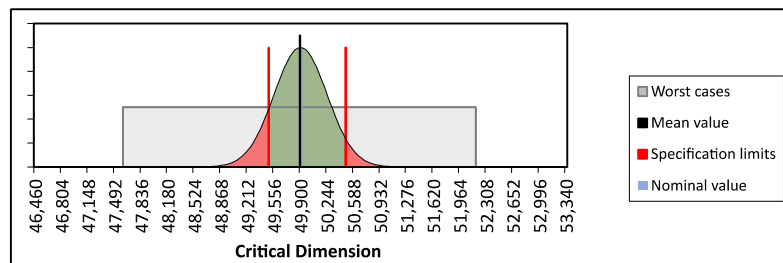
$$DFS = \pm |(FEATURE_{LMC} - FEATURE_{MMC}) / 2| = \pm |(6.3 - 5.7) / 2| = \pm 0.3$$

Item	Technical Product Documentation			Specification						
	Description of component/Assy	num.	Rev.	num.	Description of dimension	Nominal	Tol. +	Tol. -	s	k
01	base	003	02	(05)	Surface profile		0,250	-0,250	1,00	3,0
					UZ shift	0,10			1,00	3,0
					Datum Feature Shift (DFS)		0,200	-0,200	1,00	3,0
					TED	12,50			1,00	3,0
02	base	003	02	(06)	Assembly shift, screw 5mm		0,600	-0,600	1,00	3,0
									1,00	3,0
03	plate	004	02	(06)	Assembly shift, screw 5mm		0,650	-0,650	1,00	3,0
									1,00	3,0
04	plate	004	02	(05)	Surface profile		0,300	-0,300	1,00	3,0
					UZ shift	-0,20			1,00	3,0
					Datum Feature Shift (DFS)		0,300	-0,300	1,00	3,0
					TED	37,50			1,00	3,0

Fig. 7.21: Extract from the input for the total length stack-up using the bolt as alignment with material condition and functional specification.

The extract from the outputs tab is shown in Fig. 7.22. The use of the Material Condition adds the Datum Feature Shift, therefore two contributions are added to the stack-up compared to the previous case. The variability of the output increases slightly.

It is therefore confirmed also in this case that the use of a material condition is not beneficial when the alignment depends on feature of sizes.



	RSS	Adjusted RSS
$C_p = (USL - LSL) / (2 \cdot 3\sigma)$	0,48	0,32
$C_{pk_u} = (USL - \mu) / (3\sigma)$	0,58	0,39
$C_{pk_l} = (\mu - LSL) / (3\sigma)$	0,39	0,26
$C_{pk} = \min[C_{pk_u}, C_{pk_l}]$	0,39	0,26

	RSS	Adjusted RSS
	PPM	
Above USL probability	40562	122455
Below LSL probability	122455	219110
Out of tolerance probability	163016	341565

Fig. 7.22: Extract from the outputs for the total length stack-up using the bolt as alignment with material condition and functional specification.

7.3.5 Comparison

The cases that have been presented so far are now compared. The first comparison will address the differences coming from different design options: which feature to use for alignment. The second comparison, assuming the alignment relies on the bolt, will address the effect of material condition and a properly defined functional specification.

The comparison between different assembly conditions using the same geometric specification is shown in Fig. 7.23. The first obvious difference that can be seen is that while the explicit alignment feature ensures the output statistical distribution is well within specification limits (both C_p and C_{pk} greater than one), using the bolt as alignment results in a much larger output statistical distribution and a significant increase in the number of scraps (by a factor of 10^3). It should be highlighted that the output statistical distribution for the alignment through the bolt represents a best-case scenario since a Gaussian distribution of the assembly shift is assumed; the real distribution might even be wider.

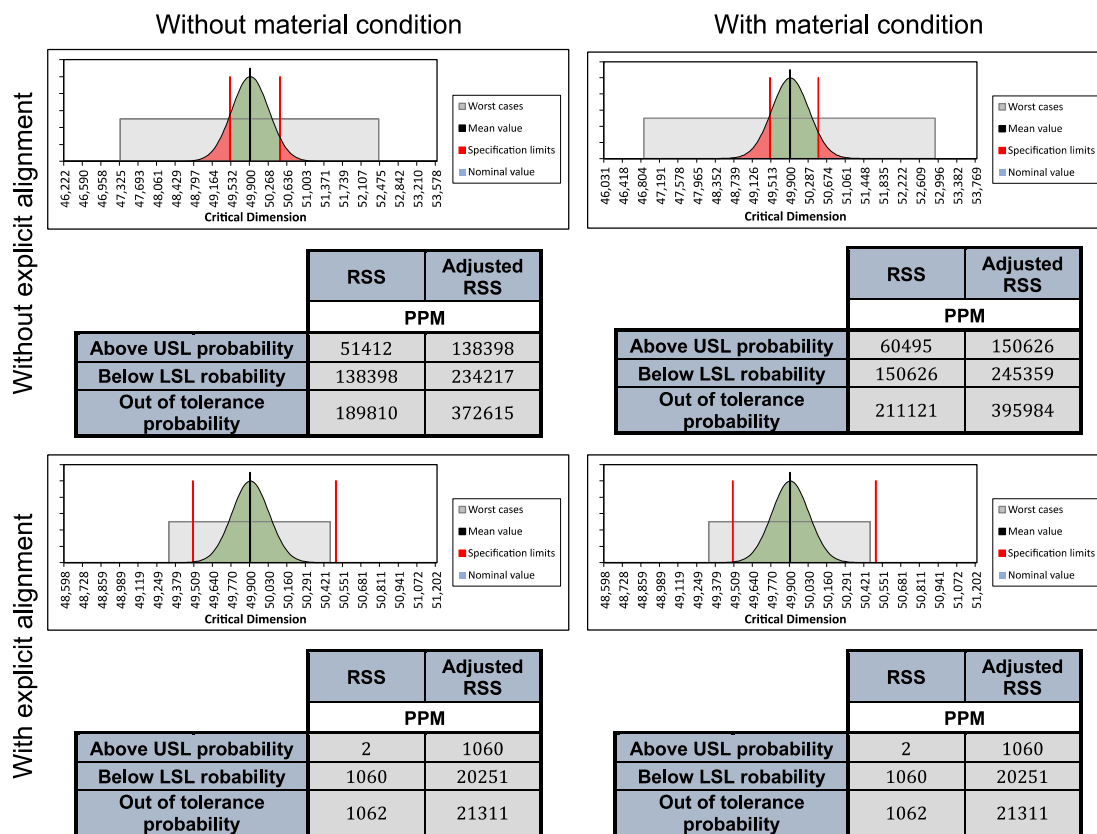


Fig. 7.23: Comparison between the result obtained with the same geometric specification changing the assembly condition.

Since the tolerance values are the same for these specifications and the topology is almost the same, the production cost can be considered comparable (or even the same). The result is that at the same production cost, choosing to base the alignment on the bolt gives a far worse result compared to the use of an explicit alignment feature.

This proves, once again, that bolted connections should never be used to guarantee alignment if the requirement is critical. It might be noted that, as presented in the previous chapter, if a pattern of bolts is used, the effect of the assembly shift might be mitigated and, therefore, help with the alignment. The precise computation of the effect is still difficult and, so far, may be achieved only with Monte Carlo simulation (see future research agenda, chapter 13 on page 271).

These considerations do not apply if the alignment is guaranteed with dowel pins since, in this case, the clearance is minimal by design.

The comparison between different specifications for the same assembly condition is shown in Fig. 7.24. In this case, the alignment is given by the bolt, and it has already been discussed that this is not the most efficient way of managing the assembly. Nonetheless, in industry, this situation often occurs, and it is important to find solutions that can help mitigate the effect of the assembly shift.

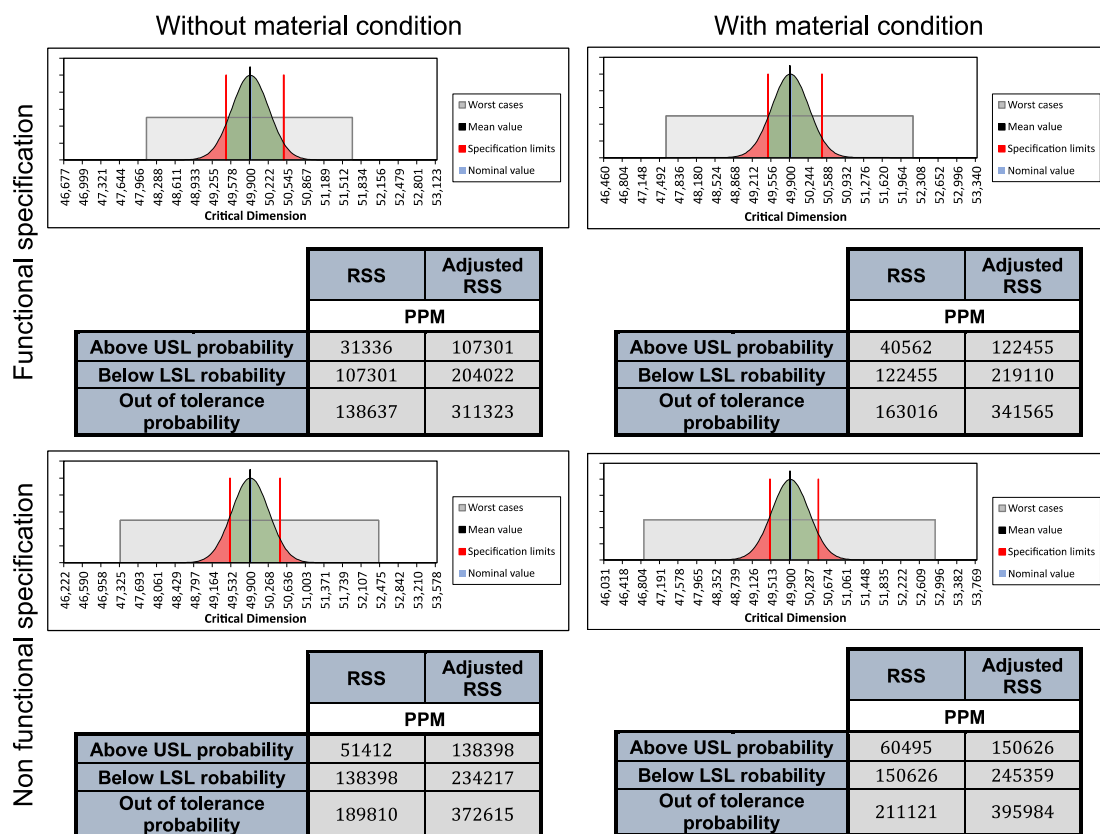


Fig. 7.24: Comparison between the result obtained with different geometric specifications with the same assembly condition.

With the given tolerance values, it can be seen that none of the proposed specifications fulfills the functional requirements. Nonetheless, significant differences can be seen when comparing the different cases.

Considering the functional specification, the application of the material requirements increases the number of estimated scraps by 17.58 %, while considering the non-functional specification, the number of scraps increases by 11.23 %. Therefore, in both cases, the application of the material condition decreases the quality of the assembly and may not be a good solution. A definitive answer can only be derived by computing the cost of the scrap compared to the savings coming from the application of the material requirement. The tolerance stack-up gives the possibility to economically evaluate the solution, allowing sound decisions. If the stack-up is used for tolerance synthesis according to a pre-defined metric (e.g., C_p and C_{pk} greater or equal to one) starting from a worst solution will inevitably lead to tighter tolerance values, and therefore, higher manufacturing costs.

Considering the differences between the use of a functional specification versus a non-functional one, it can be seen that a non-functional specification always estimates a larger number of scraps. If the case without material condition is considered, the non-functional specification results in 36.91 % more scraps; considering the case with material condition, it leads to 29.51 % more scraps. Inevitably, using a non-functional specification induces having tighter tolerances than actually needed. Indeed, the higher number of scraps derives from a tolerance stack-up that does not represent the assembly conditions. Since the functional specification, as defined in this work, describes the assembly conditions, the stack-up that can be created is the “shortest” possible, meaning that it has the least contribution possible. The result is that a tolerance synthesis based on a functional specification allows larger tolerances when compared to other possible geometric specifications that do not consider the assembly conditions.

7.4 || Conclusions

The aim of this chapter was to demonstrate the potential of tolerance stack-up as a design tool, both for validating design assumptions on the nominal model and for evaluating alternatives in geometric specifications. Tolerance stack-up is a valuable tool for comparing different design options by analyzing output metrics such as C_p , C_{pk} , or scraps number.

In the case study presented, the old design rule that advises against using bolted connections for guaranteed alignment was investigated. The evidence from the tolerance stack-up confirms the validity of this empirical rule, providing yet another proof.

The effect of material condition was also analyzed statistically, confirming that the maximum material condition precisely describes the assemblability requirement but should be avoided when precise alignment is needed.

Furthermore, the impact of a functional specification versus a non-functional one was studied. As previously postulated in this work, it was proven that a functional specification that accurately describes the assembly conditions allows the creation of “shorter” tolerance stack-ups, which, in turn, permits larger tolerances to be assigned during the tolerance synthesis phase.

In conclusion, tolerance stack-up represents a powerful tool in the hands of designers to validate design assumptions and optimize their designs when used wisely. By leveraging tolerance stack-up analyses, designers can make informed decisions and improve the overall quality of their designs.

8 || Correlation of functional and manufacturing specifications for deformable assembly⁵

The beauty of physics lies in the extent which seemingly complex and unrelated phenomena can be explained and correlated through a high level of abstraction by a set of laws which are amazing in their simplicity.

Melvin Schwartz

Nowadays, non-rigid parts, such as injection-molded plastic and thin sheet-metal components, which undergo deformation during assembly, are increasingly common in industrial products. Due to the manufacturing process, some parts may exhibit significant deformation, exceeding functional limits. However, during the assembly process, these parts can be manipulated to achieve functional configurations. As a result, the functional geometrical specifications (i.e., ISO GPS) relevant to assembly cannot be directly transferred to the individual sub-assembly parts. Instead, the manufacturing geometrical specifications of these parts should be based on a “free state condition” (see ISO 10579 [108]). A clarifying example can be found in section 8.4.

In many industrial cases, the relationships between functional and manufacturing specifications are often not systematically managed. The existence of multiple documents (functional, manufacturing, and verification specifications) creates a multi-pole structure with hierarchical relationships, requiring a rigorous correlation (see ISO/TS 21619/2018 [37]). When dealing with rigid parts and assemblies, tolerance stack-ups can be used to achieve this correlation, and the tolerance transfer method [54] represents a valid option. However, there is a lack of standardized procedures to correlate the functional specification (or “as assembled”) to the manufacturing specification (“free state”) for deformable or compliant assemblies.

In the case of non-rigid bodies, literature provides approaches based on Finite Element Method (FEM) simulation. Many contributions focus on sheet metal parts: assemblies commonly used in the aerospace and automotive sectors. Sellem and Rivière [109] propose a mechanical approach using influence coefficient matrices to compute tolerances for welded, bolted, riveted, or

⁵ The context of this chapter is mainly derived from a paper already published by the author [165].

glued sheet metal parts. Liu and Hu [110] present a mono-dimensional strategy called the “offset finite element model” to predict sheet metal assembly variability in spot-welded parts. Liu, Hu, and Woo [111] discuss the differences between “series” and “parallel” assemblies, finding that parallel assemblies exhibit smaller variability compared to individual part variability. The Influence Coefficient method [112] was developed to link the assembly's spring-back to the free-state condition, considering shape defects and contact modeling [113,114]. These approaches are limited to thin-walled parts, and a summary of these methodologies can be found in the literature [115].

Stockinger et al. [116] present an approach considering elastic deformation in sheet metal parts for tolerance stack-ups, validated through experimental results and compared to different commercial solutions integrating 3DCS™ by Dimensional Control Systems® and CATIA V5™ workbench TAA™ (Tolerance Analysis of deformable Assemblies) by Dassault Systèmes®, where FEM simulation is used to analyze assembly process deviations.

Radvar-Esfahlan and Tahan [117] propose the Generalized Numerical Inspection Fixture (GNIF) methodology to perform fixtureless inspections of freeform surfaces on non-rigid thin-walled parts. This methodology considers the part's deformation as isometric, meaning that the geodesic distance between any two internal points does not change during deformation. Correspondent points between the CAD model and the acquired freeform model are defined using this assumption. Further developments to this framework introduce improved boundary conditions [118] and automation [119]. Lindau et al. [120] propose a method to compensate for information lost in a fully clamped configuration, simulating the clamped state with FEM simulation and the method of influence coefficient, using a three-point supporting setup. Morse and Grohol [121] develop an efficient methodology for fixtureless inspection of non-rigid parts by executing FEM simulation on the nominal geometry independently from actual data.

Raymauld et al. [122] propose a methodology for performing virtual measurements of constrained state thin-walled parts made of polymers.

Recent trends driven by the digitization of product systems and the implementation of the digital twin concept have enabled the prediction of product geometrical quality in the early design phase, as discussed by Maropoulos and Ceglarek [123]. The Digital Twin concept, first developed at NASA and presented in 2010 [124], is defined as “*an integrated multi-physics, multi-scale, probabilistic simulation of a vehicle or system that uses the best available physical models, sensor updates, fleet history, etc., to mirror the life of its flying twin.*” In the context of mechanical assemblies, the main purpose of a Digital Twin is the verification and validation of product design and the definition of its characteristics [125], enabling digital variation management [126,127]. A notable characteristic of a Digital Twin is the bidirectional real-time communication: physical-digital and digital-physical. Its implementation for geometrical assurance allows selective assembly and real-time process adjustment [128–131]. The use of neural networks embedded in Digital Twins or as meta-models for predicting assembly variability [129,132] and spring-back during manufacturing [133] has also been tested.

While full model simulation may be suitable for early design phases for development and optimization purposes, simplified models are crucial for real-time applications during production [127]. However, the concurrent engineering paradigm implies that the early design phase alone cannot be strictly defined, and the product geometry itself is developed in parallel with the production process [134]. Consequently, the need for simplified meta-models or surrogate models extends to the design phase as well.

In the literature, sheet metal parts and/or parts with thin-walled geometry have been primarily addressed, with no specific works focusing on general non-rigid large parts. In this context, a “non-rigid large part” refers to a part where not all the geometry is equally influenced by the assembly process, implying that local stiffer portions are not deformed but only translated and/or rotated. It is also assumed that the part, once assembled, reaches a stable configuration. Furthermore, the methodologies presented in the literature are optimized for inspection or tolerance stack-up applications. Since they represent a post-processing of acquired data, if used for quality control, they need to be repeated after each inspection cycle. The need for simplified generic models was also highlighted by Kaufmann et al. in an in-depth analysis of the model presented in the literature [135].

In a first preliminary iteration of the proposed framework [136], a procedure for correlating the functional geometrical specification to the manufacturing specification, applied to large injection-molded parts, was presented. This methodology suggests a correlation procedure between the geometric specifications in the “as produced” (free) state and the “as assembled” (functional) state to be performed at the start-up of production, in order to define free state tolerance limits for inspection during mass production. The procedure utilizes FEM simulation and is based on a formal definition of datum systems and geometric tolerances as defined by ISO GPS standards. However, the methodology relies on the non-realistic hypothesis that the assembly process can completely recover the initial deformation at the assembly features, resulting in the best-case scenario where the maximum possible reduction is achieved.

Therefore, to fill this gap, a methodological framework for correlating the manufacturing specification and the functional specification applied to large non-rigid parts, taking into consideration the elastic spring-back of the assembly is presented in this chapter. The Influence Coefficient Method, widely applied in sheet metal assemblies, is used to determine the spring-back of the assembly features. This chapter presents and discusses a methodology that allows for the creation of a linearized model to simulate the constrained state using a “restricted skin model” approach.

8.1 || Methodology description

The overall proposed methodology can be seen in Fig. 8.1. In brief, the parts in the free state are inspected based on the manufacturing specification, and the deviations in the free state are

recorded to generate the free state restricted skin model. The assembled state restricted skin model is simulated starting from the free state restricted skin model using a linearized model. It is then virtually inspected based on the functional specification. The deviations in the assembled state are recorded and correlated with the deviations in the free state.

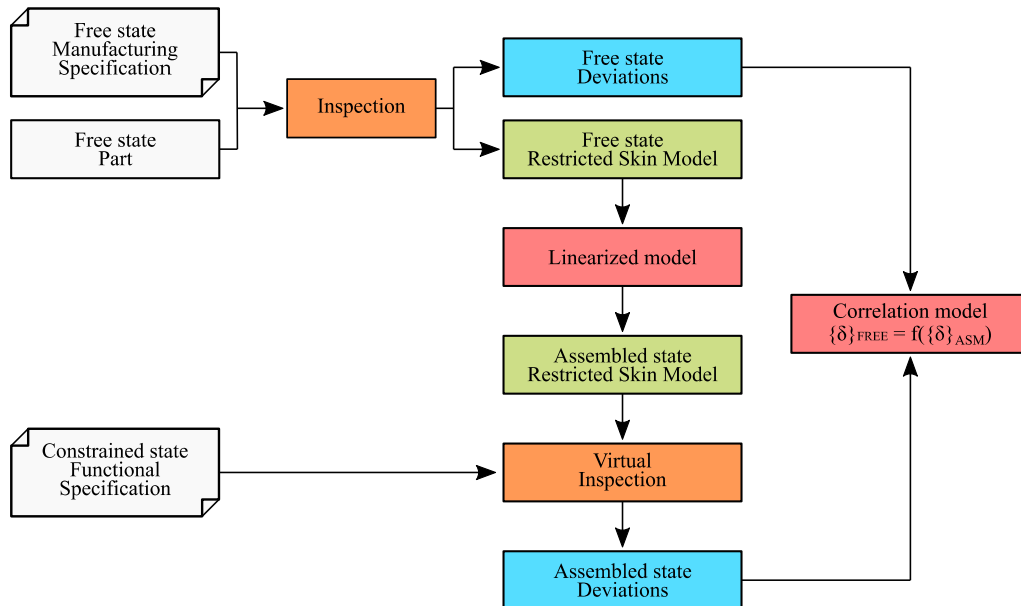


Fig. 8.1: General workflow to correlate functional (design) and manufacturing specifications.

The core concepts described in this chapter include the definition of the restricted skin model and the discussion of the linearized model.

The methodology is presented through the evaluation of the assembly between two large non-rigid parts. If more than two parts need to be assembled, the result of the first assembly operation can be considered as a new single part that receives a third part, and so on. For both parts, a coherent functional specification is assumed to be available. Two classes of geometrical features can be identified for both parts: the mutual assembly features (features that come into contact when the two parts are assembled) and other functional features. It is important to establish a proper functional datum system for both parts to ensure a correct geometrical specification.

The assembly process is considered to consist of four general steps: locating and placement in the fixture, clamping, joining, and releasing [137,138]. No deformation caused by the joining process is considered in this methodology, although its contribution could be easily added as presented in a previous study [114].

For the first part, n degrees of freedom are assigned to the assembly features, and a total of m degrees of freedom are assigned to the other functional features. The degrees of freedom can represent rigid geometrical deviations (such as rigid translation or rotation), a set of point deviations for a given feature (e.g., sampling points on a flat surface to consider form deformations), or deviations in derived geometry (such as axis or mid-plane). An example of each type of input-output

degrees of freedom and its geometrical interpretation is shown in Fig. 8.2. The use of a set of points for tolerance analysis, without considering deformability, is also mentioned in a previous study [139].

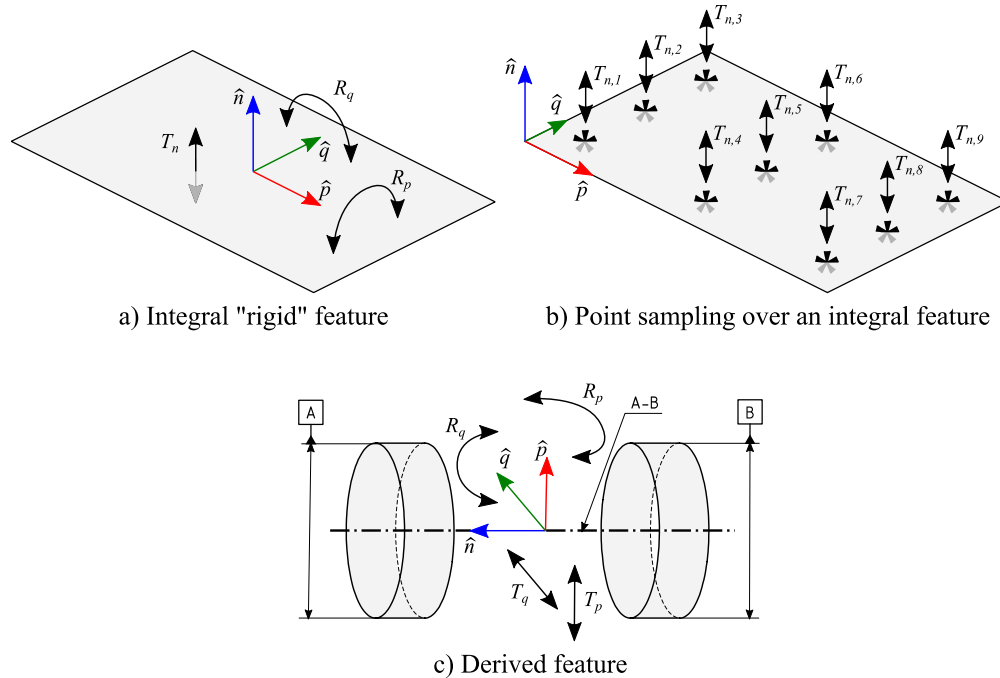


Fig. 8.2 : Types of possible input-output degrees of freedom.

8.1.1 Matrix computation

Throughout a simulation, a sensitivity matrix $[A_1]$ ($m \times n$) is evaluated, which links the m outputs degrees of freedom to the n input degrees of freedom. Simultaneously, a reduced stiffness matrix $[K_1]$ ($n \times n$) is computed, linking the n input degrees of freedom to the n constrain forces. To obtain these reduced matrices, n FEM simulation are performed by applying a unit deviation in one input degree of freedom at a time while keeping all others at null deviation. It is important to note that the reliability of the FEM simulations, as an input to the model, significantly impacts the accuracy of the proposed methodology. The simulation parameters such as mesh, boundary conditions, contact modeling, etc., should be carefully evaluated for each specific case.

The same matrices are also evaluated for the second component: $[A_2]$ ($p \times n$) and $[K_2]$ ($n \times n$). It should be noted that the degrees of freedom applied to the assembly features of the second component need to be mapped from the first component, as shown in, Fig. 8.3.

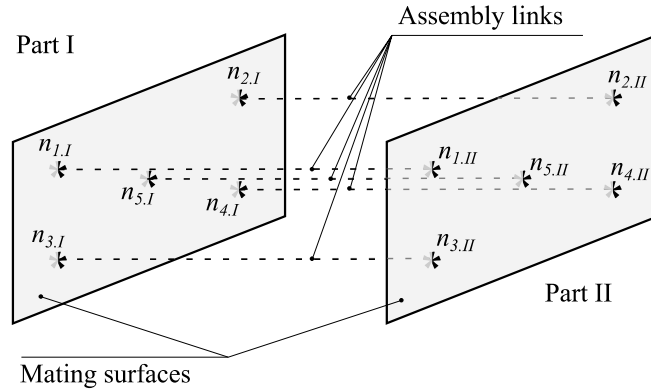


Fig. 8.3 : The input degrees of freedom are mapped on the second part mating feature creating an assembly link per each of them.

The assembly needs to be evaluated as it becomes stiffer compared to both single parts. By considering only the input degrees of freedom, a reduced stiffness matrix can be evaluated for the assembly, denoted as $[K_{asm}]$ ($n \times n$), which links the assembly deviation to the constraining forces.

8.1.2 Assembly feature deviation

Once the matrices are evaluated, the first step is to calculate the deviation of the assembly features using the Influence Coefficient Method [7], given by equation (8-1). The derivation of the formula is omitted here for the sake of brevity, but it is well-documented and available in the literature.

$$\{\delta_n\} = [K_{asm}]^{-1} [K_1] \{\delta_1\} [K_{asm}]^{-1} [K_2] \{\delta_2\} \quad (8-1)$$

Where:

- $\{\delta_n\}$ represents the deviation associated with the n input degrees of freedom after the assembly.
- $\{\delta_1\}$ represents the free state deviation associated with the n input degrees of freedom for the first part.
- $\{\delta_2\}$ represents the free state deviation associated with the n input degrees of freedom for the second part.

8.1.3 Deviation of other functional elements

The overall methodology is based on the assumptions of linear constitutive relations and small deviations from nominal. As a result, the superposition principle is employed to determine the deviation from the nominal of an actual geometry when constrained, by summing the different contributions.

Three contributions are taken into account: the free state deviation, the deviation caused by fixturing, and the elastic spring back, leading to the final formula.

$$\{\delta_m\}_{TOT} = \{\delta_m\}_{FREE} - [A_1]\{\delta_1\} + [A_1]\{\delta_n\} \quad (8-2)$$

The formula is written for the first part of the assembly, where:

- $\{\delta_m\}_{TOT}$ represents the deviation associated with the m output degrees of freedom after the assembly.
- $\{\delta_m\}_{FREE}$ represents the free state deviation associated with the m output degrees of freedom for the first part and should be evaluated by means of inspection of the part in free state condition.
- $-[A_1]\{\delta_1\}$ represents the deviations associated with the m output degrees of freedom for the first part if the n input degrees of freedom of the non-ideal actual part are forced to their nominal position (i.e., fixturing).
- $[A_1]\{\delta_n\}$ represents the deviations associated with the m output degrees of freedom for the first part due to the elastic spring back.

The equation (8-2) can also be rewritten in a more structured manner as follows:

$$\{\delta_m\}_{TOT} = \{\delta_m\}_{FREE} + \{-[A_1] + [A_1][K_{asm}]^{-1}[K_1]\}\{\delta_1\} + \{[A_1][K_{asm}]^{-1}[K_2]\}\{\delta_2\} \quad (8-3)$$

If considering the second part, the equation becomes:

$$\{\delta_p\}_{TOT} = \{\delta_p\}_{FREE} + \{[A_2][K_{asm}]^{-1}[K_1]\}\{\delta_1\} + \{-[A_2] + [A_2][K_{asm}]^{-1}[K_2]\}\{\delta_2\} \quad (8-4)$$

Besides the two sensitivity matrices, $[A_1]$ and $[A_2]$, already defined, four additional sensitivity matrices can be defined:

- $[A_{11}] = -[A_1] + [A_1][K_{asm}]^{-1}[K_1]$ represents the assembled state sensitivity matrix for the first part relative to the first part deviations.
- $[A_{12}] = [A_1][K_{asm}]^{-1}[K_2]$ represents the assembled state sensitivity matrix for the first part relative to the second part deviations.

- $[A_{22}] = -[A_2] + [A_2][K_{asm}]^{-1}[K_2]$ represents the assembled state sensitivity matrix for the second part relative to the second part deviations.
- $[A_{21}] = [A_2][K_{asm}]^{-1}[K_1]$ represents the assembled state sensitivity matrix for the second part relative to the first part deviations.

Both equations (8-3) and (8-4) can then be written compactly.

$$\{\delta_m\}_{TOT} = \{\delta_m\}_{FREE} + [A_{11}]\{\delta_1\} + [A_{12}]\{\delta_2\} \quad (8-5)$$

$$\{\delta_p\}_{TOT} = \{\delta_p\}_{FREE} + [A_{21}]\{\delta_1\} + [A_{22}]\{\delta_2\} \quad (8-6)$$

These two equations, along with equation (8-1), can be used to evaluate the constrained state. These three equations form the core of the proposed linearized model.

It is noteworthy that these three equations can also be used to propagate the uncertainty associated with the input quantities, such as the free-state measurement uncertainty.

A summary of the procedure to create the proposed linearized model can be seen in Fig. 8.4.

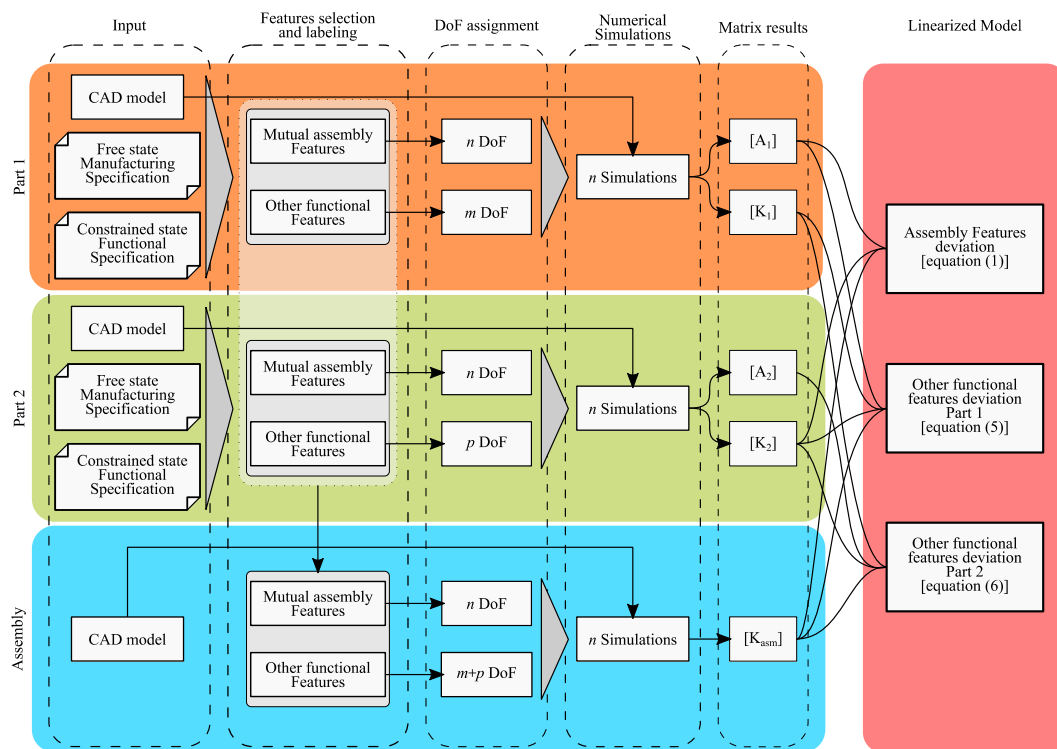


Fig. 8.4 : The general workflow to generate the proposed linearized model. DoF stands for Degree of Freedom.

8.1.4 Specification Correlation

Using the aforementioned workflow for both the free state and simulated constrained state allows for the determination of geometrical deviations in the functional features. These deviations can be in the form of rigid feature translation and/or rotation or as a set of point deviations, which account for form errors. As a result, the obtained deviations can be considered a “restricted skin model” representation, in contrast to the “full” skin model that considers all topological boundaries of the part, including form deviations [140].

Digital inspection can be conducted according to the ISO GPS standard. The manufacturing specification is used for inspecting the free state part, while the functional specification is used for inspecting the constrained state part. This approach provides geometrical deviations in accordance with ISO 17450-1:2011 and ISO 1101:2017 [38,141] for both states.

Consequently, it becomes possible to create a statistical correlation model between the free state deviation and the simulated constrained state, considering all possible combinations of assembly among the available parts. This correlation model can be utilized to define manufacturing limits for the free state that statistically guarantee the predefined functional limit.

8.1.5 Model validation

The proposed methodological framework has undergone testing to verify and validate its assumptions. The testing involved different case studies, each designed to evaluate and stress different steps of the procedure.

Firstly, a simplified mono-dimensional case was tested. In this case, an analytical definition was available for all the previously described sensitivity matrices. As a result, no FEM simulation was required, allowing for the identification of methodological flaws independent of FEM model inaccuracies.

Secondly, a case study was conducted to demonstrate the effectiveness of the sensitivity matrix in simulating the output degrees of freedom using FEM simulation. This case study aimed to show that the reduced model could yield the same results as a full FEM simulation.

Thirdly, a case study focused solely on the elastic spring back at the assembly features was presented. This case study aimed to explore the impact of elastic spring back on the assembly.

Lastly, based on the findings from the third case study, two samples were produced, and the results were compared to actual measurements.

Overall, these case studies were performed to test and validate different aspects of the proposed methodology, ensuring its robustness and effectiveness.

Case study 1

The setup of the monodimensional test case is illustrated in Fig. 8.5. It involves two idealized components, each with one input and one output. Each elastic element has a nominal length of 100 mm.

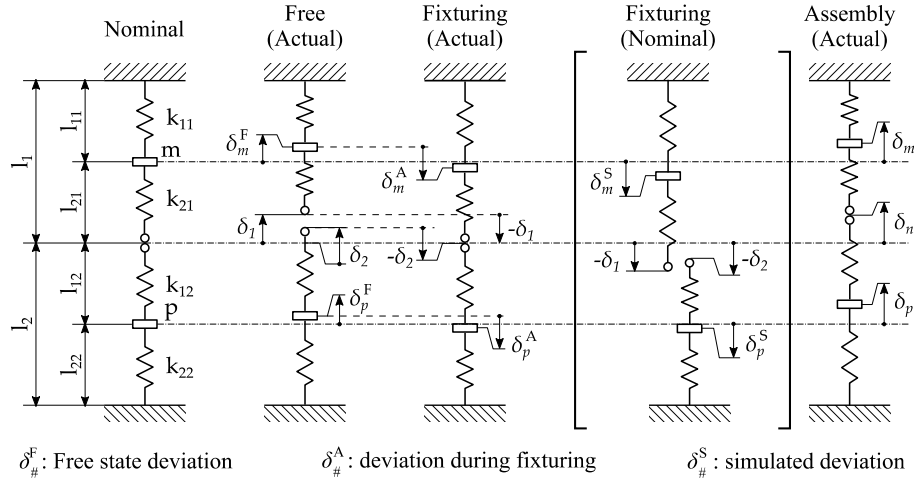


Fig. 8.5 : The monodimensional case study.

In Tab. 8.1, all the tested configurations can be seen. Various combinations of stiffness and free state deviation were examined to verify the results of the framework.

Tab. 8.1: Configurations tested to verify the framework.

Test case	$\{\delta_1\}$ [mm]	$\{\delta_m\}_{FREE}$ [mm]	$\{\delta_2\}$ [mm]	$\{\delta_p\}_{FREE}$ [mm]	k_{11} [N/mm]	k_{21} [N/mm]	k_{12} [N/mm]	k_{22} [N/mm]
1.1	10	0	0	0	1000	800	10^9 *	10^9 *
1.2	10	0	0	0	1000	800	400	500
1.3	10	0	5	0	1000	800	400	500
1.4	10	0	-5	0	1000	800	400	500
1.5	10	5	-5	-3	1000	10^{-9} *	10^{-9} *	500
1.6	10	5	-5	-3	1000	800	10^{-9} *	10^{-9} *
1.7**	10	5	0	0	1000	800	Variable	variable

* Values of 10^9 and 10^{-9} are used to simulate respectively an infinitely rigid component and an infinitely compliant component.

** Test case 1.7 is used to analyze how the second component stiffness influences the spring-back value.

Each combination was selected to challenge the model and generate specific cases where the final output could be deduced. The expected outcomes for each case can be found in Tab. 8.2.

Tab. 8.2: Expected simulation results.

Test case	Expected results		
	$\{\delta_n\}$	$\{\delta_m\}_{TOT}$	$\{\delta_p\}_{TOT}$
1.1	0	$-10 < \{\delta_m\}_{TOT} < 0$	0
1.2	$0 < \{\delta_n\} < 10$	$\{\delta_m\}_{TOT_1} < \{\delta_m\}_{TOT} < 0$	> 0
1.3	$\{\delta_n\} > \{\delta_n\}_2$	–	–
1.4	$\{\delta_n\} < \{\delta_n\}_2$	$-10 < \{\delta_m\}_{TOT} < \{\delta_m\}_{TOT_2}$	–
1.5	0	5	–3
1.6	10	5	–3

Case study 2

The case study designed to demonstrate the effectiveness of the sensitivity matrix, as proposed in the framework, is illustrated in Fig. 8.6. Assuming that the elastic spring back is accurately estimated by the model (MIC), the results obtained through the reduced model are compared to those obtained with full FEM simulation to validate the capability of the proposed sensitivity matrix in accurately estimating the deviations in output degrees of freedom.

The assembly feature is defined as a deformable planar surface and is described with 12 degrees of freedom. The output degrees of freedom are considered as the translation and rotation of the upper cylinder, as shown in Fig. 8.6.a).

For FEM simulations, the software Patran/NASTRAN was used. The geometry is discretized with two-dimensional FEM elements (CQUAD4). To record the deviation of the output degrees of freedom, two service nodes are placed in the nominal position at the extreme points of the cylinder axes and connected to one node of the cylinder in the corresponding extreme section with a rigid link (RBE2), as depicted in Fig. 8.6.b). To verify the assumption that the cylinder behaves as a rigid element, the same service node is connected to the relevant FEM node in the corresponding section using spring elements (CELAS1). If the cylinder behaves as a rigid element, no stress should be recorded within the spring elements.

Five different free-state deviations for the assembly feature were tested and are listed in Tab. 8.3. The deviation values were randomly generated based on a truncated Fourier series.

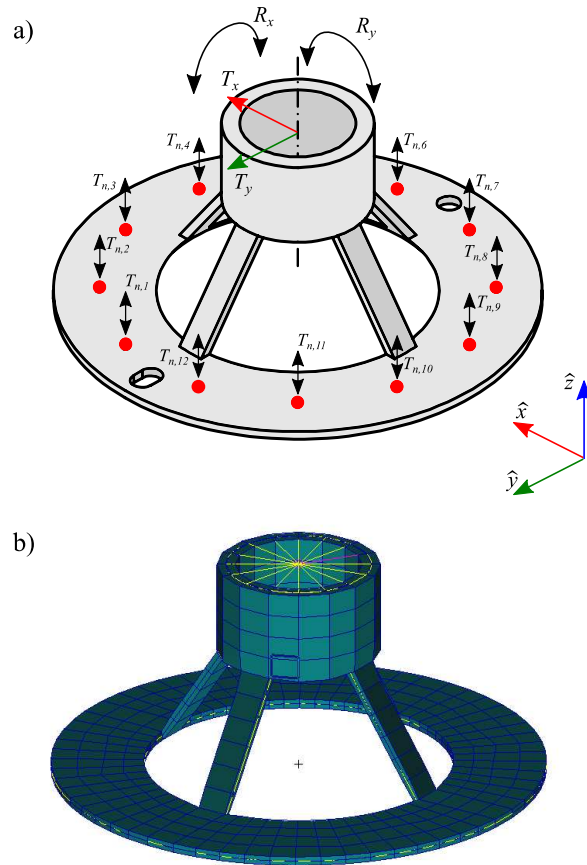


Fig. 8.6: The case study used to prove the sensitivity matrix's effectiveness, a) CAD model, b) FEM model.

Tab. 8.3: Configuration tested for case study 2.

Test case	$\{\delta_n\}_1$	$\{\delta_n\}_2$	$\{\delta_n\}_3$	$\{\delta_n\}_4$	$\{\delta_n\}_5$	$\{\delta_n\}_6$	$\{\delta_n\}_7$	$\{\delta_n\}_8$	$\{\delta_n\}_9$	$\{\delta_n\}_{10}$	$\{\delta_n\}_{11}$	$\{\delta_n\}_{12}$
	[mm]	[mm]	[mm]	[mm]	[mm]	[mm]	[mm]	[mm]	[mm]	[mm]	[mm]	[mm]
2.1	1.582	1.502	0.702	-0.112	-1.179	-1.094	-0.716	-0.982	-0.702	-0.408	0.313	1.094
2.2	0.889	0.809	0.702	0.581	-0.486	-1.094	-1.408	-1.675	-0.702	0.285	1.006	1.094
2.3	-1.608	-1.413	-0.648	0.463	0.660	1.010	1.089	0.547	0.648	0.403	-0.140	-1.010
2.4	-1.708	-1.250	-0.848	0.636	0.560	1.010	1.189	0.374	0.848	0.230	-0.040	-1.010
2.5	-1.716	0.547	-0.148	-0.057	-0.833	1.010	2.582	1.066	0.148	-0.463	-0.033	-1.010

Case study 3

Case study 3 is designed to test the elastic spring back at the assembly features. The setup is illustrated in Fig. 8.7, where two simple parts are involved: the base (Fig. 8.7.b) and Fig. 8.7.e), and the top (Fig. 8.7.a) and Fig. 8.7.d)). The assembly is performed by gluing the two parts together using a fixture.

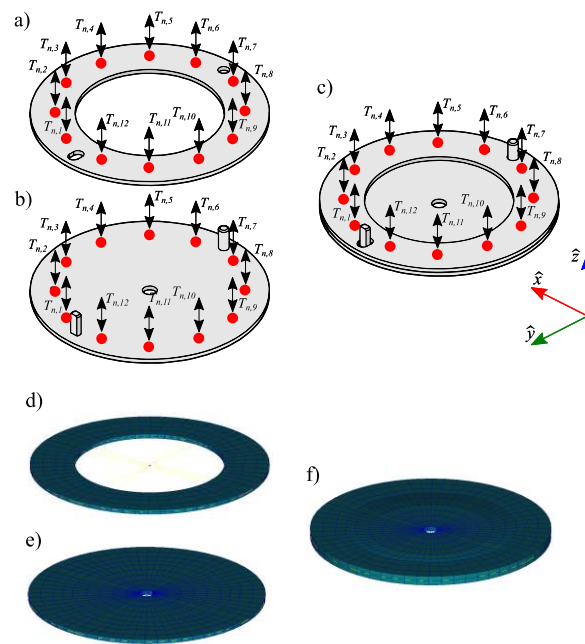


Fig. 8.7: The case study used to test the elastic spring back.

Both assembly features are described with 12 degrees of freedom, as shown in Fig. 8.7.a) and Fig. 8.7.b). The simulations are performed using Patran/NASTRAN, and the geometry is discretized with bidimensional FEM elements (CQUAD4), as depicted in Fig. 8.7.d), e), and f).

Due to the polynomial approximation of the FEM simulation, numerical errors in the stiffness matrix are inevitable. Theoretically, the sum of any row of the stiffness matrix should be equal to zero, but in practice, a residual error is always present. This residual error leads to a resultant fixturing force, even for rigid translations of the assembly features, which is not physically meaningful. Although this residual force is small compared to the forces caused by actual assembly feature deformation, it can estimate a rigid spring back translation when passed through the inverse of the assembly stiffness matrix. To avoid this issue, the input deviations need to be filtered by their mean value, which represents a rigid translation. This filtering helps eliminate the numerical error.

Residual errors in the stiffness matrix can be attributed to the fact that the FEM solver computes only a certain number of significant digits. In some cases, the residual error can be significant enough to make the solution unstable, resulting in elastic spring back that exceeds the input deviations or occurs in the opposite direction. This effect was studied on a simplified geometry,

as shown in Fig. 8.8. In this case, two identical parts are joined together, and deformations are considered only on one part.

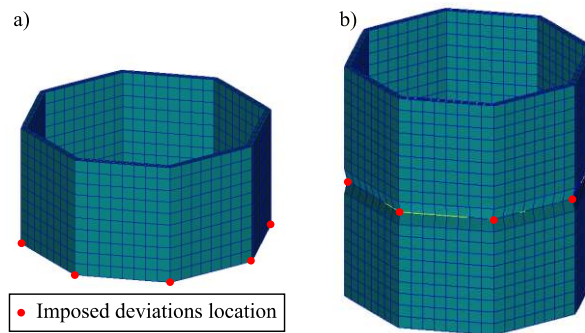


Fig. 8.8: The geometry used to test the instability of the problem.

The full model in this case exhibits physically sound behavior. However, when the stiffness matrices are truncated and the less significant digits are used, the spring back diverges more towards the opposite side compared to the input deviations, as shown in Fig. 8.9.

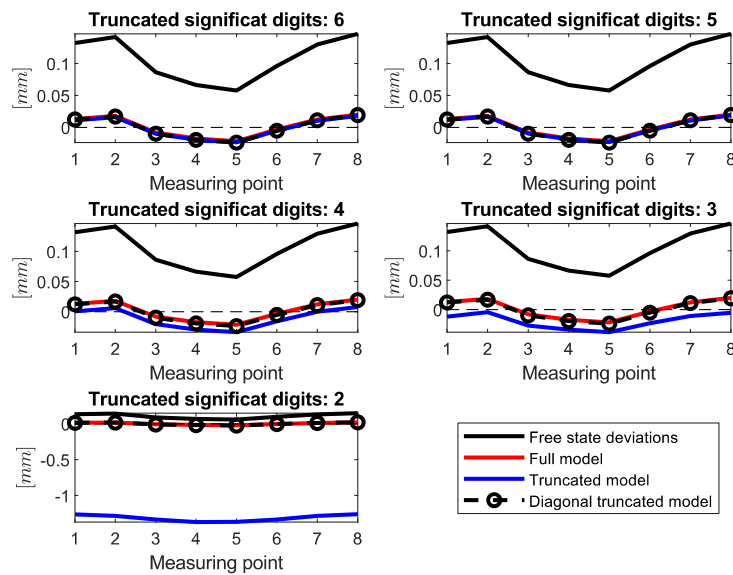


Fig. 8.9: Effect of the truncation of the stiffness matrices on the elastic spring back simulation.

To mitigate this numerical effect, only the diagonal components of the stiffness matrices are considered. The fixturing forces ($-[K] \cdot \{\delta_1\}$) do not have actual values, but since the same transformation is applied to both the component and assembly stiffness matrices, the resulting assembly forces are correctly converted into spring back deviations, as shown in Fig. 8.9. The diagonal model appears to be more stable compared to the full model: even with only two significant digits in the stiffness matrices, the spring back is comparable to that obtained with the full model.

Therefore, to avoid numerical instability, only the diagonal elements of the stiffness matrices are used in the model for case study 3.

The different configurations tested for case study 3 can be seen in Tab. 8.4.

Tab. 8.4: Configuration tested for case study 3.

Test case	$\{\delta_i\}_1$	$\{\delta_i\}_2$	$\{\delta_i\}_3$	$\{\delta_i\}_4$	$\{\delta_i\}_5$	$\{\delta_i\}_6$	$\{\delta_i\}_7$	$\{\delta_i\}_8$	$\{\delta_i\}_9$	$\{\delta_i\}_{10}$	$\{\delta_i\}_{11}$	$\{\delta_i\}_{12}$	
	[mm]	[mm]	[mm]	[mm]	[mm]	[mm]	[mm]	[mm]	[mm]	[mm]	[mm]	[mm]	
3.1	$\{\delta_1\}$	0.500	0.500	0.500	0.500	0.500	0.500	0.500	0.500	0.500	0.500	0.500	
	$\{\delta_2\}$	1.000	1.000	1.000	1.000	1.000	1.000	1.000	1.000	1.000	1.000	1.000	
3.2	$\{\delta_1\}$	0.000	0.000	0.000	0.000	0.000	0.000	0.000	0.000	0.000	0.000	0.000	
	$\{\delta_2\}$	1.582	1.502	0.702	-0.112	-1.179	-1.094	-0.716	-0.982	-0.702	-0.408	0.313	1.094
3.3	$\{\delta_1\}$	1.582	1.502	0.702	-0.112	-1.179	-1.094	-0.716	-0.982	-0.702	-0.408	0.313	1.094
	$\{\delta_2\}$	-1.582	-1.502	-0.702	0.112	1.179	1.094	0.716	0.982	0.702	0.408	-0.313	-1.094
3.4	$\{\delta_1\}$	-1.708	-1.250	-0.848	0.636	0.560	1.010	1.189	0.374	0.848	0.230	-0.040	-1.010
	$\{\delta_2\}$	-1.716	0.547	-0.148	-0.057	-0.833	1.010	2.582	1.066	0.148	-0.463	-0.033	-1.010

Test case 3.1 is proposed to check whether the model can correctly handle rigid translations. The expected result is a null spring back since no deformation is applied to the assembly feature during the joining operation.

Test case 3.2 checks whether the simulated spring back is physically sound. Part 1 is considered nominal, while part 2 has a simulated deviation with a zero average value. It is expected that the spring back will be in the same direction as the free state deviation of part 2 but with a lower value.

Test case 3.3 proposes mirrored free-state deviations between the two parts. Since part 1 (base) is stiffer than part 2 (top), it is expected to have a small spring back towards the free state deviation of part 1.

Finally, test case 3.4 presents random free state deviations, making it difficult to predict any particular spring back result.

Case study 4

Case study 4 is designed to validate the model against actual data. The same geometry presented in case study 3 was additively manufactured using a formlabs® Form 3™ apparatus and the formlabs® Tough 1500 resin, see Fig. 8.10.a),b),c), and d).

The geometry of the parts was manually distorted to obtain significant deviations from the nominal shape. The base and top parts were 3D scanned using a 3D structured light scanner (Aurum3D), and the data were processed in GOM Inspect to extract the twelve free state deviations at the assembly features.

The two parts were then glued together using epoxy adhesive, ensuring that they remained flat during the gluing process using a custom fixture. The assembled structure (Fig. 8.10.e) and f)) was measured using the same procedure as the individual free-state parts.

The free state deviations obtained from the 3D scanning were used as input for the model, following the approach explained in case study 3. The results obtained from the model were compared with the actual values measured in the assembly to assess the accuracy of the model.

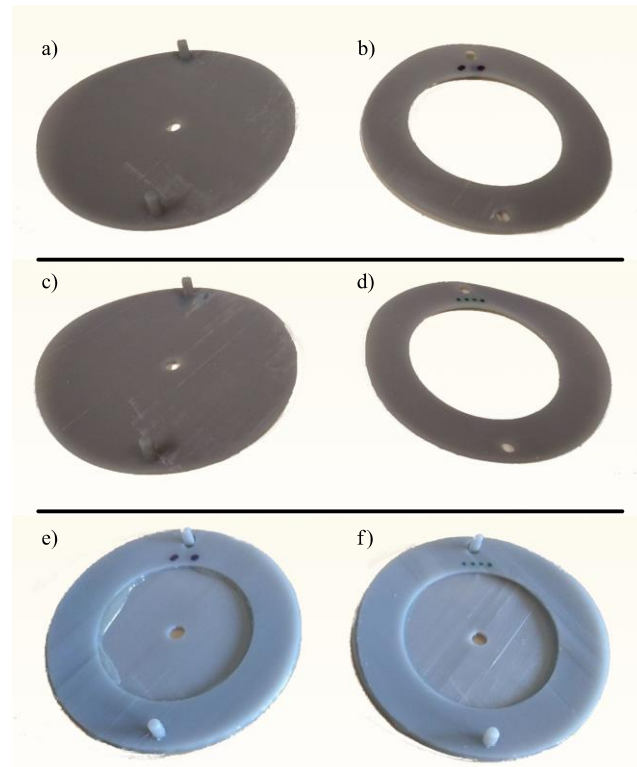


Fig. 8.10: Actual geometries used for case study 4.

8.2 || Results

8.2.1 Results case study 1

Matrices computation

For the presented case study, the matrices collapse into numerical values. The analytical formulation for each of them is described below.

$$[A_1] = \frac{k_{21}}{k_{11} + k_{21}} \quad (8-7)$$

$$[K_1] = \frac{k_{11} \cdot k_{21}}{k_{11} + k_{21}} \quad (8-8)$$

$$[A_2] = \frac{k_{12}}{k_{12} + k_{22}} \quad (8-9)$$

$$[K_2] = \frac{k_{12} \cdot k_{22}}{k_{12} + k_{22}} \quad (8-10)$$

$$[K_{asm}] = \frac{(k_{11} + k_{21})(k_{12} \cdot k_{22}) + (k_{12} + k_{22})(k_{11} \cdot k_{21})}{(k_{11} + k_{21})(k_{12} + k_{22})} \quad (8-11)$$

In a non-simplified case, these matrices would need to be determined using FEM simulation. Therefore, there is no analytical solution available for any additional sensitivity matrix that needs to be studied.

Assembly feature deviation

In this simple case, all the sensitivity matrices can be defined analytically. Equation (8-1) can then be written as follows.

$$\begin{aligned} \{\delta_n\} = & \frac{(k_{11} \cdot k_{21})(k_{12} + k_{22})}{(k_{11} + k_{21})(k_{12} \cdot k_{21}) + (k_{12} + k_{22})(k_{11} \cdot k_{21})} \{\delta_1\} \\ & + \frac{(k_{12} \cdot k_{22})(k_{11} + k_{21})}{(k_{11} + k_{21})(k_{12} \cdot k_{21}) + (k_{12} + k_{22})(k_{11} \cdot k_{21})} \{\delta_2\} \end{aligned} \quad (8-12)$$

Deviation of other functional elements

The compact equation derived to directly evaluate the deviation of the other functional elements, equations (8-5)-(8-6), can be expressed as follows.

$$\begin{aligned} \{\delta_m\}_{TOT} = & \{\delta_m\}_{FREE} \\ & + \frac{k_{21}}{(k_{11} + k_{21})} \left[\frac{(k_{11} \cdot k_{21})(k_{12} + k_{22})}{(k_{11} + k_{21})(k_{12} \cdot k_{21}) + (k_{12} + k_{22})(k_{11} \cdot k_{21})} - 1 \right] \{\delta_1\} \\ & + \left[\frac{(k_{21} \cdot k_{12} \cdot k_{22})}{(k_{11} + k_{21})(k_{12} \cdot k_{21}) + (k_{12} + k_{22})(k_{11} \cdot k_{21})} \right] \{\delta_2\} \end{aligned} \quad (8-13)$$

$$\begin{aligned} \{\delta_p\}_{TOT} = \{\delta_p\}_{FREE} + & \left[\frac{(k_{11} \cdot k_{21} \cdot k_{12})}{(k_{11} + k_{21})(k_{12} \cdot k_{21}) + (k_{12} + k_{22})(k_{11} \cdot k_{21})} \right] \{\delta_1\} \\ & + \frac{k_{12}}{(k_{12} + k_{22})} \left[\frac{(k_{12} \cdot k_{22})(k_{11} + k_{21})}{(k_{11} + k_{21})(k_{12} \cdot k_{21}) + (k_{12} + k_{22})(k_{11} \cdot k_{21})} - 1 \right] \{\delta_2\} \end{aligned} \quad (8-14)$$

Test Case results

The results obtained using the described methodology for the test cases described in Tab. 8.1 can be seen in Tab. 8.5.

Tab. 8.5: Simulation results.

Test case	Simulation results		
	$\{\delta_n\} [mm]$	$\{\delta_m\}_{TOT} [mm]$	$\{\delta_p\}_{TOT} [mm]$
1.1	0.000*	-4.444	0.000*
1.2	6.667	-1.481	2.963
1.3	8.333	-0.741	1.481
1.4	5.000	-2.222	4.444
1.5	2.500**	5.000	-3.000
1.6	10.000	5.000	4.500**

* Actual values below 10^{-5} .

** Result non-conformal to the expected ones.

The results obtained from the first six tests (Tab. 8.5) are in line with the expected results (as presented in Tab. 8.2), except for the spring-back of test 1.5 and the deviation of the second component of test 1.6. These two discrepancies are legitimate because it is not possible to impose a stiffness value of zero and, therefore, the result diverges.

The results for test case 1.7 are summarized in Fig. 8.11. It can be highlighted that the spring-back due to the deviation of part one decreases linearly with the influence that the very same part has on the assembly stiffness.

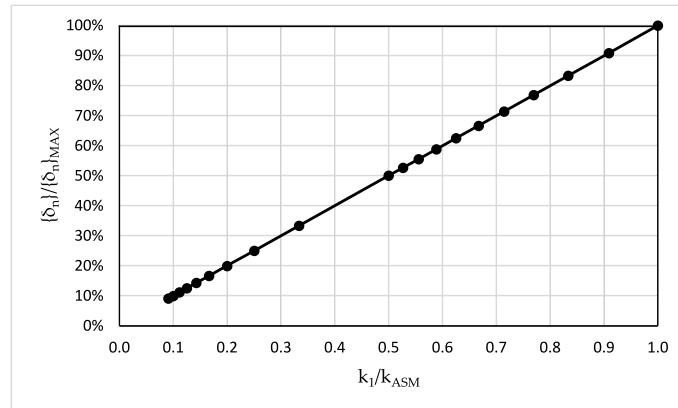


Fig. 8.11: Result for test case 7.

8.2.2 Results case study 2

The assumption of rigid behaviour for the output feature is verified: stresses in all spring elements are 0.0 N.

The comparison between the reduced model (sensitivity matrix) and the full FEM model can be seen in Tab. 8.6 for all configurations of test case 2.

8.2.3 Results case study 3

The results of the three test cases relevant to case study 3 can be seen in Fig. 8.12. At first glance, it is possible to see that the expected results previously summarized are met, although, especially for test case 3.3, it is difficult to see the elastic spring back. In Tab. 8.7 the numerical values for the spring back can be seen.

Tab. 8.6: Case study 2, reduced model results compared to full FEM model results.

Test case	T_x			T_y			R_x			R_y		
	Sensitivity matrix	Full FEM	Δ	Sensitivity matrix	Full FEM	Δ	Sensitivity matrix	Full FEM	Δ	Sensitivity matrix	Full FEM	Δ
	[mm]	[mm]	[mm]	[mm]	[mm]	[mm]	[deg]	[deg]	[deg]	[deg]	[deg]	[deg]
2.1	-0.399	-0.399	3.3E-8	-1.178	-1.178	2.1E-7	2.476	2.474	-1.4E-3	-1.069	-1.069	7.8E-5
2.2	-0.444	-0.444	1.7E-8	-1.131	-1.131	4.2E-8	2.623	2.621	1.7E-3	-1.000	-1.000	6.0E-5
2.3	0.319	0.139	-1.5E-8	1.259	1.259	8.1E-8	-2.598	-2.596	1.7E-3	0.649	0.649	6.0E-6
2.4	0.347	0.347	-6.8E-8	1.359	1.359	5.3E-8	-2.587	-2.586	1.6E-3	0.637	0.637	8.2E-6
2.5	0.128	0.128	3.1E-8	1.591	1.591	-9.6E-8	-3.942	-3.936	6.0E-3	-0.593	-0.593	1.4E-5

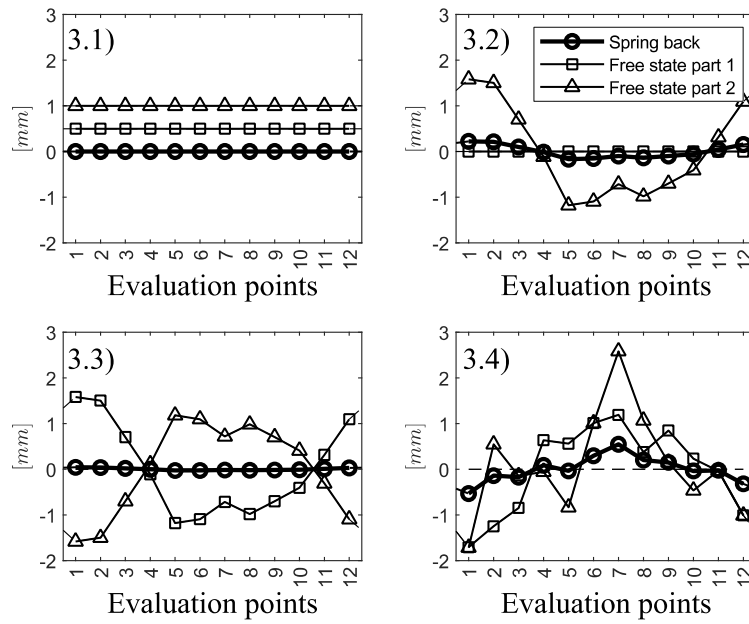


Fig. 8.12: Result for case study 3.

Tab. 8.7: Configuration tested for case study 3.

Test case	$\{\delta_n\}_1$	$\{\delta_n\}_2$	$\{\delta_n\}_3$	$\{\delta_n\}_4$	$\{\delta_n\}_5$	$\{\delta_n\}_6$	$\{\delta_n\}_7$	$\{\delta_n\}_8$	$\{\delta_n\}_9$	$\{\delta_n\}_{10}$	$\{\delta_n\}_{11}$	$\{\delta_n\}_{12}$
	[mm]	[mm]	[mm]	[mm]	[mm]	[mm]	[mm]	[mm]	[mm]	[mm]	[mm]	[mm]
3.1	0.000	0.000	0.000	0.000	0.000	0.000	0.000	0.000	0.000	0.000	0.000	0.000
3.2	0.221	0.212	0.098	-0.016	-0.167	-0.153	-0.100	-0.139	-0.098	-0.057	0.044	0.153
3.3	0.041	0.036	0.018	-0.003	-0.028	-0.028	-0.018	-0.024	-0.018	-0.011	0.008	0.028
3.4	-0.534	-0.142	-0.173	0.085	-0.038	0.295	0.544	0.200	0.148	-0.039	-0.024	-0.320

8.2.4 Results case study 4

The results of the comparison between the proposed framework and the actual values measured in the two samples are summarized in Fig. 8.13. It can be noted that in both cases, the differences are in the range of $\pm 0.2 \text{ mm}$, even if the scale of the deviations is different.

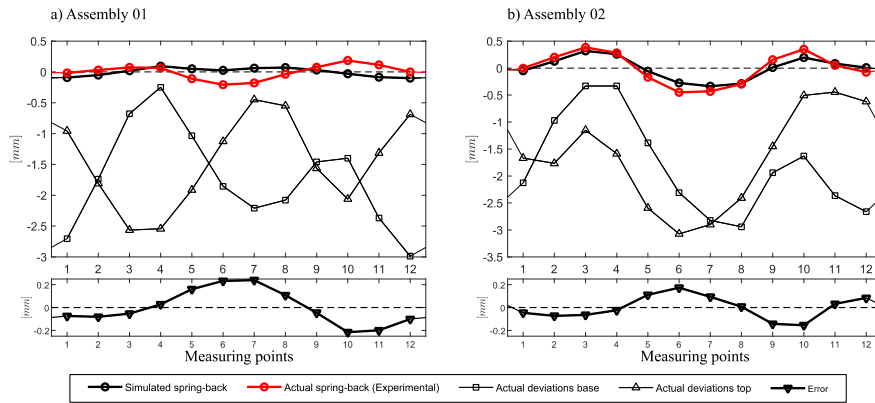


Fig. 8.13: Comparison between the result obtained with the proposed framework and the actual values measure in the assembly.

8.3 || Considerations on the model

8.3.1 Limits of application

The test cases from 1.1 to 1.6 were used to check if the proposed model can react accordingly to what is physically sound.

Test case 1.1 considers that the second element had the nominal geometry while being infinitely rigid. The only deviation was on the assembly feature of the first component. Unfortunately, since infinite rigidity cannot be imposed, a value of 10^9N/mm (i.e., 10^8 times the first component rigidity) was used instead. Even with this approximation, the result is compliant with the theoretical result: there is no spring-back at the assembly feature, the second component is undeformed, and the first component output degree deviation is opposite to the free state deviation of the assembly feature, coherently with the assembly procedure.

Test case 1.2 introduced finite rigidity to the second component. Therefore, a spring-back, in agreement with the free state deviation of the assembly feature of the first component, was expected and observed through simulation. The deviation of the first part's output decreases compared to the previous case where its deviation, starting from the nominal position, was due to the fixturing only. Due to the spring-back, it now leans back to its nominal position. This time, the second component's output also shows a deviation in the same direction as the spring-back.

In test case 1.3, starting from the previous one, a deviation in the assembly feature (i.e., input) of the second component is introduced in the same direction as the deviation on the first component. In this configuration, both parts contribute to the spring-back, and thus, they can be considered as two distinct contributions. Each contribution points in the same direction as the free

state deviation. Therefore, a greater spring-back value is expected compared to the previous case. The model provides a result that aligns with the theoretical assumption. In this case, the deviation of the output degrees of freedom is disregarded.

Test case 1.4 assumes an opposite deviation to the second part's assembly feature. This time, the spring-back should be lower than in test case 2 since the deviations of the two parts compensate for each other. The output degree of freedom on the first part should have a greater absolute value compared to the second test case. Both results given by the model are consistent.

In test case 1.5, a deviation is introduced in all functional features, and the stiffnesses k_{21} and k_{12} , which link the assembly features to the output degrees of freedom, have null rigidity. Therefore, during assembly, no force is needed, and consequently, no further deviation should be observed in the output degrees of freedom, and no spring-back should occur. In this case, the model results align with the theoretical assumption for the output degree of freedom, but a non-null spring-back is predicted. However, this inconsistency can be explained. The model does not allow for a stiffness value of zero, so a value of 10^{-9}N/mm was used instead. Even though this value is very small, the assembly force is different from zero. At the same time, the assembly stiffness has the same order of magnitude as the near-zero imposed stiffness. Therefore, even a small assembly force results in a non-null spring-back.

Test case 1.6 uses null stiffness for the second part. Therefore, the second part should not exchange forces with the first one, resulting in a complete spring-back: deviation in part one and no deviation in the output degree of freedom of part two. The model correctly simulates the deviation in part one, but the deviation due to the spring-back in the second part is not null. The discrepancy can be explained by the same effect seen in the previous case: the inability to set null stiffnesses leads to divergent results.

In addition to the one-dimensional case study, the model was tested with FEM simulation in case study 3. The expected results for the proposed case were achieved, showing no unexpected behaviors. The case study was designed to be far from the problematic cases shown in the one-dimensional case study.

Considering all the evidence, it can be stated that the proposed model is generally able to correctly interpret the theoretical behavior. The cases in which it fails are due to the inability to correctly set the required stiffness for the specific case. Nevertheless, a null stiffness is not realistic in an actual application. However, special attention is required in defining the model in cases where the stiffness ratio between the two parts is high.

8.3.2 Assembly with more than two parts

The result of test case 1.7 demonstrates a linear correlation between the spring-back resulting from the deviation of the first component and the influence of the part on the assembly stiffness. In other words, the stiffer the component, the greater the spring-back. In the example, a

two-component assembly was considered. By applying the superimposition of effects to an assembly with more than two parts, the overall spring-back will be the sum of each individual contribution. As the number of parts in the assembly increases, each part will contribute less to the assembly stiffness. This means that the overall spring-back will be the sum of different terms that will be significantly lower compared to the free state deformation. Each contribution to the spring-back is likely to be randomly directed in space, thereby compensating for each other. Therefore, in an assembly where the mean free state deviations of the mating features are randomly distributed, a small spring-back is expected in comparison to the free state deviation.

8.3.3 The advantages of a hybrid approach

This methodology can be considered a hybrid approach, hereinafter referred to as the restricted skin model. Some features are discretized as skin models, considering their form deviations, while others are treated as rigid features, considering only their derived elements and/or associated degrees of freedom. The result is a lighter model with a lower number of degrees of freedom compared to traditional skin model approaches, which typically involve a higher number of degrees of freedom. In cases where a “full” skin model approach is used, creating a linearized model that links all possible sources of variation may not be practically feasible. In industrial applications, where form error is not functionally relevant, the proposed method allows for the neglect of form deviations in the linearized model. Additionally, the model can be more accurate than non-skin model approaches where a contact model cannot be utilized.

The use of a linearized model requires performing FEM simulations at the beginning to create the model (i.e., $3n$ simulations). Subsequently, all combinations can be simulated in real-time by solving the three equations (equations (8-1)-(8-5)-(8-6)). The simulation process (FEM) can also be optimized using the super-element method [142]. The model is completely independent of the actual mean deviations, allowing for quick reuse of the model during production to adjust manufacturing specification limits in the event of process drifting. It can also be used to set dedicated limits for different production lines or plants with minimal additional effort.

Case study 2 was designed to verify whether the sensitivity matrix applied to the restricted skin model can accurately estimate the deviations of the output degrees of freedom compared to the full FEM simulation. From the results presented in Tab. 8.6, it can be observed that the difference between the reduced model and the full FEM model is negligible. Therefore, it can be concluded that the proposed hybrid approach effectively estimates the results of a full model with reduced computational effort.

8.3.4 Experimental validation

Case study 4 allows for experimental validation of the proposed model. Two assemblies were considered and deterministically evaluated. In the first assembly, the deviations of the two mating surfaces were almost opposite in direction, resulting in a mitigation of the effects. As expected, the simulated spring-back is small compared to the simulated spring-back of the second assembly, where the free state deviations were almost in the same direction. In this second case, there is no mitigation. The reduced spring-back, compared to the free state deviations, is due to the assembly stiffness, which increases super-linearly, while the spring-back force is given by a linear sum of the fixturing forces.

The difference between the simulated spring-back and the actual values falls within the range of $\pm 0.2 \text{ mm}$, even though the spring-back of the first assembly is much smaller than that of the second assembly. The result is that, for the second assembly, there is a better fit between the simulated and actual values due to the scale. Since the error is similar in both cases, it can be interpreted as an effect of the non-uniform glue layer thickness, which adds a level of uncertainty. Considering the uncertainty caused by the glue layer and the measuring process, the methodology is considered experimentally validated.

8.4 || A possible application

The inspiration for developing this model comes from the experience gained while working with Electrolux on the geometric specification development for a washing machine tub. In this case, the tub is composed of two polymer flanges that are deformed and friction welded together, while the bearing seats and shoulders remain undeformed. This case falls within the scope of the proposed methodology.

To demonstrate a possible industrial application, a plastic tank that presents similar problems and issues as those analyzed together with the industrial partner is considered. Some preliminary evaluations for the industrial case study, using a simpler model that neglects elastic spring-back, were published in the literature by the Design Tools and Methods in Industrial Engineering Laboratory and can be referred to as [136].

The assembly consists of two non-rigid parts: a main body and a top part. Once assembled with plastic rivets, the tank needs to be installed in place, and the top opening needs to be located in a specific position. A possible functional specification for the assembly, consistent with the aforementioned description, can be seen in Fig. 8.14.

The tank top is further considered for analysis. A possible functional and manufacturing specification for the part is proposed in Fig. 8.15. As it is a non-rigid part, the ISO 10579 standard is referenced, and all call-outs addressing functionality refer to the “as assembled” state, while all call-outs addressing manufacturing refer to the free state condition or “as produced” state.

In this case, both the functional and manufacturing specifications are represented in the same drawing. However, it is possible that the datum system is not the same for both cases, thus requiring separate documents, or the use of layers in a digital medium (e.g., MBD Models).

The proposed methodology aims to correlate corresponding values between the functional specification and the manufacturing specification (e.g., t_7 and t_{15}). If a feature property is not influenced by deformation, such as the diameter of a hole that doesn't change significantly, a direct link can be established, and therefore the same tolerance value should be found in both specifications (e.g., t_{10} and t_{18} might be the same). However, the location of the same hole may experience significant drift during assembly. In this case, its free state location tolerances must be carefully correlated to the as-assembled state. Since only its location is of interest, the feature may be considered as a rigid feature and described by just four parameters, as depicted in Fig. 8.2.

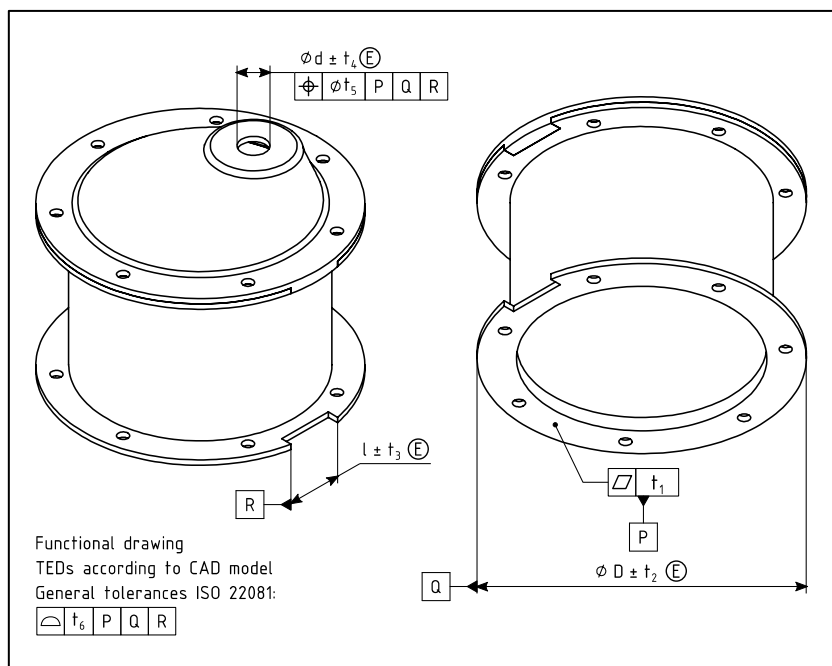


Fig. 8.14: Functional specification for the tank assembly.

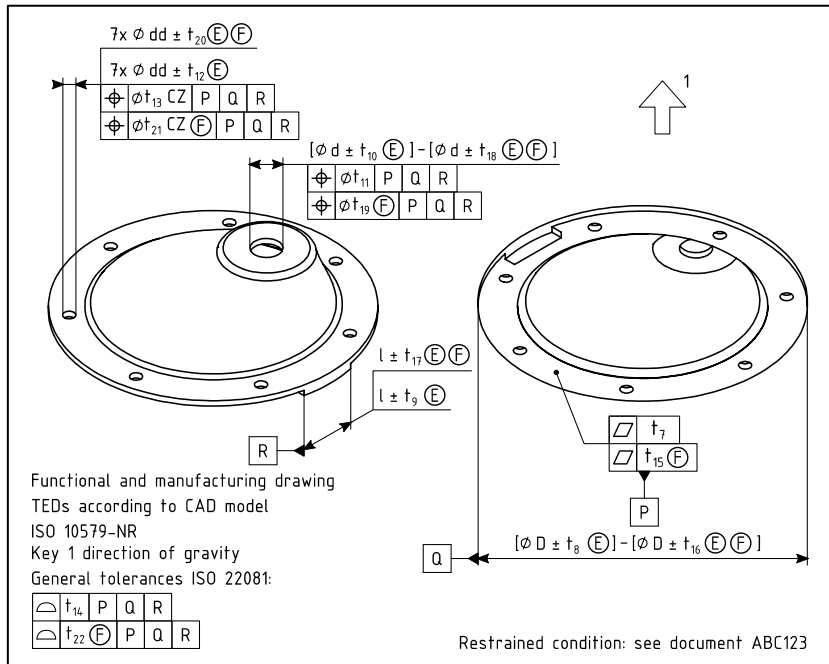


Fig. 8.15: Functional and manufacturing specifications for the tank top.

A link between this example and the mono-dimensional test case presented in section 3 can be highlighted. First, the tank top can be considered as “Part 1,” and the tank body as “Part 2.” The input degree of freedom of Part 1 can be linked to the primary datum of the tank top, while the output degrees of freedom can be linked to a rigid feature deviation of the top opening. Similarly, the input degree of freedom of Part 2 can be linked to the assembly surface of the tank body, and the output degree of freedom can be linked to the deviation of the primary datum in the assembly.

9 || Definition of Verification specification within the ISO GPS system⁶

The man of science has learned to believe in justification, not by faith, but by verification.

Thomas Huxley

The duality principle, described within the ISO Geometrical Product Specification (GPS) standards [76], presents a perspective where the verification conceptually mirrors the specification. While this is a valuable model, further refinement is required to accommodate the different aims of inspection as the manufacturing process evolves. If one were to infer that the duality principle ideally implies a one-to-one correspondence between specification and verification, then the creation of the *geometric functional specification* and *geometric manufacturing specification* would imply only two unique verifications exist. However, inspections are performed with different aims for both functional and manufacturing purposes during the product development cycle, and a means of differentiating verification strategies is needed.

This observation underscores the need for geometric inspection-oriented information that may be captured unambiguously. The work reported here aims to elaborate on the definition of a *geometric verification specification* exploring its usage in the product development lifecycle for the reasons explained in the following section.

9.1.1 Geometric verification specification

ISO/TS 21619 [37] defines the *verification specification* as a “document stating verification-process-related requirements” that is derived from, and dependent on, higher-level specifications (i.e., functional and manufacturing specifications) through a process of transformation. This technical specification does not suggest how this transformation takes place or how the resulting documents are used.

⁶ The context of this chapter is mainly derived from a paper already published by the author [166].

There is limited literature providing insights regarding “verification specifications” in the domain of mechanical assemblies and parts. It is worth noting the statement by Woo that carefully created verification specifications allow for avoiding divergence from the designated procedure and/or aim over time [61].

NASA's System Engineering Handbook points out a list of 18 items that are conveyed in the verification procedure and 11 items that shall be present in the verification report [62]. Even though this work is not related to mechanical assemblies it is worth noting that items in the verification procedure (e.g., calibrations intervals, data recording procedures, measuring equipment, single operations sequence, etc.) contribute to an understanding of the overall verification procedure uncertainty.

The hierarchy of specifications requires that the *geometric verification specification* be subordinate to the *geometric functional and/or manufacturing specifications*. One important part of the *geometric verification specification* is the management of verification uncertainty. If any qualified operator performs the inspection by strictly adhering to this specification, the estimated (budgeted) measurement uncertainty should be met and comparable measurement results across multiple instruments and facilities should be achieved.

The *geometric verification specification* is not intended to be a static document throughout the development cycle. The main reasons for the evolution of the specification are the increasing knowledge of the manufacturing process and the changes in resource availability.

In the following section different geometric verification purposes will be analyzed, highlighting the specificities that lead to different versions of a *geometric verification specification*. Next, the specific information needed in a verification specification will be presented and discussed. Finally, a case study will be presented.

9.2 || Verification purpose

The metrological inspection of mechanical parts has two main objectives: the determination of conformity to a GPS specification and the support of the manufacturing process. These two objectives can be further subdivided based on the character of the information needed from the inspection. For instance, a geometric functional inspection can be performed for supplier qualification, inbound batch approval, selective assembly, etc. while a geometric manufacturing inspection could be used for process tuning, statistical process control (SPC), in-line checks, etc. These applications are briefly discussed in the following subsections.

9.2.1 Supplier qualification

Supplier qualification provides confidence that a supplier can provide a functional part. The customer's interest is in the functionality and should not be interested in the manufacturing process, leading to a functionally based inspection. Usually, 30 to 50 parts are considered and all of the tolerances in the geometric functional specification are checked. Since this type of inspection is performed at the beginning of production for a limited number of parts, there is almost no time constraint. Consequently, this type of check is the closest to the direct application of the duality principle to the *geometric functional specification*. Nonetheless, valuable information can be added to drive the verification procedure, as discussed in section 9.3.

9.2.2 Inbound batch approval

A customer may be interested in checking whether subsequent incoming batches are within geometrical functional limits even if the supplier was qualified. The batch approval may be held to a specific timeframe set by the warehouse schedule. For this reason, the speed of the inspection is essential and a trade-off among different possibilities is necessary. For instance, a small sample may be fully checked according to the geometric functional specification; a larger sample may be checked only for pre-defined Critical to Quality (CTQ) tolerances or by using functional gauges (go/no-go test).

9.2.3 Selective assembly

Selective assembly is a strategy used when the manufacturing process is not capable of producing parts that guarantee interchangeable assembly [143]. Inspection can be used to cluster the parts in different groups based on a critical assembly characteristic; each class can then be paired with a specific class of the mating part ensuring interchangeability within the paired classes. Since functionality is addressed in this case, it is certainly a geometric functional inspection, albeit different from the previously described ones. Traceability between the measurement and the actual feature (measurand) is needed: agreed-upon binning or marking needs to be prescribed to track the parts.

9.2.4 Manufacturing/assembly process tuning

Manufacturing processes initially need to be calibrated to find appropriate process parameters to achieve the expected geometric quality. Simulation is a viable tool to define the preliminary process parameters, but the ground truth can be seen only in the produced parts. Consequently, parts need to be inspected based on the *geometric manufacturing specification* assessing the actual performance of the process. The measurands associated with this type of geometric inspection need to be consistent with the quantity controlled by the manufacturing process. If the location of a cylindrical Feature of Size (FoS) is only reported by the minimum tolerance zone containing the non-ideal feature [38,141], then any directional information allowing for process tuning is missing. Therefore, the directional quantities to be extracted from the location tolerance need to be defined, paying particular attention to the coordinate reference system to avoid ambiguity regarding the direction of the deviations.

9.2.5 Statistical process control

The aim of SPC is to evaluate whether the manufacturing process remains stable with only chance deviations. Depending on the details of the manufacturing process, a certain level of covariance among similar “critical to quality” tolerances can be expected during production. In this case, verifying all the dimensions gives redundant information. A subset of the tolerances can be chosen for SPC, reducing inspection time. Knowledge of the manufacturing process is used to refine the specification so that key performance tolerances can be defined and/or updated. As with process tuning, directionality can play an important role in the inspection and the same considerations from the previous section apply.

Work by Zang and Lu [144] reported on standardization in China of quality-oriented statistical tolerancing where tolerances are assigned to a population of parts. There have been efforts in this field [145] for the life of the ISO GPS system, but the results in both standards and practice are still difficult to generalize.

9.2.6 In-line checks

In-line checks are essential for safety-critical applications and/or when the economic risk of allowing nonfunctional parts in the production line is high; therefore, 100% of the production is inspected. The check is performed at either of two points: the exit of a manufacturing step (manufacturing inspection) or entering the assembly line (functional inspection). In both cases, the time needed to perform the inspection is critical and results must be obtained at the pace of the production line. Careful attention is needed in the definition of the inspected quantities, allowing

reproducible inspection across different production sites. Previous research developed a methodology to assess the economic impact of metrology in manufacturing, giving a tool to identify economically sound inspections [146].

9.3 || Contents of the verification specification

To drive the different geometric verification procedures, the *geometric verification specification* needs a sufficient set of information to support the corresponding “parent” specifications and to decrease the ambiguity in the inspection procedure.

Before initiating the inspection process, the first task is the identification of each specification (i.e., ballooning) which assigns an ID to each tolerance. Different personnel may follow different strategies to assign the IDs, so it is preferable that a unique identifier be assigned at the specification stage. This could be achieved on the drawing with a number between angle brackets (i.e., <#>); members of ISO TC213 are discussing the possibility of standardizing this technique. Patterns of features may have a single call-out assigning the same tolerance to each feature; these must be identified as separate tolerances for each feature for analysis and reporting.

The next step in inspection planning is the association of each tolerance to the proper metrological equipment. To ensure that measurements made in different plants can be directly compared, the same measurands should have comparable expanded uncertainties. An uncertainty requirement shall be added (based on the case) containing a: statement of the target uncertainty (U_T) as described in ISO 14253-2 [147], requirement that each quantity shall be reported with its expanded uncertainty or conformity will be determined using a specified decision rule and/or acceptable risk for each tolerance [148,149].

As there is no direct translation from a datum reference frame to a cartesian coordinate system, the explicit indication of the coordinate system allows the identification of the correct information for process tuning, and avoids misinterpretations.

During the actual inspection many contributors to uncertainty are present, some of which can be managed through a dedicated geometric specification. ISO 14253-2:2011 reviews and describes ten categories of uncertainty: *environment*, *reference element of measurement equipment*, *measurement equipment*, *measurement setup*, *software and calculations*, *metrologist*, *measuring object*, *the definition of the characteristic*, *measuring procedure*, and *physical constant* [147]. Some of these are addressed below, with commentary regarding the management of their impact using the *geometric verification specification*.

For dimensional inspection, the thermal *environment* is the most significant contributor (20 °C per ISO 1:2016) although other environmental variables such as humidity, illumination, thermal equilibrium, and time/spatial gradients of variables are also important. In particular, in-line inspections may need a statement of environmental conditions.

Software and calculation are often anathema to standard practice. Modern metrology software has such a vast array of options that collecting all the settings that can be applied during measurement may be impossible. Two of the most important parameters are the choice of filters and association criteria. These have a strong impact on the geometric inferences drawn from raw measurement points and should be specified based on the manufacturing process, inspection equipment, and intended output of the geometric verification. The designer may have limited information about manufacturing and inspection but should be consulted to ensure that the functional requirements are adequately captured by these choices.

The selection and use of *measuring equipment* are intentionally omitted from geometric product specifications, separating verification from the specified geometry. While traceability is required for most industrial measurements, the means of attaining it is not.

The specifics regarding *measuring set-up* (i.e., how the measuring equipment is used) cannot be completely captured geometrically. Nonetheless, it may be useful to suggest a measuring set-up (possibly in a separate document) to allow a different plant with similar equipment to mirror the set-up or for an experienced metrologist to adapt the set-up to a different piece of equipment.

The importance of the *measurement object* (i.e., how the measuring equipment and set-up interact with the object) is reflected in two ways. Firstly, the workpiece has geometric deviations (based on the manufacturing process) that will interact with choices made about measurement, and secondly, the workpiece is not perfectly rigid – despite the implied assumption of rigidity in the functional specification. For instance, it may be useful to state the direction of gravity in the verification specification and the part placement in the measuring system.

A relevant contributor to the measurement uncertainty is the *measuring procedure*; the same equipment used in the same environmental conditions can produce very different measured values if different procedures are followed. A comprehensive description of the measuring procedure will include points already discussed in this list. In addition, other requirements such as the order or measurements and the number of sampled points can appear in a separate document.

Finally, the *metrologist* themselves contributes to the overall uncertainty, often when making choices regarding the items discussed above. The metrologist remains the free variable in the whole idea of the geometric verification specification.

9.4 || Case study

To show the applicability and the usefulness of a dedicated *geometric verification specification* the concepts explained above have been implemented in a case study. The example consists of a simple spacer with eight through-holes. From a functional point of view, the spacer needs to establish a distance between two mating parts and eight pins need to pass through without interference. A geometric functional specification, consistent with this functional description, is presented in Fig. 9.1. The median plane of the mating surfaces is the primary datum, and the pattern

becomes the secondary datum, therefore defining a symmetric datum system in accordance with the four possible mounting positions. This type of drawing allows for describing the pure functionality in the cleanest way possible; no unnecessary tolerances and indications are added.

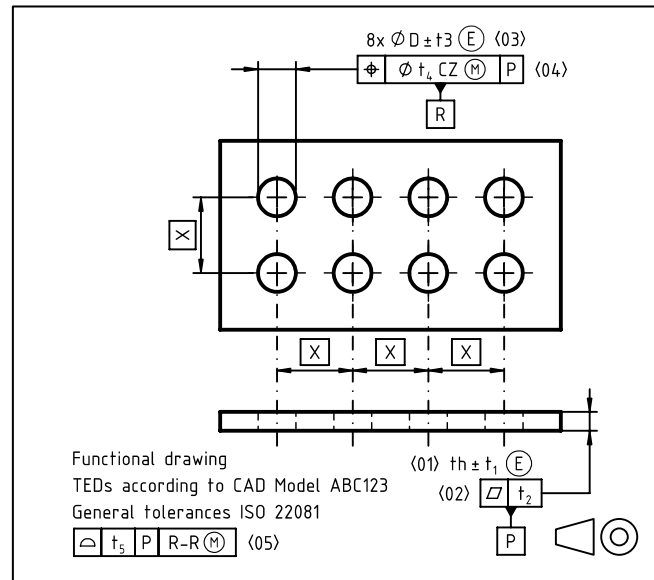


Fig. 9.1: Geometric functional specification for the case study.

Let us assume that the most severe assembly risk is caused by errors in the pattern of through holes. Misalignment of the pins through the holes must be avoided to prevent damaging the mating parts during assembly. The thickness check is less critical since the spacer can be replaced without damage if its thickness is out of specification. Based on these assumptions about criticality, each spacer will be subjected to an in-line check entering the assembly process; a geometric verification specification for this check is now created. As the hole pattern is primarily two-dimensional, the inspection is performed with an optical system: the part is positioned on the measuring platform and the holes are sampled through image recognition. The pattern is then compared to the virtual condition to ensure assembleability.

Fig. 9.2 shows a possible verification geometric specification for this purpose; the primary datum is assigned to the bottom surface and the pattern is checked in dimension and position. The primary datum is not checked directly, but reflects the placement of the part on the measuring device. Given the measuring principle, the 2D holes sampling already integrates 3D deviation effects to the virtual condition.

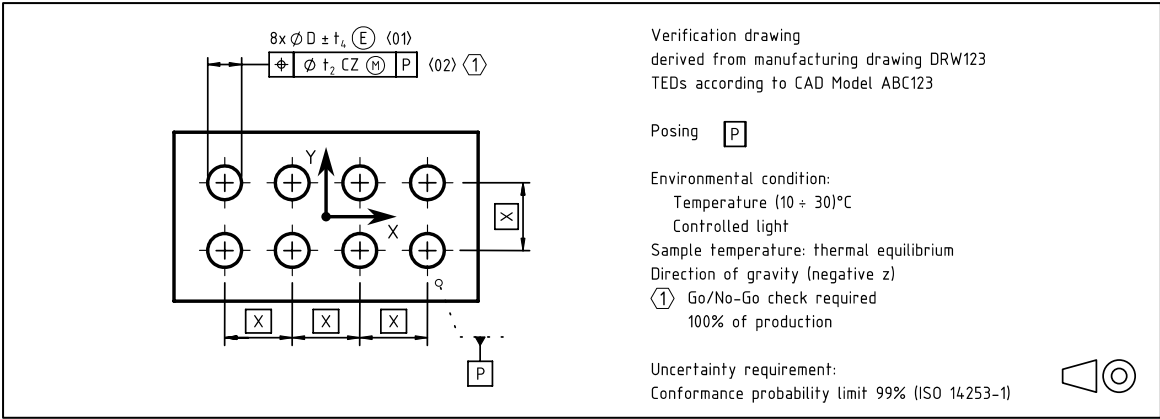


Fig. 9.2: Geometric verification specification dedicated to in-line functional check.

Other data included in this verification specification are: parent functional specification, part posing, environmental conditions, part temperature range, type of assessment (go/no-go check), and a decision rule statement. Since it is an optical inspection, the requirement of constant light conditions is added. Being an inline check, the ambient temperature cannot be controlled precisely, the limits are established to comply with the uncertainty statement. If the check needs to be reproduced in a second plant and/or the equipment needs to be updated, this type of specification clarifies exactly the requirements that need to be respected.

Moving upstream to the manufacturing process, we assume the part is produced by a CNC milling machine. A possible geometric manufacturing specification is shown in Fig. 9.3. Here the datum system reflects the fixturing in the milling machine, removing the symmetry of the specification. Care must be used when changing the location of a pattern form a self-defined reference system to an external one [150].

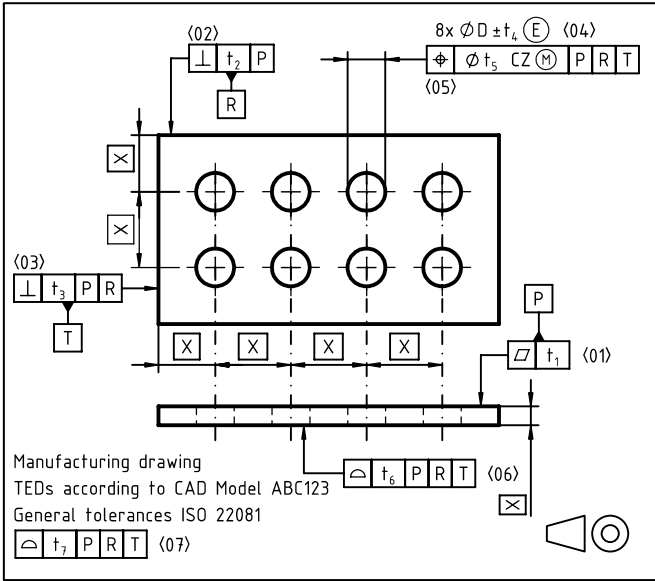


Fig. 9.3: Geometric manufacturing specification for the case study.

The manufacturing drawing targets the production process, which guides the geometric verification specification in a way that can provide tuning and feedback to this process; the result can be seen in Fig. 9.4. As it is assumed that the geometry is produced by a combination of milling and drilling, the quantities more likely to exhibit errors are the hole positions in the plane; the orientation errors are likely to be negligible.

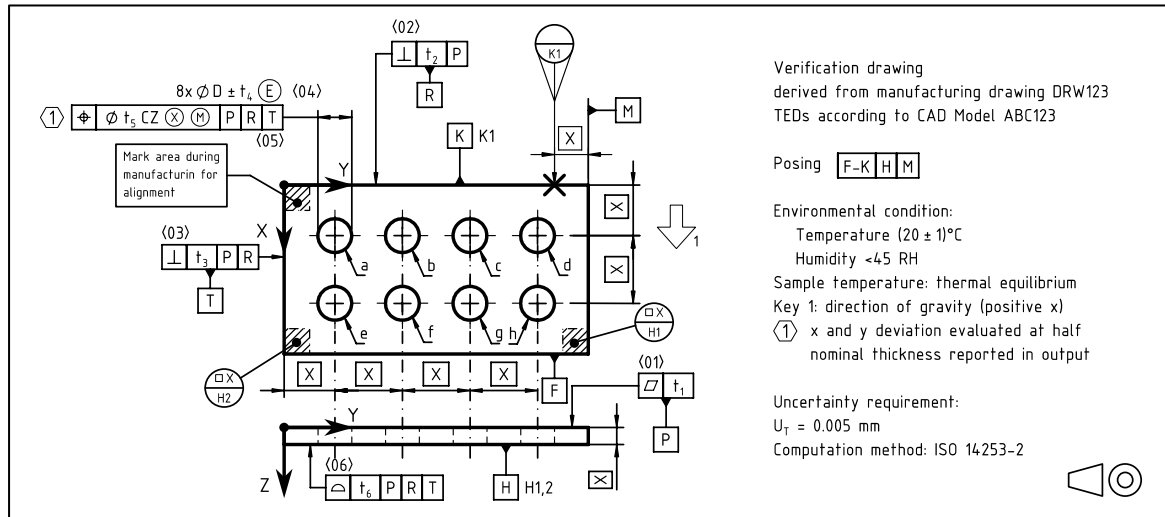


Fig. 9.4: Geometric verification specification dedicated to process tuning

The alignment marking for orientation and the specific naming for each item in the pattern to establish traceability are added. The posing, Fig. 9.5, is described using the datum symbols even if they do not belong to the manufacturing datum system. The use of movable datum targets allows a detailed description of the posing itself. One feature is part of both datum systems but is identified with two names since for the manufacturing datum system it is considered as integral feature (datum R); for the pose description only one point is considered (movable datum target K1). The discussion with experts from the ISO/TC 213 has pointed out that the concept of Contacting Feature ([CF] modifier) may be used instead of a movable datum target for this type of specific usage. Indeed the concept of movable datum target is still under debate within the ISO/TC 213⁷.

⁷ The ISO/TC 213 expert Bertrand Nicquevert is thanked for this input, further consideration shall be made in future research.

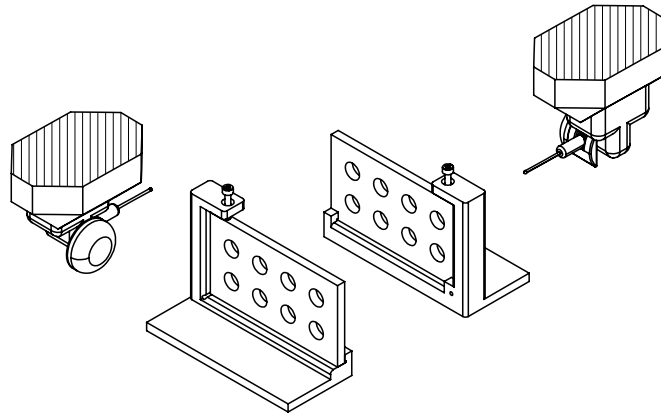


Fig. 9.5: Example of posing described by the verification geometric specification in Fig. 9.4

The reference system is explicitly indicated and flag note 1 describes the type of quantity that is requested when assessing the hole locations. The deviations of interest are the deviation of the intersection point between the axis of the maximum inscribed cylinder and the nominal median plane from the nominal axis. Therefore an association criterion is needed to avoid ambiguity in the determination of the deviation: the associated maximum inscribed feature is invoked. Further, the reporting of x and y deviations in the coordinate system indicated allows effective feedback to the manufacturing process.

9.5 || Conclusions

This chapter refines a definition of the *geometric verification specification*; its different aims for metrological inspection are presented and discussed, showing that different requirements in terms of measurement time and results needed will influence the specification. Requirements to control uncertainty contributors in the metrological process are also included in this specification. This work falls within the context of “Design for Metrology” where the design needs meet the constraints of a measurement process [63]: the functional design is still respected, but verification-specific information is captured in the verification specification.

A remaining question is “should the designer be responsible for this information, or the metrologist?” It is unreasonable to ask designers to become experts in the field of metrology and the knowledge required to wisely choose the right measurand/process while assuring the appropriate uncertainty is beyond the capability of a common metrology operator. The responsibility should be given either to specialized personnel capable of linking metrology and design, or to appropriate teams with the combined knowledge needed.

The example given shows a possible interpretation for a simple part. The current ISO GPS system provides adequate symbology for the geometric requirements of verification specifications. Nonetheless, it is also evident that for specific applications such as the requirement to report

directional deviations of features, there is room for improvement, e.g. defining appropriate symbology.

The development of geometric verification specifications provides challenges both for research and standardization and is worthy of deeper investigations to fully define its application within the ISO GPS system, beyond the current ISO/TS 21619. The use of a geometric verification specification to support SPC and capability index computation can be explored, and test cases of these specifications could be subjected to industrial review to verify the benefits in industrial contexts. As yet, this work still does not address the actual conversion of a higher-level specification into a geometric verification specification, nor does it address industrial constraints to its application. Both points are suitable for future research.

10 || Use of real statistics for statistical assembly simulation

In the pursuit of knowledge, real statistics are the compass, while simulations are mere guesses.

Anonymous

The need for a high volume of interchangeable parts in the modern industrial context first required the formalization of nominal dimensions and tolerances [151,152]. Globalization and offshore outsourcing added complexity to tolerancing management, considering factors such as delivery time and assessing the quality of inbound batches. Alternatively, information, such as measuring reports, can be shared in real-time by the supplier and used as a starting point for an assembly simulation. If the measured data is shared in its raw format (e.g. cloud point), it may be used to generate a “skin model” or non-ideal surface model [38,153] of the manufactured parts, which can be used for the assembly simulation [153–156]. Statistical metrics could be shared instead (e.g. mean, standard deviation, cp, cpk, etc.), and in this case, the smallest tolerance zone that fits the measured data, natural tolerance, could be defined. These fitted tolerance zones may be used for stack-up tolerance analysis [157,158].

To perform tolerance analysis, many different models can be found in the literature and were already briefly presented in section 5.2. In the context of the vector-loop model, different methods for solving non-linear tolerance analysis are possible, such as the linearized method, system moments, quadrature, reliability index, Taguchi Method, and Monte Carlo simulation. A review of these methods can be found in Kenneth and Spencer [95].

Gao et al. [159] compared the DLM (Direct Linearized Method), a generalization of the vector-loop model, and Monte Carlo Simulation, finding that the DLM is accurate in determining the assembly variations, but it is not accurate in predicting assembly rejects when highly nonlinear constraints are in place, as mean shifts and skewed output distribution result from non-linearities. The SOTA (Second-order tolerance analysis) Method was developed to combine the advantages of the Monte Carlo method with the computation speed associated with the DLM. The SOTA uses the method of system moments (MSM) [102,103,160] to link the output statistical moments, and both first and second-order models were developed. It proved to meet the expectation with a

rejection estimation comparable to the Monte Carlo using 10^6 samples with a computational effort five orders of magnitude less [161].

The benefits of a second-order model for tolerance analysis in the design phase were already discussed in the literature, as it can simulate highly nonlinear assembly functions with accuracy comparable to the ones obtained with the Monte Carlo simulation [161].

When highly non-normal input (i.e., non-normal distributions), such as the ones that may result from actual production batches, are used the behavior of the variational method (as the SOTA method) is not documented. The Monte Carlo simulation still represents an approach that can simulate such conditions by discretizing all the distributions into a finite number of samples that are combined by sampling the output distribution. A large number of samples are required to guarantee accuracy, resulting in high computational time. For this reason, the use of a variational method may be convenient.

The MSM, as presented in [102], allows two variations: a linear and a second-order approach, depending on the number of terms included in the Taylor series that approximate the assembly function. Another key aspect that needs to be considered is the expansion pole for the series, which can be chosen in different positions: nominal, tolerance midpoint, and input distribution mean.

This chapter aims to compare different settings for MSM implemented in the SOTA Method for assembly simulation and/or partial assembly simulation, e.g., virtual assembly with parts including “as-designed” tolerances and others with “as-produced” natural tolerances. The partial assembly simulation may represent a formal methodology to quantify the rejection rate when a batch is accepted by derogation.

10.1 || Method of System Moments

10.1.1 Linear Model limits

The scaled statistical moments of the output distribution using a linear model are found with equations (10-1), (10-2), (10-3), and (10-4).

$$\mu_i = \mu_1(U_i) = \bar{u}_i \quad (10-1)$$

$$\sigma_i = \sqrt{\mu_2(U_i)} = \sqrt{\sum_{j=1}^n b_j^2 \sigma_j^2} \quad (10-2)$$

$$\beta_{1_i} = \frac{\mu_3(U_i)}{\sigma_i^3} = \frac{\sum_{j=1}^n b_j^3 \sigma_j^3 \beta_{1_j}}{\sqrt{[\sum_{j=1}^n b_j^2 \sigma_j^2]^3}} \quad (10-3)$$

$$\beta_{2_i} = \frac{\mu_4(U_i)}{\sigma_i^4} = 3 + \frac{\sum_{j=1}^n b_j^4 \sigma_j^4 \gamma_{2_j}}{[\sum_{j=1}^n b_j^2 \sigma_j^2]^2} \quad (10-4)$$

\bar{u}_i is the value that the output (U_i) assumes when all the input variables x_j are set to the values where the sensitivities are quantified (expansion pole).

The sensitivities of the output (U_i) with respect to the input variable (x_j) are represented by:

$$b_j = \frac{\partial U_i}{\partial x_j}$$

γ_{2_j} is the excess kurtosis ($\gamma_{2_j} = \beta_{2_j} - 3$) that represents the difference in kurtosis between the given distribution and a normal one. All the steps to get to the last set of equations are not displayed for the sake of brevity (but can be found in appendix B on page 299).

From equation (10-1), the mean of the output distribution depends only on the expansion point chosen for the Taylor series. But, from Fig. 10.1, it is possible to see that the mean value of the output depends on the shape of the functional equation that remaps the input distribution. Therefore, it can be assumed that both the functional equation derivatives and the input distribution parameters influence the mean of the output.

From equation (10-2), the variance of the output depends on the slope of the functional equation and the variance of the input. At the same time, it is well known that equation $\mu_2(U_i) = E(U_i^2) - [E(U_i)]^2 = E(U_i'^2)$ is always valid, being one of the possible definitions given to the variance. Since we have already discussed that the value of the mean depends on the full shape of the functional equation and the input distribution shape, it can be derived that the variance depends on these parameters too (higher-order derivatives of the functional equation and higher statistical moments) being the expected value for the square of the output distribution.

From equation (10-3), it is possible to see that the skewness of the output distribution depends only on the skewness of the distribution of the inputs: if the skewness of all the input distributions is null, the skewness of the output distribution is automatically null. This is proven wrong by looking at Fig. 10.1 in which it can be seen that in the case of a non-linear functional equation, the output distribution is asymmetric even if the input is normal. It is possible to state that the skewness of the output distribution is a function of the higher-order derivatives of the functional equation of the system.

From equation (10-4), it is possible to see that the output statistical distribution departs from normality ($\beta_2 = 3$) only if the input distributions are non-normal. In other words, it can be said that

the excess kurtosis depends only on the excess kurtosis of the input variables. It is not possible to arrive at a proper conclusion from Fig. 10.1, since it is not possible to quantify the kurtosis for the output distribution that is displayed in the figure. A complete study on second-order equations is needed to determine which parameters the kurtosis depends on.

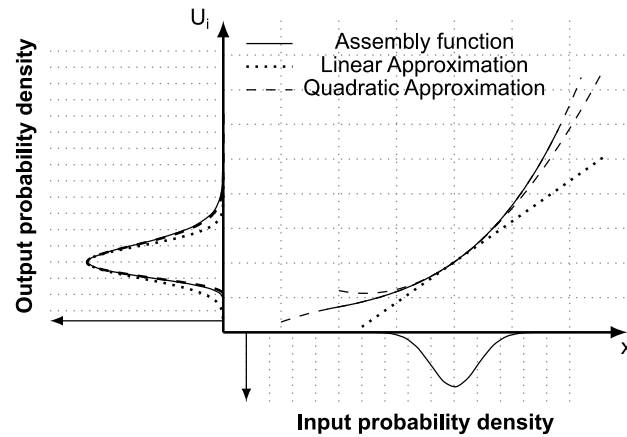


Fig. 10.1: Input and output probability distribution for a single-input/single-output system, comparison among actual non-linear assembly function, linear approximation, and a quadratic approximation.

10.1.2 Second-order model contributions

Using a second order model equations from (10-1) to (10-4) becomes really complex [102,103,160]. The full second-order model, if the first four output's statistical moments are desired, requires knowing the first eight statistical moments of the input distributions [102] as follow.

$$E(U_i) = f(U_i', \mu_2)$$

$$E(U_i^2) = f(U_i', U_i'', \mu_2, \mu_3, \mu_4)$$

$$E(U_i^3) = f(U_i', U_i'', \mu_2, \mu_3, \mu_4, \mu_5, \mu_6)$$

$$E(U_i^4) = f(U_i', U_i'', \mu_2, \mu_3, \mu_4, \mu_5, \mu_6, \mu_7, \mu_8)$$

The scaled statistical moments of the output distribution are a function of the latter, but it is not possible to determine if they are also dependent on all the statistical moments involved in the $E(U_i^n)$ definitions. It can't be excluded that the contributions of higher statistical moments compensate each other.

The following considerations will be based on what is possible to graphically determine from Fig. 10.1 for a single-input/single-output system.

By looking at Fig. 10.1, the shape of the statistical distribution stretches if it is mediated by a second-order functional equation: the mode depends on the value of the functional equation while the mean of the output shifts from it. The deformation of the statistical distribution will be greater if the input distribution is more spread: the shift of the mean from the mode depends both on the second-order derivatives and the standard deviation of the input variables.

The effect of the second-order derivatives stretches the bell toward the positive direction and compresses it towards the negative direction. Therefore, it can't be detected a clear direct influence on the output standard deviation by the second-order derivatives. At the same time, it can be assumed that the standard deviation depends both on the skewness and kurtosis of the input distribution: the input distribution statistical moments can accentuate or mitigate the deformation impressed by the functional equation second-order derivatives. For example, if the input distribution in Fig. 10.1 had a negative skewness, it means that the probability on the area that extends the output probability towards the positive direction have a thinner tail with the effect of decreasing the spread of the output distribution.

The skewness depends on the second-order derivative of the functional equation and the standard deviation since they deform the shape of the distribution. It is also possible to assume that the asymmetry of the output distribution depends on the skewness and kurtosis interaction with second-order derivatives since it was already discussed that they can increase or decrease the deformation of the output distribution. There is no graphical way to determine in which way the 5th or 6th statistical moments affect the distribution shape since there is no graphical interpretation for them.

For the kurtosis, it is possible to repeat the same considerations made for the skewness.

10.2 || Case Study

Among commercial software, CETOL6sigma implements the SOTA Method. One of the options of the software is the possibility to custom set different statistical distributions as input. Three different statistical distributions are supported: the uniform, the Gaussian (a.k.a. Normal), and the SMLambda (Standard Moment Lambda) distributions [162]. While the normal and the uniform distributions are widely known, the SMLambda distribution is defined by four values: mean (\bar{x} or μ), standard deviation (σ), skewness (β_1) and kurtosis (β_2). This distribution describes non-symmetrical and non-normal distributions (see Fig. 10.2), but it comes with some limitations on skewness and kurtosis [Equations (10-5)] [162], The general expression for this distribution can be found in Ramberr et al. [163].

$$\begin{aligned}
 & -2 \leq \beta_1 \leq 2 \\
 & 1.8 \cdot \beta_1^2 + 1.8 \leq \beta_2 \leq 1.25 \cdot \beta_1^2 + 5.75
 \end{aligned}
 \tag{10-5}$$

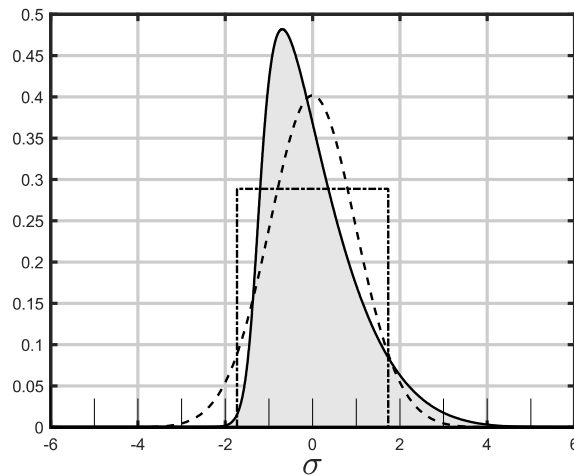


Fig. 10.2: SMLambda distribution with a mean value of 0, standard deviation, skewness and excess kurtosis of 1; compared with a normal distribution (dashed line) and a uniform distribution (dash dotted line).

The software allows for both first-order and second-order tolerance analysis. However, the more detailed description provided by the second-order analysis comes with a higher computational cost. For a problem with n variables, n^2 more values need to be computed.

Both types of analysis allow the software to choose the central point of the expansion for the Taylor series: CAD nominal values, Distribution mean, or Tolerance midpoint. When tolerances are symmetrical with respect to the nominal values and the statistical distributions are symmetrical, these three points coincide [162].

Once measurements have been performed, and the statistical moments are evaluated, it is possible to find values outside the limit given by the SMLambda distribution [Equation (10-5)]. However, strategies to find the best fitting SMLambda distribution to fit experimental data go beyond the aims of this work.

10.2.1 The assembly

The “Seat Latch” assembly, which is one of the training models in CETOL6sigma, was chosen as a case study. Real statistics were simulated for the “Side plate” part.

A virtual batch of sixteen geometries was created using CAE process simulation: the nominal geometry was imported into MAGMASOFT, and the results for the metal casting simulation, obtained by changing process parameters, were exported as .stl files, see Fig. 10.3.

The samples with random deformations in size, shape, and orientation were inspected in GOM Inspect, where each feature's real size (if applicable) and the deviations from nominal, in terms of translations and rotations, were exported. These data were then converted into deviations expressed in the same reference system used in CETOL6sigma. For each dimensional variable, the first four scaled statistical moments about the mean were computed.

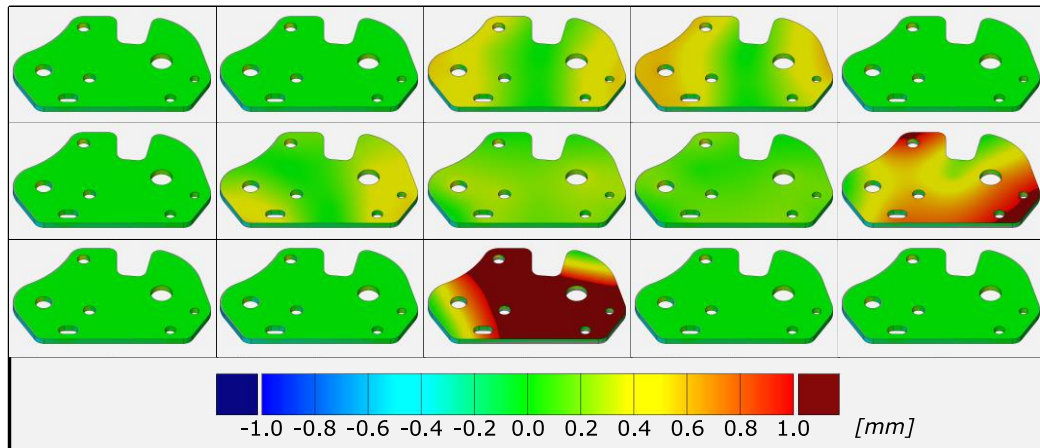


Fig. 10.3: Simulated real geometries, surface comparison in GOM Inspect.

When the skewness and kurtosis values were out of acceptable limits, the closest admissible values were used to fit the SMLambda distribution to the real data.

The moments were then used in the CETOL6sigma model to simulate the real distribution's impact on tolerance stack-up. Two functional dimensions (outputs), "X-POS" and "Y-POS," were selected for display. These dimensions describe the position, with respect to the side plate, of the hole where the cable that engage the mechanism is joint. The output statistical distribution was then recorded after performing four kinds of analysis among the six available:

- Linear analysis centered on the tolerance midpoint.
- Linear analysis centered on the mean of the input distribution.
- Second-order analysis centered on the tolerance midpoint.
- Second-order analysis centered on the mean of the input distribution.

The analysis in which the pole of the Taylor expansion is set on the CAD nominal was not considered, as it was coincident with the pole centered on the nominal value, since no asymmetric tolerances were present in the model.

10.3 || Results

The simulated real distributions are significantly away from normality and could only be described by an SMLambda distribution (Fig. 10.4). The computed statistical moments are used as input variables.

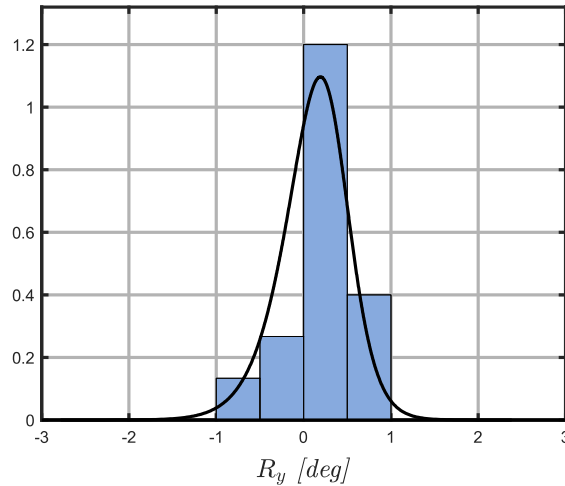


Fig. 10.4: Distribution for rotation about y-axes for the cylinder marked as Cylinder 2.

10.3.1 Critical dimension “Y-POS”

Fig. 10.5 shows the results of the output statistical distribution for the linear and second-order analyses centered on the tolerance midpoint.

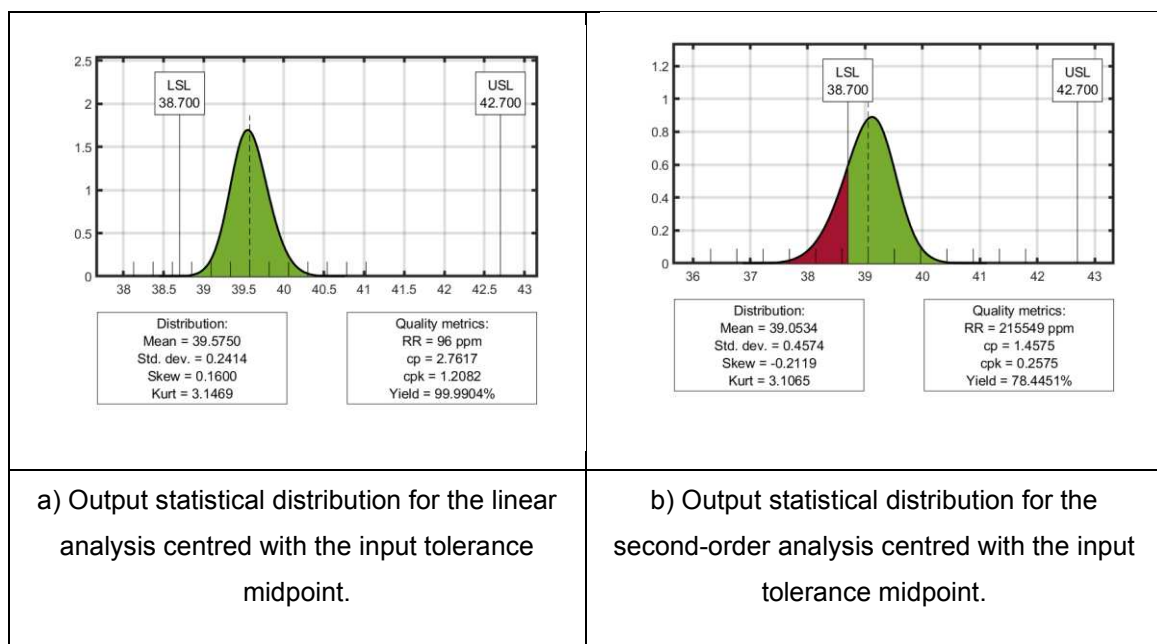


Fig. 10.5: Output statistical distribution for the analysis centred with the input tolerance midpoint.

The output distribution is considerably different in the two cases: the mean shifts by -0.5216 mm , (13.07 % of the tolerance width), resulting in a different percentage of parts within tolerance (yield): 99.99 % for the linear analysis and 78.45 % for the second-order analysis.

The results obtained by centering the Taylor expansion with the mean values of the input variables can be seen in Fig. 10.6.

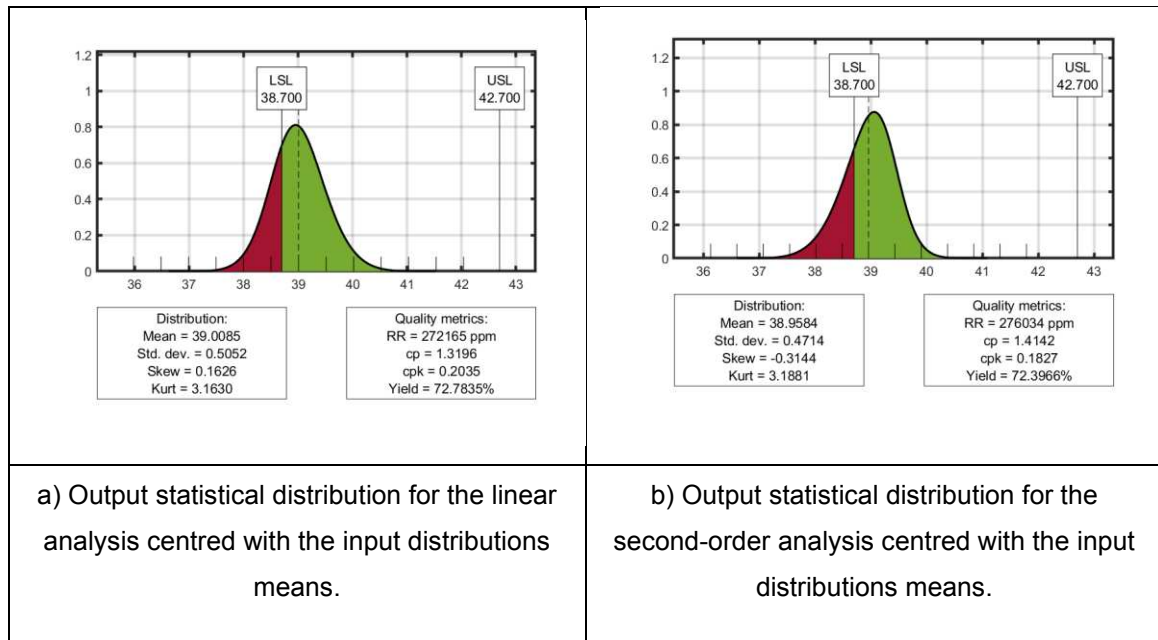


Fig. 10.6: Output statistical distribution for the analysis centred with the input distributions means.

A smaller difference in the mean can be noted (1.25 % of the tolerance width), and the acceptability rate is now comparable (72.78 % for the linear and 72.40 % for the second-order analysis). Nonetheless, it is noteworthy that the skewness changes sign.

The differences when changing the expansion pole for the linear analysis can be noted by comparing Fig. 10.5,a) and Fig. 10.6,a). The mean value shifts by 14.16 % of the tolerance width, and the standard deviation shifts by 6.60 % of the tolerance width, resulting in the yield given by the analysis centered with the input distribution means being less than 1 % away from second-order analysis yields (centred with the input distributions means).

Analyzing Fig. 10.5,b) and Fig. 10.6,b), the differences in the output distribution for a second-order analysis when the expansion point is changed can be seen. The distribution shape is similar for both cases (negative skew), with the mean shifting by 2.38 % of the tolerance width. As a result, the acceptability rate goes from 78.44 % to 72.40 %.

For this critical dimension, the output distribution is heavily influenced by the types of analyses performed. As can be seen in Fig. 10.7, the distribution obtained with the linear analysis centered on the tolerance midpoint is far away from the others.

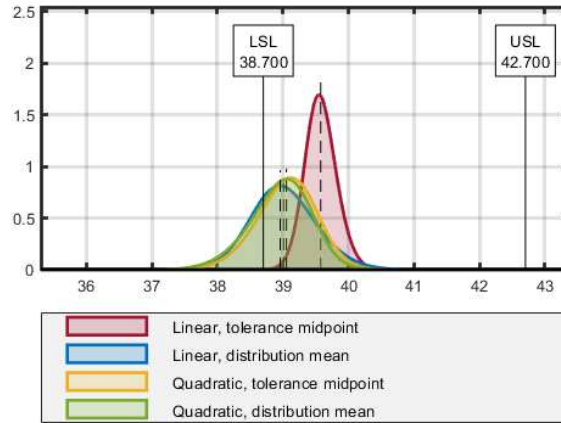


Fig. 10.7: Comparison among the output statistical distribution obtained for the critical dimension “Y-POS”.

10.3.2 Critical dimension “X-POS”

Considering now the critical dimension “X-POS,” a significantly different behavior can be noted. In Fig. 10.8 the four outputs are almost overlapped, meaning that this critical dimension is not influenced by the type of analysis.

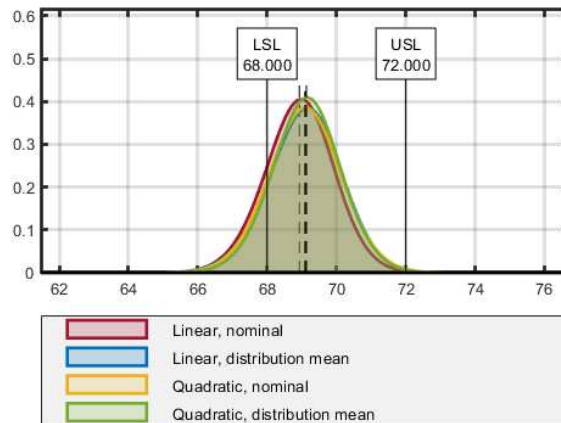


Fig. 10.8: Comparison among the output statistical distribution obtained for the critical dimension “X-POS”.

Overall, the acceptability rate ranges from 82.35 % to 87.17 % , the mean maximum difference is 5.12% of the tolerance width, and the standard deviation maximum difference is 1.65 % of the tolerance width.

10.4 || Discussion

The analysis of the Method of System Moments showed that the linear model neglects many contributions to the final output, potentially leading to unreliable results.

10.4.1 The mean shift

It was shown that the mean of the output depends on both the curvature of the functional equation and the shapes of the input distributions. However, the linear model assumes that the mean of the output depends solely on the expansion pole, leading to a mean shift that can significantly impact the yield. This mean shift and its effect on yield due to the functional equation curvature were already discussed [159]. Additionally, the shape (skewness and kurtosis) of the input also has a similar impact, as it can either amplify or mitigate the mean shift caused by the functional equation curvature. However, in a tolerance stack-up with multiple inputs, each individual input shift may partially compensate for each other.

This effect was clearly observed in the case study. The critical dimension “Y-POS” exhibited a significant mean shift, while the “X-POS” showed almost no mean shift. Notably, both dimensions pertain to the same feature but in different directions. Hence, the same assembly can behave differently in terms of critical dimensions based on their specific directions.

10.4.2 Critical dimension “Y-POS”

The critical dimension “Y-POS” is chosen for further discussion regarding the influence of different types of analysis, as the other dimension (X-POS) has been found to be not influenced.

Among the four outputs, the one obtained with a linear analysis and the expansion pole centered on the tolerance midpoint is significantly different from the other three (Fig. 10.6). This indicates that the choice of the expansion pole is crucial when using a linear model. However, when the expansion pole is set to the input distribution mean, the results of the linear model are nearly overlapped with the second-order results. It is important to note that the skewness changes sign when the second-order model is applied, indicating that the linear model fails to accurately

determine the output distribution shape. Nevertheless, if the expansion pole is chosen carefully, the yield result can be close to the second-order results.

When comparing the second-order results, it can be observed that the differences are small when the expansion point is changed. This can be explained by the fact that the second-order model considers both the mean shift due to the functional equation curvature and the input mean. As a result, the choice of the expansion point has less impact on the output distribution shape in the second-order analysis compared to the linear analysis.

10.5 || Conclusions

The chapter aimed to compare different settings for MSM implemented in the SOTA Method for assembly simulation and/or partial assembly simulation using actual statistics as inputs, thereby conducting virtual simulation analysis. The software CETOL6sigma was used as a benchmark since it allows the use of such inputs.

Different behaviors were observed for different critical dimensions (outputs). Considering the critical dimension that presented significant differences, it is shown that different types of analysis lead to different results, particularly for yields, in the presence of non-linear inputs. The full second-order tolerance analysis was already proven to give better results in the presence of highly non-linear functional equations. In our study case, the assembly has a functional equation close to linearity, but highly non-linear inputs were used.

The linear model centered on the nominal value simply cannot adequately represent reality. The result for this analysis gives an acceptability rate estimation that is completely different from the result of the second-order analysis. At the same time, the linear model centered on the input distribution means gives a result in line with the second-order analysis. Therefore, it can be concluded that, in the case of highly non-linear input distributions, the expansion pole for the Taylor series should be selected as the input distribution mean.

The following best practice can be extrapolated:

- For non-linear assemblies, e.g., when rotations are predominant, the second-order analysis should be used.
- For non-symmetric tolerance zones, the expansion point should be set on the tolerance midpoint or input distribution means.
- For non-normal input distributions, the second-order analysis should be used.
- When using real statistics, the second-order analysis centered on input distribution means should be used.

In general, it is always advisable to check the linearity assumption by performing a second-order analysis. The check should be performed for all critical dimensions in the model since the behavior of each dimension can be different.

11 || An industrial application, the ELECTROLUX case study

*I'd rather have half of my idea change the world than my whole idea
be a few papers in a journal*

Rodney Brooks

In this final chapter, the aim is to provide a snapshot of an actual implementation of the framework that has been presented throughout this thesis in an actual industrial case. In the following part of the activity that has involved the Design Tools and Methods in Industrial Engineering Laboratory of the University of Padova in collaboration with Electrolux SpA will be presented. Unfortunately, due to the industrial nature of the activities, intellectual property protection, and the non-disclosure agreement signed by the parties involved, this chapter cannot go into the details of the implementation but it will be limited to the general strategy that has been followed and that could be easily adapted and used in a different industrial scenario.

The industrial implementation is based on three pillars (see Fig. 11.1) that enable a structured implementation of the system. The first pillar is the training. The second pillar is the technical documentation, and the third one is the deployment strategy.

The training is not limited to the training itself (frontal lessons), it comprehends all the activities needed to custom-fit a training strategy for the actual industrial body considering its size, structure, and territorial distribution. Therefore, the contents need to be carefully evaluated: the order on which different ISO GPS topics are presented is essential for a deep understanding of the system and different industrial bodies may have different interests. For instance, the methodologies to deal with deformable bodies might not be relevant for an industry exclusively dealing with milled parts. Training itself, without a tutoring phase aiming to see the content of the training applied to actual case studies coming from the industry, is not very useful and is soon left behind. For this reason, a tutoring phase shall be carefully scheduled to keep the participants in the training interested in the topic. All these training-related activities need to be scheduled and tracked to keep control of the progress that is made: a control body, under the name of the technical committee, shall be defined, as presented in section 11.1. A more comprehensive presentation of the training phase is given in section 11.2.

The technical documentation pillar comprehends the activities needed for the creation of internal documentation needed to set a list of internal rules for the implementation of the ISO GPS system. The pure application of international standards might result difficult without further guidance given by the internal technical documentation. The same technical committee already mentioned is responsible for coordinating and distributing the technical documentation that is composed of: an ISO GPS Competence and training manual, ISO GPS guidelines, Drawing Standards, Working Instructions, and templates and instructions for specific modules. A more detailed overview is given in section 11.3.

Finally, the last pillar is the deployment strategy, always under the responsibility of the technical committee. Its main contents are the definition of a step-by-step procedure for the ISO GPS implementation starting from the definition of pilot projects and the diffusion of the knowledge acquired to other projects up to the official switch-on for the whole organization. The definition of tools to keep the process traceable is also needed to allow for continuous correction of the process.

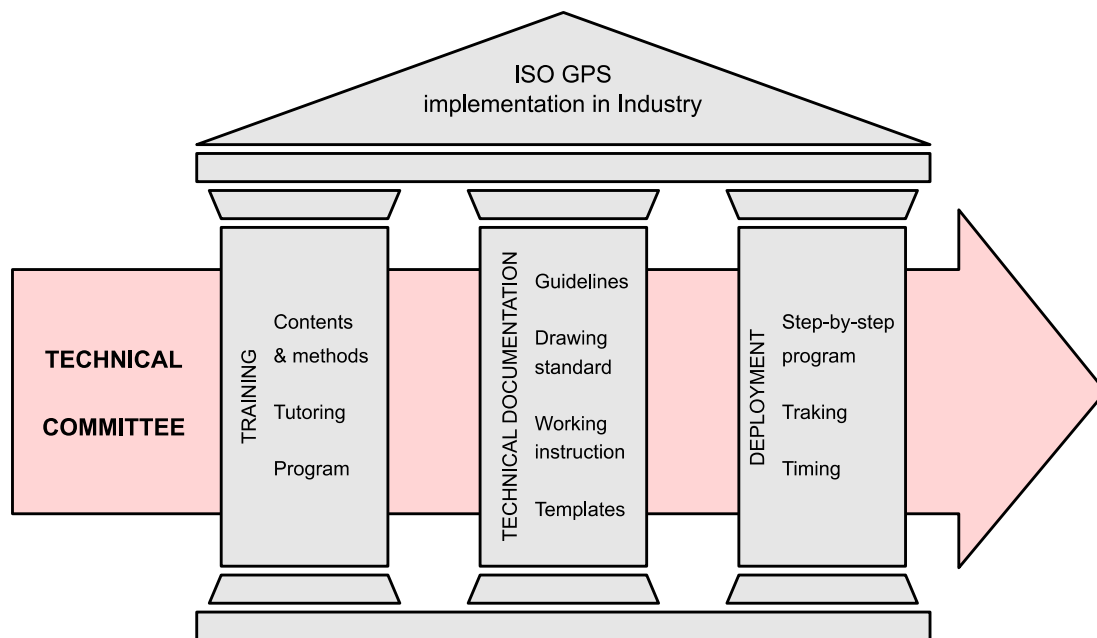


Fig. 11.1: Pillars for the ISO GPS implementation in Industry.

The current industrial application at Electrolux has spanned over four years, beginning in 2020 and scheduled to continue until the end of 2024. The extended timeline of this implementation is partly due to the trial-and-error adjustments needed to establish the implementation procedure. Subsequent repetitions of the process may require less time.

During the first two years, only the design department was involved in training and tutoring initiatives. Concurrently, key case studies were selected and examined in collaboration with the designers responsible for these sub-assemblies/components.

Following this initial phase, experts from Manufacturing, Engineering, and Metrology participated in a second round of training, which also expanded the number of designers receiving dedicated training.

Starting a couple of months after the initial training phase, tutoring has consistently remained active.

The expected benefits of implementing the ISO GPS system in the industry can be summarized as follows:

- Enhanced design clarity.
- More realistic design specifications.
- Streamlined flow of information within Technical Product Documentation.
- Reduction in manufacturing costs (fewer non-conforming parts).
- Improved assembly processes.
- Consistent and reliable inspection methods.

When combined, these factors contribute to achieving reliable product quality. Furthermore, the sharing of corporate knowledge is simplified, and effective outsourcing practices can be implemented.

11.1 || Technical committee

As previously mentioned, the Technical Committee is responsible for implementing the ISO GPS methodology at Electrolux, with its main objective being to support the implementation of this methodology. Its primary deliverables, representing the outcomes of its work, include:

- Rolling out specific plans and timelines.
- Defining stakeholders.
- Establishing a RACI matrix (Responsible, Accountable, Consulted, and Informed) for the ISO GPS process.
- Defining support materials, which were also referred to as technical documentation.
- Identifying Key Performance Indicators (KPIs) to monitor the progress of case studies.
- Assessing risks in accordance with ISO 9001.
- Managing the transitional phase by setting priorities and rules for handling previously defined designs (legacy).

To accomplish these goals, the Technical Committee was formed, consisting of various professional figures. The primary responsibility rested with internal members of the R&D quality department, assisted by three external consultants from the University of Padova, including myself, as well as Professors Gianmaria Concheri and Roberto Meneghello. This team also included three

other individuals from the R&D quality department involved in developing internal standards for the industrial partner.

Because this process involved multiple departments, professionals from other departments were consulted. In the early phases, the main department involved was Global PDM (Product Data Management) and PLM (Product Lifecycle Management), responsible for exploring how to implement the framework into the organization's worldwide PLM software architecture.

The first two major tasks undertaken by the Technical Committee were defining the process and assessing risks. Defining the process involved simulating the implementation of the new framework for a new product to determine the rollout steps. This phase was crucial for risk evaluation, as required by ISO 9001.

Risk assessment involved gathering feedback from various stakeholders, both internal and external. Internally, the main stakeholders were defined by the proposed framework (refer to Fig. 2.5 at page 49), including the design department (comprising all designers involved in product development), the manufacturing department (involving all professionals involved in the workshop floor), and the quality control department (comprising all professionals involved in quality control). Given Electrolux's multinational and complex external supply chain, the framework depicted in Fig. 2.6 at page 51 also had to be considered. Therefore, external stakeholders were regarded as suppliers, along with all professionals involved in managing supplier relationships, such as the purchasing office. The primary methods for collecting stakeholder inputs were interviews and gathering questions and feedback during training sessions.

By analyzing these interactions among different internal and external stakeholders, the RACI (Responsible, Accountable, Consulted, and Informed) matrix could be initially drafted. This matrix formalizes the expanded responsibility principle presented in Chapter 2. At each step of the process involving the creation of a geometric specification, a responsible figure is defined, indicating the professional responsible for that step. Simultaneously, the accountable figure is identified, responsible for approving the outcome (deliverable) of the step. The responsible and accountable figures may be the same or different individuals. The RACI matrix also specifies who needs to be consulted for each step to contribute their expertise and who needs to be directly informed about the delivery of the outcome. This rigorous procedure facilitates the implementation of the top-down vision advocated by the proposed framework.

Some universal criticalities, not specific to any particular industrial case, have been identified. These include the misalignment of external suppliers, the risk of designers having to fill knowledge gaps, and transitional phase management.

The first point becomes more critical as the industrial organization grows, as the number of external suppliers can increase significantly. However, it can also be seen as an opportunity. A large industrial organization can act as a catalyst for innovation and encourage suppliers to bridge knowledge gaps, benefiting the entire industry.

The second point is typically one of the first concerns raised by designers during training. Nevertheless, it is a false problem because, as evident from the results of the industrial survey, designers are already responsible for the entire geometric specification process. Filling the gaps can be seen as a challenge related to the transitional phase.

This brings us to the last point, which can become more challenging as the industrial organization grows, given the need to align more people and departments. The solution to this problem lies in a proper definition of the transitional phase by the Technical Committee.

In addition to managing training, the priorities for the Technical Committee include creating technical documentation, which, among other things, details technical aspects and outlines mitigation strategies against the identified criticalities. Careful consideration is also needed for the integration of the process into the PLM software.

11.2 || Training

Training constitutes the first pillar of ISO GPS implementation in industry. However, as the industrial survey demonstrated (see chapter 1), traditional training often falls short in delivering satisfactory results. Therefore, it is essential to meticulously design training that aligns with the integration of ISO GPS effectively.

Many commercial ISO GPS training programs typically offer courses ranging from 8 to 24 hours. Often, these courses are primarily designed to unlock commercial opportunities for selling software packages. Such courses provide only a surface-level understanding of the ISO GPS system and lack the depth and customization required to meet the specific needs of clients.

The training program developed for our industrial partners follows a different approach. It doesn't adhere to fixed time limits and has evolved over a span of more than two years. The current structure includes various modules tailored to different professionals, ensuring that each participant receives the necessary information to excel in their role. Additionally, a tutoring phase runs concurrently with the training, enabling participants to witness the practical application of the ISO GPS system in their specific product contexts.

11.2.1 Training modules

As previously mentioned, the final training program was divided into various training modules. Each module consists of different lessons, each lasting for 2 hours, with no more than one lesson per week.

This setup was chosen because it allows participants to maintain their maximum focus throughout the lessons. It also provides them with time between lessons to reflect on the content presented and return to subsequent lessons with questions or remarks. Furthermore, it ensures

that the disruption to the organization's operations, as professionals are temporarily away from their desks, is limited each time.

The training units are presented in the following list:

- **Basics** (2x2h): Introduction to ISO GPS standards and fundamentals of the integrated ISO GPS/ASME GD&T approach.
- **How to Read** (3x2h): Methodological approach to reading and comprehending a detailed drawing.
- **How to Write** (5x2h): Methodological approach to creating a detailed drawing with geometrical specifications.
- **How to Compute** (4x2h): Methodological approach to calculating dimensional and location tolerances for shaft-hole connections, ensuring assemblability, and performing tolerance stack-up computations.
- **How to Measure** (2x2h): Methodological approach to reading a specification, defining measurands, admissible variability, and reference frames, leading to an inspection procedure.
- **Case studies** (3h): Presentation of actual case studies from the industrial organization.

A detailed training agenda is provided in Appendix C on page 301.

This training setup represents the result of two years of adjustments and was delivered to over 50 professional figures from various departments. In the following sub-section, the initial training phase will be presented.

11.2.2 Ambassador phase

At the outset of the collaboration with Electrolux, the training modules, as presented in the previous sub-section, had not yet been developed, and a different strategy was pursued. During this phase, the objective was to train a core group of experts capable of managing the transitional phase and the subsequent extended training phase.

In 2020, a total of twelve designers were selected, chosen for their heightened sensitivity to the topic. The content of the training was similar to the one previously described but organized differently.

One significant issue that arose during this initial phase concerned the distinction between training and tutoring. As mentioned earlier, the tutoring phase is essential to enable professionals to witness the real application of the system. However, during this initial iteration, the transition between training and tutoring was not clearly defined, and too many actual cases were introduced during the lessons. While it may seem ideal to base training on real cases, it is not always the case when dealing with professionals from the industry. Different designers among the participants came from different business units and already had specific interests in certain products. As a result, when real cases were presented, only a few participants were genuinely interested in the specific

application, while others were not because the product differed significantly from what they typically worked on.

This situation led to prolonged discussions related to Phase 0 (Chapter 3 on page 63), which were clearer to the designer responsible for the product but not as clear to other participants.

This experience prompted the formalization of the training modules as presented previously and initiated the initial dissemination phase, as detailed in the following sub-section.

11.2.3 Initial dissemination phase

The initial dissemination phase officially commenced in 2022 and involved the delivery of training modules to over 50 professionals from various departments within Electrolux.

The first step involved defining the competence and training matrix. Based on the modules described in sub-section 11.2.1, each department was assigned specific mandatory modules, suggested modules, and optional modules by the technical committee.

The complete matrix is extensive and cannot be displayed here. However, in Fig. 11.2, we provide an example involving only the general department. The actual matrix is more detailed and takes into consideration the specific requirements of different business units within the organization.

	Training Units				
	Basic	H2R	H2W	H2C	H2M
R&D	Mandatory	Mandatory	Mandatory	Mandatory	Optional
Manufacturing Engineering	Mandatory	Mandatory	Mandatory	Suggested	Optional
Quality Control	Mandatory	Mandatory	Optional	Optional	Mandatory
Purchasing	Mandatory	Mandatory	Optional	Optional	Optional
Suppliers	Mandatory	Mandatory	Suggested	Optional	Mandatory

 Mandatory
 Suggested
 Optional

Fig. 11.2: Competence and Training matrix (example).

Based on this matrix, the professionals selected for the initial dissemination phase were invited to attend the relevant lessons. The training program lasted for approximately six months.

11.3 || Technical documentation

The technical documentation collects all the internal documents that define the geometric specification process in its entirety, from the training strategies to the management of drawings in the PLM software.

To achieve this, three main documents are needed:

- **Guidelines:** These are owned by the R&D department and describe the ISO GPS methodological approach in its broader sense, starting from the training approach.
- **Drawing standard:** This document is owned by the PDM-PLM Program Manager and states how drawings with geometrical specifications according to ISO GPS need to be handled.
- **Working Instruction:** These are also owned by the PDM-PLM Program Manager and specify how to deal with drawings containing geometric specifications inside the PLM software and how to manage referencing codes for traceability.

Further details can be found in the next subsections.

11.3.1 Guideline ISO GPS

The document describes the preparation of Technical Product Documentation within the industrial body. It also supports the proper reading and interpretation of any Technical Product Documentation document.

The main contents can be summarized as follows:

- Types of information in TPD and types of TPD documents.
- Who is entitled to manage TPD information and documents.
- Language for geometric representation and tolerancing specification (i.e., ISO-GPS).
- Methodology for TPD preparation.

11.3.2 Drawing standard

The Drawing Standard serves as the reference for creating new drawings or revising existing ones. This standard establishes the minimum requirements for preparing drawings. The requirements outlined in this document are crucial for standardizing practices and ensuring consistent interpretation.

In addition to ISO standards, this document incorporates internal-specific drawing requirements. The key contents can be summarized as follows:

- Guidelines on handling general tolerances.
- Definition of Critical To Quality (CTQ) dimensions.
- Mandatory identification for tolerance specifications.
- Guidelines for distinguishing between Functional and Manufacturing specifications.
- References to ISO GPS Guidelines and Drawing Working Instructions.

11.3.3 Working Instructions

The Working Instructions document is less susceptible to generalization because it explains how to handle drawings containing Geometric Specifications within the specific PLM environment of the industrial organization. Due to these reasons, this thesis cannot provide further details about this document.

11.3.4 Drawings management

The Drawing management process involves translating the geometric specification model, as presented in chapter 2, into an actual industrial case. It's important to distinguish between industrial design (aesthetic) and technical design (technical representation). The drawing management process is illustrated in Fig. 11.3.

The starting point begins with industrial design, where the aesthetics of the product are defined, and aesthetic requirements are established. During this stage, attention is focused on the external surfaces visible to the end customers. Aesthetic requirements, such as defining maximum gaps between parts, play a significant marketing role as they can influence the perception of quality by customers.

In the technical office, responsible for the technical design, the mechanical CAD model is initially created. This model should represent all parts within the product, whether visible or invisible to the customer. At this stage, the primary focus is on functionality. Therefore, the CAD model should not consider manufacturing constraints, such as draft angles. Including such manufacturing requirements in the CAD model might make it challenging to update, and these requirements may not be fully defined in the early stages.

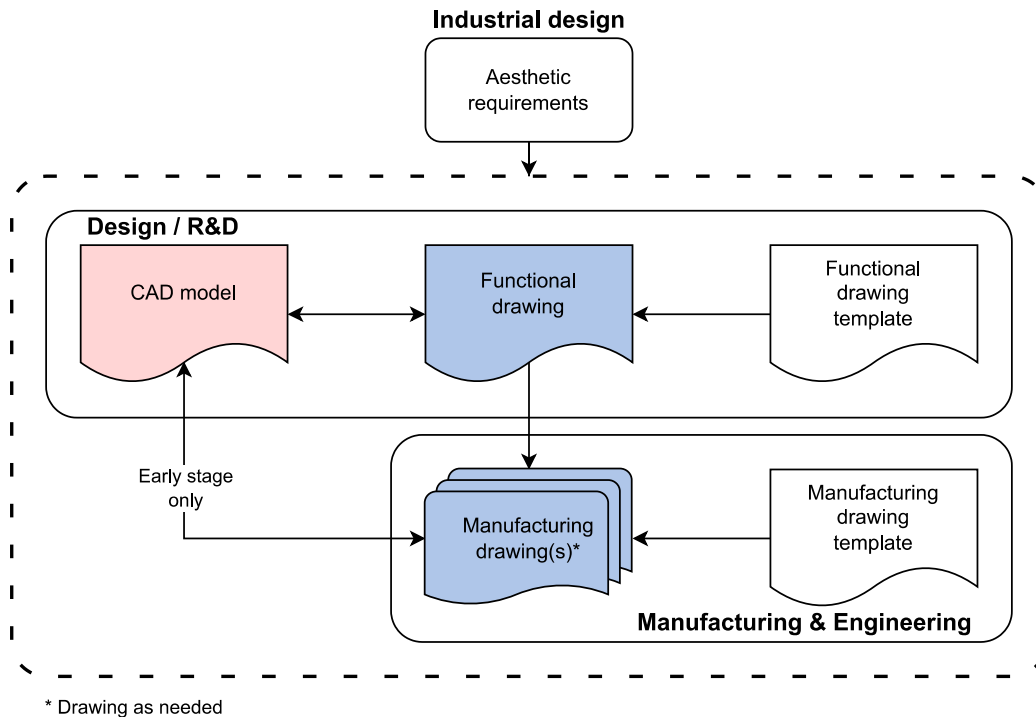


Fig. 11.3: Drawings management.

The CAD model must pay special attention to the interfaces between the parts that make up the product because modifications to these geometries can lead to significant changes in the entire product.

This CAD model is utilized to create Functional Drawings that convey functional geometric specifications. Since the primary focus is on functionality, function takes precedence over geometry, and drawing templates can be established. For example, the functionality of a hinge remains relatively consistent within certain limits. When creating functional geometric specifications for a new hinge, corresponding features that satisfy the same functional requirements as previous models can be identified. Therefore, performing phase 0, as presented in chapter 3, becomes more straightforward. Once a specific feature that addresses a particular functional need is identified, the required tolerances can be found in the template.

Functional drawings serve as input for the industrialization of the product, which involves defining the manufacturing process required to produce each component. Functional drawings are linked to the same original CAD models. At this stage, all constraints arising from the manufacturing process need to be taken into account. Possible modifications to the CAD models or functional specifications may be considered in the early stages. This phase resembles the Engineering Change Request (ECR) process, as presented in Fig. 2.5 at page 49.

Templates can also be employed for manufacturing drawings. These templates compile information about references used for manufacturing alignments and process parameters applicable to specific situations.

Templates encapsulate the prior knowledge accumulated within the industrial organization regarding the specific product and/or manufacturing process. Therefore, templates serve not only as examples of drawings but also as technical reports that explain the functional features, justify their selection, and guide the designer in replicating the same process for a product with similar functionality.

11.4 || Deployment in Electrolux

The deployment phase at Electrolux is currently underway. However, details cannot be disclosed at this time.

Presently, the training is being extended to various business areas, and the technical documentation is being prepared and evaluated by different stakeholders. The step-by-step roll-out procedure is under discussion and will soon be approved by Electrolux. This will set the official switch-on date for the new system, which will be systematically implemented.

12 || Conclusions

I am turned into a sort of machine for observing facts and grinding out conclusions.

Charles Darwin

This work aims to establish a new vision for the ISO GPS system and its implementation in the industry. The focus is on assessing and defining methodologies and tools to manage the tolerancing process in the industrial product development life cycle.

A survey conducted in the Italian market has shown that the penetration of the ISO GPS system is lacking. The difficulties in implementing the system are shared by both industry and academia. To overcome these implementation difficulties, this work proposes a novel geometric specification management approach. In this framework, attention is given to the responsibility for geometric specification and its sharing throughout the product development life cycle. The “standard” responsibility principle, as defined in the standard, is overcome by adopting an extended responsibility principle in which all the actors involved in product development are called upon to operate together, taking responsibility for their respective areas and expertise. The designer is not required to take care of the overall process.

The implementation of such a framework necessitates distinguishing between different types of geometric specifications: functional, manufacturing, and verification specifications. The existence and relationships of these documents open up different research gaps and questions that have been analyzed throughout this work.

A procedure based on Design for Assembly (DfA) analysis to recognize and classify functional features has been presented, aiding the designer in focusing on functionality and helping to create “pure” functional specifications. The integration of this methodology into the geometry specification integrated procedure developed at the Design Tools and Methods in Industrial Engineering Laboratory of Padova is also shown in this work.

The proposed procedure for geometric specifications is inherently a top-down approach in which product requirements are shifted step by step from the system, to sub-systems, and single components. In this vision, a methodology to handle tolerance stack-ups in a top-down approach is presented and discussed.

Tolerance stack-ups are also used to analyze the rejection rate of patterns of fits where the boundary condition design criterion cannot guarantee assimilability due to an alignment requirement. An analytical methodology to deal with patterns with a multiplicity of two is presented and discussed, overcoming traditional methods where an arbitrary fit is used as zero for the stack-up, thereby limiting the result.

The alignment problem is further studied, proving once more that using bolted connections to guarantee alignment is not ideal. Nonetheless, the effect of different geometric specifications is analyzed, giving a designer a guide on the effect of different modifiers and their impact on alignment.

The existence of manufacturing specifications as a separate entity from the functional one leads to the correlation problem between the two. The issue is even more challenging if deformable components are considered. A methodological framework to correlate functional and manufacturing specifications for deformable components is presented and validated experimentally.

The concept of verification specifications is also explored, and a possible interpretation in line with the standard is proposed. In the ISO GPS system, verification specifications are mentioned, but no actual explanation of their contents or usage is provided.

In the field of design using metrology, the usage of real statistics from actual production batches is explored. Using the Second Order Tolerance Analysis (SOTA) method, different settings are tested, showing that when dealing with real statistical data, linear analysis can lead to misleading results. Guidelines are then extrapolated and stated.

Lastly, the implementation of the proposed framework in an actual industrial environment is shown and discussed. The adaptations needed for the theoretical framework are also demonstrated and discussed.

The research process has always been linked to an actual industrial application. This means that issues were collected by collaborating with industry on actual case studies. Methodologies and tools to overcome these issues were then analyzed from a theoretical point of view, proposing an academic solution. The proposed solutions were then tested in an industrial environment to explore their actual applicability and define the adaptations needed for practical usage.

The process of collecting issues from industry meant that a non-linear path was followed in the research activity. The result shows in this thesis come from a rearrangement of all the activity is a more structured and usable way.

This work can be seen both as an ending and a starting point. It is an ending point for my research activities relevant to my PhD program. However, it equally stands as a vibrant prologue to future research endeavors, poised to propel the realization of a more effective and streamlined ISO GPS system implementation in industry. For this reason, as also stated in the introduction, “the main purpose of this document is to establish a new vision for the system and be the starting point for future research lines and activities.” Further work will be needed in the future to explore all possible repercussions of the proposed vision.

With the objective of laying the groundwork for extended research and innovative endeavors, this document inherently assumes a pioneering role in shaping the trajectory of forthcoming research streams and initiatives. It effectively establishes the foundation for a paradigm shift towards enhanced proficiency in the domain of industrial geometric specification management.

13 || Future research agenda

A leader is one who knows the way, goes the way, and shows the way.

John C. Maxwell

Now, at the end of this work, it is time to start tracing the feeble line showing future possible evolutions, expanding radially from what was presented here. In Fig. 13.1, each of the contents presented throughout this thesis is located within the research gap scheme. Consequently, it is straightforward to see gaps that still need to be covered. All of these gaps, of course, represent possible future evolutions. Plausible evolution for each of the contributions presented in this work will also be presented in this chapter.

Looking at the missing gaps, two main future research items can be defined. Firstly, the definition of specification efficiency. When dealing with functional geometric specifications, how can we be sure to deal with the most efficient specification possible? The concept of efficient geometric specification lies behind the possibility to allow for maximum variability (larger tolerances) while still respecting functional requirements. There are two main contributors that lead to tighter tolerances in tolerance synthesis: the number of tolerances in the stack-up and the sensitivity factors. The number of tolerances is related to the specification scheme itself. For instance, if the geometric specification does not consider the assembly requirements, longer stack-ups are needed (see chapter 7). The sensitivity factors are related to the nominal geometry of the product. When trying to optimize a geometric specification, both the specification scheme and the geometry need to be considered. The specification efficiency might be based on Computer Aided Tolerancing simulation. The preliminary idea is to define the efficiency as the inverse of the output (Key Characteristics) bound when all input tolerances are set to be unitary. An efficiency can be defined for each functional equation $U_i = f_i(x_j)$ where U_i is the stack-up output, and x_j the stack-up inputs. Under these hypotheses and using a variational model for statistical tolerance analysis, the efficiency for each functional equation can be defined as follows.

$$\epsilon_i = \frac{1}{2k \cdot \sqrt{(\nabla^T f_i)^2 \cdot \{\alpha_j\}}} \quad (13-1)$$

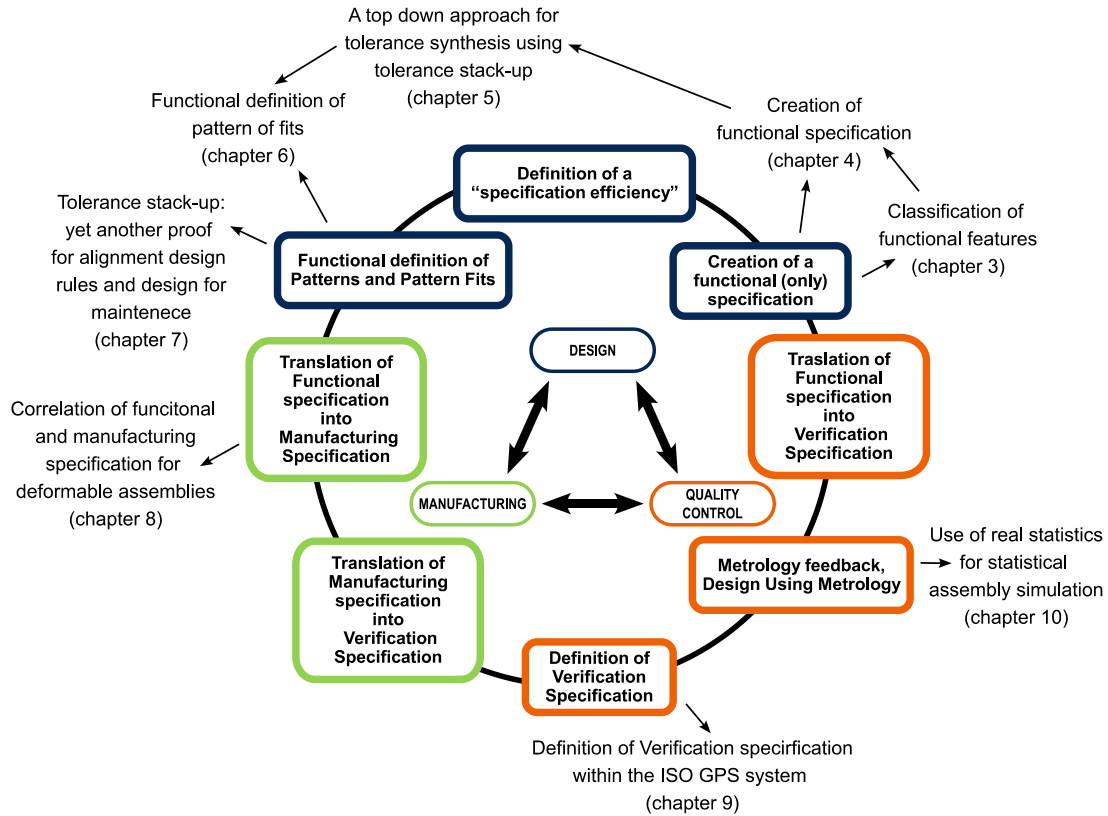


Fig. 13.1: graphical representation of the research gaps and the contributions in this thesis.

Where k is the coverage factor, $\nabla^T f_i$ is the gradient of the functional equation representing the geometry contribution, and $\{\alpha_j\}$ is a vector depending on the type of tolerance. Eventual correction coefficients shall be investigated, and the merging of different efficiencies coming from different functional equations for the same component shall be defined.

Also, the conversion of functional or manufacturing specifications into verification specifications shall be investigated. A proper methodological framework shall be defined starting from the proposed definition. Constraints related to the actual industrial application of the concept should also be studied.

Once all the gaps are covered, a radial expansion can be performed.

Regarding the definition of functional specifications, the methodology could be expanded by proposing a structured approach considering additional specifications on waviness and roughness.

Regarding the functional definition of patterns of fits, two interesting evolutions might be considered. The first one is still in the analytical domain and consists of the analytical extension of the methodology to patterns of any multiplicity. The first step is defining an interpolation function for

the rejection rate as a function of the number of fits. The rejection rate function is bounded between 0 and 1 for any value of n (number of fits). If the boundary condition design criterion is not respected, the limit of the function for an infinite number of fits is one $\lim_{n \rightarrow +\infty} R(n) = 1$. With these hypotheses, an exponential interpolating equation can be assumed in the form of:

$$R(n) = 1 - [1 - \theta_2]e^{-\frac{1}{\theta_1}(n-2)} \quad (13-2)$$

Where θ_2 is the rejection rate of a couple of fits, and θ_1 represents the time constant. An analytical model aiming to estimate θ_1 (and θ_2) as function of the fits parameters may be defined. The model for θ_2 is not essential since this value can be already analytically defined.

Alternatively, the β coefficient can be derived from equation (6-8):

$$\beta(n) = 1 - \frac{n^{-1}\sqrt{1 - R(n)}}{R(2)} \quad (13-3)$$

If equation (13-2) is considered as correct, it is possible to obtain that β is a convergent function for $n \rightarrow \infty$ and that the value of $\beta(\infty)$ is:

$$\beta(\infty) = \frac{1}{r(\infty)} \left(1 - e^{-\frac{1}{\theta_1}}\right) \quad (13-4)$$

Where $r(\infty)$ is the rejection rate for a couple of fits pertaining to an infinite pattern.

The interpolating equation for β becomes:

$$\beta(n) = \theta_1 - [\theta_1 - 1]e^{-\theta_2(n-2)} \quad (13-5)$$

Where $\theta_1 = \beta(\infty)$ and therefore can be determined analytically. The determination of the coefficients needed for the regression is currently under investigation following a DoE approach.

Another opportunity lies in the numerical solution of the problem through Monte Carlo simulation. The solution of the linear pattern considering interference only along one line is quite straightforward and was already implemented to verify the analytical solutions that were presented. The numerical solution allows considering patterns of any shape, also considering the real interference that could occur in any direction. In this case, a virtual assembly routine shall be programmed to detect the maximum interference and look for a relative position between the two parts allowing assemblability. Currently, a pseudocode is under evaluation and looks promising.

For the correlation between functional and manufacturing specifications, the model shall be completed considering the statistical correlation between functional and manufacturing tolerance values. The same procedure presented in this work shall be followed for different simplified

assemblies, and a proper regression model shall be implemented. The regression model may also be created using real data from physical measurements.

Looking at the concept of verification specification, an interesting project might investigate the advantages of using such a concept in the industry through specific industrial surveys. The possible outcome of such an investigation might help in defining even more the content, usage, and definition of geometric verification specification with respect to what was presented in this thesis.

At this point, coming back to the beginning of this work. The proposed survey shall be extended internationally, at the European level first and worldwide after. At the time of writing, international collaborations are ongoing to achieve this goal. The outcome of such an extension will increase the statistical significance of the survey with more entries. At the same time, it will allow a comparison of the situation in different geographical areas.

Moreover, a comparison across different industrial sectors shall be performed. So far, this type of analysis was not possible due to the limited number of entries from some of the industrial sectors.

Finally, a project has already been written regarding the digitalization of the geometrical specification process using the MBD (Model-Based Definition) approach. The project will study and analyze Model-Based Definition (MBD) tools. The capabilities of the MBDVidia software tool will be investigated, with a particular focus on the practical implementations that this solution can offer to local businesses. They will investigate the compatibility of this software tool with commonly used CAD packages, as well as with CAT simulation tools and metrological inspection tools. The MBD module of SolidWorks, a widely used CAD solution among Small and Medium Enterprises (SMEs), will also be examined. Simultaneously, research to assess the actual adoption of these tools at the local and national levels through targeted surveys will be conducted. Obstacles that hinder their adoption in the industrial sector and possible strategies to facilitate a smoother transition for companies towards Industry 4.0 will be defined. Methodologies that can find immediate industrial applications for MBD, with the aim of improving intra and inter-company communication, will be developed. The possibility of defining layers of information within the same CAD model to consolidate all the necessary geometric and dimensional information in a single format for product development will also be explored.

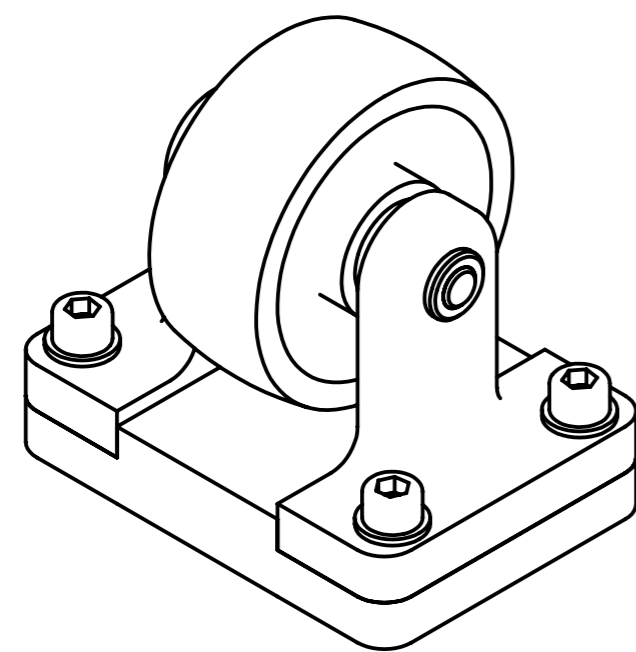
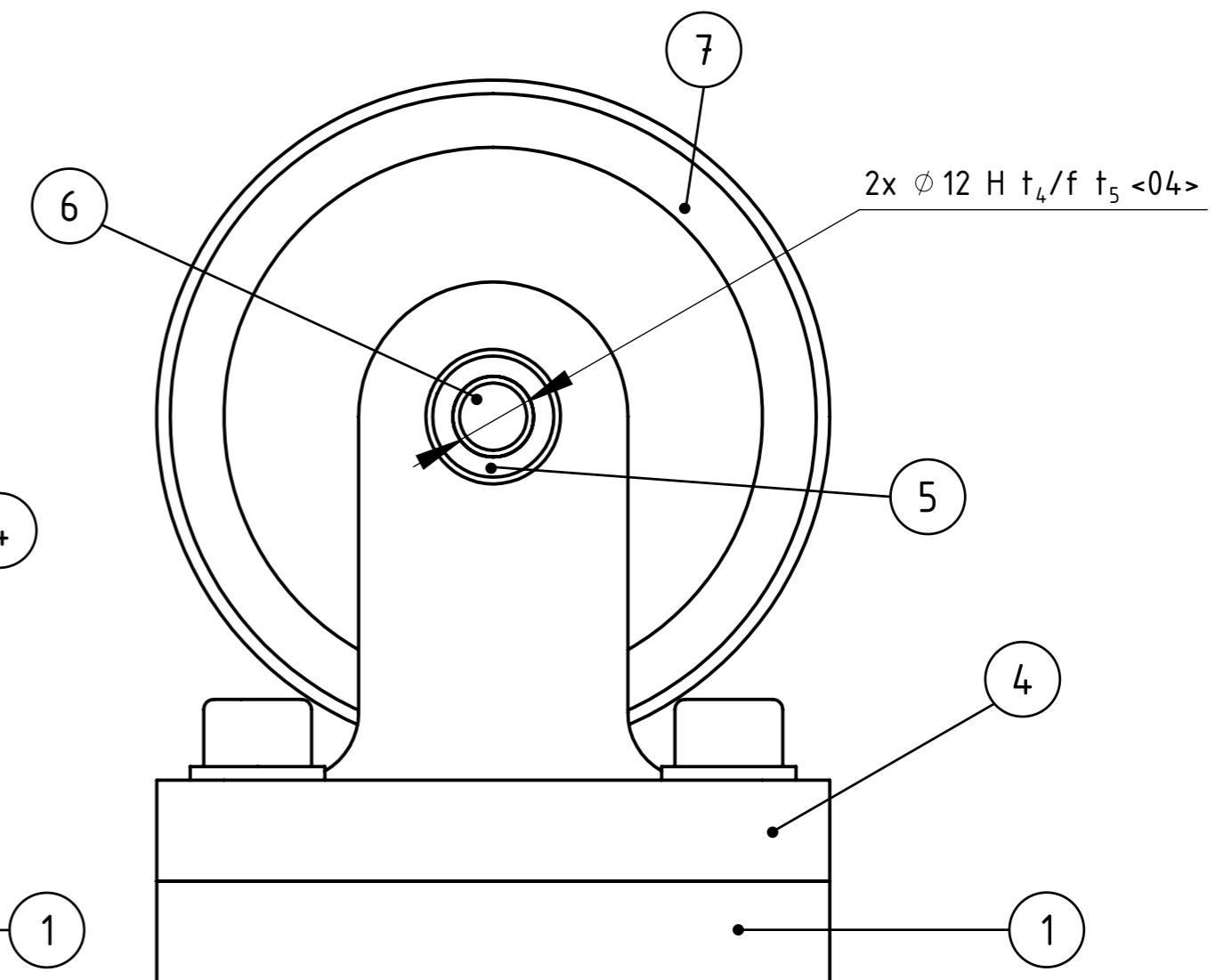
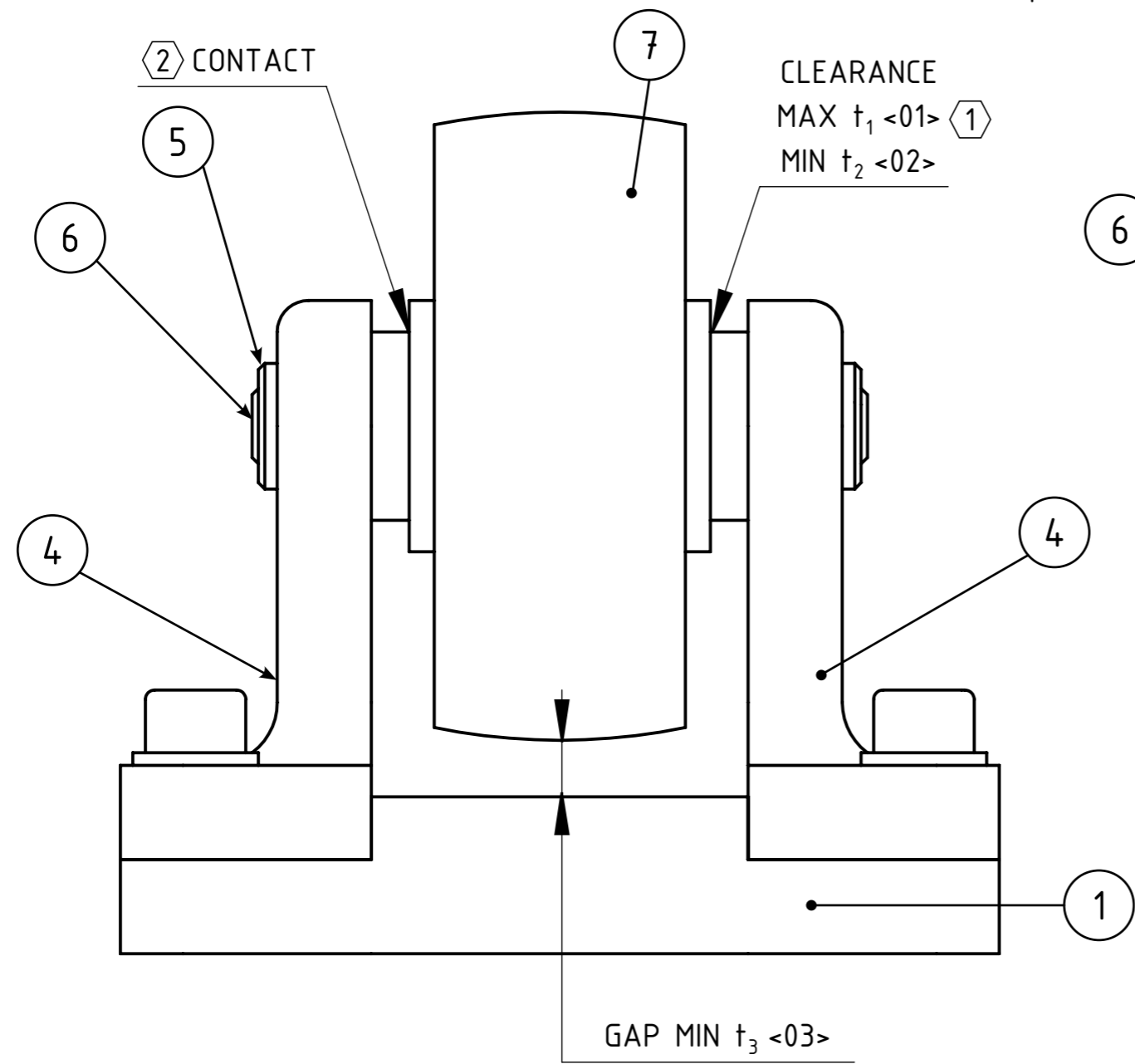
Appendices

A || Geometric Specification 2D drawings for the case study of chapter 4

In this appendix all actual drawing coming from the case study presented throughout chapters 3 and 4 will be presented in their entirety.

A.1 || Assembly Drawing

The first drawing to be presented is the one relevant to the full assembly.



Components list:

- 1 - Base (D-0001-02-01-2023)
- 4 - Riser (D-0001-02-02-2023)
- 5 - Bushing (D-0001-02-03-2023)
- 6 - Shaft (D-0001-02-04-2023)
- 7 - Wheel (D-0001-02-05-2023)

Sub-assemblies list:

- 2 - Riser_asm (D-0001-01-01-2023)
Components: 4 & 5
- 3 - Wheel_asm (D-0001-01-02-2023)
Components: 6 & 7

Functional Drawing

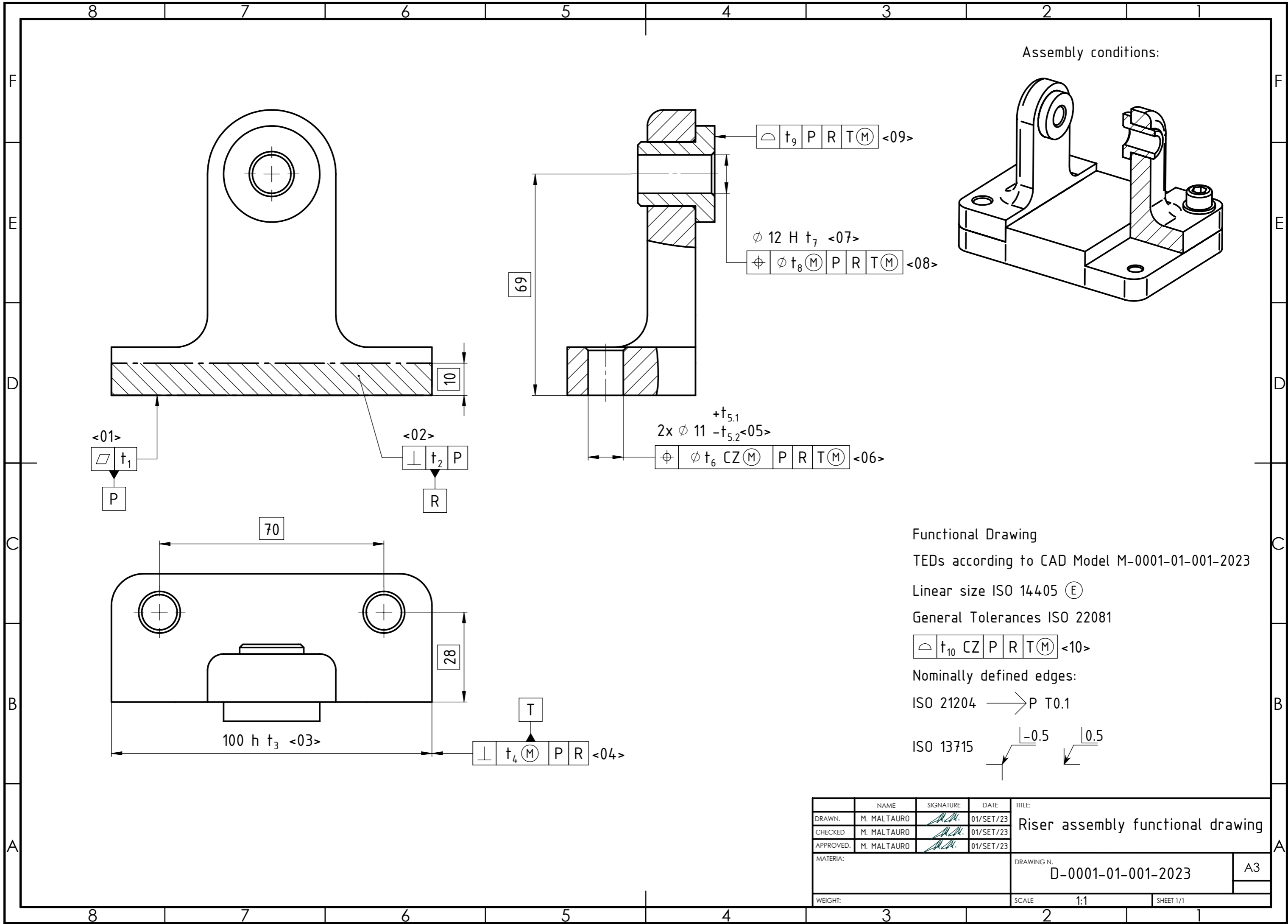
TEDs according to CAD Model
M-0001-00-001-2023
Linear size ISO 14405 (E)
Requirement 1 valid only if
condition 2 is respected

	NAME	SIGNATURE	DATE	TITLE:
DRAWN.	M. MALTAURO	<i>M.M.</i>	01/SET/23	Final assembly functional drawing
CHECKED	M. MALTAURO	<i>M.M.</i>	01/SET/23	
APPROVED.	M. MALTAURO	<i>M.M.</i>	01/SET/23	
MATERIA:				DRAWING N.
				D-0001-00-001-2023
WEIGHT:				SCALE 1:1
				SHEET 1/1

A3

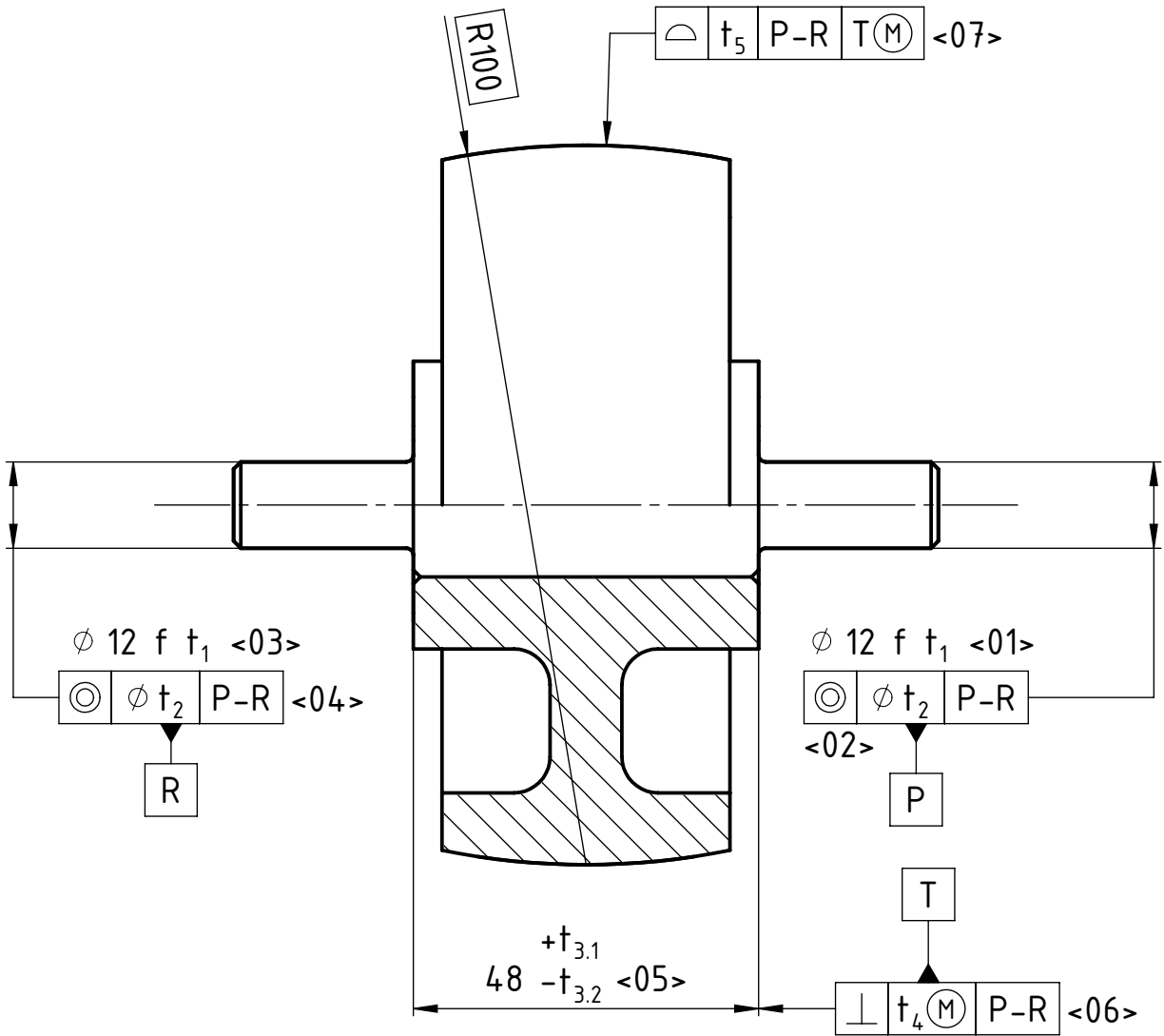
A.2 || Sub-assembly Drawings

In a top down approach, after the full assembly drawing, the sub-assembly drawings follows.

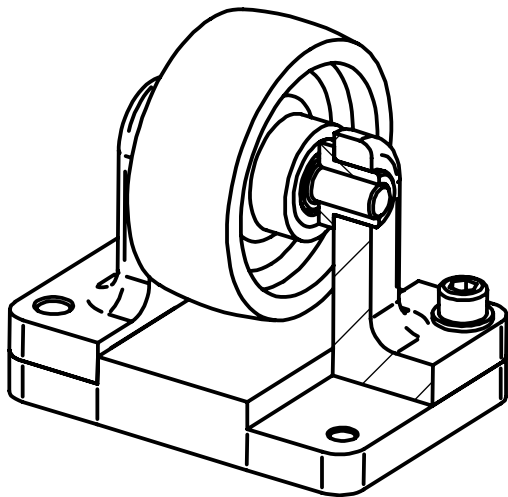


	NAME	SIGNATURE	DATE	TITLE:
DRAWN.	M. MALTAURO	<i>M. Maltauro</i>	01/SET/23	Riser assembly functional drawing
CHECKED	M. MALTAURO	<i>M. Maltauro</i>	01/SET/23	
APPROVED.	M. MALTAURO	<i>M. Maltauro</i>	01/SET/23	
MATERIA:				DRAWING N.
				D-0001-01-001-2023
WEIGHT:				SCALE 1:1
				SHEET 1/1

A3



Assembly conditions:



Functional Drawing

TEDs according to CAD Model

M-0001-01-002-2023

Linear size ISO 14405 (E)

General Tolerances ISO 22081

t_6 CZ P-R T(M) <08>

Nominally defined edges:

ISO 21204 \rightarrow P T0.1

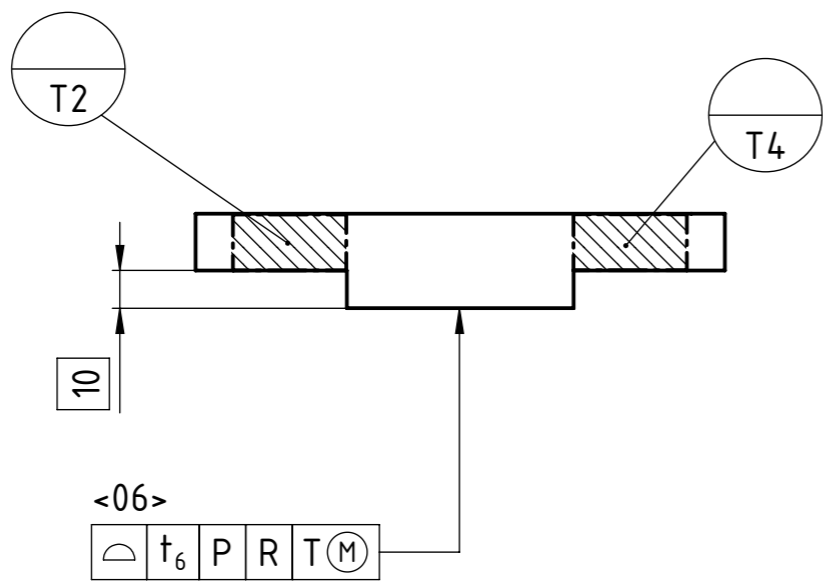
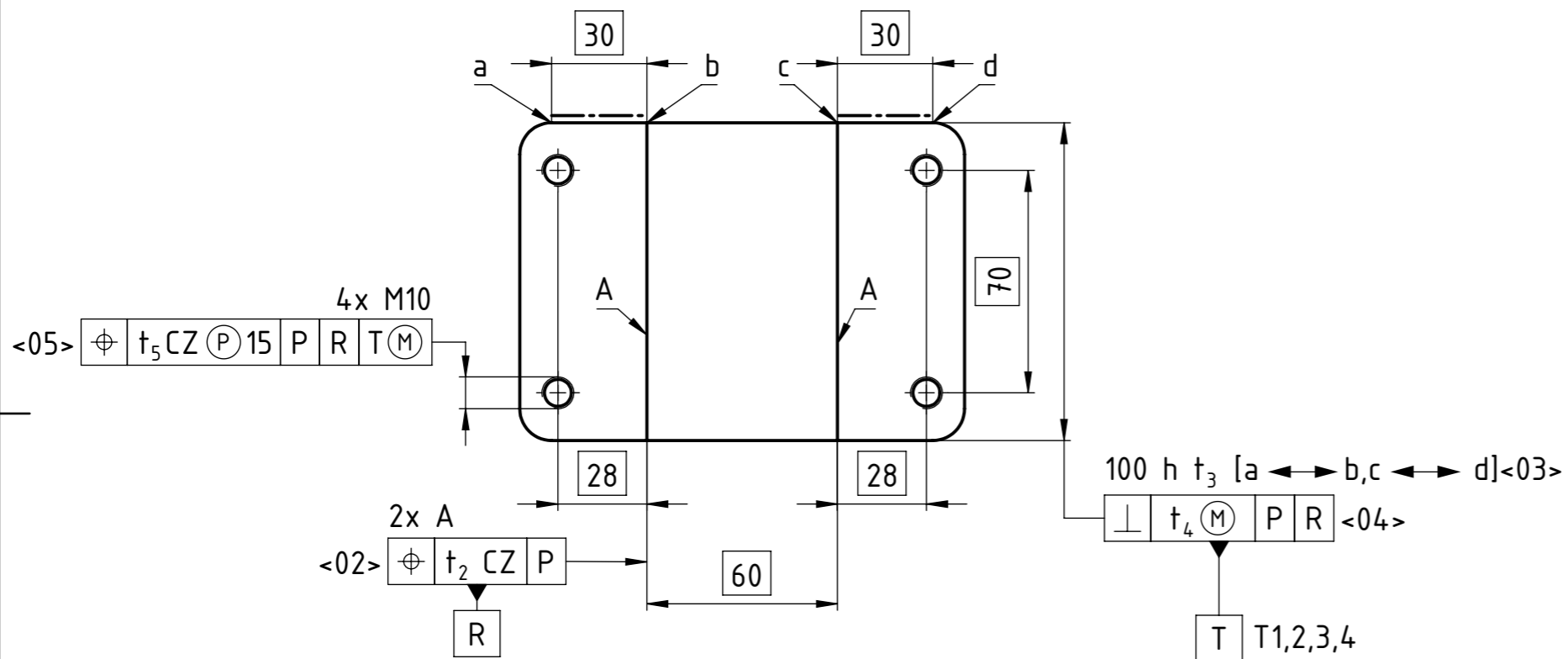
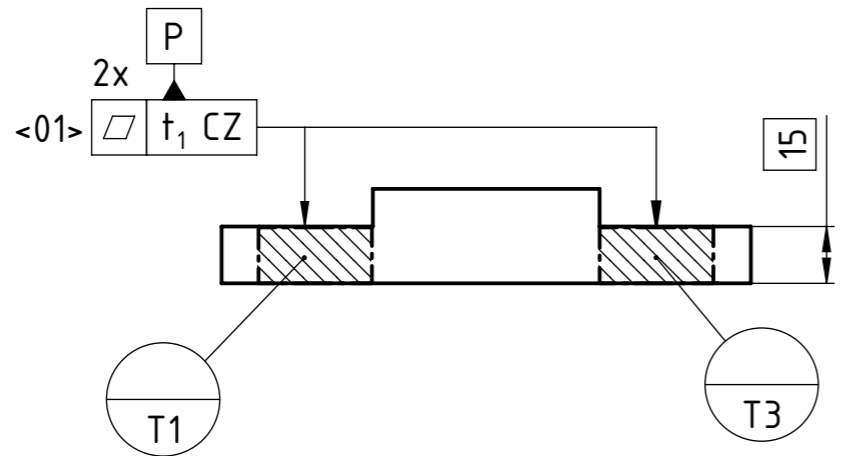
ISO 13715 $\begin{matrix} \swarrow -0.5 \\ \searrow 0.5 \end{matrix}$

	NAME	SIGNATURE	DATE	TITLE:
DRAWN.	M. MALTAURO	<i>M. Maltauro</i>	01/SET/23	Wheel assembly functional drawing
CHECKED	M. MALTAURO	<i>M. Maltauro</i>	01/SET/23	
APPROVED.	M. MALTAURO	<i>M. Maltauro</i>	01/SET/23	
MATERIA:				DRAWING N.
				D-0001-01-002-2023
WEIGHT:				SCALE
				1:1
				SHEET 1/1

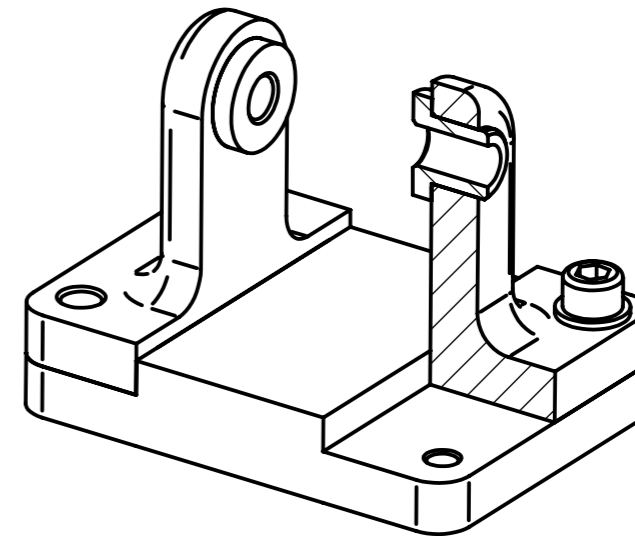
A4

A.3 || Part Drawings

Finally, all part drawings are presented in the following.



Assembly conditions:



Functional Drawing

TEDs according to CAD Model M-0001-02-001-2023

Linear size ISO 14405 (E)

General Tolerances ISO 22081

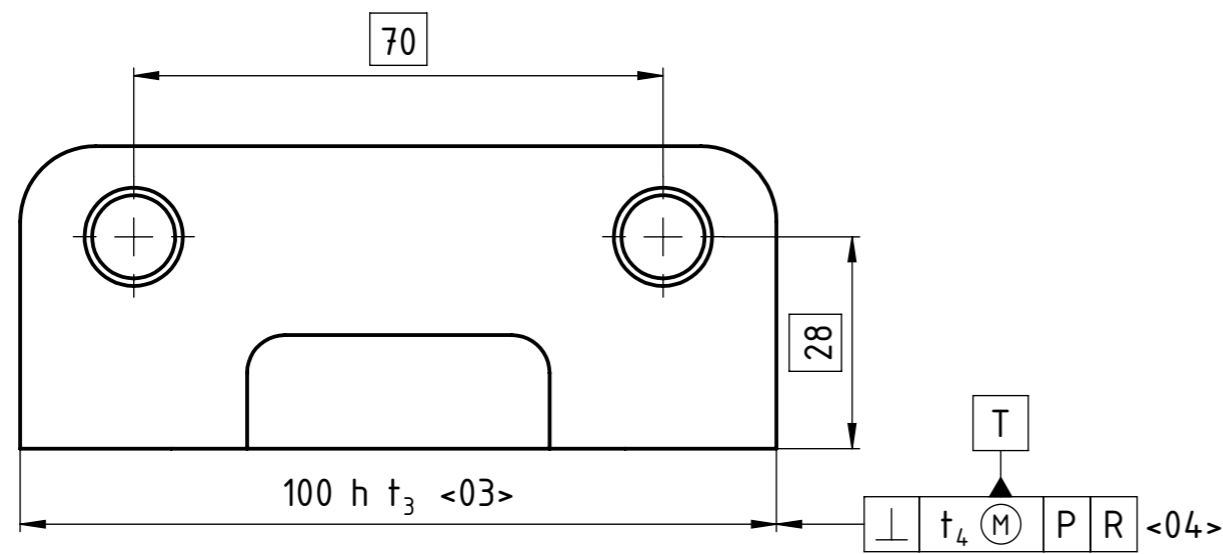
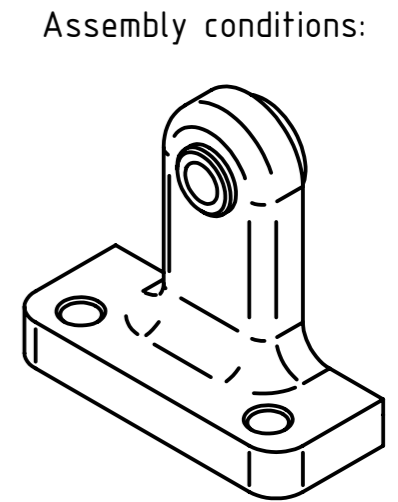
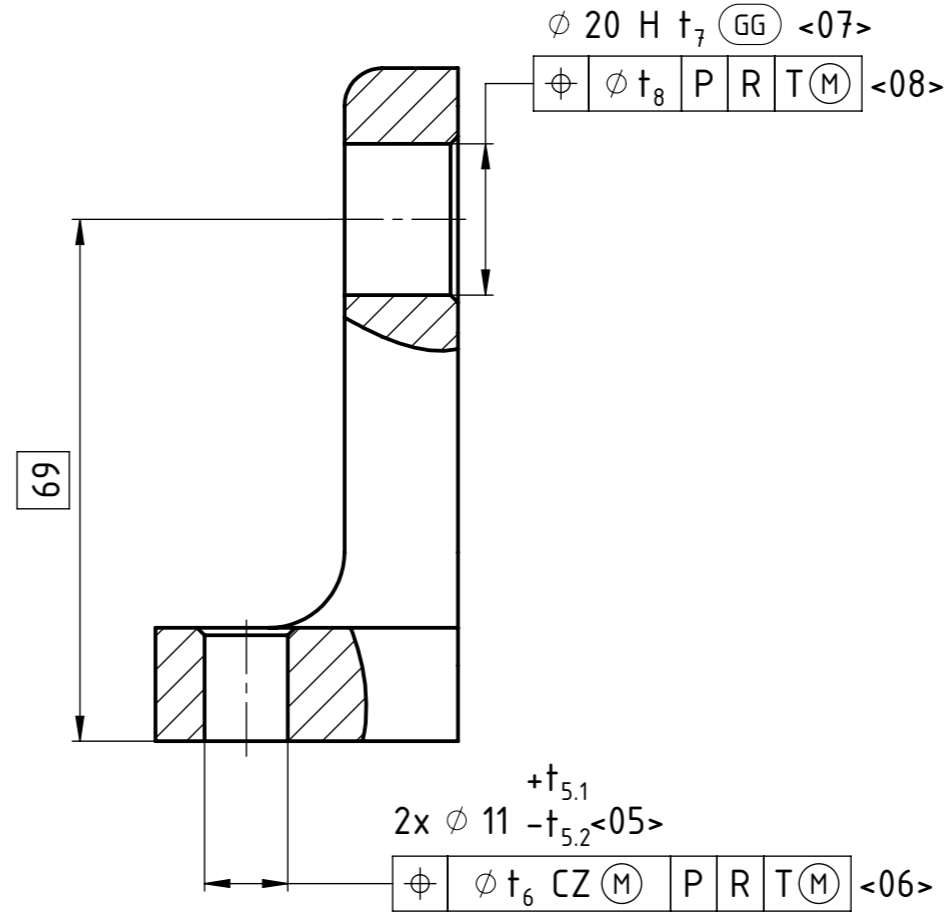
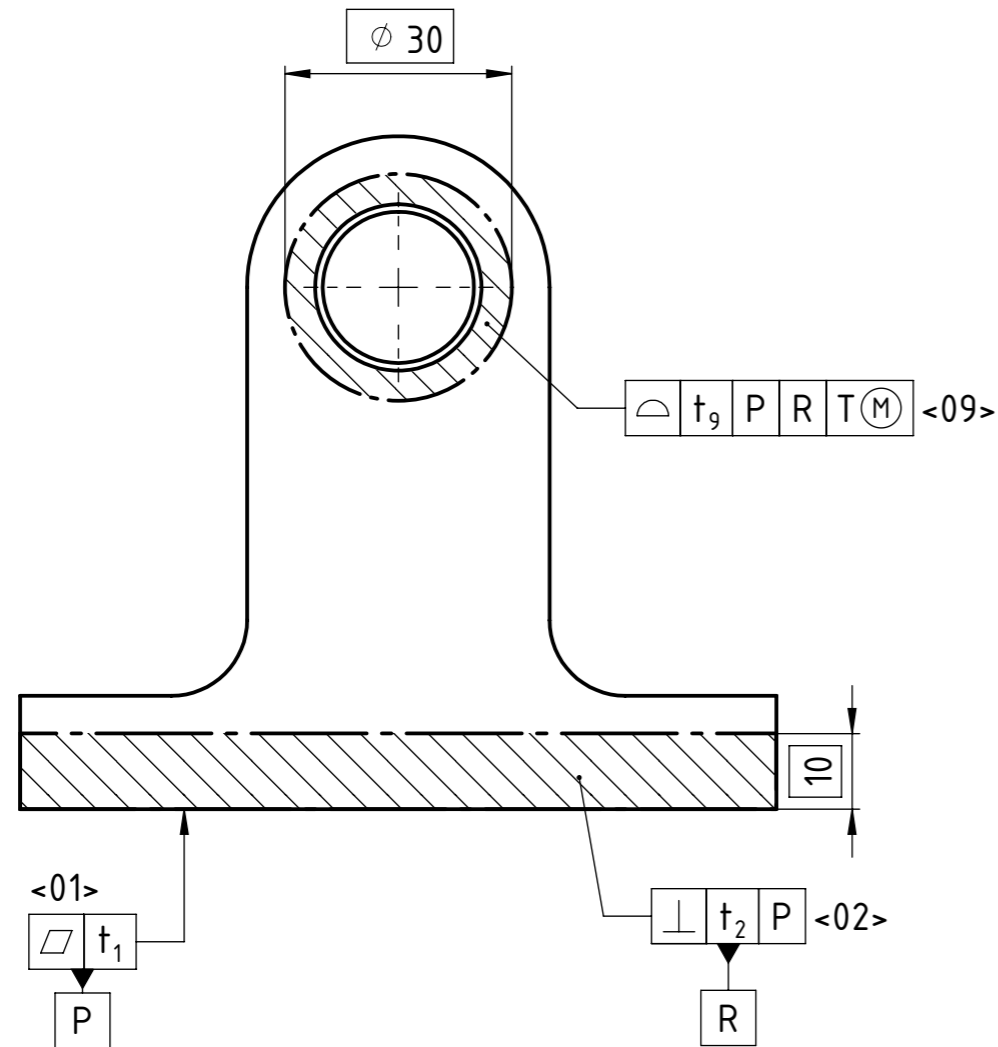
\ominus t_7 CZ P R T (M) <07>

Nominally defined edges:

ISO 21204 \rightarrow P T0.1

ISO 13715 \swarrow -0.5 \searrow 0.5

	NAME	SIGNATURE	DATE	TITLE:
DRAWN.	M. MALTAURO	<i>M. Maltauro</i>	01/SET/23	Base functional drawing
CHECKED	M. MALTAURO	<i>M. Maltauro</i>	01/SET/23	
APPROVED.	M. MALTAURO	<i>M. Maltauro</i>	01/SET/23	
MATERIA:				DRAWING N.
				D-0001-02-001-2023
				A3
WEIGHT:				SCALE 1:2
				SHEET 1/1



Functional Drawing
 TEDs according to CAD Model M-0001-02-002-2023

Linear size ISO 14405 (E) (GG)

General Tolerances ISO 22081

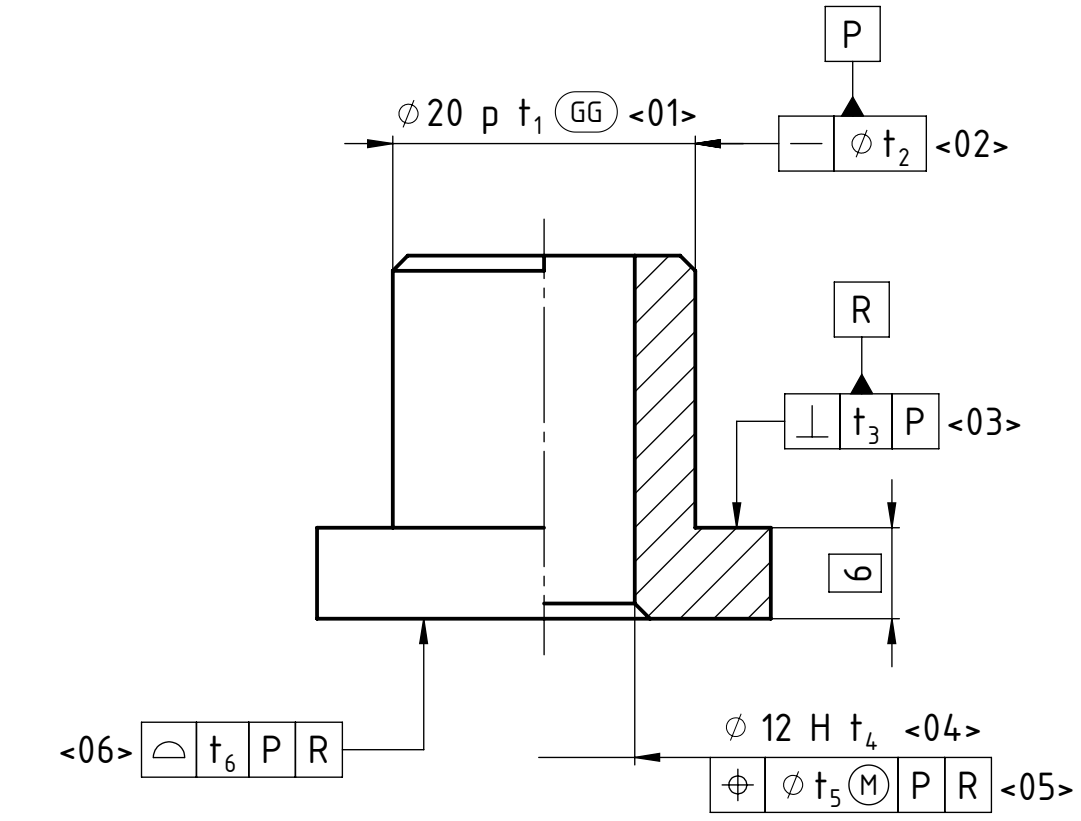
$\ominus t_{10}$ CZ P R T M <10>

Nominally defined edges:

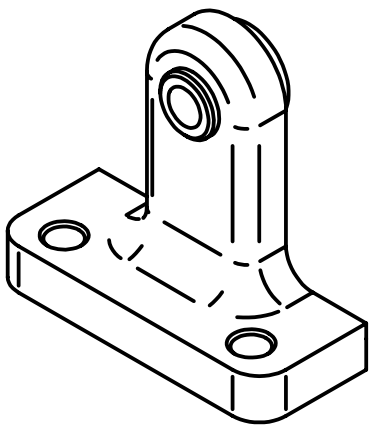
ISO 21204 \rightarrow P T0.1

ISO 13715 \swarrow $\begin{matrix} -0.5 \\ 0.5 \end{matrix}$

	NAME	SIGNATURE	DATE	TITLE:
DRAWN.	M. MALTAURO	<i>M. Maltauro</i>	01/SET/23	Riser functional drawing
CHECKED	M. MALTAURO	<i>M. Maltauro</i>	01/SET/23	
APPROVED.	M. MALTAURO	<i>M. Maltauro</i>	01/SET/23	
MATERIA:				DRAWING N. D-0001-02-002-2023
WEIGHT:				A3
SCALE 1:1				SHEET 1/1



Assembly conditions:



Functional Drawing

TEDs according to CAD Model

M-0001-02-003-2023

Linear size ISO 14405 (E) (GG)

General Tolerances ISO 22081

$\frac{\Delta}{t_7}$ CZ P R <07>

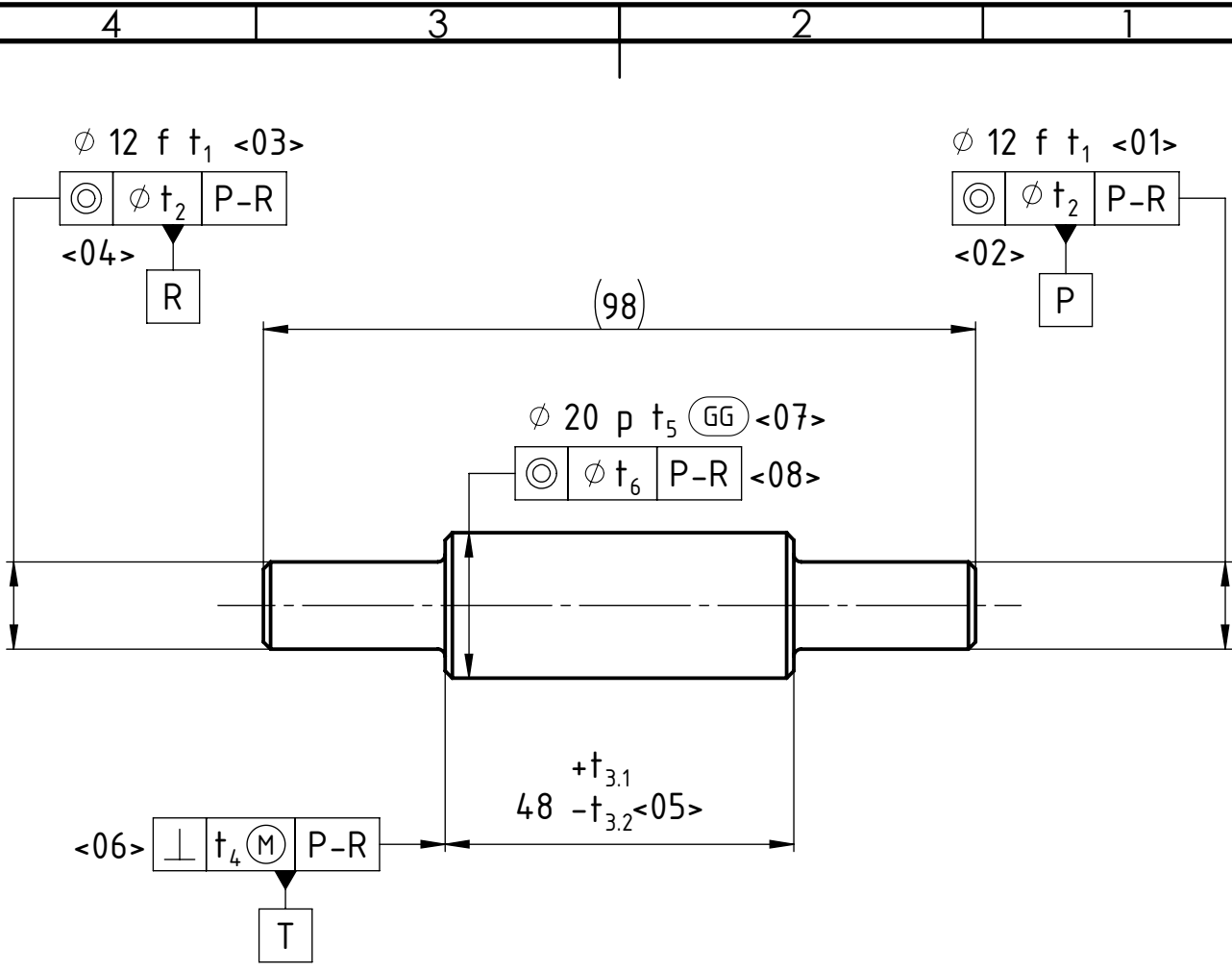
Nominally defined edges:

ISO 21204 \rightarrow P T0.1

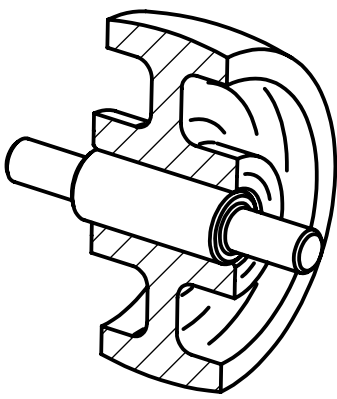
ISO 13715 $\begin{matrix} | -0.5 \\ | 0.5 \end{matrix}$

	NAME	SIGNATURE	DATE	TITLE:
DRAWN.	M. MALTAURO	<i>M.M.</i>	01/SET/23	Bushing functional drawing
CHECKED	M. MALTAURO	<i>M.M.</i>	01/SET/23	
APPROVED.	M. MALTAURO	<i>M.M.</i>	01/SET/23	
MATERIA:				DRAWING N.
				D-0001-02-003-2023
WEIGHT:				SCALE
				2:1
				SHEET 1/1

A4



Assembly conditions:



Functional Drawing
 TEDs according to CAD Model
 M-0001-02-004-2023

Linear size ISO 14405 (E) (GG)
 General Tolerances ISO 22081

$\frac{\Delta}{r}$ t_7 CZ P-R T (M) <09>

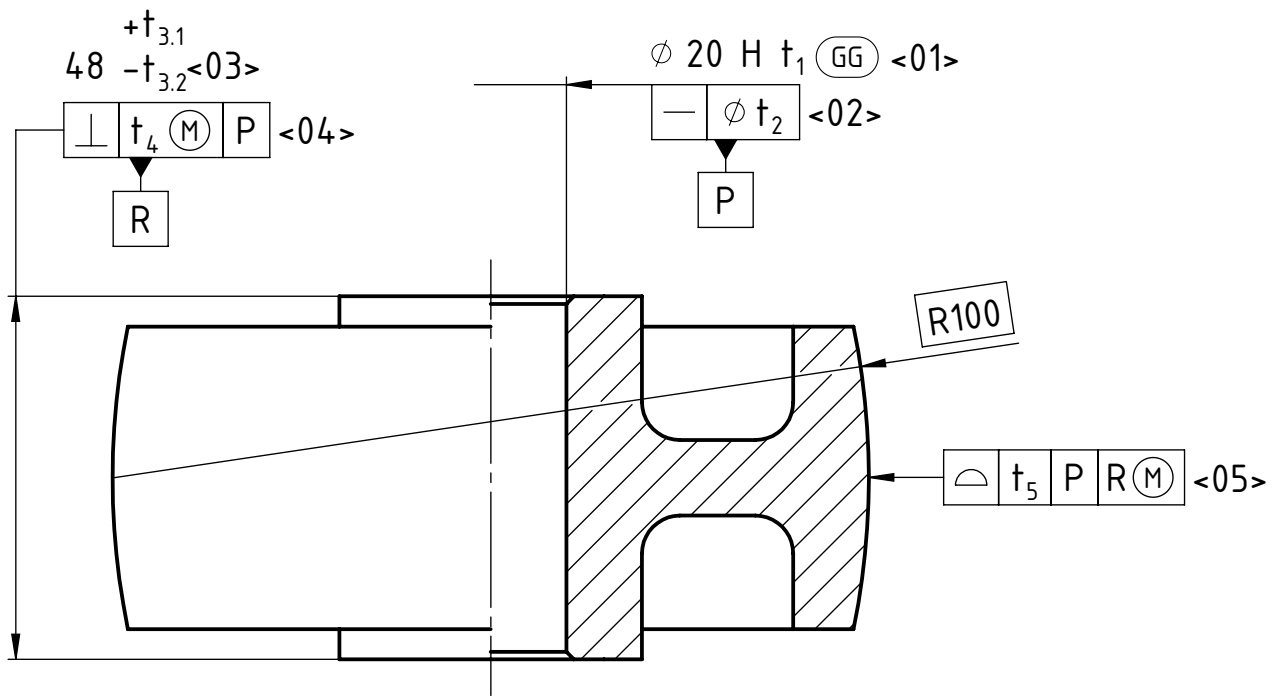
Nominally defined edges:

ISO 21204 \rightarrow P T0.1

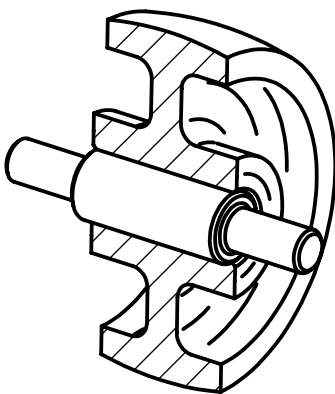
ISO 13715 \swarrow $\frac{-0.5}{\sqrt{r}}$ \searrow $\frac{0.5}{\sqrt{r}}$

	NAME	SIGNATURE	DATE	TITLE:
DRAWN.	M. MALTAURO	<i>M. Maltauro</i>	01/SET/23	Shaft functional drawing
CHECKED	M. MALTAURO	<i>M. Maltauro</i>	01/SET/23	
APPROVED.	M. MALTAURO	<i>M. Maltauro</i>	01/SET/23	
MATERIA:				DRAWING N. D-0001-02-004-2023
WEIGHT:				SCALE 1:1 SHEET 1/1

A4



Assembly conditions:



Functional Drawing

TEDs according to CAD Model

M-0001-02-005-2023

Linear size ISO 14405 (E) (GG)

General Tolerances ISO 22081

$\text{半} t_6 CZ P R (M) <06>$

Nominally defined edges:

ISO 21204 $\longrightarrow P T0.1$

ISO 13715 $\begin{matrix} | -0.5 \\ | 0.5 \end{matrix}$

	NAME	SIGNATURE	DATE	TITLE:
DRAWN.	M. MALTAURO	<i>M.M.</i>	01/SET/23	Wheel funcitonal drawing
CHECKED	M. MALTAURO	<i>M.M.</i>	01/SET/23	
APPROVED.	M. MALTAURO	<i>M.M.</i>	01/SET/23	
MATERIA:				DRAWING N.
				D-0001-02-005-2023
WEIGHT:				SCALE
				1:1
				SHEET 1/1

A4

B || Derivation of equation for statistical tolerance analysis

The four statistical raw moments, for the output, can be written as follow for a linear analysis [162][102].

$$E(U_i) = 0$$

$$E(U_i^2) = \sum_{j=1}^n b_j^2 \mu_2(x_j)$$

$$E(U_i^3) = \sum_{j=1}^n b_j^3 \mu_3(x_j)$$

$$E(U_i^4) = \sum_{j=1}^n b_j^4 \mu_4(x_j) + \sum_{j=1}^{n-1} \sum_{k=j+1}^n 6 b_j^2 b_k^2 \mu_4(x_j) \mu_4(x_k)$$

Where b_j represent the sensibility of the output U_i with respect to the input variable x_j :

$$b_j = \frac{\partial U_i}{\partial x_j}$$

The raw moments are used to find the central moments:

$$\mu_1(U_i) = E(U_i) + \bar{u}_i = \bar{u}_i$$

$$\mu_2(U_i) = E(U_i^2) - [E(U_i)]^2 = E(U_i^2)$$

$$\mu_3(U_i) = E(U_i^3) - 3 E(U_i^2)E(U_i) + 2[E(U_i)]^2 = E(U_i^3)$$

$$\mu_4(U_i) = E(U_i^4) - 4 E(U_i^3)E(U_i) + 6 E(U_i^2)[E(U_i)]^2 - 3 [E(U_i)]^4 = E(U_i^4)$$

Where \bar{u} is the value that the output (U_i) assumes when all the input variables x_j are set to the values where the sensitivities are quantified (expansion pole).

By combining together these equations it is possible to find the scaled moments of the output distribution.

$$\mu_1(U_i) = \bar{u}_i$$

$$\sigma_i = \sqrt{\mu_2(U_i)} = \sqrt{\sum_{j=1}^n b_j^2 \sigma_j^2}$$

$$\beta_{1i} = \frac{\mu_3(U_i)}{\sigma_i^3} = \frac{\sum_{j=1}^n b_j^3 \sigma_j^3 \beta_{1j}}{\sqrt{[\sum_{j=1}^n b_j^2 \sigma_j^2]^3}}$$

$$\beta_{2i} = \frac{\mu_4(U_i)}{\sigma_i^4} = 3 + \frac{\sum_{j=1}^n b_j^4 \sigma_j^4 \gamma_{2j}}{[\sum_{j=1}^n b_j^2 \sigma_j^2]^2}$$

Where γ_{2j} is the excess kurtosis ($\gamma_{2j} = \beta_{2j} - 3$) that represent the difference in kurtosis between the given distribution and a normal one.

C || Training agenda

In this appendix a detailed agenda of the training modules as resented in sub-section 11.2.1 on page 259 is presented.

Hours	Day	Topic	Description
2	1	Geometrical Product Specifications: general introduction	Introduction to ISO Geometrical Products Specification standards and their use in modern industry.
2	2	Geometrical Product Specifications: integrated ISO GPS/ASME GD&T methodology fundamentals	Basic concepts of the integrated ISO GPS/ASME GD&T approach to geometrical specification.
2	3	How to Read (H2R) methodology - part A	Methodological approach to the reading and comprehension of a detailed drawing with geometrical specifications.
1	4	How to Read (H2R) methodology - part B	Methodological approach to the reading and comprehension of a detailed drawing with geometrical specifications.
1		H2R basic topics: Geometric tolerances hierarchy and interpretation	Presentation of the definitions of geometric tolerances and their hierarchy.
1		H2R basic topics: Datum System - hierarchy and interpretation	Construction of a part reference system defined by the Datum System. Association of part dof to Datum Features.
0,5	5	H2R advanced topics: General tolerances	Interpretation of general tolerances for dimensional and geometrical tolerances: former and current practice.
0,5		H2R advanced topics: Non Rigid Parts (ISO 10579) and examples	Interpretation of geometrical specifications for deformable bodies, e.g., injection moulded parts, sheet metal etc, in accordance with ISO 10579 with examples.
2	6	How to Write (H2W) methodology - Part A	Methodological approach to the write a detailed drawing with geometrical specifications - part A.
2	7	How to Write (H2W) methodology - Part B	Methodological approach to the write a detailed drawing with geometrical specifications - part B.

1	8	H2W advanced topics: Dependency/independency principles and envelope requirement	How to deal with the dependency and independency principle, differences between ISO GPS/ASME GD&T interpretation and the envelope requirement as a functional indication for mating geometries.
1		H2W advanced topics: Linear sizes according ISO 14405-1	The correct use of linear sizes according to ISO 14405-1: what is a linear size and what is not, in other words, when to use them wisely.
1	9	H2W advanced topics: Dimensions other than linear sizes (ISO 14405-2)	The correct specification for what is not a linear size: the use of TEDs (Theoretically Exact Dimensions) and geometrical tolerances according to ISO 14405-2.
1		H2W advanced topics: The Boundary Condition concept. MMC and LMC modifiers (with applications)	Maximum Material Condition and Least Material condition, how to use them to relax the tolerance zone still ensuring functionality.
1	10	H2W advanced topics: Datum System and Datum targets	Datum system management for actual components: taking the next step beyond the basic examples in the standards and the use of datum targets.
1		H2W advanced topics: Profile tolerances and additional symbols (UZ, OZ)	The use of profile tolerances, when to use them and how to modify to our will their effect using additional indicators.
0,5		Specification of a pattern of elements (SZ, CZ, ><). Projected tolerance zone (P)	The use of patterns in geometrical specification: how to correctly invoke patterns according to the standard and take the best out of them through examples.
0,5	11	How to Compute (H2C) methodology: Position tolerances assignment	Methodological approach to the computing dimensional and location tolerance for shaft-hole connections assuring assemblability.
1		H2C methodology: Introduction to Tolerance Stack-up analysis: worst case and statistical approaches	Different computation models for tolerance analysis: pros and cons of worst case and statistical approaches.
2	12	H2C methodology: Linear geometric tolerance stack-up analysis	How to easily create a monodimensional linear tolerance stack-up starting from a geometrical specification.
2	13	H2C methodology: Tool for the computation of Stack-up Analyses - part 1	Presentation of the excel file model for the computation of stack-ups in R&D and ME, with examples - part 1.
1	14	H2C methodology: Tool for the computation of Stack-up Analyses - part 2	Presentation of the excel file model for the computation of stack-ups in R&D and ME, with examples - part 2.
1		H2R advanced topics: application examples in Electrolux (by Ambassadors)	Presentation of actual case studies from Electrolux presented by ISO GPS Ambassadors.
2	15	H2R advanced topics: application examples in Electrolux (by Ambassadors)	Presentation of actual case studies from Electrolux presented by ISO GPS Ambassadors.

2	16	How to Measure (H2M) Methodology	Methodological approach to the reading of a specification aiming to define the measurand, its admissible variability, and the reference frame leading to an inspection procedure. Conformance and non-conformance to specifications.
1	17	H2M advanced topics: Coordinate metrology	The use of Coordinate Metrology to check conformity to a geometrical specification: measurement equipments, environment and equipment set-up,...
1			Procedures for the measurement of geometrical specifications: part 1.
1	18	H2M advanced topics:	Procedures for the measurement of geometrical specifications: part 2.
1			Traceability. Uncertainty. Errors sources. Calibrations.

D || Scientific production and tutored dissertations

D.1 || Journal publications

Maltauro, M., Passarotto, G., Meneghello, R., Concheri, G. : Bridging the gap between design and manufacturing specifications for non-rigid parts using the influence coefficient method. The International Journal of Advanced Manufacturing Technology 172, 579-897 (2023). <https://doi.org/10.1007/s00170-023-11480-4>

Ciocca, L., **Maltauro, M.**, Pierantozzi, E., Breschi, L., Montanari, A., Andreucci, L., Meneghello, R.: Evaluation of trueness and precision of removable partial denture metal frameworks manufactured with digital technology and different materials. The Journal of Advanced Prosthodontics 15(2), 55-62 (2023). <https://doi.org/10.4047/jap.2023.15.2.55>

Ciocca, L., **Maltauro, M.**, Cimini, V., Breschi, L., Montanari, A., Andreucci, L., Meneghello, R.: Analysis of the trueness and precision of complete denture bases manufactured using digital and analog technologies. The Journal of Advanced Prosthodontics 15(1), 22-32 (2023). <https://doi.org/10.4047/jap.2023.15.1.22>

Sponchiado, R., Rosso, S., Dal Fabbro, P., Grigolato, L., Elsayed, H., Bernardo, E., **Maltauro, M.**, Ucheddu, F., Meneghello, R., Concheri, G., Savio, G.: Modeling Materials Coextrusion in Polymers Additive Manufacturing. Materials 16(2), 820 (2023). <https://doi.org/10.3390/ma16020820>

Ciocca, L., **Maltauro, M.**, Cimini, V., Breschi, L., Meneghello, R.: Outdoing best-fit approaches for the manufacturing accuracy evaluation of complete denture bases. International Journal on Interactive Design and Manufacturing (IJIDeM) 17, pages1389–1397 (2023). <https://doi.org/10.1007/s12008-022-01162-y>

D.2 || Full paper peer review conference proceedings

Maltauro, M., Morse, E. Towards a Definition of “Geometric Verification Specifications” Within the ISO GPS System. *Procedia CIRP* 119, pp. 339–344 (2023).

<https://doi.org/10.1016/j.procir.2023.03.101>.

Maltauro, M., Meneghello, R., Concheri, G.: Conformity Rate Estimation for Shaft-Hole Pattern Fit Not Compliant with the Boundary Condition Design Criterion. In: Gerbino, S., Lanzotti, A., Martorelli, M., Mirálbes Buil, R., Rizzi, C., and Roucoules, L. (eds.) *Advances on Mechanics, Design Engineering and Manufacturing IV - Proceedings of the International Joint Conference on Mechanics, Design Engineering and Advanced Manufacturing, JCM 2022, June 1-3, 2022, Ischia, Italy*. pp. 1256–1267. Springer International Publishing, Cham (2023) . <https://doi.org/10.1007/978-3-031-15928-2\ 110>

Maltauro, M., Meneghello, R., Concheri, G., Pellegrini, D., Viero, M., Bisognin, G.: A Case Study on the Correlation Between Functional and Manufacturing Specifications for a Large Injection Moulded Part. In: Gerbino, S., Lanzotti, A., Martorelli, M., Mirálbes Buil, R., Rizzi, C., and Roucoules, L. (eds.) *Advances on Mechanics, Design Engineering and Manufacturing IV - Proceedings of the International Joint Conference on Mechanics, Design Engineering and Advanced Manufacturing, JCM 2022, June 1-3, 2022, Ischia, Italy*. pp. 1268–1278. Springer International Publishing, Cham (2023). <https://doi.org/10.1007/978-3-031-15928-2\ 111>

D.3 || Full paper non peer review conference proceedings

Pelizzari, J., **Maltauro, M.**, Campagnolo, A., Uccheddu, F., Meneghetti, G.: Valutazione della resistenza a fatica multiassiale di giunti saldati a tratti in acciaio per applicazioni automotive con il metodo della tensione di picco. In: *Atti del 50° convegno nazionale AIAS - Associazione Italiana per l'Analisi delle Sollecitazioni* (2021)

D.4 || Abstract conference proceedings

Ciocca, L., Meneghello, R., **Maltauro, M.**, “A METROLOGICAL PILOT STUDY TO COMPARE DIGITAL AND ANALOGIC ARTICULATORS FOR COMPLETE DENTURES”, *ICP2023, Prosthodontics on Pathways to Healthy Ageing, 30/08–02/09 2023*. (2023) <https://www.icp-conference.com/wp-content/uploads/2023/08/ICP-2023-London-Program-Book.pdf>

Maltauro, M., Meneghello, R., Concheri, G.: Bridging the Gap between Design and Metrology using Statistical Tolerance Analysis. In: Booklet of abstracts ENBIS and Mathmet joint workshop - Mathematical and Sstatistical Methods for Metrology – 30-31 May 2023. pp. 34-35 (2023). <http://www.msmm2023.polito.it/allegati/Booklet%20of%20abstracts.pdf>

Cimini, V., **Maltauro, M.**, Meneghello, R., Breschi, L., Ciocca, L.: METROLOGICAL TEST OF ACCURACY OF THREE METHODS FOR FABRICATING DIGITAL COMPLETE DENTURES. In: Abstract Collegio dei Docenti Universitari di discipline Odontostomatologiche ETS – Digital dentistry: la sfida del presente verso il futuro. pp. 348. Dental Cadmos (2022). <https://dx.doi.org/10.19256/abstract.cduo.17.2022>

Pierantozzi, E., **Maltauro, M.**, Meneghello, R., Breschi, L., Ciocca, L.: TRUENESS AND PRECISION OF DIGITALLY MANUFACTURED FRAMEWORKS FOR REMOVABLE PARTIAL DENTURE. In: Abstract Collegio dei Docenti Universitari di discipline Odontostomatologiche ETS – Digital dentistry: la sfida del presente verso il futuro. pp. 349. Dental Cadmos (2022). <https://dx.doi.org/10.19256/abstract.cduo.17.2022>

D.5 || Pre-prints

Maltauro, M., Meneghello, R., Concheri, G. : Tolerance specifications management in industrial product design cycle. Preprint. (2023). <https://doi.org/110.21203/rs.3.rs-2556637/v1>

D.6 || Co-tutored students' dissertations

Fontana, D.: Generalizzazione della stima del tasso di conformità per pattern di accoppiamenti albero-foro. (Generalization of conformity rate estimation for shaft-hole pattern fit) Dipartimento di Ingegneria Industriale - DII, Bachelor degree in Aerospace Engineering. Tutor: Concheri G. Co-tutor: Maltauro, M. (2022/2023)

Barjami, A.: Incertezza ed errori dello scanner intraorale. Dalla revisione della letteratura al confronto sperimentale di tre dispositivi di ultima generazione. (Uncertainty and errors of the intraoral scanner. From the literature review to the applied comparison of three next generation devices). Dipartimento di Neuroscienze - DNS, 6 years single cycle degree in Dentistry and orthodontics. Tutor : Graiff, L. Co-tutor: Maltauro, M. (2022/2023)

Zanin, M.: Generazione automatica dello schema di specifica geometrica funzionale per un elettrodomestico Electrolux. (Automatic functional geometric specification scheme generation for

an Electrolux household appliance). Dipartimento di Tecnica e Gestione dei Sistemi Industriali - DTG, Master degree in Product Innovation Engineering. Tutor: Menghello, R. Co-tutor: Concheri, G., Maltauro, M. (2022/2023)

Carraro, M.: Progettazione e specificazione geometrica funzionale del profilo alare per un drone ad ala fissa. (Design and geometrical specification of a wing airfoil for a fixed-wing drone). Dipartimento di Ingegneria Industriale - DII, Master degree in Aerospace Engineering. Tutor: Picano, F. Co-tutor: Maltauro, M. (2021/2022)

Passarotto, G.: Gestione delle specifiche geometriche per componenti non rigidi: implementazione del metodo dei coefficienti di influenza. (Geometric specifications management for non-rigid parts: implementation of the influence coefficient method). Dipartimento di Ingegneria Industriale - DII, Master degree in Mechanical Engineering. Tutor: Concheri, G. Co-tutor: Meneghello, R., Maltauro, M. (2021/2022)

Andretta, A., Campagnaro, C., Casa, L., Fasolo, C., Scortegagna, A.: Analisi e revisione di sottoassiemi meccanici di un elettrodomestico Electrolux della linea dishwasher. (Analysis and revision of mechanical subassemblies of an Electrolux dishwasher line appliance). Dipartimento di Tecnica e Gestione dei Sistemi Industriali - DTG, Bachelor degree in Product Innovation Engineering. Tutor: Meneghello, R. Co-tutor: Maltauro, M. (2021/2022)

De Checchi, F.: Reverse Engineering mediante scanner 3D multifunzione: verifica delle prestazioni e ottimizzazione per la stampa 3D. (Reverse Engineering with a multifunctional 3D scanner: performance verification and optimization for 3D printing). Dipartimento di Tecnica e Gestione dei Sistemi Industriali - DTG, Master degree in Product Innovation Engineering. Tutor: Menghello, R. Co-tutor: Maltauro, M. (2020/2021)

Pellegrini, D.: Gestione delle specifiche geometriche in Electrolux. Studio di correlazione tra specifica funzionale e di produzione di un corpo lavante. (Geometric specifications management in Electrolux. Correlation between functional and manufacturing specification for a washing group.). Dipartimento di Ingegneria Industriale - DII, Master degree in Mechanical Engineering. Tutor: Meneghello, R. Co-tutor: Concheri, G., Maltauro, M. (2020/2021)

Longo, M.: Analisi Funzionale di un Elettrodomestico per il Lavaggio dei Tessuti. (Functional Analysis of an Appliance for Fabrics Washing). Dipartimento di Tecnica e Gestione dei Sistemi Industriali - DTG, Bachelor degree in Mechanical and Mechatronic Engineering. Tutor: Meneghello, R. Co-tutor: Maltauro, M. (2020/2021).

Bibliography

- [1] ISO International Organization for Standardization, ISO 14638:2015 - Geometrical product specifications (GPS) - Matrix model, (2015).
- [2] ISO International Organization for Standardization, ISO/TR 14638:1995 - Geometrical product specification (GPS) - Masterplan, (1995).
- [3] E. Morse, J.Y. Dantan, N. Anwer, R. Söderberg, G. Moroni, A. Qureshi, X. Jiang, L. Mathieu, Tolerancing: Managing uncertainty from conceptual design to final product, CIRP Ann. 67 (2018) 695–717. <https://doi.org/10.1016/j.cirp.2018.05.009>.
- [4] ISO International Organization for Standardization, ISO 9000:2015 - Quality management systems - Fundamentals and vocabulary, (2015).
- [5] ASME, ASME Y14.5 - 2018 - Dimensioning and Tolerancing, (2019) 344.
- [6] ISO International Organization for Standardization, ISO 17450-2:2012 - Geometrical product specifications (GPS) - General concepts - Basic tenets, specifications, operators, uncertainties and ambiguities, (2012).
- [7] L. Pierre, B. Anselmetti, N. Anwer, On the usage of least material requirement for functional tolerancing, in: Procedia CIRP, 2018: pp. 179–184. <https://doi.org/10.1016/j.procir.2018.04.068>.
- [8] ISO International Organization for Standardization, ISO/R 286:1962 - SO system of limits and fits — Part I : General, tolerances and deviations, (1962).
- [9] A.S. for E. Education, American Standard Drawings and Drafting Room Practice, (1935).
- [10] American Society for Engineering Education, American Standard Drawings and Drafting Room Practice, (1946).
- [11] ISO International Organization for Standardization, ISO 286-1:2010 - Geometrical product specifications (GPS) - ISO code system for tolerances on linear sizes - Part 1: Basis of tolerances, deviations and fits, (2010).
- [12] S. Parker, Notes on Design and Inspection of Mass Production Engineering Work, (1940).
- [13] D. of G.M.C. Engineering Dept., Chevrolet-Central Office, Chevrolet Draftsman's Handbook, (1940).
- [14] bsi, BS 308:1943 - Engineering drawing office practice, (1964).
- [15] bsi, BS 308:1953 - Engineering drawing office practice, (1953).
- [16] ISO International Organization for Standardization, ISO/R 1101-1:1969 - Tolerance of Form

- and of Position - Part 1 - Generalities, Symbols, Indications on Drawings, (1969).
- [17] H.S. Nielsen, *The ISO Geometrical Product Specifications Handbook - Find your way in GPS*, ISO International Organization for Standardization, 2012.
- [18] S. Parker, *Drawing and Dimensions*, Sir Isaac Pitman & Sons, LTD., London, 1956.
- [19] P. Chiabert, F. Lombardi, M. Orlando, Benefits of geometric dimensioning and tolerancing, *J. Mater. Process. Technol.* 78 (1998) 29–35. [https://doi.org/10.1016/S0924-0136\(97\)00459-7](https://doi.org/10.1016/S0924-0136(97)00459-7).
- [20] ISO International Organization for Standardization, *ISO 14405-1:2016 Geometrical product specifications (GPS) — Dimensional tolerancing — Part 1: Linear sizes*, (2016).
- [21] J. Schuldt, R. Hofmann, S. Gröger, Introduction of a maturity model for the assessment of the integration of the GPS system in companies, *Procedia CIRP.* 92 (2020) 129–133. <https://doi.org/10.1016/j.procir.2020.05.188>.
- [22] J. Schuldt, S. Gröger, The assessment of the ISO GPS system implementation with a GPS maturity model, *Procedia CIRP.* 114 (2022) 197–202. <https://doi.org/10.1016/j.procir.2022.10.027>.
- [23] E.P. Morse, C.M. Shakarji, V. Srinivasan, A Brief Analysis of Recent ISO Tolerancing Standards and Their Potential Impact on Digitization of Manufacturing, *Procedia CIRP.* 75 (2018) 11–18. <https://doi.org/10.1016/j.procir.2018.04.080>.
- [24] A. Krulikowski, *Survey Results on the Usage of ISO GPS and ASME Y14.5 Standards*, Krulikowski Consult. LLC. (2017). <https://krulikowskiconsulting.com/survey-results-on-the-usage-of-iso-and-asme-y14-5-standards/> (accessed November 17, 2022).
- [25] C. Kong, T. Li, Z. Zhang, Y. Xu, J. Luo, H. Fu, Y. Zhu, C. Ming, J. Yu, The status of delivery of ISO GPS in China: A survey, *Procedia CIRP.* 114 (2022) 100–105. <https://doi.org/10.1016/j.procir.2022.10.014>.
- [26] M.S.J. Walter, C. Klein, B. Heling, S. Wartzack, Statistical Tolerance Analysis—A Survey on Awareness, Use and Need in German Industry, *Appl. Sci.* 11 (2021) 2622. <https://doi.org/10.3390/app11062622>.
- [27] A.A. Wagire, R. Joshi, A.P.S. Rathore, R. Jain, Development of maturity model for assessing the implementation of Industry 4.0: learning from theory and practice, *Prod. Plan. Control.* 32 (2021) 603–622. <https://doi.org/10.1080/09537287.2020.1744763>.
- [28] V.D.I. VDI, *VDI-Richtlinie 4000-1 - Entwurf: Systematische Transformation und Evaluation von Produktionssystemen - Grundlagen*, (2021).
- [29] A. Schumacher, S. Erol, W. Sihn, A Maturity Model for Assessing Industry 4.0 Readiness and Maturity of Manufacturing Enterprises, *Procedia CIRP.* 52 (2016) 161–166. <https://doi.org/10.1016/j.procir.2016.07.040>.
- [30] ASME, *ASME - Geometric Dimensioning and Tolerancing Professional Certification - Applicant Information Handbook*, (2017). https://www.asme.org/wwwasmeorg/media/resourcefiles/career_education/certificationtraining/gdtp_applicationinformationhandbook.pdf (accessed February 20, 2023).

- [31] A. Wolf, Can competence and knowledge mix?, in: *Competency Based Educ. Training.*, Taylor & Francis Inc., 2005: pp. 34–46.
- [32] European Commission, Data protection - Rules for the protection of personal data inside and outside the EU., (n.d.).
- [33] MSCI Inc., GLOBAL INDUSTRY CLASSIFICATION STANDARD (GICS®) METHODOLOGY - Guiding Principles and Methodology for GICS, (2022). <https://www.msci.com/documents/1296102/11185224/GICS+Methodology+2022.pdf> (accessed February 20, 2023).
- [34] R. Piquié, L. Rivest, F. Segonds, P. Véron, An illustrated glossary of ambiguous PLM terms used in discrete manufacturing, *Int. J. Prod. Lifecycle Manag.* 8 (2015). <https://doi.org/10.1504/IJPLM.2015.070580>.
- [35] ISO International Organization for Standardization, ISO 16792:2021 - Technical product documentation - Digital product definition data practices, (2021).
- [36] ISO International Organization for Standardization, ISO 10209:2012 - Technical product documentation - Vocabulary - Terms relating to technical drawings, product definition and related documentation, (2012).
- [37] ISO International Organization for Standardization, ISO/TS 21619:2018 - Geometrical product specifications (GPS) - Types of documents with GPS, (2018).
- [38] ISO International Organization for Standardization, ISO 17450-1:2011 - Geometrical product specifications (GPS) - General concepts - Model for geometrical specification and verification, (2011).
- [39] H. Mejbri, B. Anselmetti, B. Mawussi, A recursive tolerancing method with sub-assembly generation, in: *Proc. IEEE Int. Symp. Assem. Task Plan.*, IEEE, 2003: pp. 235–240. <https://doi.org/10.1109/ISATP.2003.1217217>.
- [40] B. Anselmetti, L. Pierre, Complementary Writing of Maximum and Least Material Requirements, with an Extension to Complex Surfaces, in: *Procedia CIRP*, 2016: pp. 220–225. <https://doi.org/10.1016/j.procir.2016.02.153>.
- [41] B. Anselmetti, K. Mawussi, Computer Aided Tolerancing Using Positioning Features, *J. Comput. Inf. Sci. Eng.* 3 (2003). <https://doi.org/10.1115/1.1565074>.
- [42] H. Mejbri, B. Anselmetti, K. Mawussi, Functional tolerancing of complex mechanisms: Identification and specification of key parts, *Comput. Ind. Eng.* 49 (2005). <https://doi.org/10.1016/j.cie.2005.04.002>.
- [43] A. Ballu, H. Falgarone, N. Chevassus, L. Mathieu, A new Design Method based on Functions and Tolerance Specifications for Product Modelling, *CIRP Ann.* 55 (2006). [https://doi.org/10.1016/S0007-8506\(07\)60384-9](https://doi.org/10.1016/S0007-8506(07)60384-9).
- [44] B. Anselmetti, Generation of functional tolerancing based on positioning features, *Comput. Des.* 38 (2006). <https://doi.org/10.1016/j.cad.2006.05.005>.
- [45] J. Hu, Y. Peng, Development of a function oriented computer aided tolerancing (FOCAT) system, *Proc. Inst. Mech. Eng. Part B J. Eng. Manuf.* 225 (2011).

- <https://doi.org/10.1177/2041297510393578>.
- [46] N.P. Suh, *The Principles of Design*, Oxford University Press, 1990.
- [47] Y. Cao, H. Zhang, B. Li, Z. Wu, J. Yang, Study on functional specification scheme on interface based on positioning features, *Proc. Inst. Mech. Eng. Part B J. Eng. Manuf.* 227 (2013). <https://doi.org/10.1177/0954405413479112>.
- [48] S.M. Göhler, S. Husung, T.J. Howard, The Translation between Functional Requirements and Design Parameters for Robust Design, *Procedia CIRP.* 43 (2016). <https://doi.org/10.1016/j.procir.2016.02.028>.
- [49] P. Bourdet, L. Mathieu, C. Lartigue, A. Ballu, The Concept of the Small Displacement Torsor in Metrology, in: *Ser. Adv. Math. Appl. Sci. Vol. 40, Adv. Math. Tools Metrol. II*, WORLD SCIENTIFIC, 1996: pp. 110–122.
- [50] F. Vignat, F. Villeneuve, Simulation of the Manufacturing Process, Generation of a Model of the Manufactured Parts, in: *Digit. Enterp. Technol.*, Springer US, Boston, MA, 2007. https://doi.org/10.1007/978-0-387-49864-5_64.
- [51] F. Villeneuve, F. Vignat, Simulation of the Manufacturing Process in a Tolerancing Point of View: Generic Resolution of the Positioning Problem, in: *Model. Comput. Aided Toler. Des. Manuf.*, Springer Netherlands, Dordrecht, 2007. https://doi.org/10.1007/1-4020-5438-6_19.
- [52] H. Peng, Z. Peng, Using Small Displacement Torsor to Simulate the Machining Processes for 3D Tolerance Transfer, *IOP Conf. Ser. Mater. Sci. Eng.* 831 (2020). <https://doi.org/10.1088/1757-899X/831/1/012017>.
- [53] M. Laifa, W.B. Sai, M. Hbaieb, Evaluation of machining process by integrating 3D manufacturing dispersions, functional constraints, and the concept of small displacement torsors, *Int. J. Adv. Manuf. Technol.* 71 (2014) 1327–1336. <https://doi.org/10.1007/s00170-013-5558-9>.
- [54] B. Anselmetti, H. Louati, Generation of manufacturing tolerancing with ISO standards, *Int. J. Mach. Tools Manuf.* 45 (2005). <https://doi.org/10.1016/j.ijmachtools.2005.01.001>.
- [55] C. Mickaël, A. Bernard, 3D ISO manufacturing specifications with vectorial representation of tolerance zones, *Int. J. Adv. Manuf. Technol.* 60 (2012). <https://doi.org/10.1007/s00170-011-3638-2>.
- [56] B. Ayadi, B. Anselmetti, Z. Bouaziz, A. Zghal, Three-dimensional modelling of manufacturing tolerancing using the ascendant approach, *Int. J. Adv. Manuf. Technol.* 39 (2008). <https://doi.org/10.1007/s00170-007-1225-3>.
- [57] B. Anselmetti, ISO manufacturing tolerancing: three-dimensional transfer with analysis line method, *Int. J. Adv. Manuf. Technol.* 61 (2012). <https://doi.org/10.1007/s00170-011-3769-5>.
- [58] M. Royer, B. Anselmetti, 3D manufacturing tolerancing with probing of a local work coordinate system, *Int. J. Adv. Manuf. Technol.* 84 (2016). <https://doi.org/10.1007/s00170-015-7797-4>.
- [59] M. Royer, B. Anselmetti, 3D Manufacturing Tolerancing with Analysis Line Method Taking into Account Joining Operations During Manufacturing Process, *Procedia CIRP.* 43 (2016).

- <https://doi.org/10.1016/j.procir.2016.02.023>.
- [60] L.-M. Frère, M. Royer, J. Fourcade, Tolerance analysis using a Computer Aided Tolerancing Software: ANATOLE 3D, *Procedia CIRP*. 75 (2018). <https://doi.org/10.1016/j.procir.2018.04.079>.
- [61] S. Woo, The reliability design of mechanical system and its parametric accelerated life testing, in: *Handb. Mater. Fail. Anal. with Case Stud. from Chem. Concr. Power Ind.*, Elsevier, 2016. <https://doi.org/10.1016/B978-0-08-100116-5.00011-9>.
- [62] NASA, *NASA Systems Engineering Handbook*, NASA SP-20, Washington, DC, 2016. https://www.nasa.gov/sites/default/files/atoms/files/nasa_systems_engineering_handbook_0.pdf.
- [63] E. Morse, Design for Metrology – a new idea?, *Procedia CIRP*. 84 (2019) 165–168. <https://doi.org/10.1016/j.procir.2019.04.240>.
- [64] T. Coulson, The origin of interchangeable parts, *J. Franklin Inst.* 238 (1944). [https://doi.org/10.1016/S0016-0032\(44\)90044-X](https://doi.org/10.1016/S0016-0032(44)90044-X).
- [65] E. Buckingham, *Principles of Interchangeable Manufacturing; A Treatise on the Basic Principles Involved in Successful Interchangeable Manufacturing Practice, Covering Design, Tolerances, Drawings, Manufacturing Equipment, Gaging and Inspection*, Industrial Press, New York, 1921.
- [66] C.A. Gladman, *Drawing Office Practice in Relation to Interchangeable Components*, in: 1945. <https://doi.org/10.4271/450238>.
- [67] W.J. Durfee, The First Systematic Attempt at Interchangeability in Firearms, *Cassier's Mag. V* (1894) 469–477.
- [68] N.Z. Ishrat, *Product Management: The Art and Science of Managing Network and Communications Industry Products*, Xlibris Corporation, 2013.
- [69] ISO International Organization for Standardization, *ISO/TS 8062-2:2013 - Geometrical Product Specifications (GPS) - Dimensional and geometrical tolerances for moulded parts - Rules*, (2013).
- [70] ISO International Organization for Standardization, *ISO/IEC/IEEE 24765:2017 - Systems and software engineering - Vocabulary*, (2017).
- [71] ISO International Organization for Standardization, *ISO/IEC 2382:2015 - Information technology - Vocabulary*, (2015).
- [72] M.W. Groll, D. Heber, E/E-product data management in consideration of model-based systems engineering, *Adv. Transdiscipl. Eng.* 4 (2016) 289–298.
- [73] ISO International Organization for Standardization, *ISO 5459:2011 - Geometrical product specifications (GPS) - Geometrical tolerancing - Datums and datum systems*, (2011).
- [74] ISO International Organization for Standardization, *ISO 5458:2018 - Geometrical product specifications (GPS) - Geometrical tolerancing - Pattern and combined geometrical specification*, (2018).
- [75] ISO International Organization for Standardization, *ISO 22081:2021 - Geometrical product*

- specifications (GPS) - Geometrical tolerancing - General geometrical specifications and general size specifications, (2021).
- [76] ISO International Organization for Standardization, ISO 8015:2011 - Geometrical product specifications (GPS) - Fundamentals - Concepts, principles and rules, (2011).
- [77] D. Whitney, *Mechanical Assemblies: Their Design, Manufacture, and Role in Product Development*, Oxford University Press, New York, 2004.
- [78] G. Boothroyd, *Design for Manufacture and Assembly: The Boothroyd-Dewhurst Experience*, in: *Des. X*, Springer Netherlands, Dordrecht, 1996: pp. 19–40. https://doi.org/10.1007/978-94-011-3985-4_2.
- [79] B.R. Fischer, *Mechanical Tolerance Stackup and Analysis*, CRC Press, 2004. <https://doi.org/10.1201/9780203021194>.
- [80] P.J. Drake, *Dimensioning and Tolerancing Handbook*, McGraw Hill, 1999.
- [81] C.L. Svensen, *Drafting for Engineers*, D. Van Nostrand Company, Inc, New York, 1935.
- [82] ISO International Organization for Standardization, ISO/R 129:1959 - Engineering drawing - Dimensioning, (1959).
- [83] UNI, UNI 4820:1961 - Disegni tecnici - Definizioni e principi, (1961).
- [84] S. Kalpakjian, S. Schmid, *Manufacturing Engineering and Technology*, 5th ed., Pearson, 2008.
- [85] K.O. Kverneland, How ISO Standards Cut Manufacturing Costs, *Mach. Des.* (1998) 126–130.
- [86] A.C. Thornton, A Mathematical Framework for the Key Characteristic Process, *Res. Eng. Des.* 11 (1999) 145–157. <https://doi.org/10.1007/s001630050011>.
- [87] A. Armillotta, Allocation of geometric tolerances in one-dimensional stackup problems, *Int. J. Adv. Manuf. Technol.* 122 (2022) 1957–1973. <https://doi.org/10.1007/s00170-022-09918-2>.
- [88] R. Askri, C. Bois, H. Wagnier, N. Gayton, Tolerance synthesis of fastened metal-composite joints based on probabilistic and worst-case approaches, *Comput. Des.* 100 (2018) 39–51. <https://doi.org/10.1016/j.cad.2018.02.008>.
- [89] S. Khodaygan, A multiple objective framework for optimal asymmetric tolerance synthesis of mechanical assemblies with degrading components, *Int. J. Adv. Manuf. Technol.* 100 (2019) 2177–2205. <https://doi.org/10.1007/s00170-018-2658-6>.
- [90] C. Zhang, H. Dong, D. Wang, Y. Cheng, Tolerance synthesis for lost motion requirement of planetary gear train based on a mechanism model, *Mech. Mach. Theory.* 164 (2021) 104405. <https://doi.org/10.1016/j.mechmachtheory.2021.104405>.
- [91] M. Hallmann, B. Schleich, S. Wartzack, From tolerance allocation to tolerance-cost optimization: a comprehensive literature review, *Int. J. Adv. Manuf. Technol.* 107 (2020) 4859–4912. <https://doi.org/10.1007/s00170-020-05254-5>.
- [92] D. Vignesh Kumar, D. Ravindran, N. Lenin, M. Siva Kumar, Tolerance allocation of complex assembly with nominal dimension selection using Artificial Bee Colony algorithm, *Proc. Inst. Mech. Eng. Part C J. Mech. Eng. Sci.* 233 (2019) 18–38.

- <https://doi.org/10.1177/0954406218756439>.
- [93] D. Vignesh Kumar, D. Ravindran, M. Siva Kumar, M. Islam, Optimum tolerance synthesis of simple assemblies with nominal dimension selection using genetic algorithm, *Proc. Inst. Mech. Eng. Part C J. Mech. Eng. Sci.* 230 (2016) 3488–3508. <https://doi.org/10.1177/0954406215613366>.
- [94] W.C. Kenneth, G. Jinsong, P.M. Spencer, General 2-D tolerance analysis of mechanical assemblies with small kinematic adjustments., *J. Des. Manuf.* (1995) 263–274.
- [95] J. Gao, K.W. Chase, S.P. Magleby, Generalized 3-D tolerance analysis of mechanical assemblies with small kinematic adjustments, *IIE Trans.* 1998 304. 30 (1998) 367–377. <https://doi.org/10.1023/A:1007451225222>.
- [96] S. Gupta, J.U. Turner, Variational solid modeling for tolerance analysis, *IEEE Comput. Graph. Appl.* 13 (1993) 64–74. <https://doi.org/10.1109/38.210493>.
- [97] A. Desrochers, A. Rivière, A matrix approach to the representation of tolerance zones and clearances, *Int. J. Adv. Manuf. Technol.* 13 (1997) 630–636. <https://doi.org/10.1007/BF01350821>.
- [98] P. Lafond, L. Laperriere, Jacobian-based modeling of dispersions affecting pre-defined functional requirements of mechanical assemblies, *Proc. IEEE Int. Symp. Assem. Task Plan.* (1999) 20–25.
- [99] W. Polini, A. Corrado, Geometric tolerance analysis through Jacobian model for rigid assemblies with translational deviations, *Assem. Autom.* 36 (2016) 72–79. <https://doi.org/10.1108/AA-11-2015-088>.
- [100] A. Desrochers, W. Ghie, L. Laperrière, Application of a Unified Jacobian—Torsor Model for Tolerance Analysis, *J. Comput. Inf. Sci. Eng.* 3 (2003) 2–14. <https://doi.org/10.1115/1.1573235>.
- [101] J.K. Davidson, A. Mujezinovic', J.J. Shah, A New Mathematical Model for Geometric Tolerances as Applied to Round Faces, *J. Mech. Des.* 124 (2002) 609–622. <https://doi.org/10.1115/1.1497362>.
- [102] N.D. Cox, *Volume 11: How to perform statistical tolerance analysis*, American Society for Quality Control, Milwaukee, WI, 1986.
- [103] N.D. Cox, Tolerance Analysis by Computer, *J. Qual. Technol.* 11 (1979) 80–87. <https://doi.org/10.1080/00224065.1979.11980884>.
- [104] J.M. Bastiaan, E. Green, S. Kaye, Preliminary Study of Perceived Vibration Quality for Human Hands, *SAE Int. J. Adv. Curr. Pract. Mobil.* 1 (2019) 1741–1754. <https://doi.org/10.4271/2019-01-1522>.
- [105] ISO International Organization for Standardization, ISO 2692:2021 - Geometrical product specifications (GPS). Geometrical tolerancing. Maximum material requirement (MMR), least material requirement (LMR) and reciprocity requirement (RPR), (2021).
- [106] M. Markiewicz, E. Bachtia-Radka, S. Dudzińska, D. Grochała, Statistical Process Control Using LMC/MMC Modifiers and Multidimensional Control Charts, in: Hamrol A., Grabowska

- M., Maletic D., Woll R. Adv. Manuf. II. Manuf. 2019. Lect. Notes Mech. Eng., Springer, Cham, 2019: pp. 244–253. https://doi.org/10.1007/978-3-030-17269-5_18.
- [107] F. Scholz, Title Hole Alignment Tolerance Stacking Issues, Seattle, 1999.
- [108] ISO International Organization for Standardization, ISO 10579:2013 - Geometrical product specifications (GPS). Dimensioning and tolerancing. Non-rigid parts, (2013).
- [109] E. Sellem, A. Rivière, Tolerance Analysis of Deformable Assemblies, in: Vol. 2 24th Des. Autom. Conf., American Society of Mechanical Engineers, 1998. <https://doi.org/10.1115/DETC98/DAC-5571>.
- [110] S. Charles Liu, S. Jack Hu, An offset finite element model and its applications in predicting sheet metal assembly variation, Int. J. Mach. Tools Manuf. 35 (1995) 1545–1557. [https://doi.org/10.1016/0890-6955\(94\)00103-Q](https://doi.org/10.1016/0890-6955(94)00103-Q).
- [111] S.C. Liu, S.J. Hu, T.C. Woo, Tolerance Analysis for Sheet Metal Assemblies, J. Mech. Des. 118 (1996) 62–67. <https://doi.org/10.1115/1.2826857>.
- [112] S.C. Liu, S.J. Hu, Variation Simulation for Deformable Sheet Metal Assemblies Using Finite Element Methods, J. Manuf. Sci. Eng. 119 (1997) 368–374. <https://doi.org/10.1115/1.2831115>.
- [113] H. Atik, M. Chahbouni, D. Amegouz, S. Boutahari, Optimization tolerancing of surface in flexible parts and assembly: Influence Coefficient Method with shape defects, Int. J. Eng. Technol. 7 (2018) 90. <https://doi.org/10.14419/ijet.v7i1.8470>.
- [114] H. Atik, M. Chahbouni, D. Amagouz, S. Boutahari, An analysis of springback of compliant assemblies by contact modeling and welding distortion, Int. J. Eng. Technol. 7 (2018) 85. <https://doi.org/10.14419/ijet.v7i1.8330>.
- [115] W. Polini, A. Corrado, Methods of influence coefficients to evaluate stress and deviation distribution of flexible assemblies—a review, Int. J. Adv. Manuf. Technol. 107 (2020) 2901–2915. <https://doi.org/10.1007/s00170-020-05210-3>.
- [116] A. Stockinger, R. Lustig, H. Meerkamm, Computer-based and experimental validation of an approach to combine tolerance zones with elastic deformations, Proc. ICED 2007, 16th Int. Conf. Eng. Des. DS 42 (2007).
- [117] H. Radvar-Esfahlan, S.-A. Tahan, Nonrigid geometric metrology using generalized numerical inspection fixtures, Precis. Eng. 36 (2012) 1–9. <https://doi.org/10.1016/j.precisioneng.2011.07.002>.
- [118] V. Sabri, S.A. Tahan, X.T. Pham, D. Moreau, S. Galibois, Fixtureless profile inspection of non-rigid parts using the numerical inspection fixture with improved definition of displacement boundary conditions, Int. J. Adv. Manuf. Technol. 82 (2016) 1343–1352. <https://doi.org/10.1007/s00170-015-7425-3>.
- [119] V. Sabri, S. Sattarpanah, S.A. Tahan, J.C. Cuillière, V. François, X.T. Pham, A robust and automated FE-based method for fixtureless dimensional metrology of non-rigid parts using an improved numerical inspection fixture, Int. J. Adv. Manuf. Technol. 92 (2017) 2411–2423. <https://doi.org/10.1007/s00170-017-0216-2>.
- [120] B. Lindau, K. Wärmefjord, L. Lindkvist, R. Söderberg, Virtual Fixturing: Inspection of a Non-

- Rigid Detail Resting on 3-Points to Estimate Free State and Over-Constrained Shapes, in: Vol. 2B Adv. Manuf., American Society of Mechanical Engineers, 2020. <https://doi.org/10.1115/IMECE2020-24515>.
- [121] E. Morse, C. Grohol, Practical conformance evaluation in the measurement of flexible parts, *CIRP Ann.* 68 (2019) 507–510. <https://doi.org/10.1016/j.cirp.2019.04.076>.
- [122] S. Raynaud, V. Wolff, T.T. Dinh, O. Pareja, Modélisation et évaluation de l'incertitude de mesure lors de l'utilisation de MMT avec des pièces déformables, in: B. Larquier (Ed.), 17th Int. Congr. Metrol., EDP Sciences, Les Ulis, France, 2015: p. 13006. <https://doi.org/10.1051/metrology/201513006>.
- [123] P.G. Maropoulos, D. Ceglarek, Design verification and validation in product lifecycle, *CIRP Ann.* 59 (2010) 740–759. <https://doi.org/10.1016/j.cirp.2010.05.005>.
- [124] C. Mike Shafto, M.C.R.D.E.G.C. Kemp;, J.L.L. Wang, NASA Technology Roadmap. DRAFT Modeling, Simulation, Information Technology & Processing Roadmap Technology Area 11, (2010).
- [125] B. Schleich, N. Anwer, L. Mathieu, S. Wartzack, Shaping the digital twin for design and production engineering, *CIRP Ann.* 66 (2017) 141–144. <https://doi.org/10.1016/j.cirp.2017.04.040>.
- [126] R. Söderberg, L. Lindkvist, K. Wärmefjord, J.S. Carlson, Virtual Geometry Assurance Process and Toolbox, *Procedia CIRP.* 43 (2016) 3–12. <https://doi.org/10.1016/j.procir.2016.02.043>.
- [127] B. Schleich, K. Wärmefjord, R. Söderberg, S. Wartzack, Geometrical Variations Management 4.0: towards next Generation Geometry Assurance, *Procedia CIRP.* 75 (2018) 3–10. <https://doi.org/10.1016/j.procir.2018.04.078>.
- [128] R. Söderberg, K. Wärmefjord, J.S. Carlson, L. Lindkvist, Toward a Digital Twin for real-time geometry assurance in individualized production, *CIRP Ann.* 66 (2017) 137–140. <https://doi.org/10.1016/j.cirp.2017.04.038>.
- [129] R.S. Tabar, K. Wärmefjord, R. Söderberg, A new surrogate model-based method for individualized spot welding sequence optimization with respect to geometrical quality, *Int. J. Adv. Manuf. Technol.* 106 (2020) 2333–2346. <https://doi.org/10.1007/s00170-019-04706-x>.
- [130] R. Sadeghi Tabar, S. Lorin, C. Cromvik, L. Lindkvist, K. Wärmefjord, R. Söderberg, Efficient Spot Welding Sequence Simulation in Compliant Variation Simulation, *J. Manuf. Sci. Eng.* 143 (2021). <https://doi.org/10.1115/1.4049654>.
- [131] W. Polini, A. Corrado, Digital twin of composite assembly manufacturing process, *Int. J. Prod. Res.* 58 (2020) 5238–5252. <https://doi.org/10.1080/00207543.2020.1714091>.
- [132] L. Andolfatto, F. Thiébaud, M. Douilly, C. Lartigue, On Neural Networks' Ability to Approximate Geometrical Variation Propagation in Assembly, *Procedia CIRP.* 10 (2013) 224–232. <https://doi.org/10.1016/j.procir.2013.08.035>.
- [133] S.C. Spathopoulos, G.E. Stavroulakis, Springback Prediction in Sheet Metal Forming, Based on Finite Element Analysis and Artificial Neural Network Approach, *Appl. Mech.* 1

- (2020) 97–110. <https://doi.org/10.3390/applmech1020007>.
- [134] G. Sohlenius, Concurrent Engineering, *CIRP Ann.* 41 (1992) 645–655. [https://doi.org/10.1016/S0007-8506\(07\)63251-X](https://doi.org/10.1016/S0007-8506(07)63251-X).
- [135] M. Kaufmann, I. Effenberger, M.F. Huber, On the Development of a Surrogate Modelling Toolbox for Virtual Assembly, *Appl. Sci.* 11 (2021) 1181. <https://doi.org/10.3390/app11031181>.
- [136] M. Maltauro, R. Meneghello, G. Concheri, D. Pellegrini, M. Viero, G. Bisognin, A Case Study on the Correlation Between Functional and Manufacturing Specifications for a Large Injection Moulded Part, in: S. Gerbino, A. Lanzotti, M. Martorelli, R. Mirálbes Buil, C. Rizzi, L. Roucoules (Eds.), *Adv. Mech. Des. Eng. Manuf. IV - Proc. Int. Jt. Conf. Mech. Des. Eng. Adv. Manuf. JCM 2022*, June 1-3, 2022, Ischia, Italy, Springer International Publishing, Cham, 2023: pp. 1268–1278. https://doi.org/10.1007/978-3-031-15928-2_111.
- [137] S. Dahlström, L. Lindkvist, Variation Simulation of Sheet Metal Assemblies Using the Method of Influence Coefficients With Contact Modeling, *J. Manuf. Sci. Eng.* 129 (2007) 615–622. <https://doi.org/10.1115/1.2714570>.
- [138] Y. Li, Y. Zhao, H. Yu, X. Lai, Compliant assembly variation analysis of sheet metal with shape errors based on primitive deformation patterns, *Proc. Inst. Mech. Eng. Part C J. Mech. Eng. Sci.* 232 (2018) 2334–2351. <https://doi.org/10.1177/0954406217720231>.
- [139] J. Yang, J. Wang, Z. Wu, N. Anwer, Statistical Tolerancing based on Variation of Point-set, *Procedia CIRP.* 10 (2013) 9–16. <https://doi.org/10.1016/j.procir.2013.08.006>.
- [140] N. Anwer, A. Ballu, L. Mathieu, The skin model, a comprehensive geometric model for engineering design, *CIRP Ann.* 62 (2013) 143–146. <https://doi.org/10.1016/j.cirp.2013.03.078>.
- [141] ISO International Organization for Standardization, ISO 1101:2017 - Geometrical product specifications (GPS). Geometrical tolerancing. Tolerances of form, orientation, location and run-out, (2017).
- [142] A. Corrado, W. Polini, G. Giuliano, Super-element method applied to MIC to reduce simulation time of compliant assemblies, *Int. J. Comput. Appl. Technol.* 59 (2019) 277. <https://doi.org/10.1504/IJCAT.2019.099197>.
- [143] G. Lanza, B. Haefner, A. Kraemer, Optimization of selective assembly and adaptive manufacturing by means of cyber-physical system based matching, *CIRP Ann.* 64 (2015) 399–402. <https://doi.org/10.1016/j.cirp.2015.04.123>.
- [144] Y. Zhang, W. Lu, Development and Standardization of Quality-oriented Statistical Tolerancing in China, *Procedia CIRP.* 43 (2016) 268–273. <https://doi.org/10.1016/j.procir.2016.02.102>.
- [145] V. Srinivasan, M.A. O'Connor, Towards an ISO Standard for Statistical Tolerancing, in: *Comput. Toler.*, Springer Netherlands, Dordrecht, 1996: pp. 159–172. https://doi.org/10.1007/978-94-009-1529-9_11.
- [146] E. Savio, A methodology for the quantification of value-adding by manufacturing metrology, *CIRP Ann.* 61 (2012) 503–506. <https://doi.org/10.1016/j.cirp.2012.03.019>.

- [147] ISO International Organization for Standardization, ISO 14253-2:2011 Geometrical product specifications (GPS) — Inspection by measurement of workpieces and measuring equipment — Part 2: Guidance for the estimation of uncertainty in GPS measurement, in calibration of measuring equipment and in product verification, (n.d.).
- [148] Joint Committee for Guides in Metrology, JCGM 106:2012 - Evaluation of measurement data – The role of measurement uncertainty in conformity assessment, (2012).
- [149] ISO International Organization for Standardization, ISO 14253-1:2017 - Geometrical product specifications (GPS). Inspection by measurement of workpieces and measuring equipment. Decision rules for verifying conformity or nonconformity with specifications, (2017).
- [150] M. Maltauro, R. Meneghello, G. Concheri, Conformity Rate Estimation for Shaft-Hole Pattern Fit Not Compliant with the Boundary Condition Design Criterion, in: S. Gerbino, A. Lanzotti, M. Martorelli, R. Mirálbes Buil, C. Rizzi, L. Roucoules (Eds.), *Adv. Mech. Des. Eng. Manuf. IV - Proc. Int. Jt. Conf. Mech. Des. Eng. Adv. Manuf. JCM 2022*, June 1-3, 2022, Ischia, Italy, Springer International Publishing, Cham, 2023: pp. 1256–1267. https://doi.org/10.1007/978-3-031-15928-2_110.
- [151] B. Mills, Variation analysis applied to assembly simulation, *Assem. Autom.* 8 (1988) 41–44. <https://doi.org/10.1108/eb004233>.
- [152] S. Ma, T. Hu, Z. Xiong, Precision Assembly Simulation of Skin Model Shapes Accounting for Contact Deformation and Geometric Deviations for Statistical Tolerance Analysis Method, *Int. J. Precis. Eng. Manuf.* 22 (2021) 975–989. <https://doi.org/10.1007/s12541-021-00505-1>.
- [153] N. Anwer, A. Ballu, L. Mathieu, The skin model, a comprehensive geometric model for engineering design, *CIRP Ann.* 62 (2013) 143–146. <https://doi.org/10.1016/J.CIRP.2013.03.078>.
- [154] X. Yan, A. Ballu, Tolerance analysis using skin model shapes and linear complementarity conditions, *J. Manuf. Syst.* 48 (2018) 140–156. <https://doi.org/10.1016/J.JMSY.2018.07.005>.
- [155] A. Corrado, W. Polini, FEA integration in the tolerance analysis using Skin Model Shapes, *Procedia CIRP.* 75 (2018) 285–290. <https://doi.org/10.1016/J.PROCIR.2018.04.055>.
- [156] A. Corrado, W. Polini, Manufacturing signature in variational and vector-loop models for tolerance analysis of rigid parts, *Int. J. Adv. Manuf. Technol.* 88 (2017) 2153–2161. <https://doi.org/10.1007/s00170-016-8947-z>.
- [157] M. Marziale, W. Polini, Review of variational models for tolerance analysis of an assembly, *Proc. Inst. Mech. Eng. Part B J. Eng. Manuf.* 225 (2011) 305–318. <https://doi.org/10.1177/2041297510394107>.
- [158] A. Corrado, W. Polini, Comparison among different tools for tolerance analysis of rigid assemblies, *Int. J. Comput. Appl. Technol.* 62 (2020) 36. <https://doi.org/10.1504/IJCAT.2020.103915>.
- [159] J. Gao, K.W. Chase, S.P. Magleby, Comparison of Assembly Tolerance Analysis by the

- Direct Linearization and Modified Monte Carlo Simulation Methods, *Am. Soc. Mech. Eng. Des. Eng. Div.* 82 (1995) 353–360.
- [160] S.S. Shapiro, A.J. Gross, *Statistical Modeling Techniques*, Marcel Delcker, Inc., New York, 1981.
- [161] C.G. Glancy, K.W. Chase, A Second-Order Method for Assembly Tolerance Analysis, in: Vol. 1 25th Des. Autom. Conf., American Society of Mechanical Engineers, 1999: pp. 977–984. <https://doi.org/10.1115/DETC99/DAC-8707>.
- [162] Sigmetrix, CETOL6sigma, User Reference Manual, (2014) 198.
- [163] J.S. Ramberg, E.J. Dudewicz, P.R. Tadikamalla, E.F. Mykytka, A Probability Distribution and its Uses in Fitting Data, *Technometrics*. 21 (1979) 201–214. <https://doi.org/10.1080/00401706.1979.10489750>.
- [164] M. Maltauro, R. Meneghello, G. Concheri, Tolerance specifications management in industrial product design cycle, 2023. <https://doi.org/110.21203/rs.3.rs-2556637/v1>.
- [165] M. Maltauro, G. Passarotto, G. Concheri, R. Meneghello, Bridging the gap between design and manufacturing specifications for non-rigid parts using the influence coefficient method, *Int. J. Adv. Manuf. Technol.* 127 (2023) 579–597. <https://doi.org/10.1007/s00170-023-11480-4>.
- [166] M. Maltauro, E. Morse, Towards a Definition of “Geometric Verification Specifications” Within the ISO GPS System, *Procedia CIRP*. 119 (2023) 339–344. <https://doi.org/10.1016/j.procir.2023.03.101>.